



Femtosecond Laser ablation/ICPMS for trace element and isotope ratio measurement: application to biomineral, petroleum industry and forensic science... And poetry!

Christophe Pécheyran

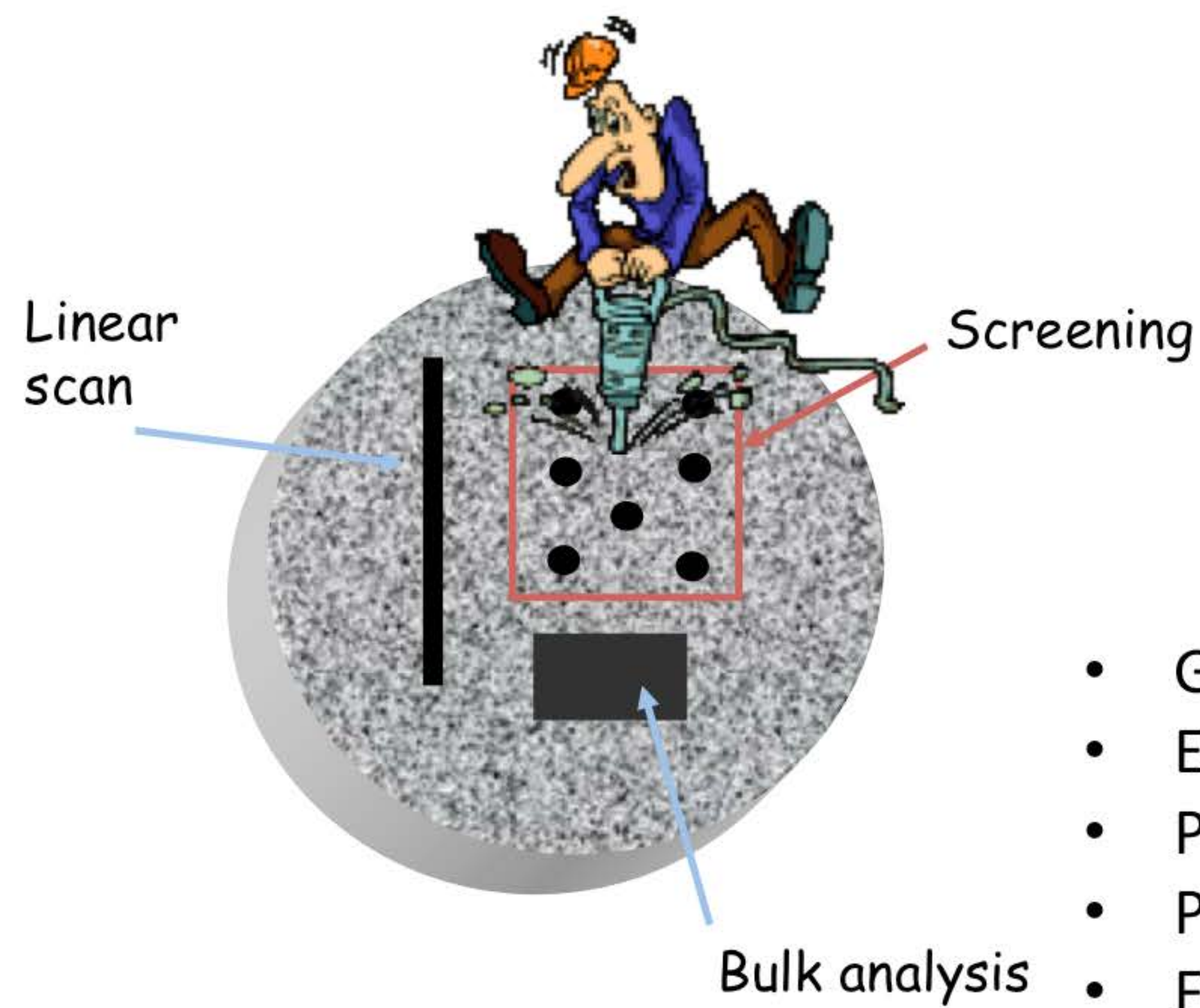
Laboratoire de Chimie Analytique Bio-Inorganique et Environnement (LCABIE),
UMR CNRS-UPPA 5254 IPREM, Hélioparc Pau Pyrénées, 64053 Pau, France

christophe.pecheyran@univ-pau.fr



Laser ablation for direct solid sampling

Direct analysis
Micro sampling (5-200 µm)
Macro sampling (>200 µm)
Minimizing invasive approach

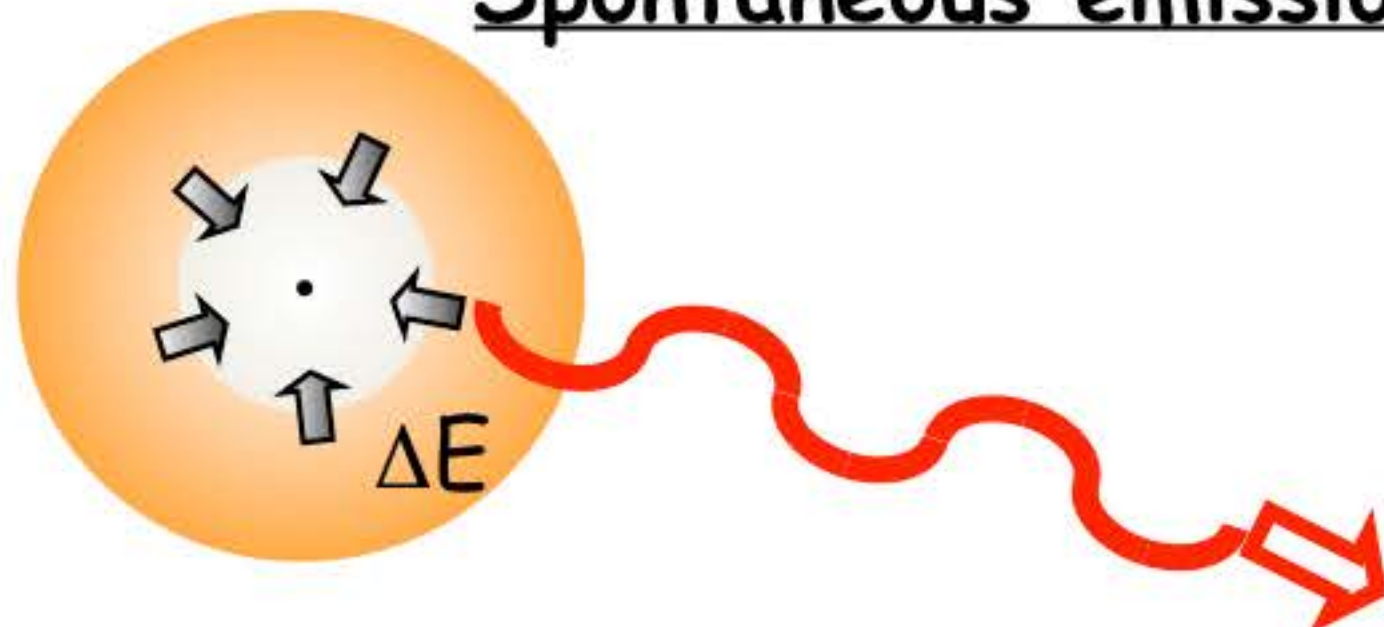


- Geosciences
- Environment
- Protéomic
- Petrochemistry
- Forensic
- Archeology
- Surface analysis...

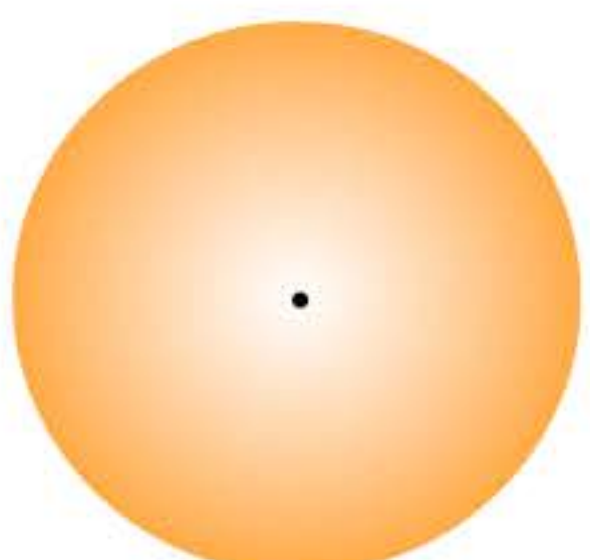
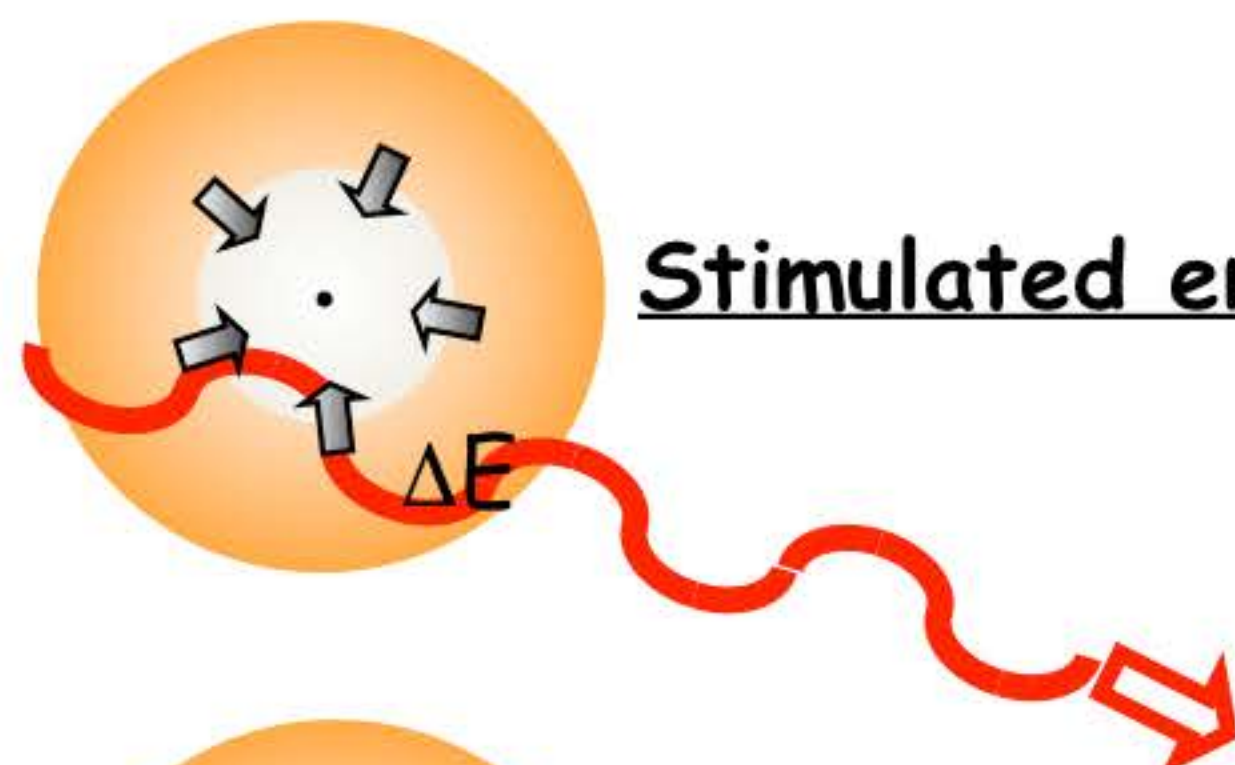


Laser basic principle

Spontaneous emission



Stimulated emission



Excited state



Ground state

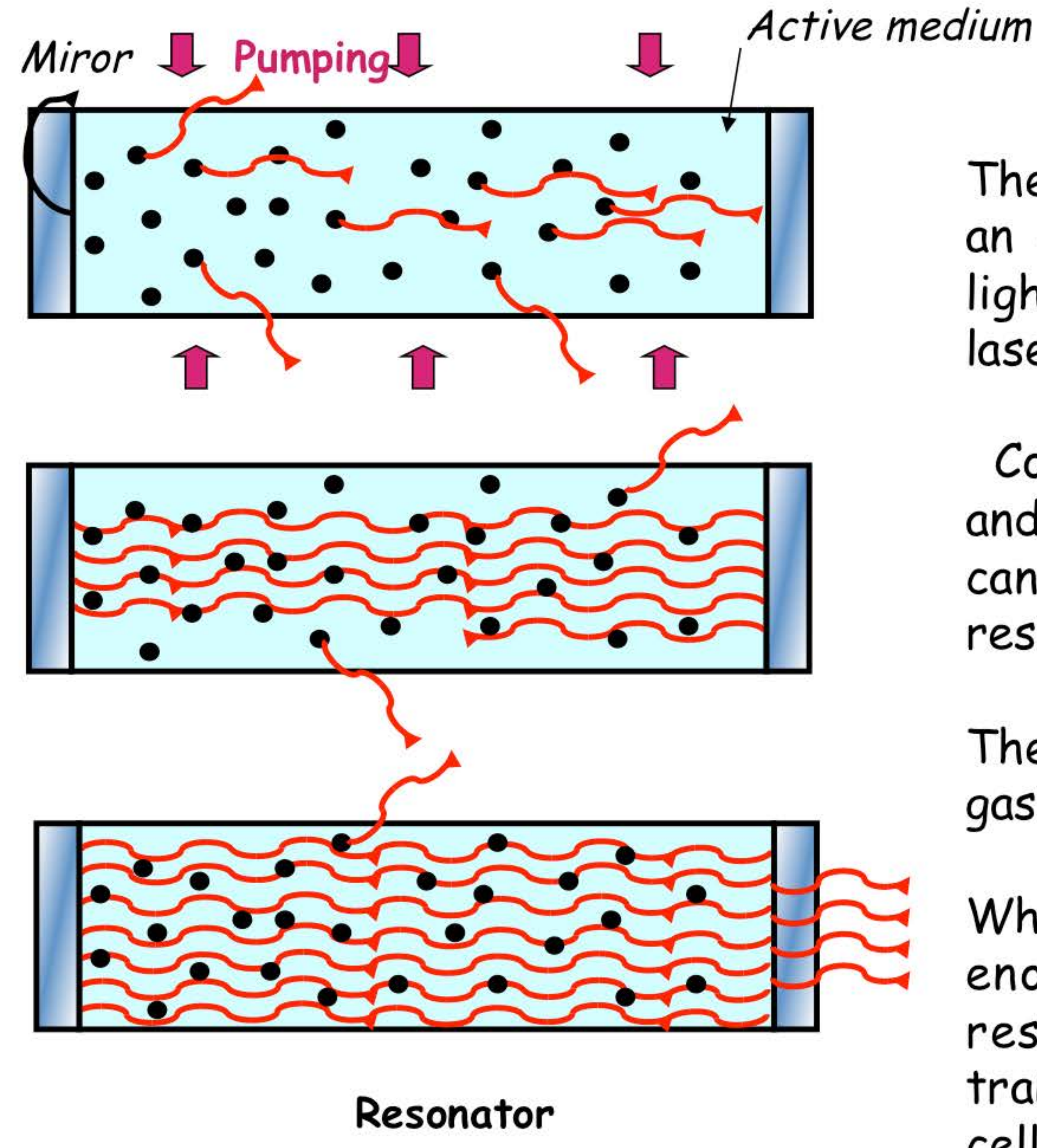
Spontaneous emission: the energy accumulated by an atom is released via the emission of a photon.

Stimulated emission (discovered by A. Einstein) : induced by a photon on a excited atom, this phenomenon leads to the emission of a photon of the same energy, same direction and phase (**coherent light**).

When a population inversion is present the rate of stimulated emission exceeds that of absorption, and a net optical amplification can be achieved

This property is used to generate laser light...

Laser basic principle



The population inversion is triggered by an external source of energy (pumping: light flash, electric source, or even lasers)

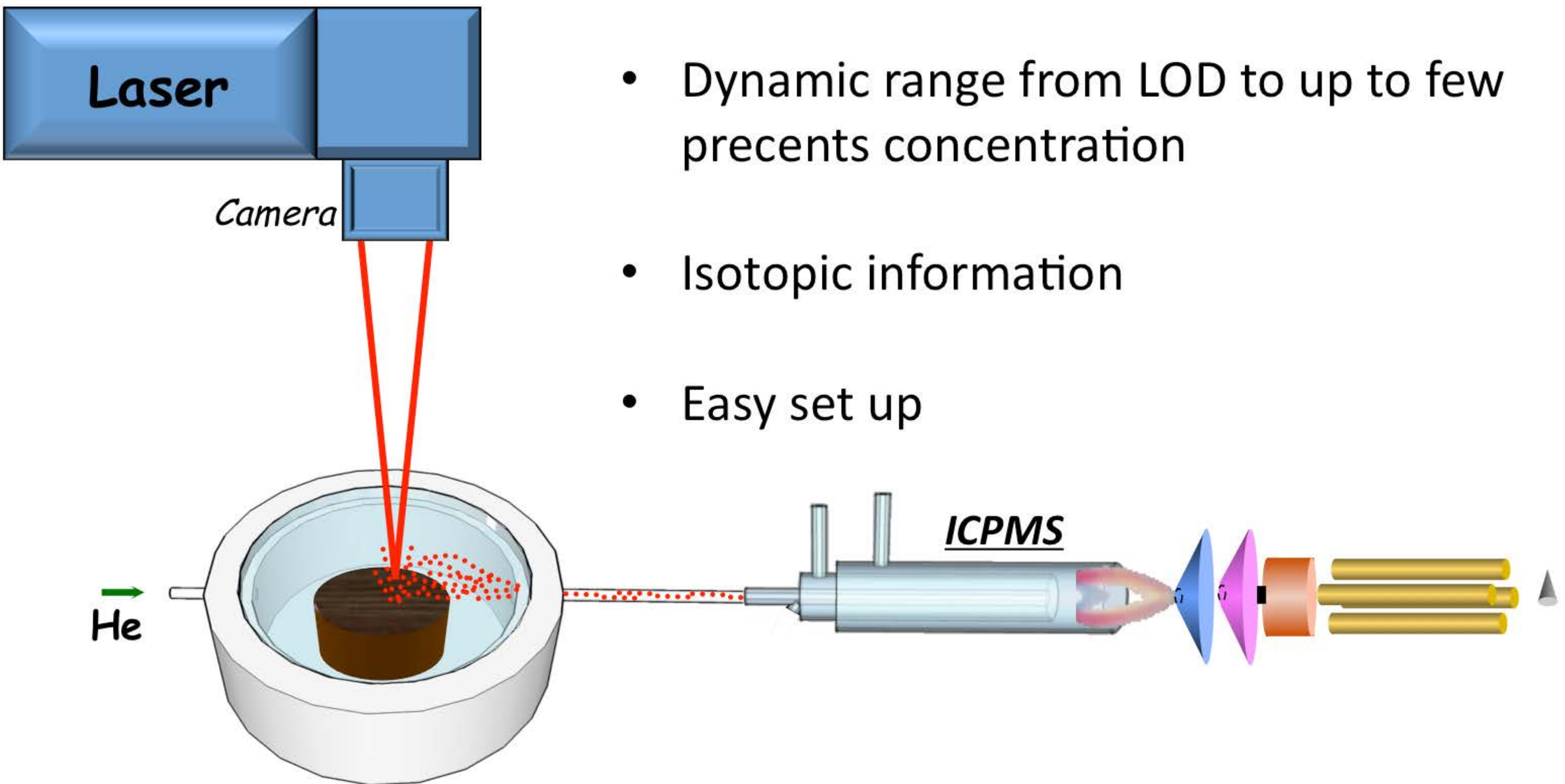
Combined with a resonator (2 mirrors and an active medium), the laser light can be accumulated in the axis of the resonator.

The active medium might be a crystal, a gas, or a liquid.

When the accumulated energy is high enough, and before destroying the resonator the end mirror is made transparent to the light (using a Pockels cell)

Laser ablation-ICPMS

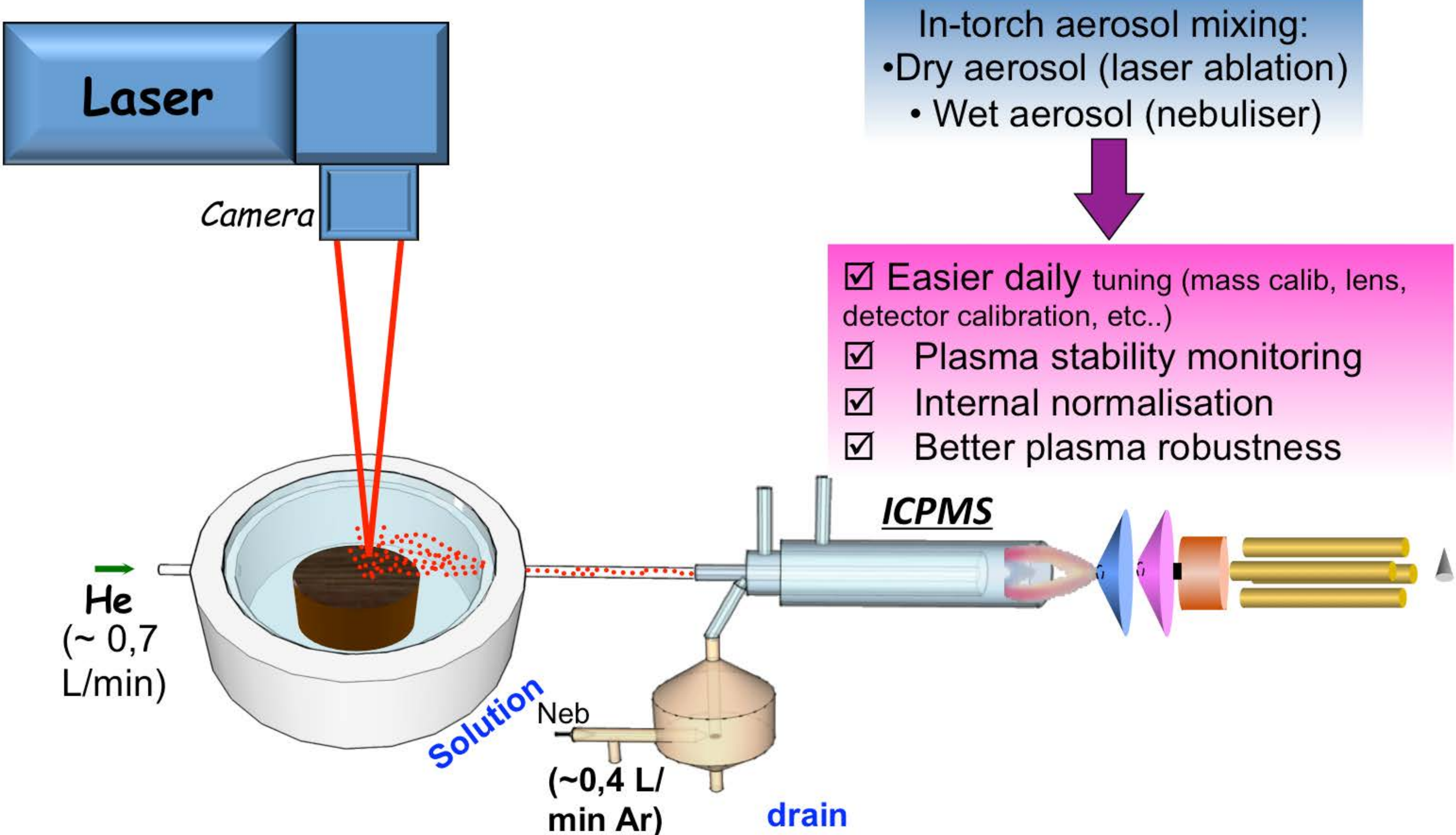
- Limits of Detection from sub ppb to ppb range
- Dynamic range from LOD to up to few percent concentration
- Isotopic information
- Easy set up



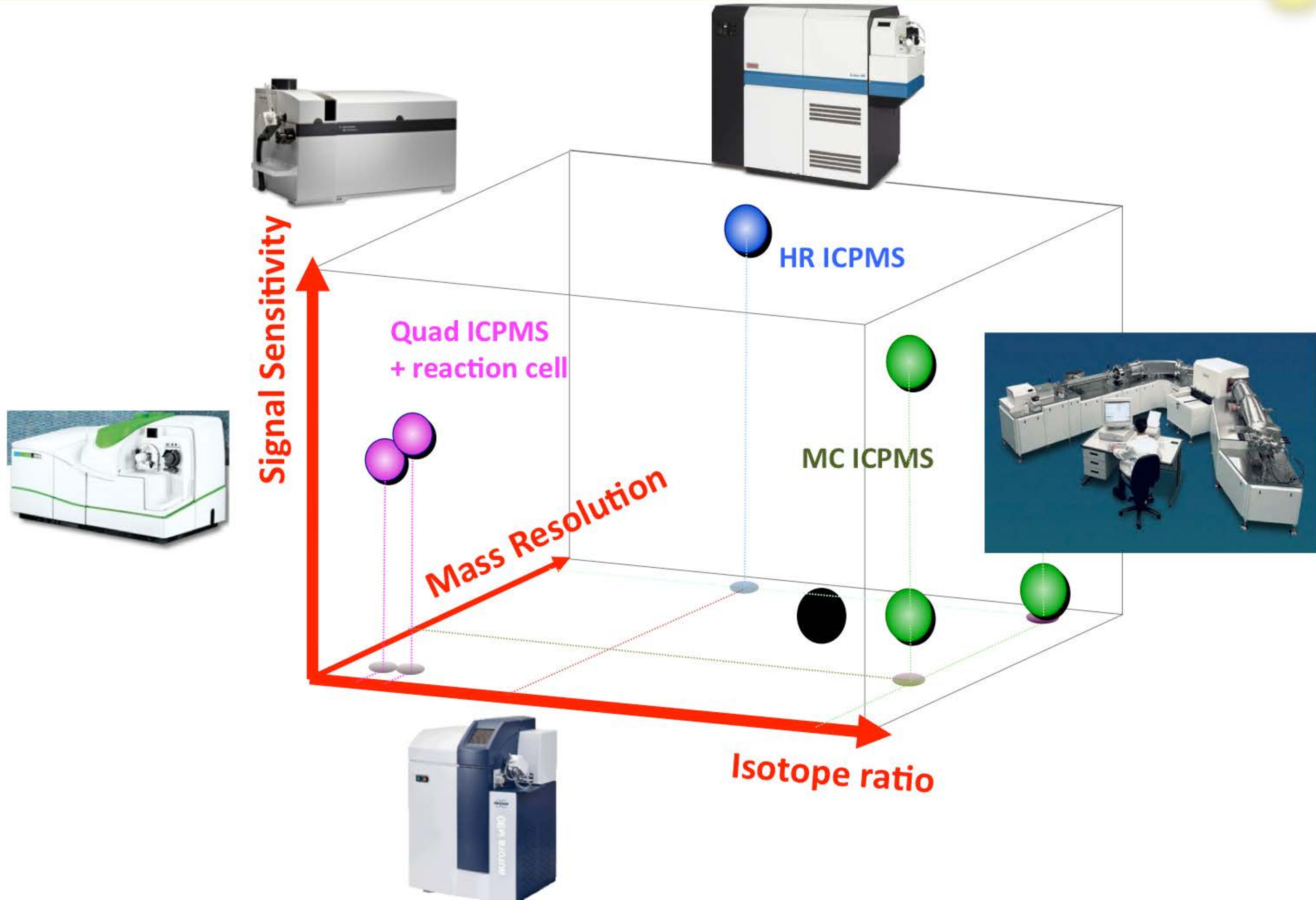
Laser ablation-ICPMS set up

Wet versus Dry plasma:

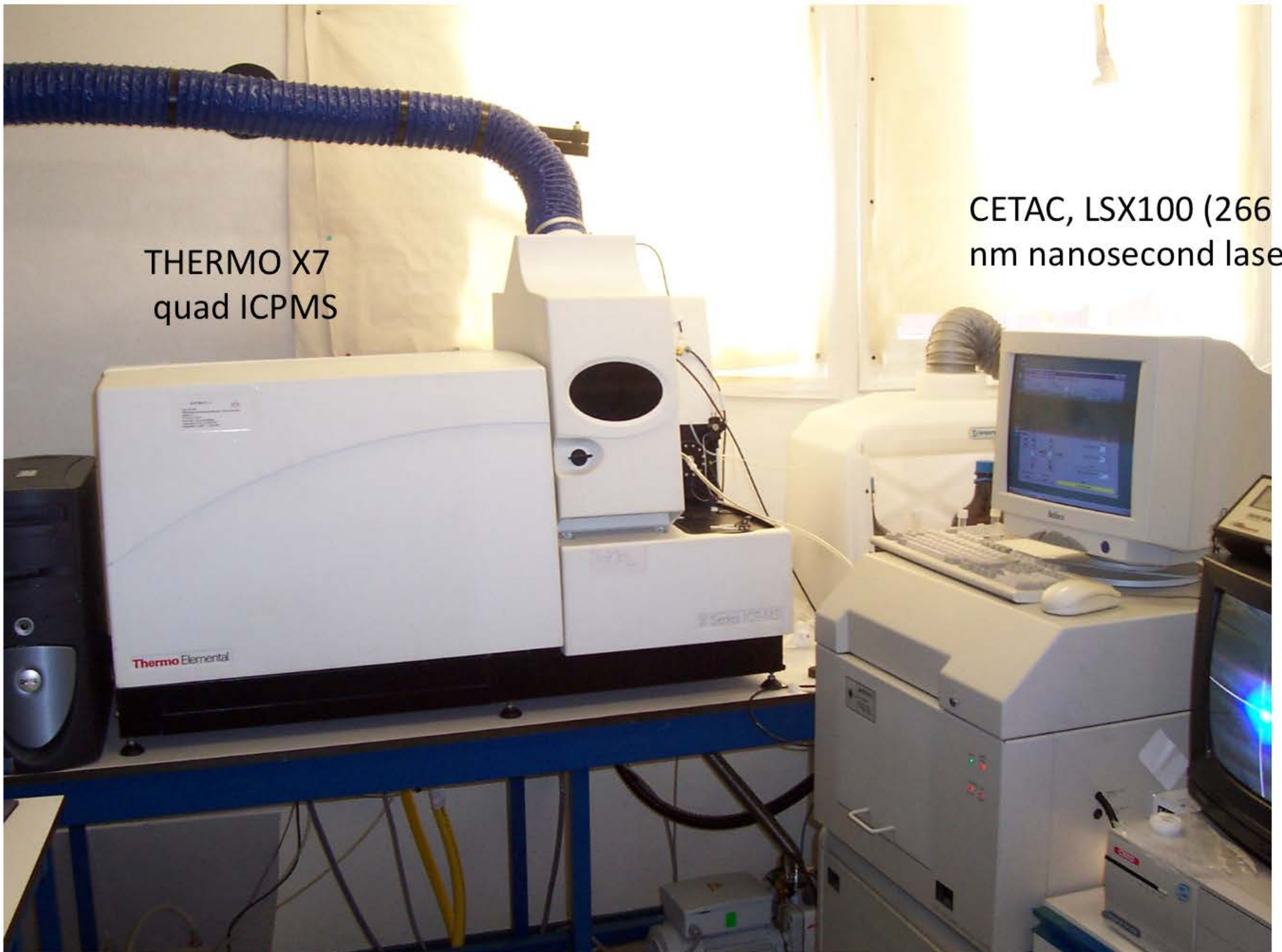
In some conditions (i.e when the oxydes level is not a problem), the LA/ICPMS coupling can be used in wet plasma configuration with some advantages:



The ICPMS family...



Laser ablation-ICPMS set up



Various laser types...

Type	Longueur d'onde	Energie/impulsion	Longueur d'une impulsion	Diamètre faisceau primaire	Fréquence de tir
	nm	J	ns	mm	Hz
CO2	10600	0.3	100-1000	2-5	100-1000
Rubis	694	1	10-100	10-25	0.1
Nd :YAG fondamental	1064	0.5	~ 4 - 100	5-10	1-20
Nd :YAG harmonique 4	266	0.003-0.009	"	"	"
Nd :YAG harmonique 5	213	> 0.001	"	"	"
KrF	248	0.002	10-100	20x10	1-100
ArF	193	0.2	10-100	20x10	1-100
Femtoseconde	196-265-8 00-257 – 515- 1030	0.0005	0.0001 – 0.0004	4	1-10000

- UV nanosecond lasers (266, 213 and 193 nm) are the most used in analytical chemistry.
- Femtosecond lasers, more expensive, though having better performance are less used.

Some definitions

Gaussian shape: the beam energy distribution of a laser is naturally gaussian: when drilling a hole, the resulting crater shape is gaussian (or conical in a first approximation)



Flat Top : some optical arrangements allow homogenising the energy profile : the resulting crater is now a cylinder.

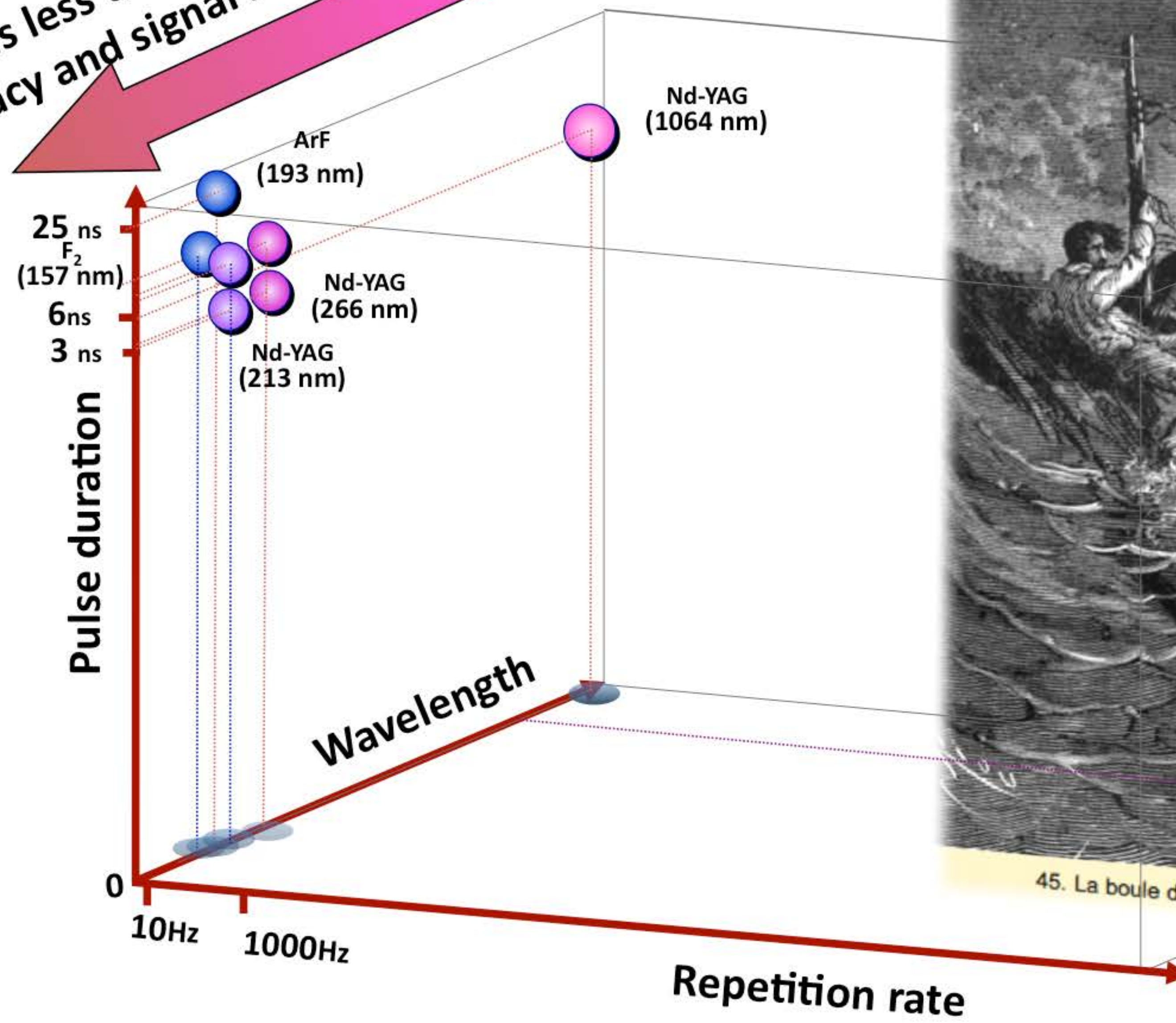


Fluence (J/cm^2) : energy per pulse/ laser beam size at the surface of the sample.

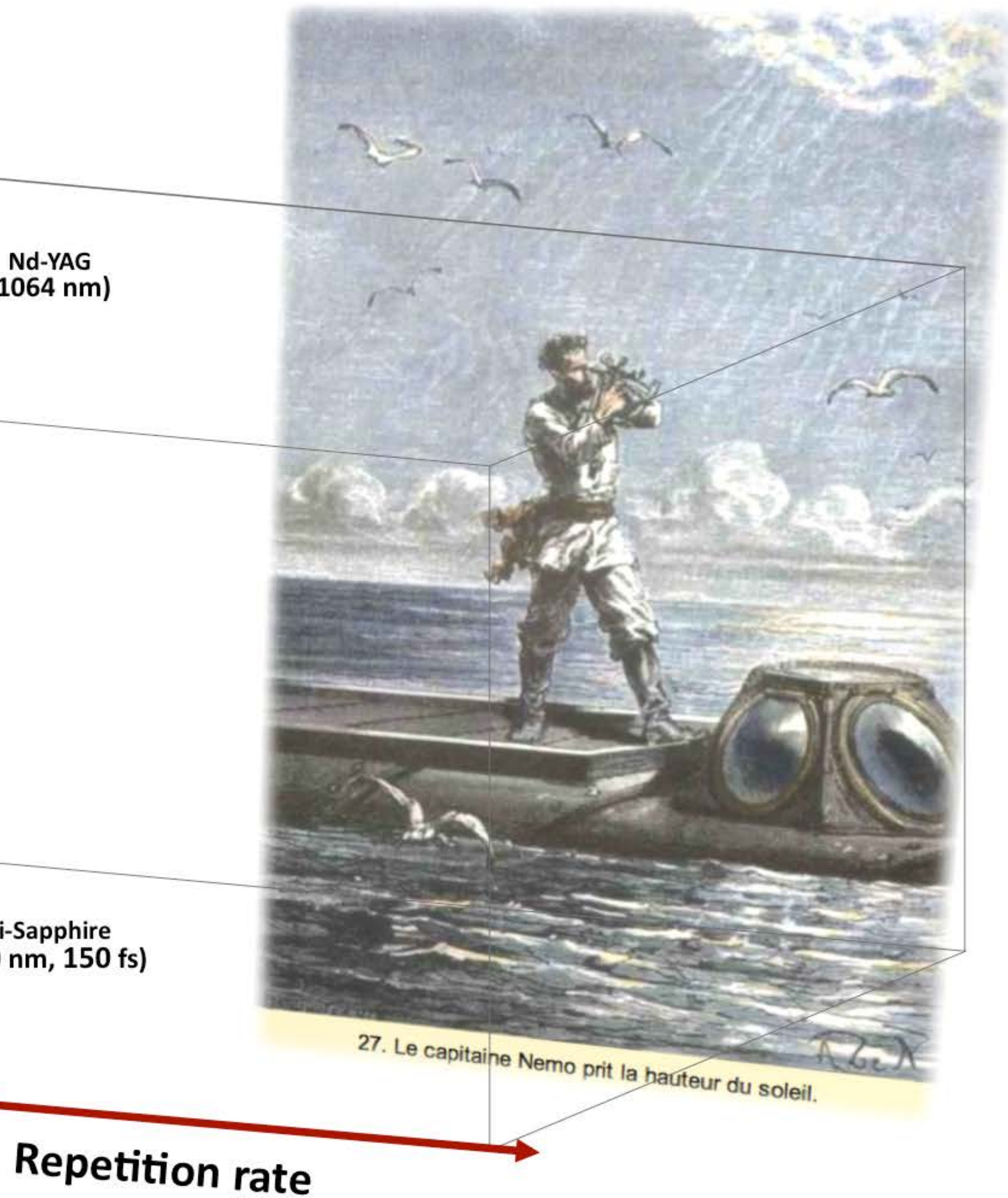
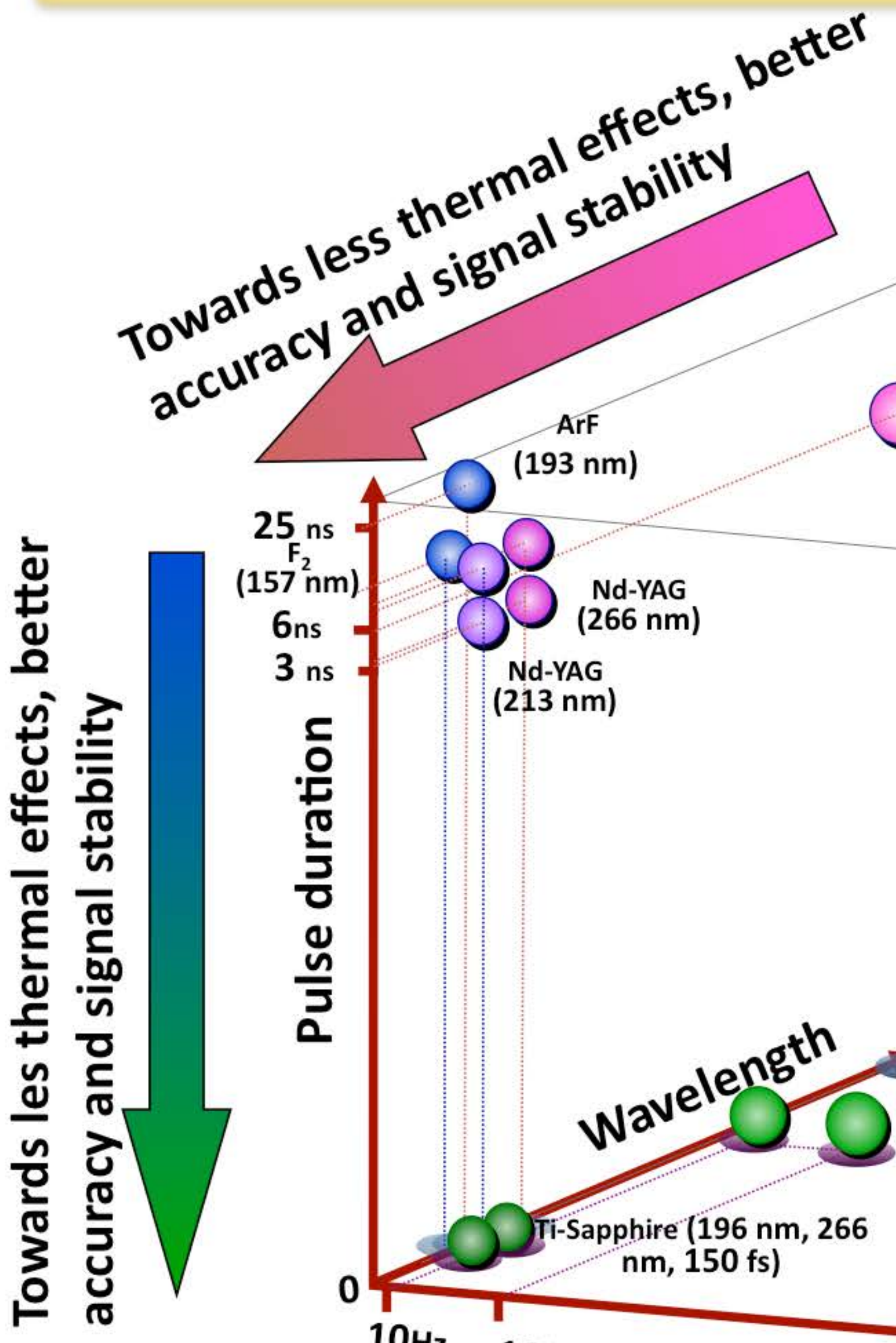
Power density (W/cm^2) : Fluence/pulse duration

LA/ICPMS since 1985 in 3D...

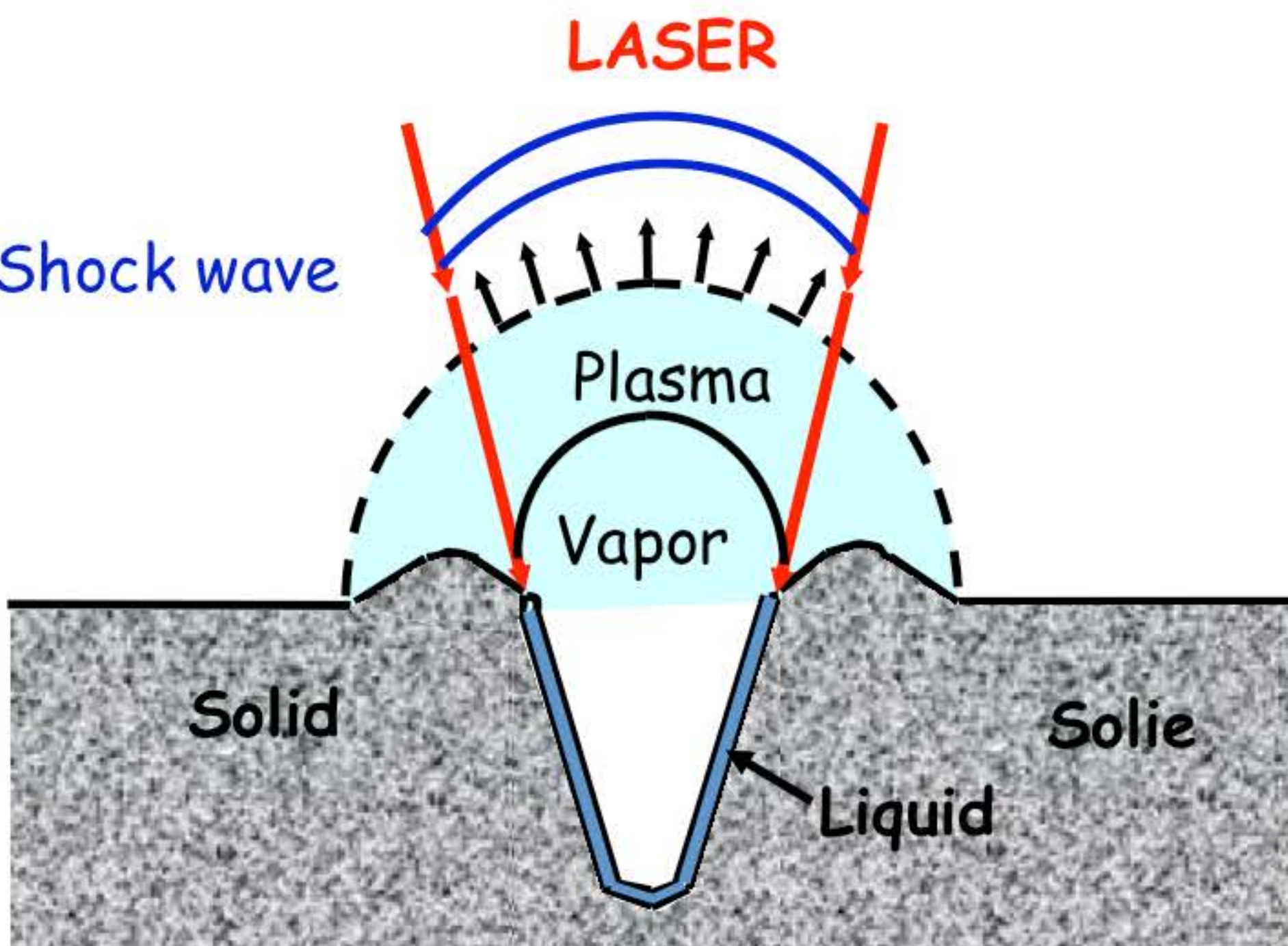
Towards less thermal effects, better accuracy and signal stability



Advances in LA/ICPMS since 2003 in 3D



Ablation processes

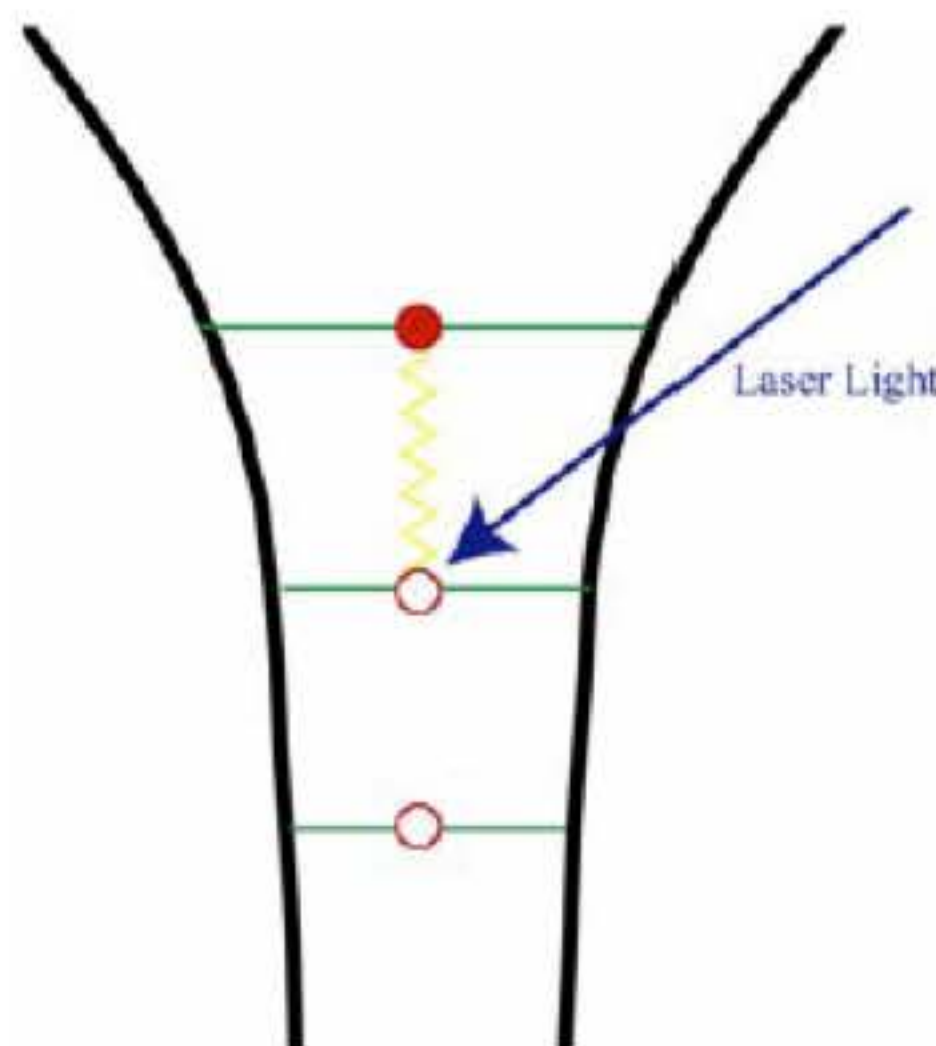


3 main processes take place during the ablation:

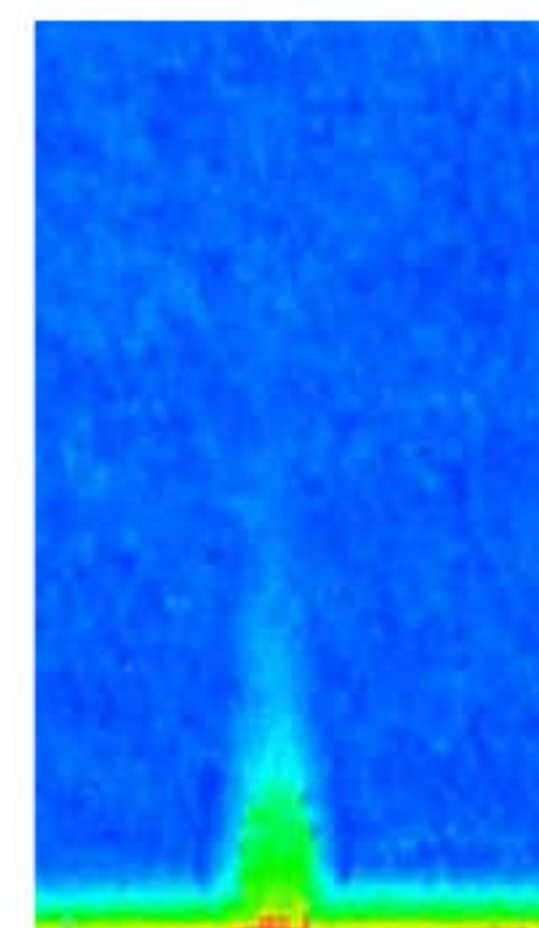
- **1st step**: the laser energy is absorbed, converted into heat. when the heat is not dissipated then melting and sublimation can occur. This occurs at low power density ($<10^6\text{W/cm}^2$). In contrast, when the power density is high enough ($>10^9\text{W/cm}^2$), ie high energy or/and short pulse duration, "spontaneous" sublimation occurs that will generate **explosion** and ejection of particles by fragmentation.
- **2^d step**: free electron occurring in the vapor phase and those formed by thermal ionisation lead to the formation of a micro plasma at the surface of the sample.
- **3rd step**: the plasma expands and generate a shock wave.

laser ablation time scale

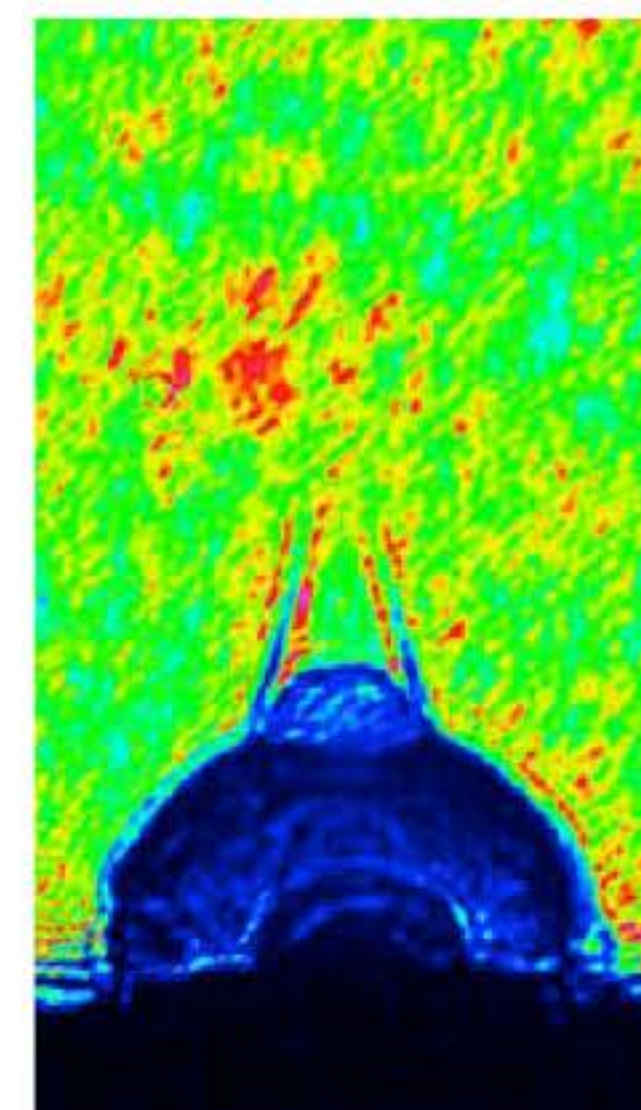
Electrons absorb
photons
Femtoseconds



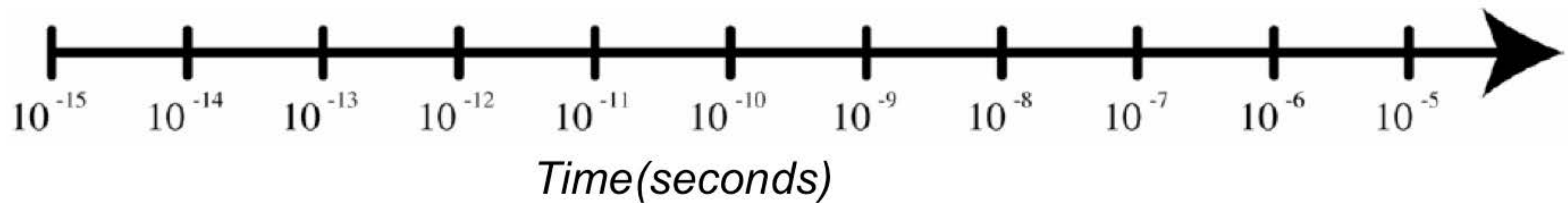
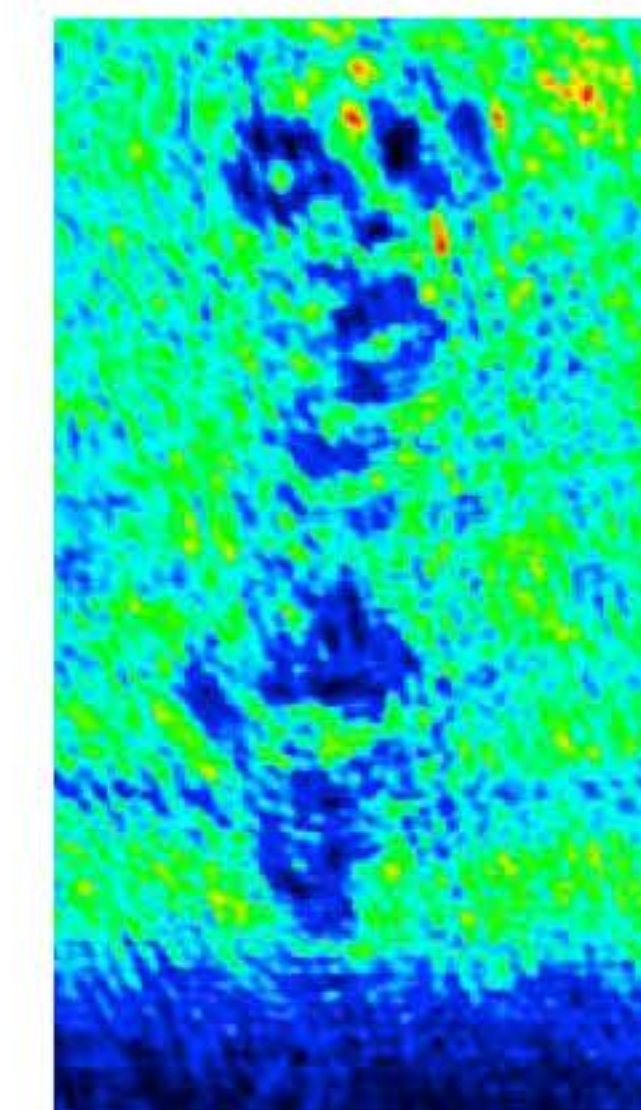
Electron emission
from the surface
Picoseconds



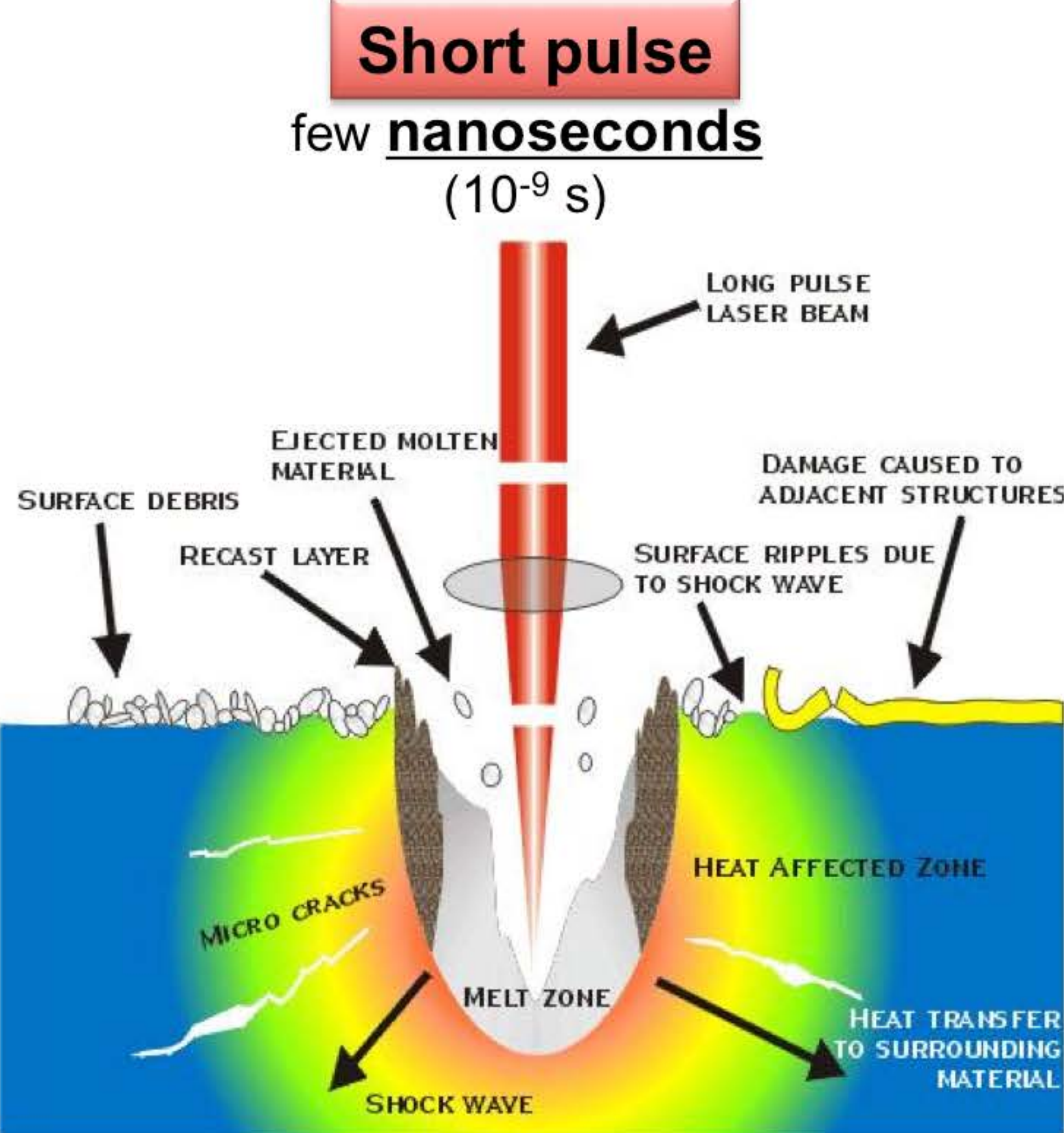
Plasma formation
Nanoseconds



Particles ejection
Microseconds



Short pulse versus Ultra Short pulse



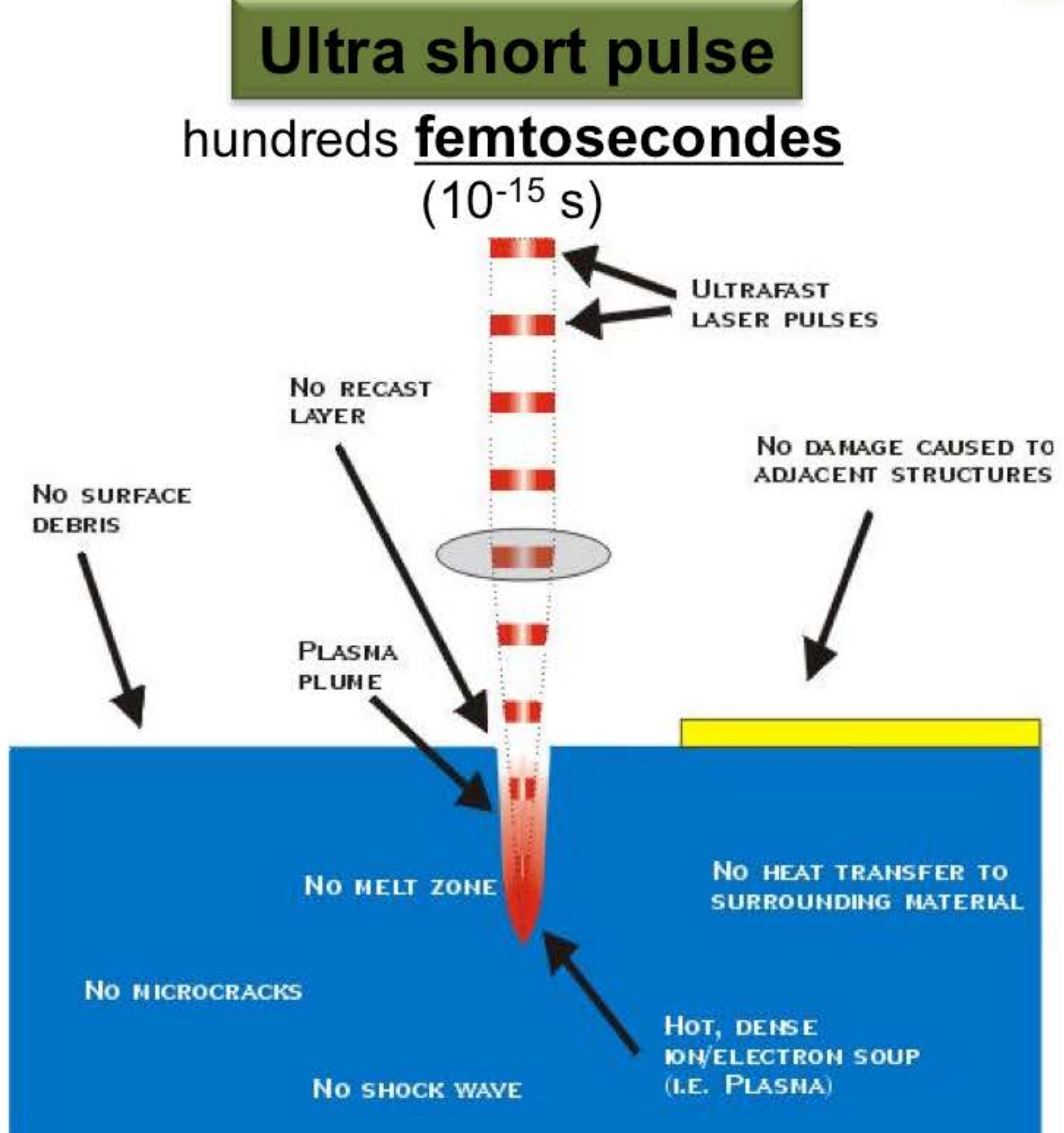
©1999 Clark-MXR, Inc.

Thermal effects

⇒ accuracy



=> in-depth resolution



©1999 Clark-MXR, Inc.

Very limited thermal effects

⇒ better accuracy (due to small particles)



⇒ better in-depth resolution



Ablation processes

At low power density (10^6 W/cm^2), the vaporisation is the dominant process and the ablated material is made of vapor, aerosol, melted particles. These conditions should be avoided as much as possible (see below).

Beyond 10^9 W/cm^2 , the process becomes explosive and thermal effects are reduced.

In addition, the micro plasma formation can interact with the sample and generate additional melting and vaporisation.

The interaction between the laser light and the sample is a dynamic process governed by the laser properties AND the sample characteristics :

LASER

Laser source Wavelength, energy, pulse duration, repetition rate
laser beam Size, focus

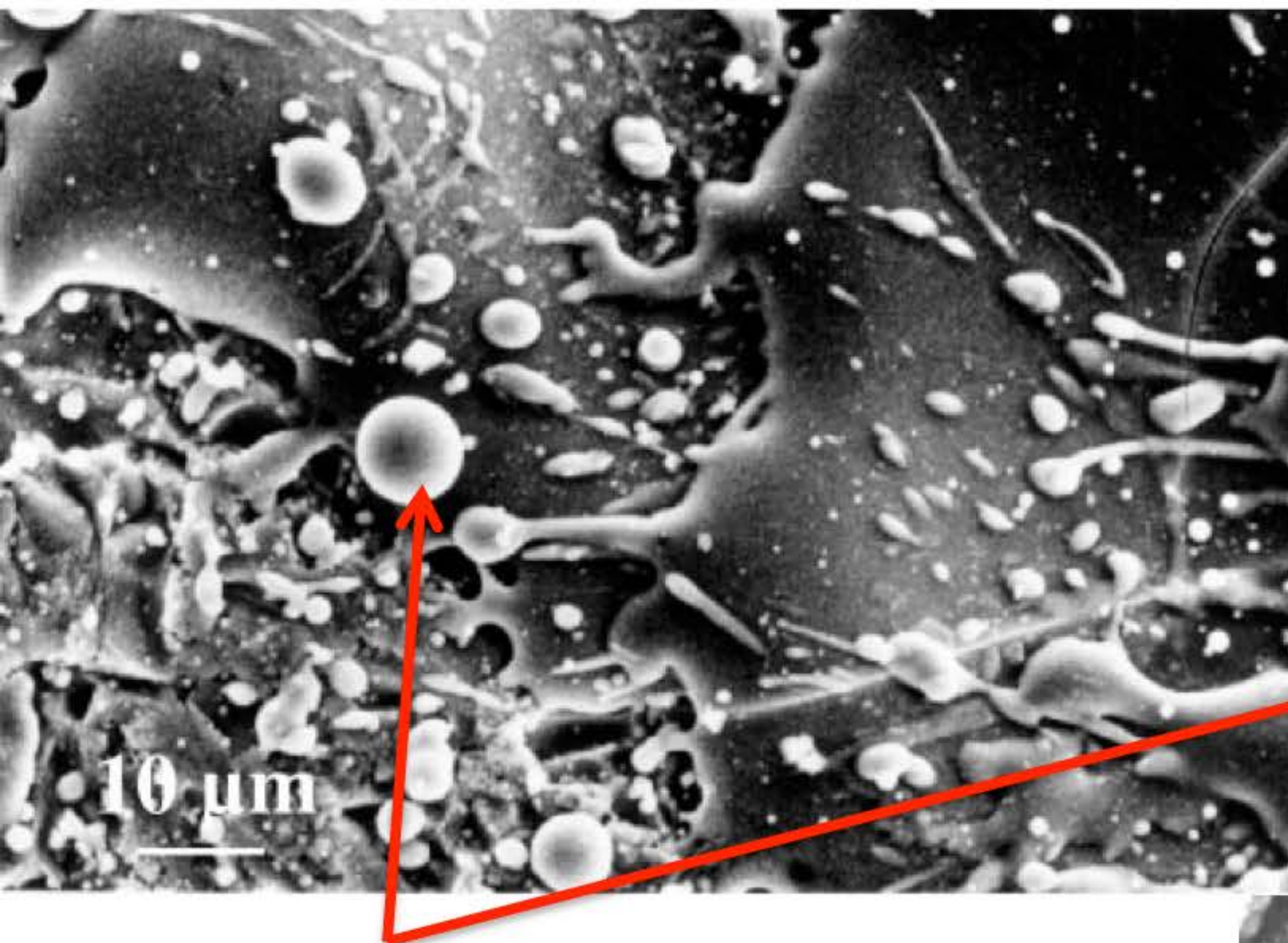
SAMPLE

Optical absorption, reflectance
Thermal conductivity, specific heat of vaporisation
Mechanic

Typical craters

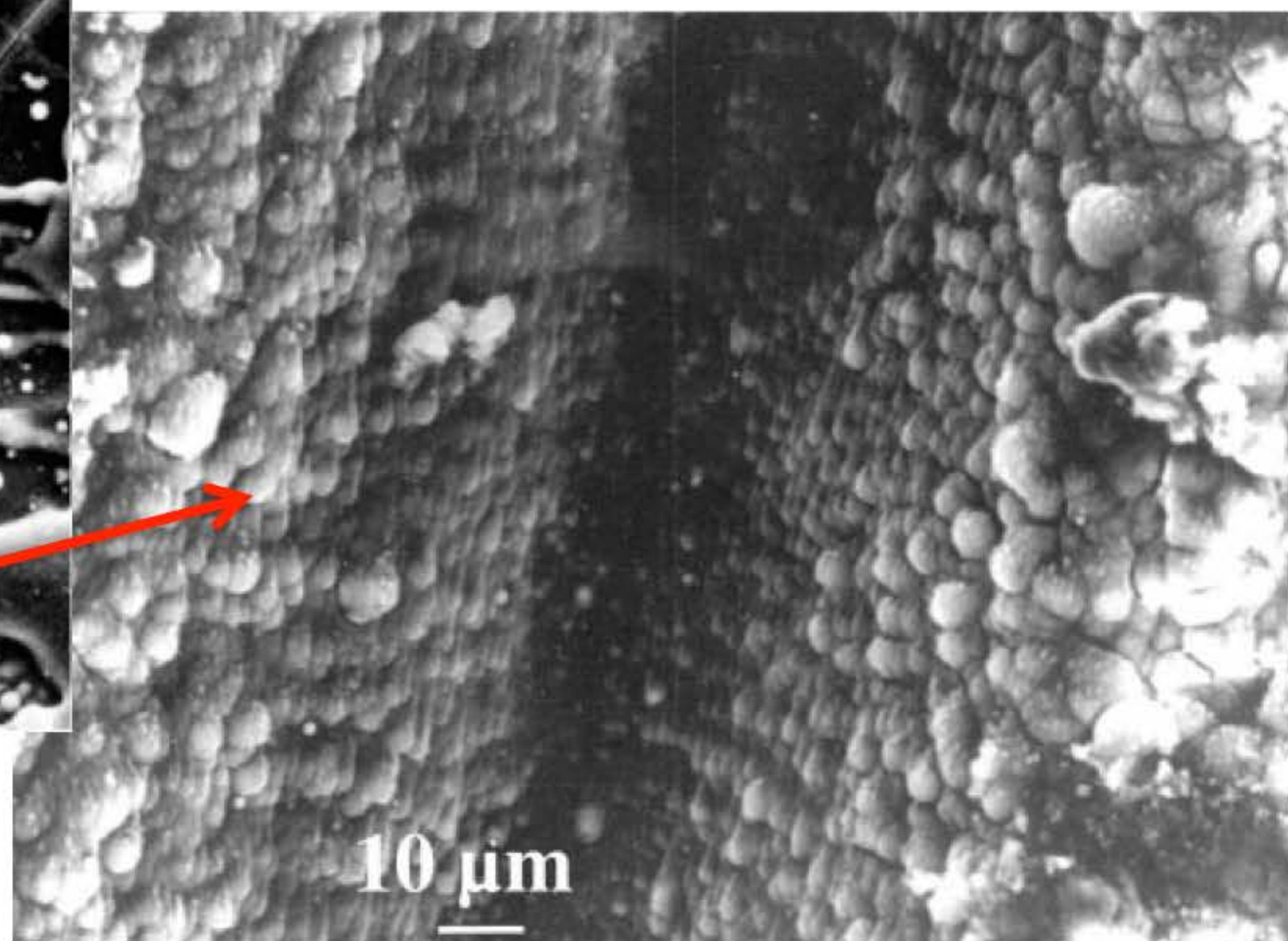
Glass samples

Nanosecond IR (1064 nm) laser:
evidence of high thermal effects (melting)



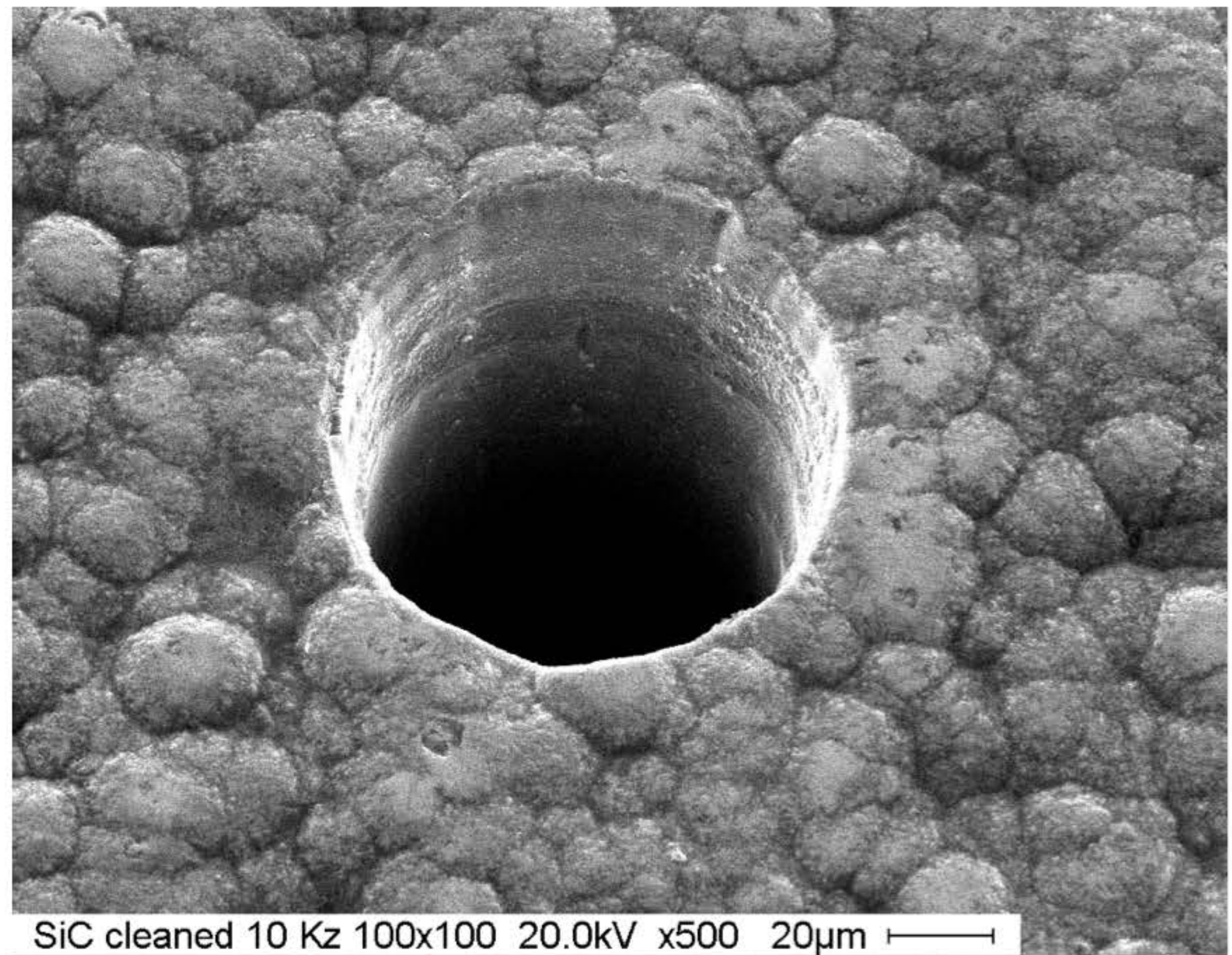
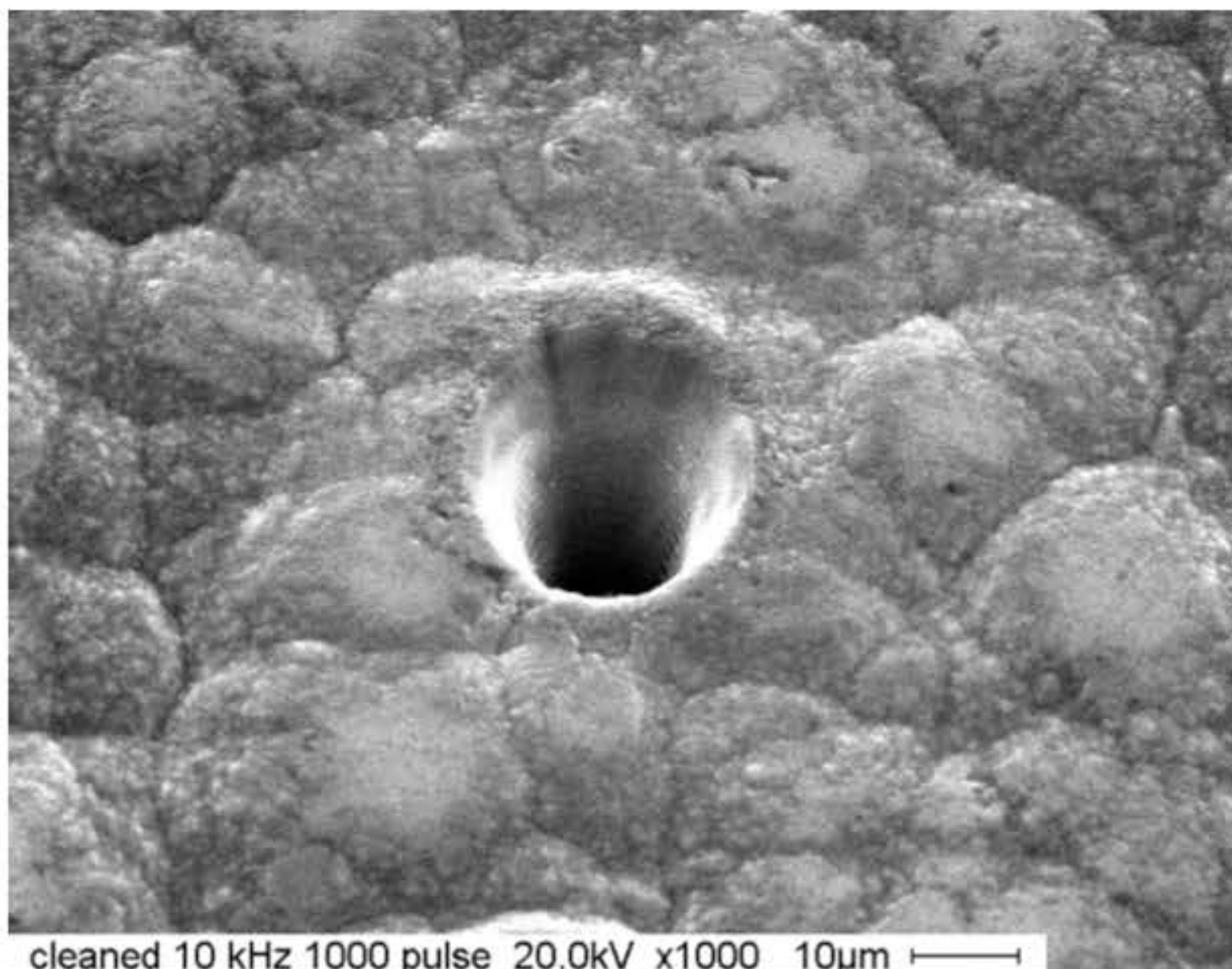
The chemical composition of the spheres
might differ from the initial material
composition...

Nanosecond UV (266 nm) laser. reduced
thermal effects, but still there...



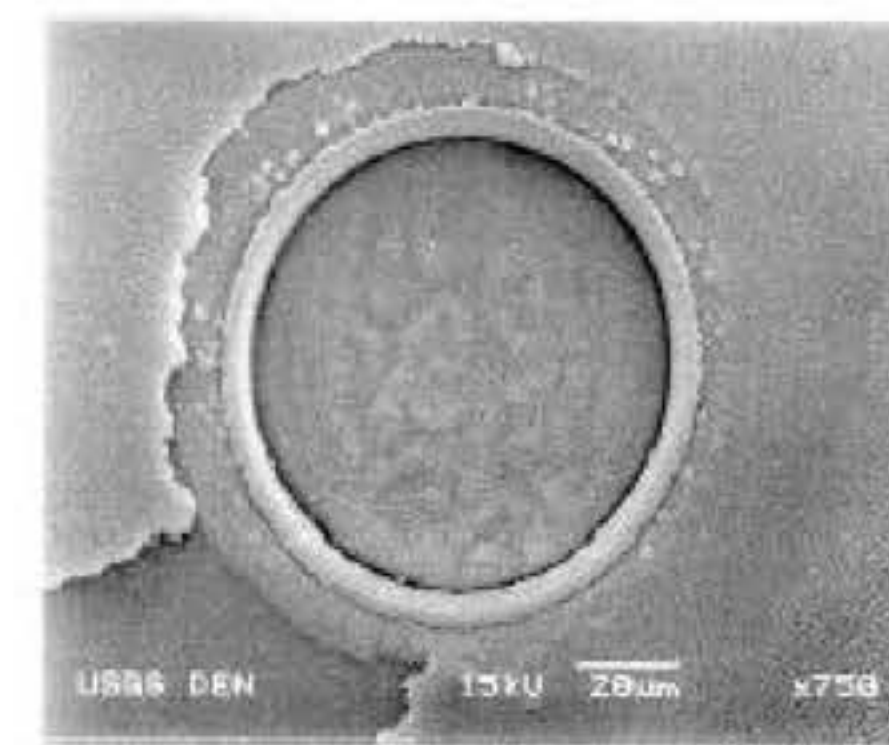
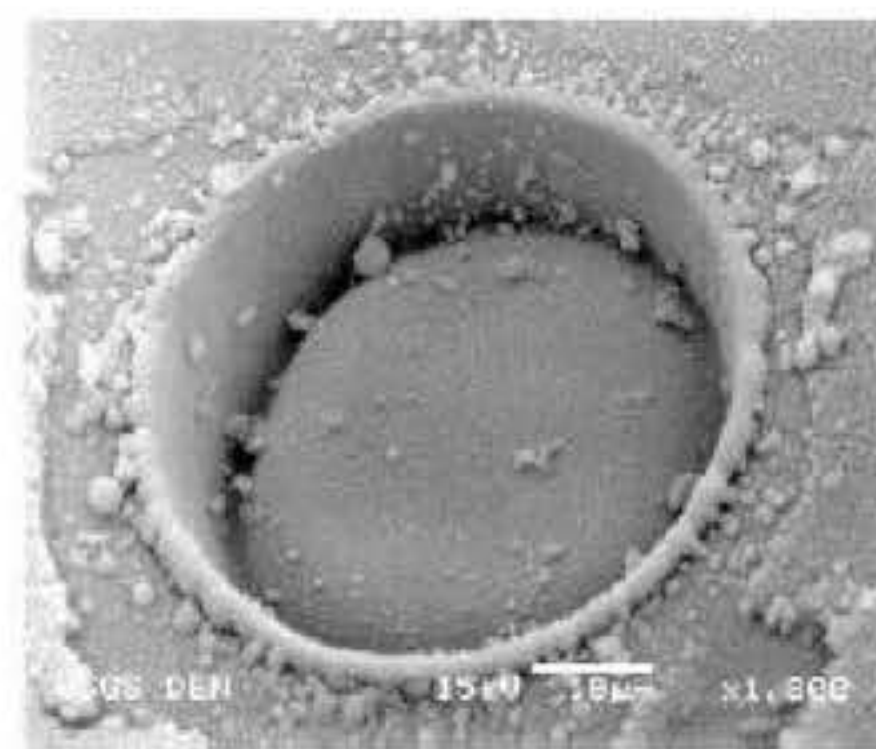
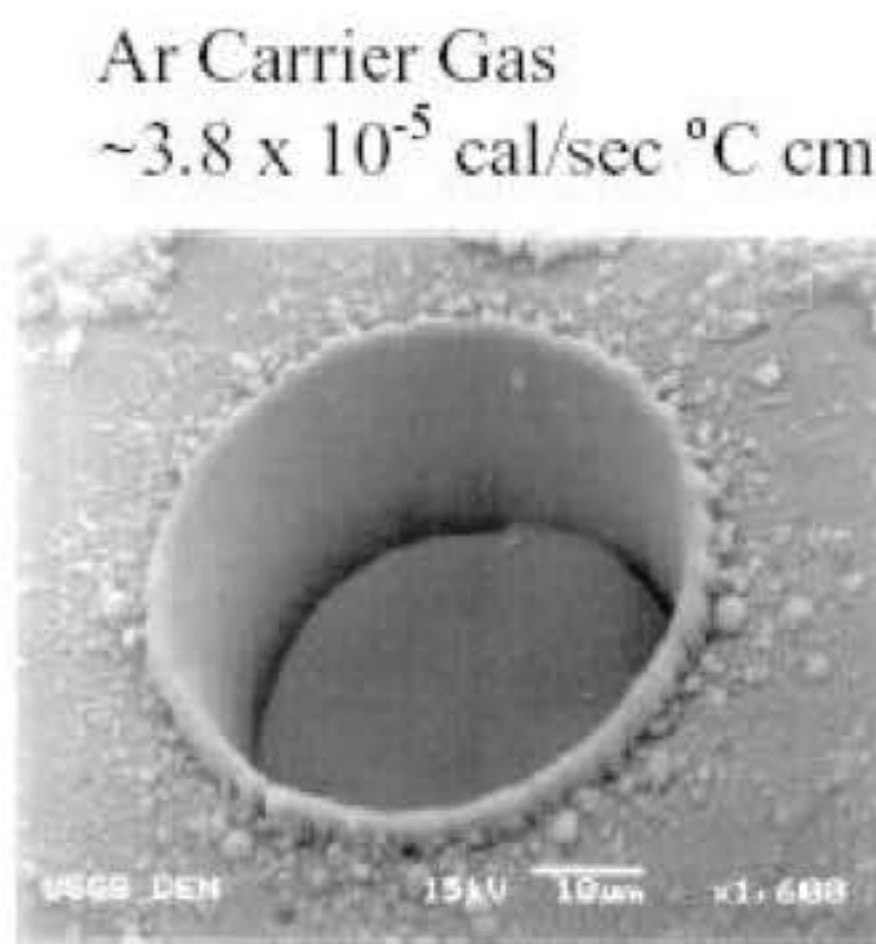
Typical craters

**SiC ablated with femtosecond IR
(1030 nm).**
No evidence of significant thermal
effects



Carrier gas

Carrier gas influence: the analytical performances are better when Ar is replaced by He : => better cooling effect (then smaller particles), and particles are more easily extracted from the bottom of the crater. The particles are however better transported in an Ar stream, that's why Ar is added post ablation cell. The sensitivity improvement is about 2-3 when using He in the ablation cell.



In addition, the spectral background being reduced when adding He in the ICPMS, LOD are finally improved by a factor 10 (this phenomenon is more pronounced at 193 nm compared to 266 nm).

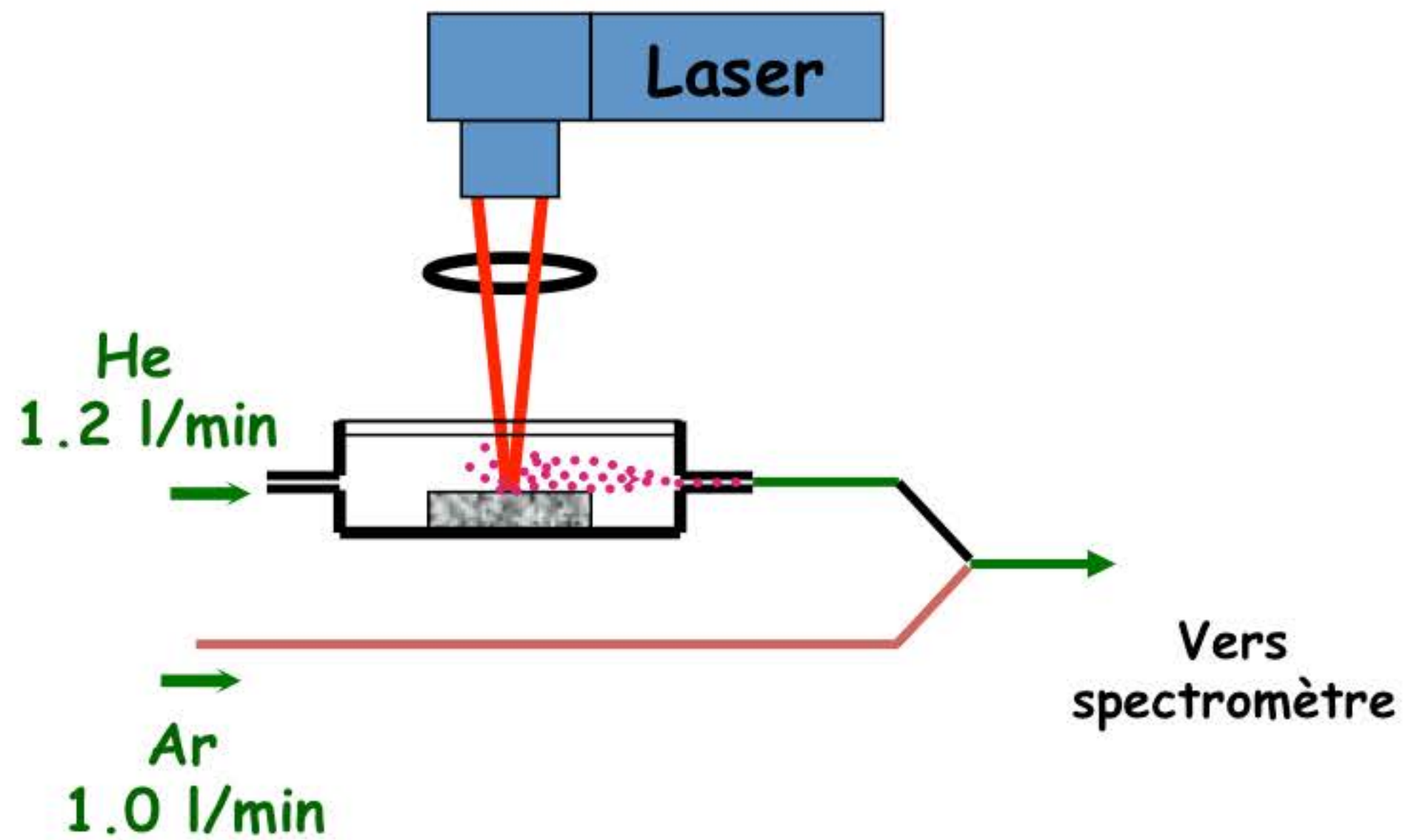


Figure 7: Gas Effects: Crater Characteristics in NIST 612 Glass (images courtesy of USGS Denver CO, USA)

Cetac LSX 200 – 266 nm

D. Gunther et al, JAAS, 1999, 14, 1363-1368

Sample preparation

LA/ICPMS requires very limited sample preparation. However flat sample surface generally facilitates laser focussing (better visualisation).



Powders (eg: clays, sands, aerosols, sediments, etc) must be fixed:

- ⇒ compaction (binder addition (ex : paraffin), drying and palletisation with high pressure hydraulic press).
- ⇒ Lithium borate fusion ($\text{Li}_2\text{B}_4\text{O}_7$).

Small samples must be embedded into a resin

Binders and Li borate might induce contamination.

It is well indicated to pre-clean the sample surface by ablating the desired zone with low energy (close to the ablation threshold) laser conditions; only few shots are required.

Quantification



The reason why you will need, sometimes, to spend a lot of money for high performance laser systems (from 60 k€ to >400 k€...)

Quantification

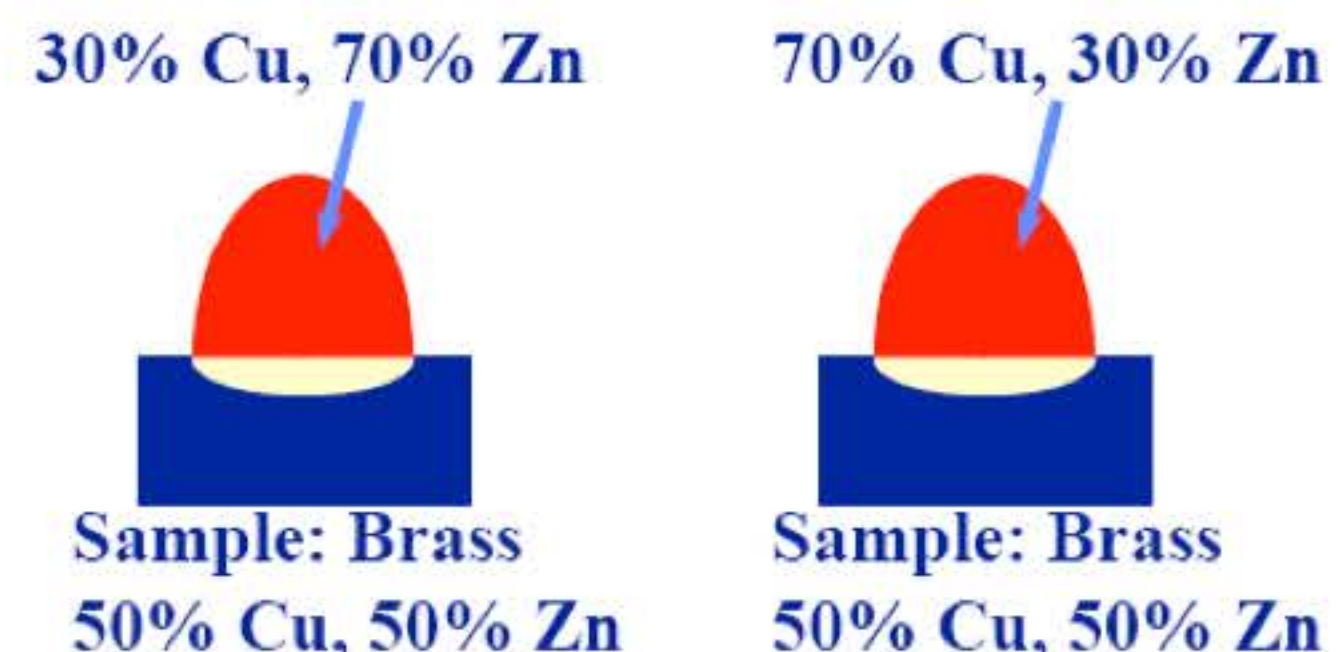
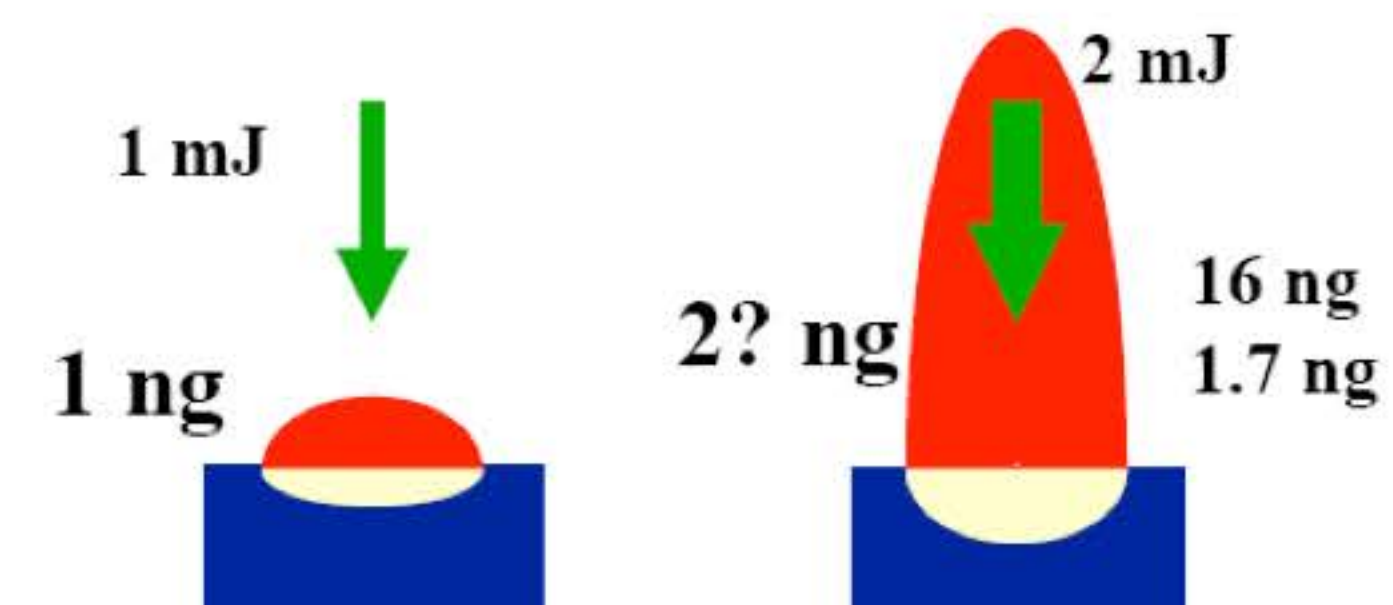
The quantification is the Achilles heel of laser ablation. Quantification is sometimes challenging because the ablation processes depends on the sample properties.

The ablation yield varies for different sample matrices (e.g. the ablation rate is not the same for copper than for glass or polymers...)

The ablated mass depends on the laser energy but not linearly : fluence (\Rightarrow focalisation), pulse duration, etc..

The detected elemental composition of the ablated mass might depends on the laser energy (elemental fractionation)

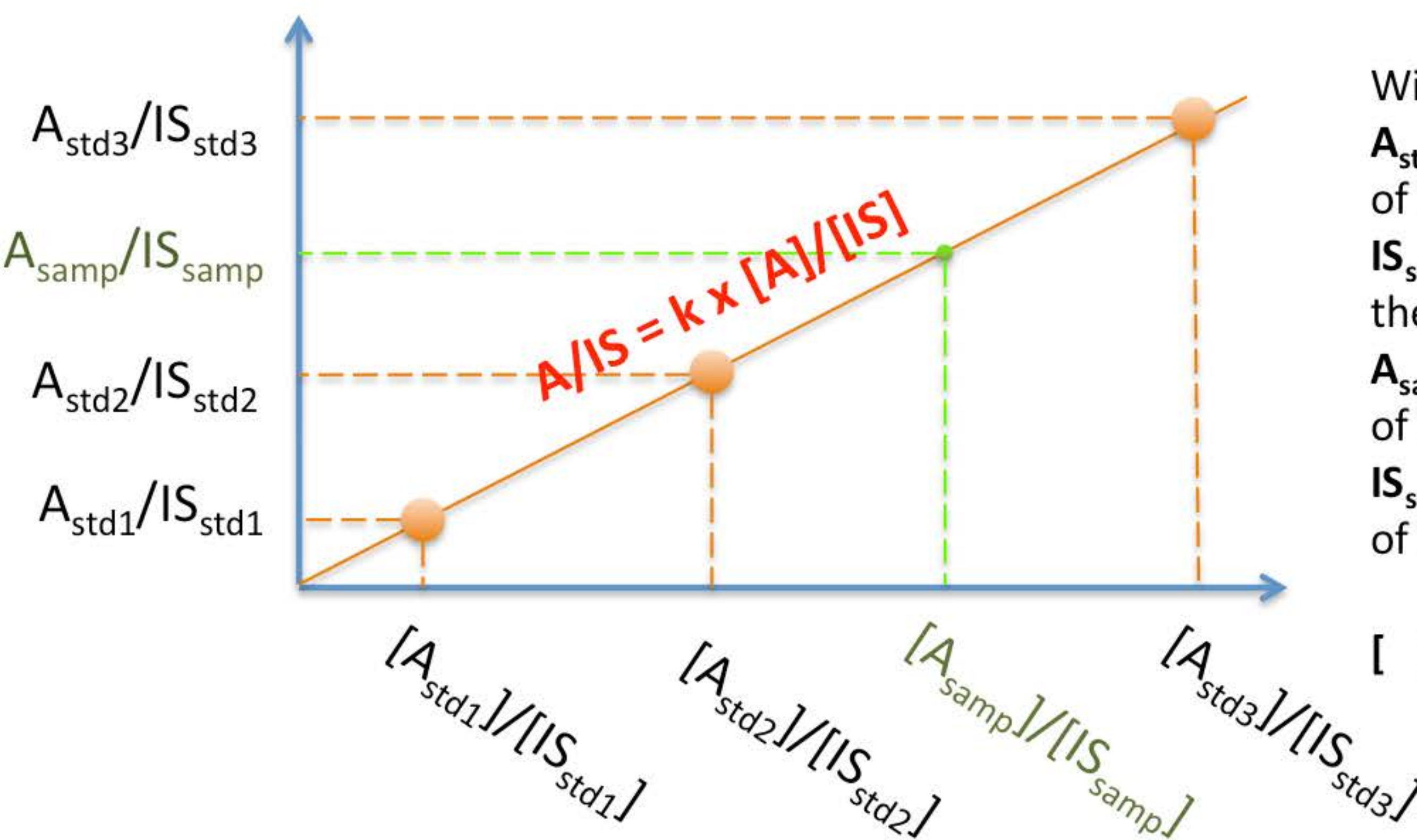
We will see later how to identify the elemental fractionation, how to calculate it and what are the physical processes behind it... And eventually how to counterbalance it or at least limit it...



Quantification: External calibration with internal standard

The quantification of a sample is generally carried out by external calibration using standards of similar matrix. For synthetic materials (glass, etc..), numerous standards are commercially available.

Bias resulting from laser ablation processes (laser energy drift, focussing problems, sample transport, etc...) and the ICPMS can be corrected using an Internal Standard (a given element that we know the concentration in the standard AND the sample). The IS must be homogenously distributed (generally part of the matrix) as it is used for normalisation. The IS in the sample can be obtained by XRF measurement for instance.



With

$A_{\text{std}i}$: NET (blank corrected) signal intensity of the Analyte for standard i

$IS_{\text{std}i}$: NET (blank corrected) signal intensity of the Internal Standard for the standard i

A_{samp} : NET (blank corrected) signal intensity of the Analyte for the sample

$IS_{\text{std}i}$: NET (blank corrected) signal intensity of the Internal Standard for the sample

[] Concentration



Quantification: External calibration with internal standard

Then, knowing the concentration of IS in the sample, the concentration of the analyte in the sample is expressed as follow :

$$[A]_{\text{sample}} = \frac{\frac{A_{\text{sample}}}{IS_{\text{sample}}} \times [IS]_{\text{sample}}}{k}$$

This equation WORKS ONLY IF the internal standard behaves similarly as the analyte in terms of laser/material interaction AND particle atomisation in the ICPMS.

For natural samples, it is not always true due to the wide range of matrices and the lack of Certified Reference Materials (CRM). This makes the quantification more challenging...

Quantification: Evidence of Elemental Fractionation

Ideally, when ablating a homogenous sample, all the elements should have the same signal profile. In fig A, a crater was drilled in CRM NIST610 (glass). It is clear that Ca and U exhibit quite similar profiles (the progressive signal extinction is due to laser fluence drop as the crater becomes deeper. One can also imagine that particles are less efficiently removed from the bottom of the crater). However, Pb profile departs from Ca and U which indicates that all the element don't behave similarly. This calls into question the use of an internal standard to correct for ablation processes drift, especially when the sample matrix differs from the standards one... The quantification is directly affected as illustrated in figB, even after internal normalisation (here Ca) as the calibration slopes differ from glass to CaCO_3 ...

THIS IS THE ELEMENTAL FRACTIONATION....

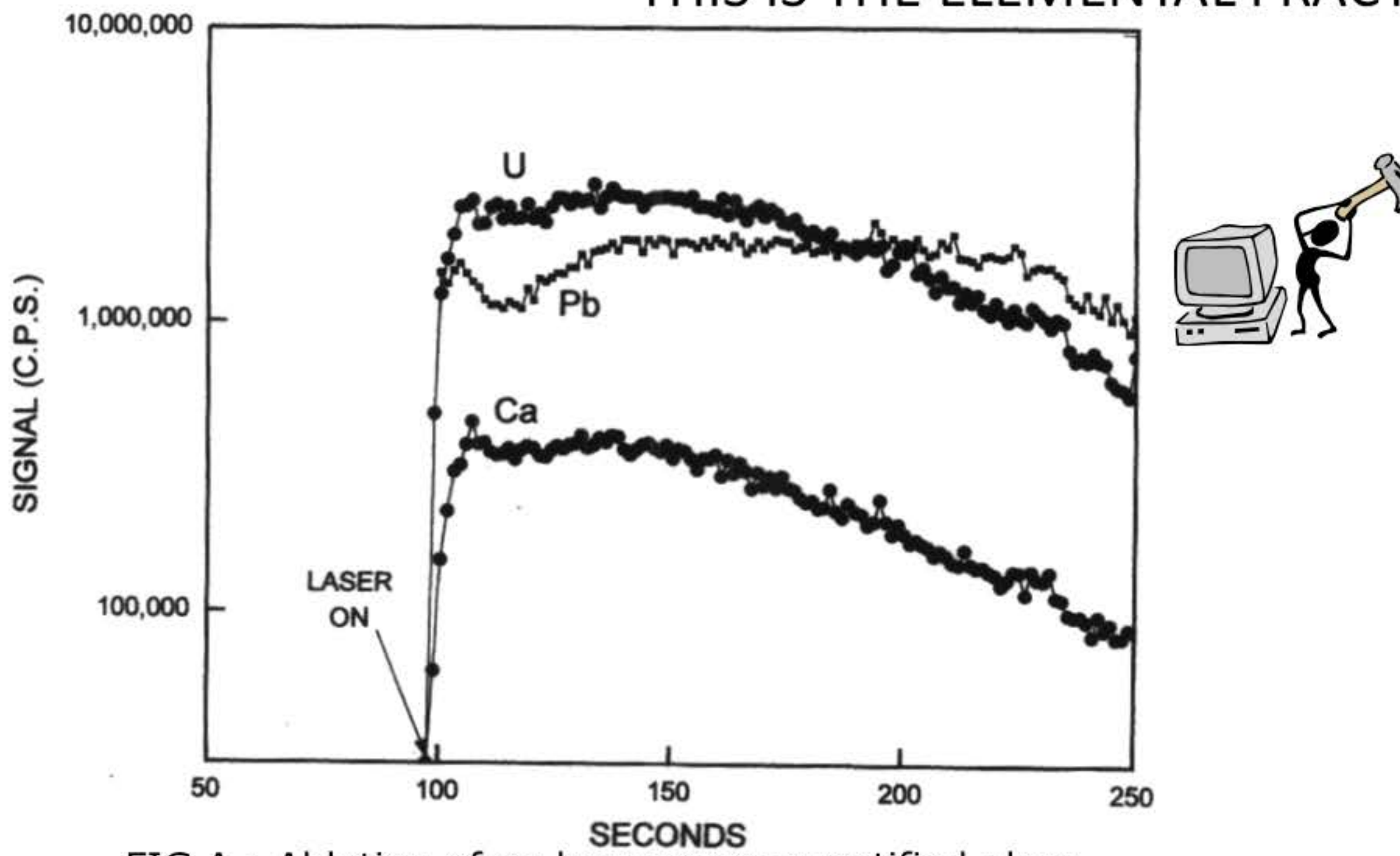


FIG A : Ablation of an homogenous certified glass sample (NIST 610). ns 266 nm laser

D. Gunther et al, Spectr. Chim. Acta, 1999, 54, 381-409

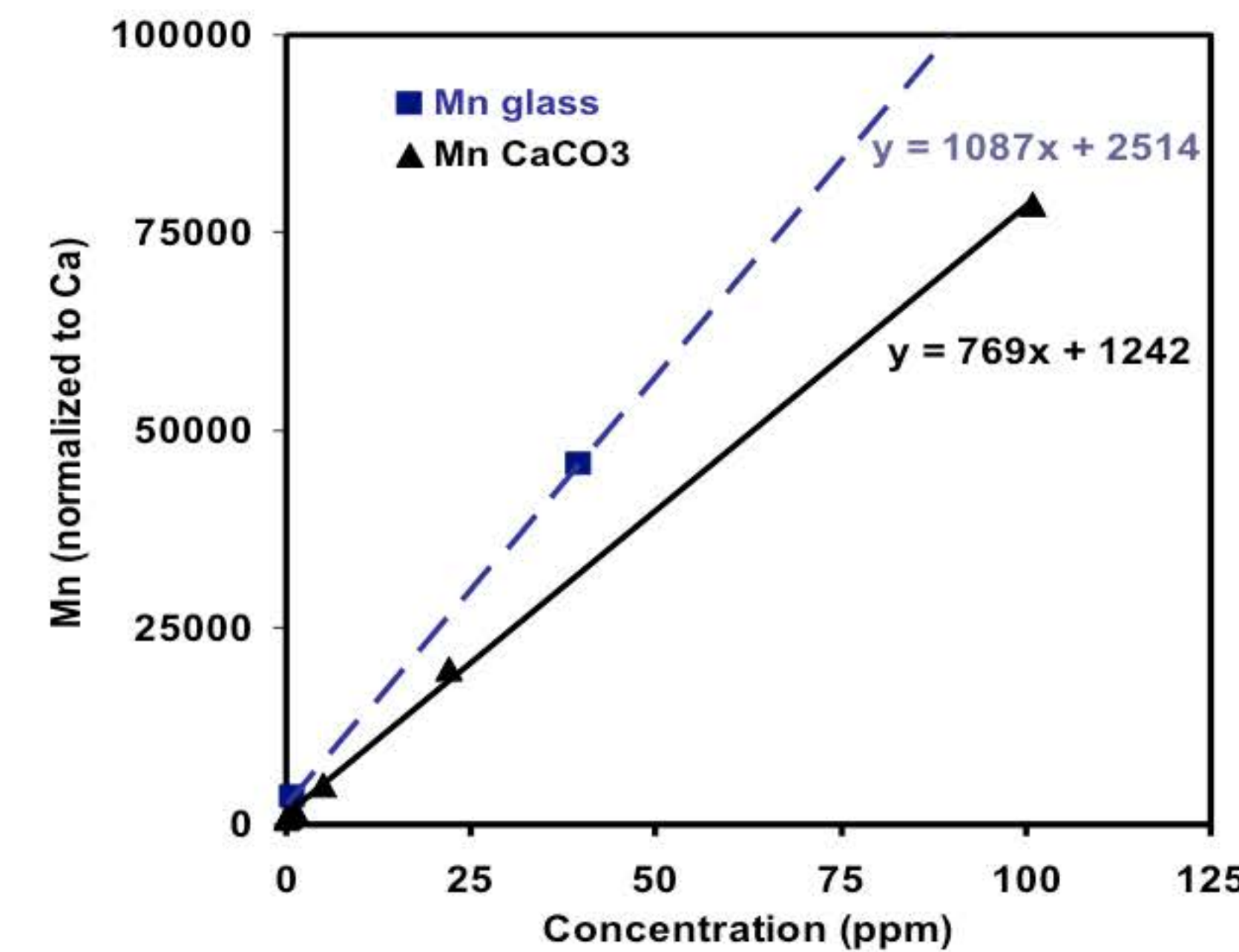


Fig B Calibration with certified glasses and CaCO_3 standards. ns 266 nm laser

25

A. Barats et al, PhD thesis - 2006

Quantification: Origin of the elemental fractionation

Two main processes can explain the elemental fractionation

1/ Selective evaporation : It appears as a result of the laser/material interaction where the vapour phase is enriched with some elements with low sublimation enthalpy : this is then a non stoichiometric sampling where the aerosol composition (particles + vapor) does not reflects the sample composition...
It is governed by the ablation conditions (temperature, the time duration of the interaction, induced plasma, the surface of interaction, etc...) and the physical properties of the sample. Melting and melted material deposited around the crater enhance this phenomenon.

This fractionation affects mostly siderophile elements (Zn, Pb, Au, Tl) whereas refractory elements (Ca, U, Th, rare earth) are less affected.

Over the course of the ablation, the sample is more and more heated (as the induced plasma interacts with the crater wall) which generated the vapor enrichment with "volatile" elements : this fractionation can be evidenced by monitoring the ratio of a "volatile element" versus a refractory element (Pb/U) : the ratio starts from a "true" value that progressively increases.

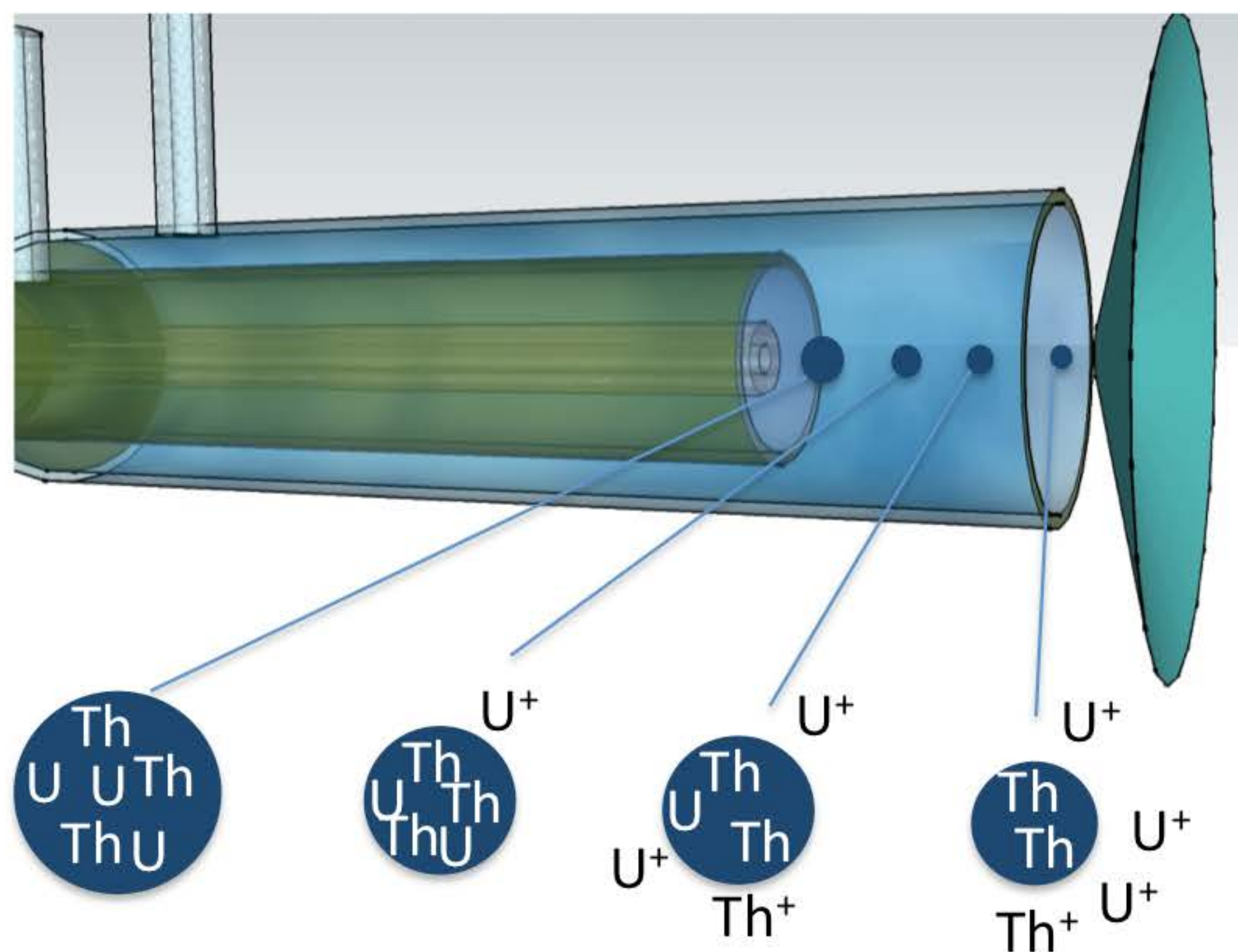
By using shorter laser wavelength (deep UV), these thermal effects (and then the fractionation indexes) are much less pronounced which explain the success of 193 nm, 213 nm or 266nm lasers.

$$\text{FI}_{1064\text{nm}} > \text{FI}_{266\text{nm}} > \text{FI}_{213\text{nm}} > \text{FI}_{193\text{nm}}$$

Quantification: Origin of the elemental fractionation

2/ Particle size: Incomplete atomisation of the laser induced particles, **into the ICP**, has been proposed more recently. Here the fractionation does not occur at the ablation site, but in the plasma of the ICPMS, the **biggest particles being less efficiently atomised (>150 nm)** than the smallest.

In these hot plasma conditions (7500 K), the most volatile elements contained in the particle diffuse more rapidly than the most refractory which generates a bias if the particle is not completely atomised : the remaining particles are then highly enriched in refractory element that will never be ionised (and then detected).

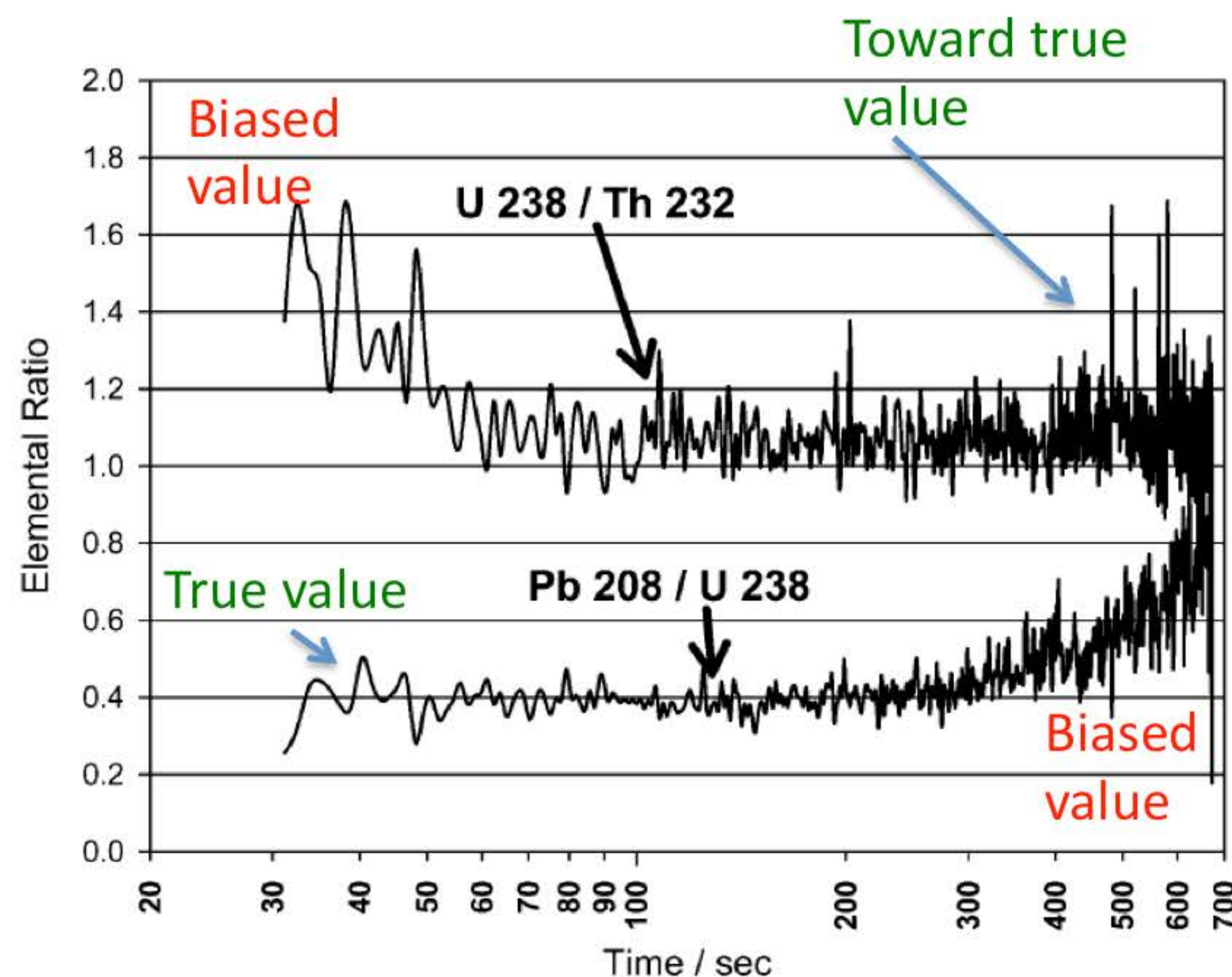


This is illustrated here with U (heat of vaporisation=417 kJ.mol⁻¹) and Th (heat of vaporisation=514 kJ.mol⁻¹)

This phenomenon is also indirectly governed by the laser wavelength since the particles size distribution is shifted towards smaller particles when using short wavelengths (see below).

Quantification: Origin of the elemental fractionation

During the ablation, the particle size distribution changes; big particles (up to $2\mu\text{m}$) being produced during the first pulses whereas smaller particles are gradually produced. The U/Th ratio is then biased at the beginning and tends towards true value at the end of the ablation.

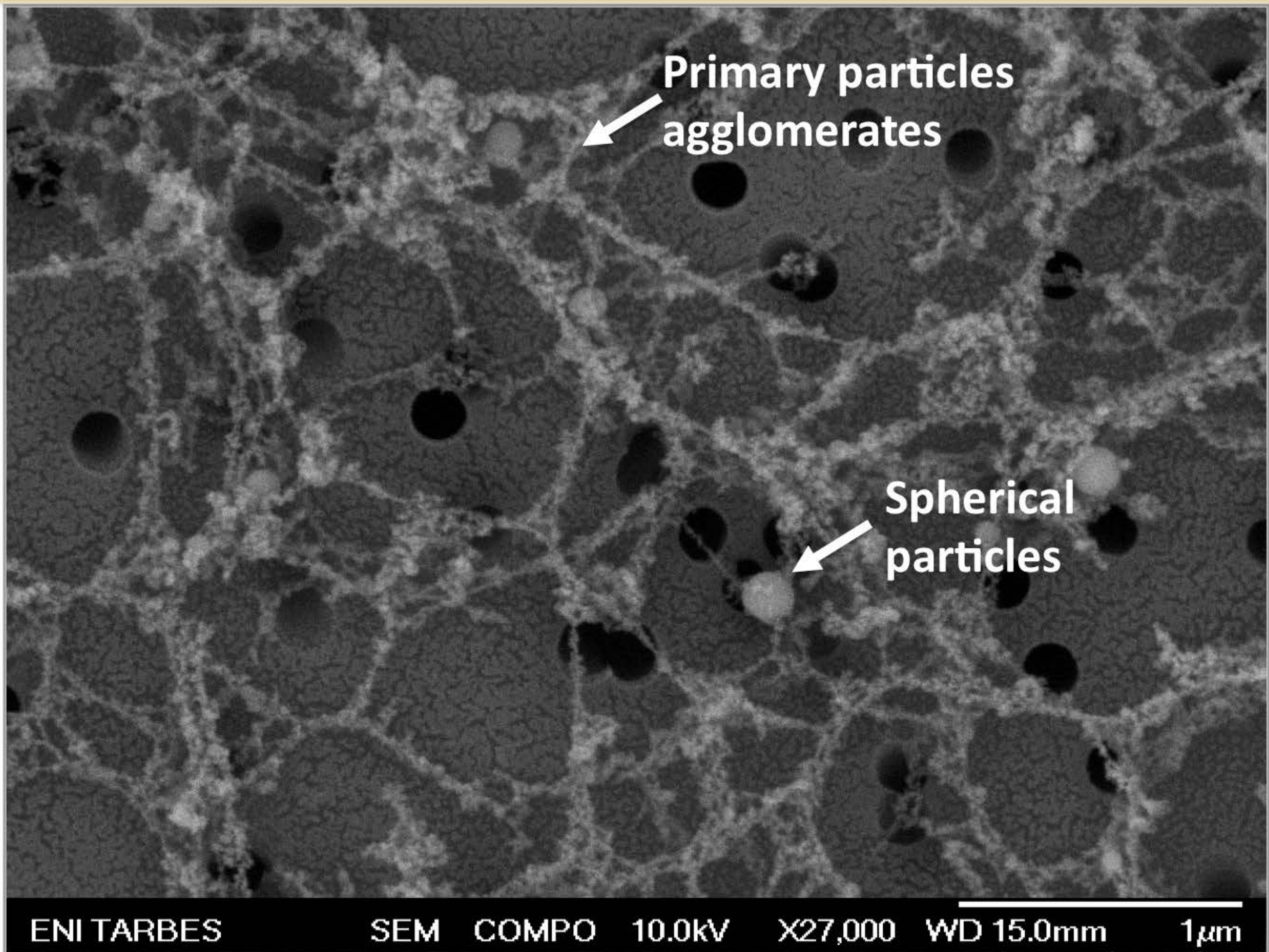


Robust ICP conditions (High power, low carrier gas, etc...) allow reducing this elemental fractionation (but it depends also on the instrument).

U and Th in the NIST 612 (or 610) are generally used for tuning the ICP since:

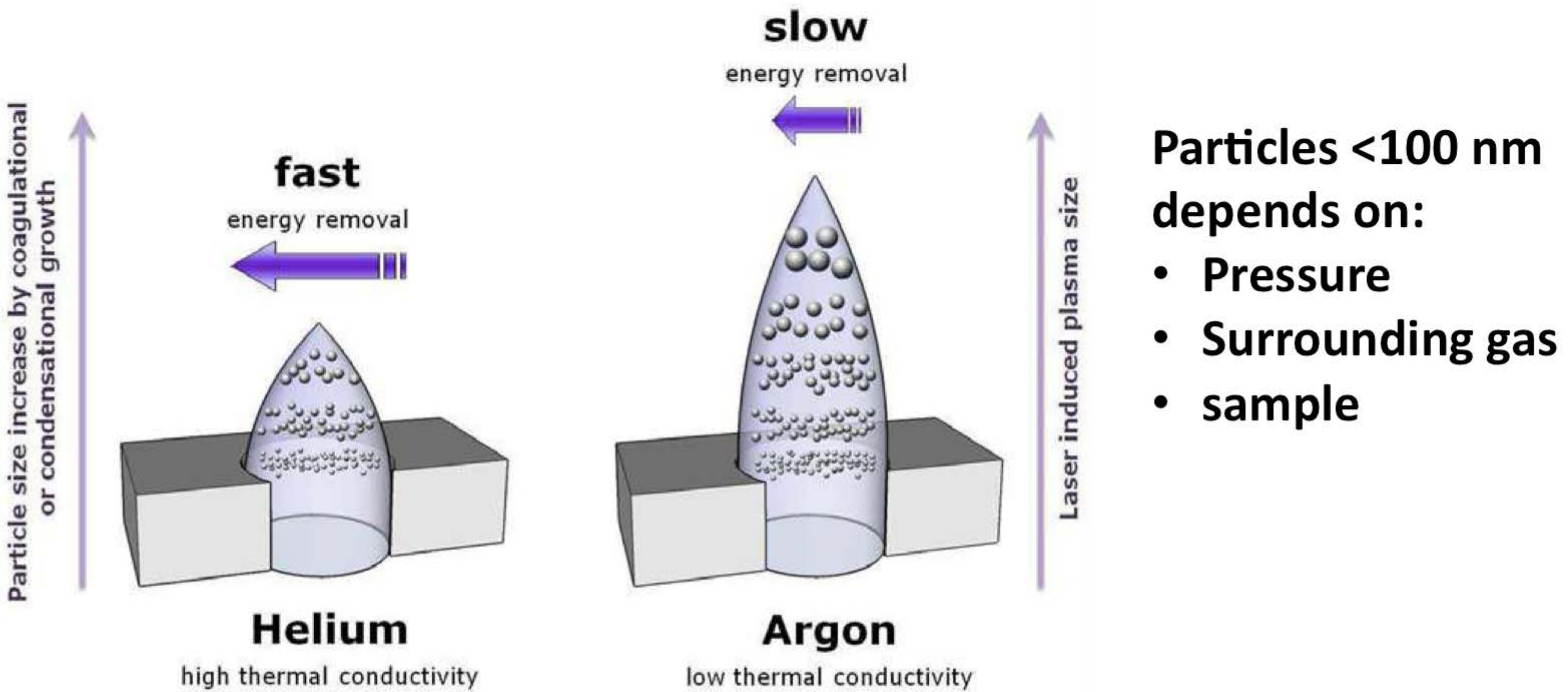
- 238U and 232Th have similar masses (they are then similarly affected by space charge effect).
- U and Th have similar ionisation potential (6,2 and 6,1 V respectively).
- $[U]=[Th]$ in these sample $U/Th=1$

The key is the particle formation...



The key is the particle formation...

1/ Primary particles generation : => Vapour phase condensation-Coagulation

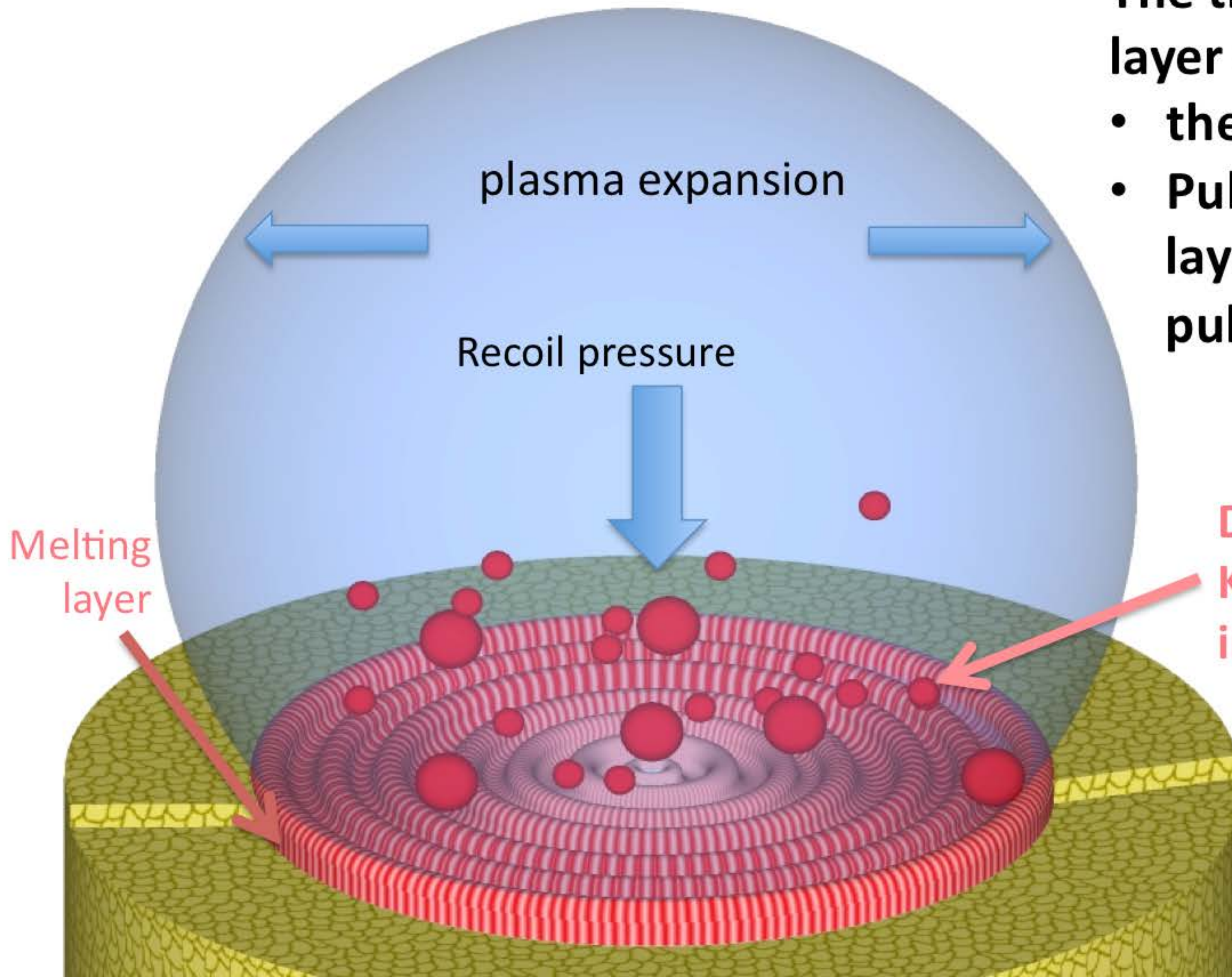


Adapté de Horn et al Applied Surf. Sci. , 2003

The key is the particle formation...

2 – Hydrodynamic sputtering (spherical particle > 100 nm)

More info in Hergenroeder J. Anal. At. Spectrom., 2006, 21, 517–524 | 517



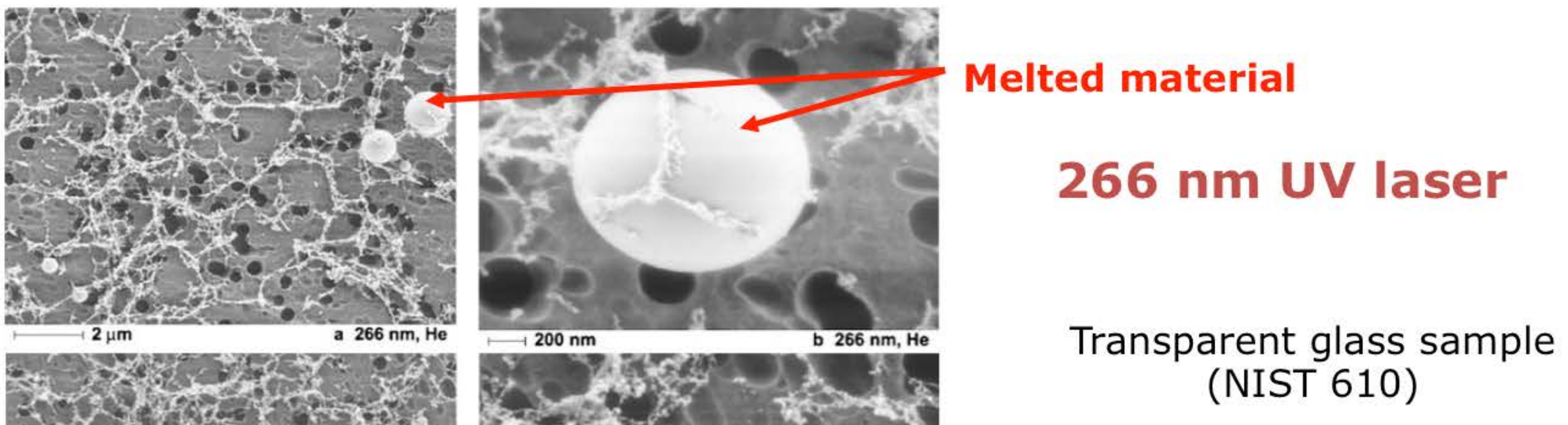
The thickness of the melting layer depends :

- the wavelength
- Pulse duration (very thin layer with femtosecond pulses)

Droplet ejection due to Kelvin-Helmholtz instabilities

Schéma d'artiste

The key is the particle formation...



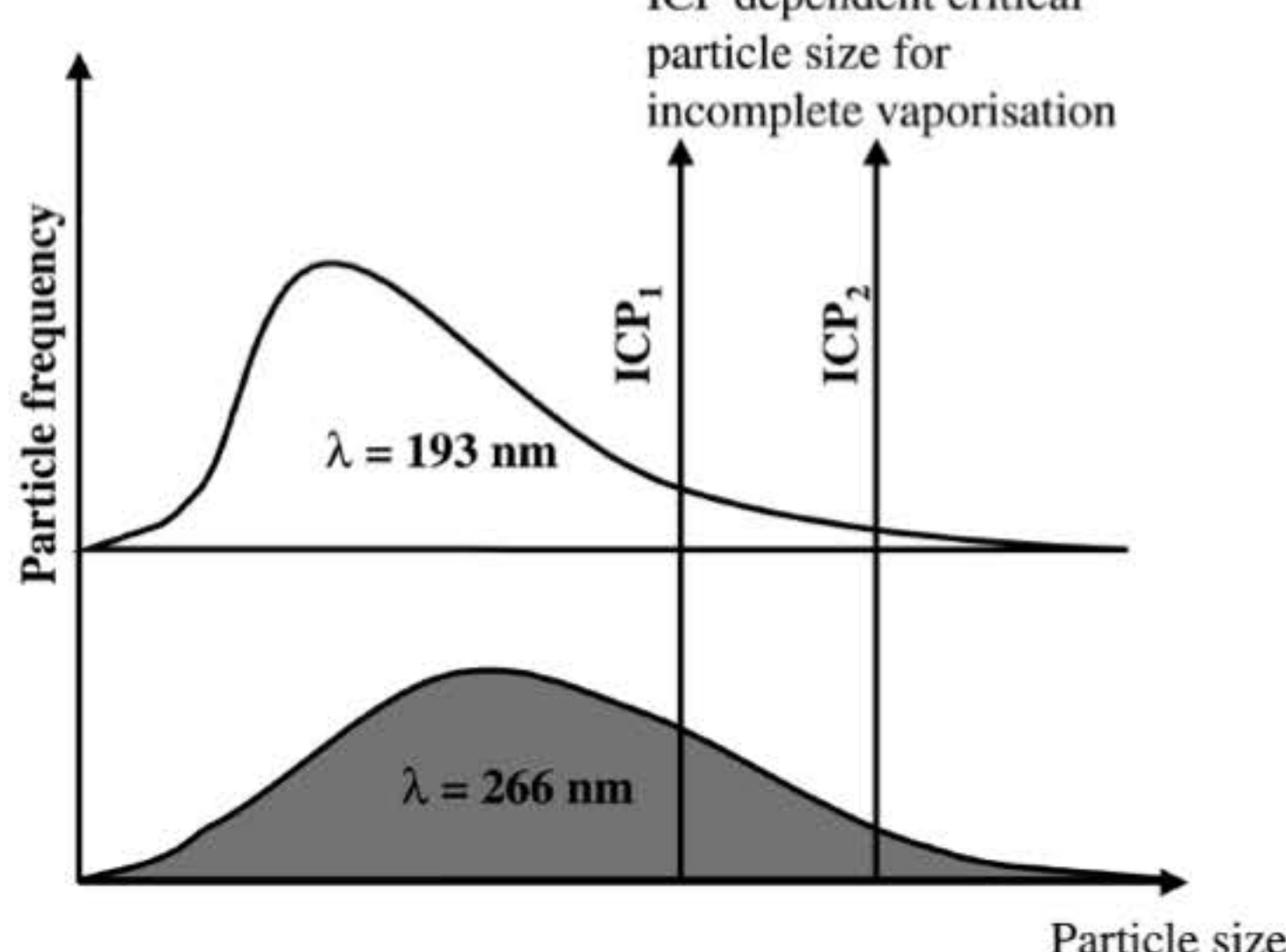
Melted material

266 nm UV laser

Transparent glass sample
(NIST 610)

193 nm UV laser

H. Kuhn et Al, abc, 2005, 383, 434-441



The aerosols is constituted by agglomerated primary particles and spherical particles resulting from melting. At 266 nm more spherical particles (and also bigger) than at 193 nm,

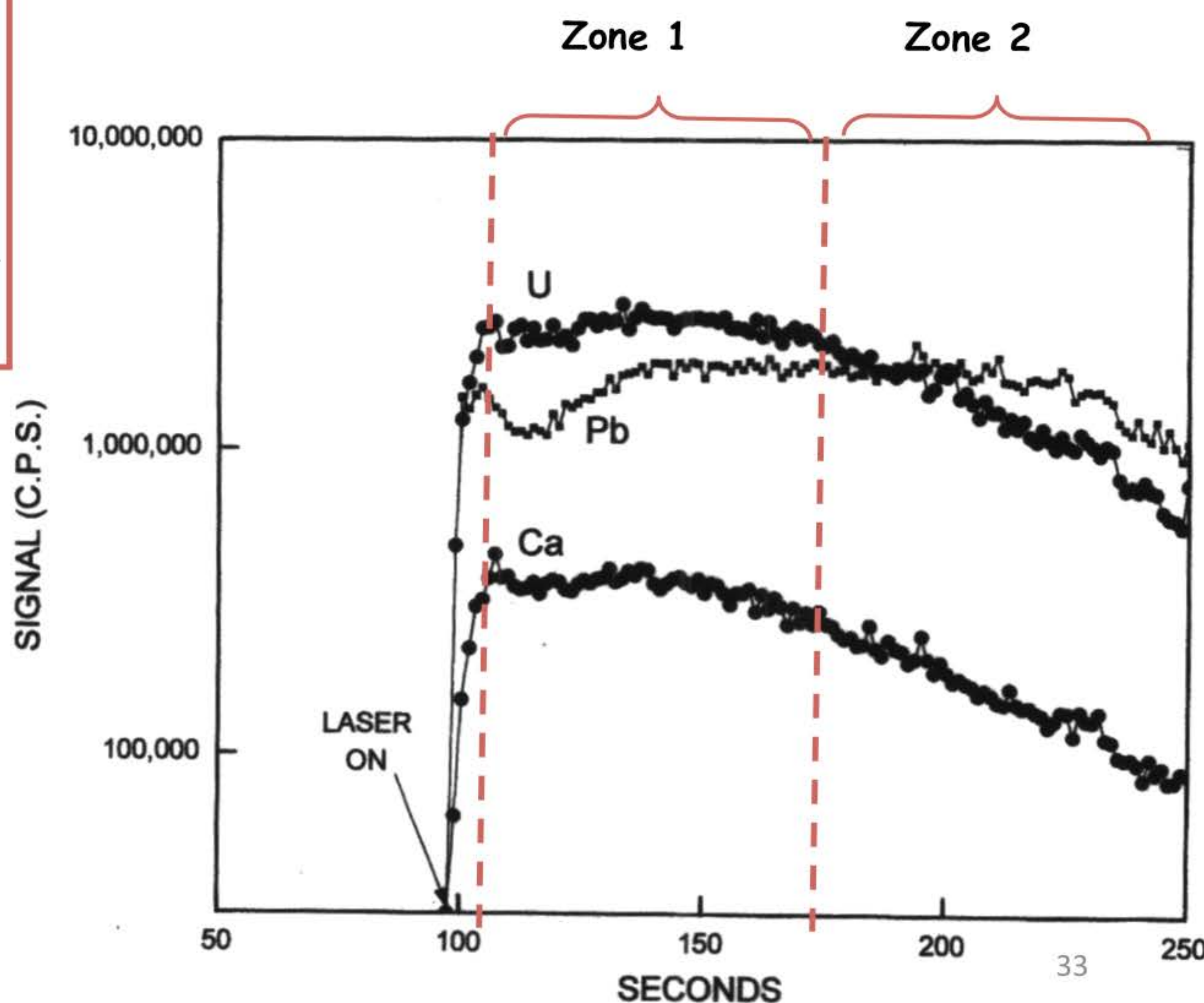
Fig. 12 Schematic diagram of influence of ICP conditions on incomplete particle vaporisation and the contribution of the latter to elemental fractionation.

M. Guillong et Al, JAAS, 2002, 17, 831-837

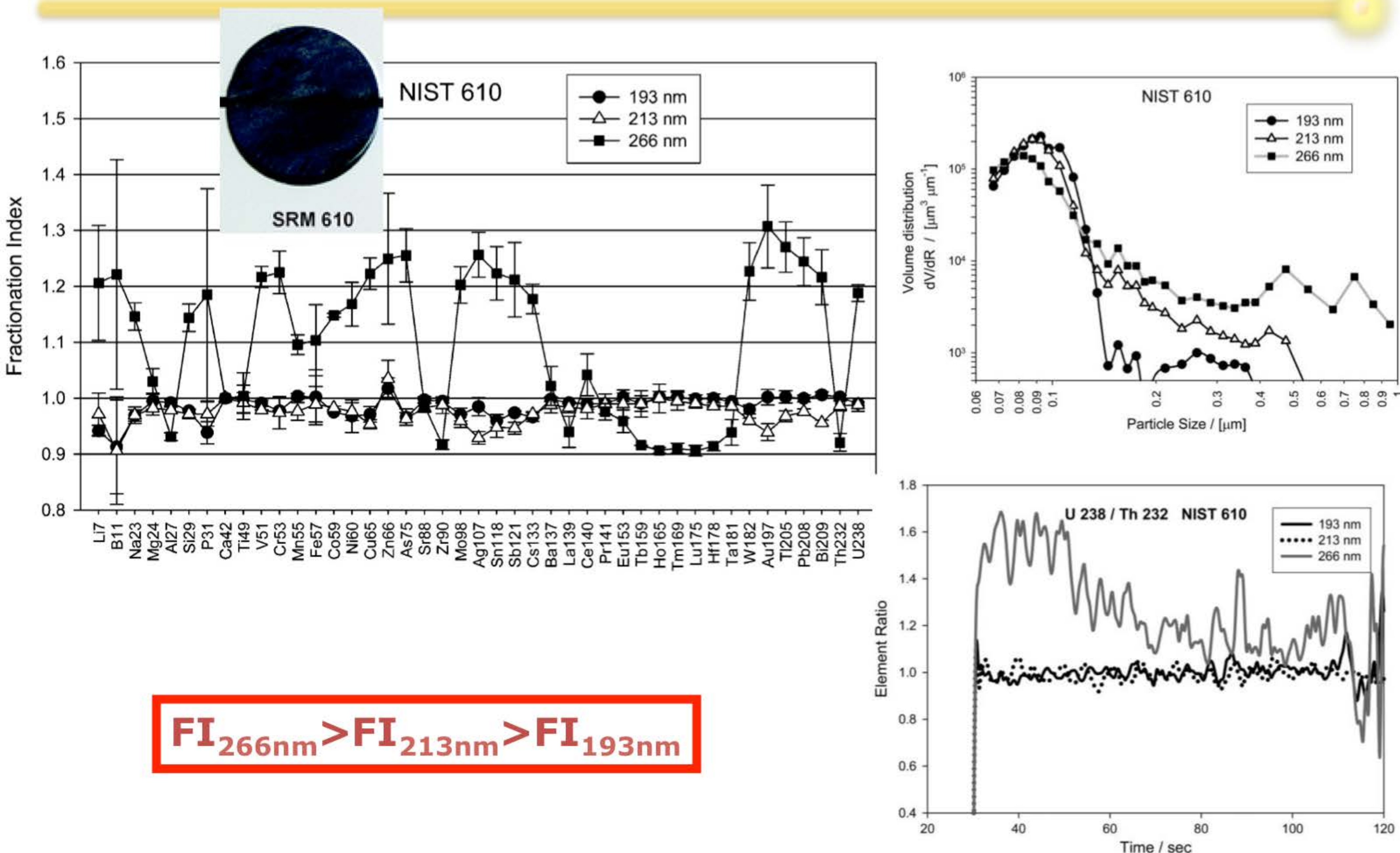
How to quantify the elemental fractionation...

For a given analyte, the fractionation index (FI) is defined with respect to another element taken as reference (generally Ca or Si). It reports the variation of the ratio over the course of the ablation taking into account 2 zones

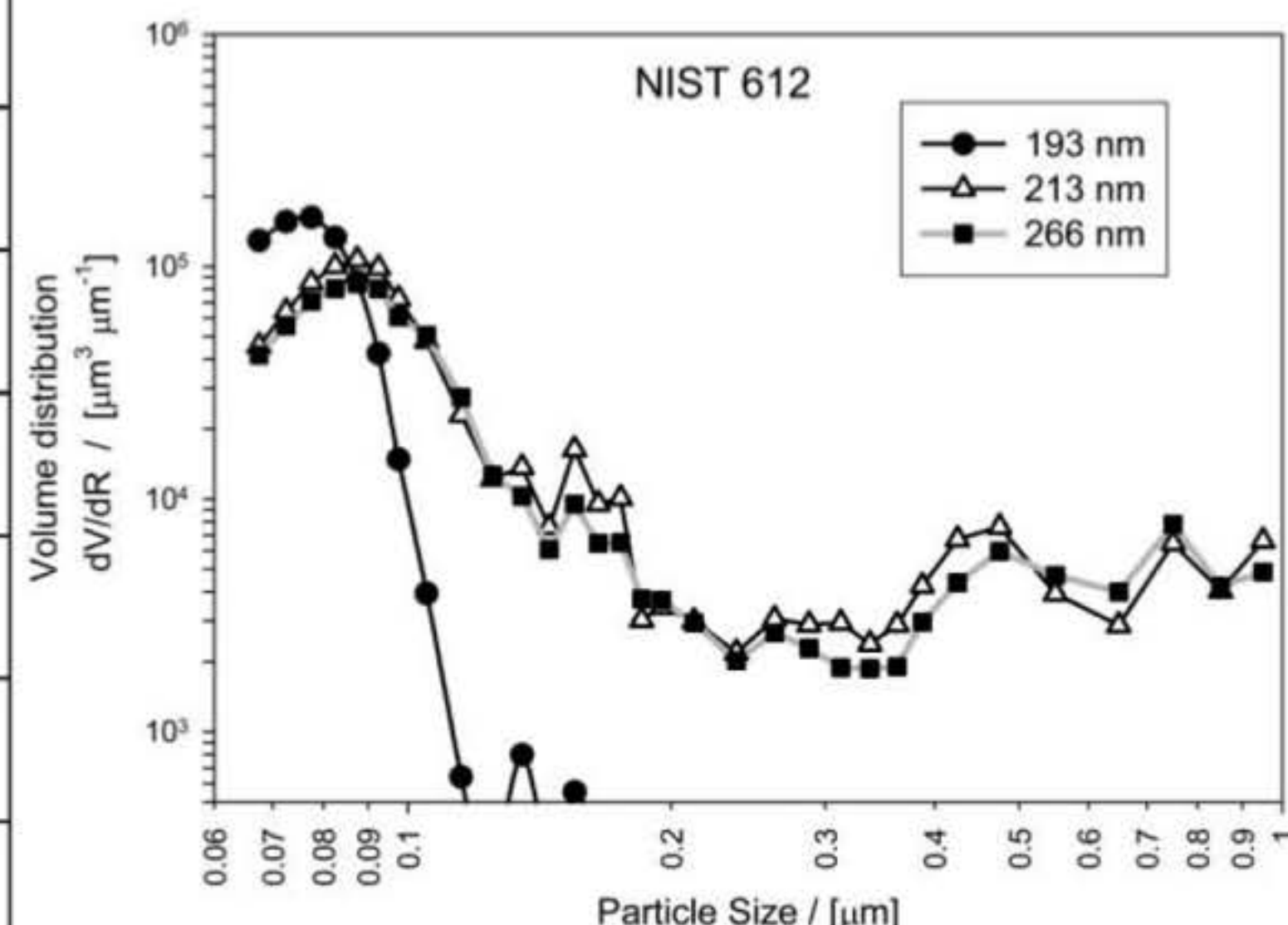
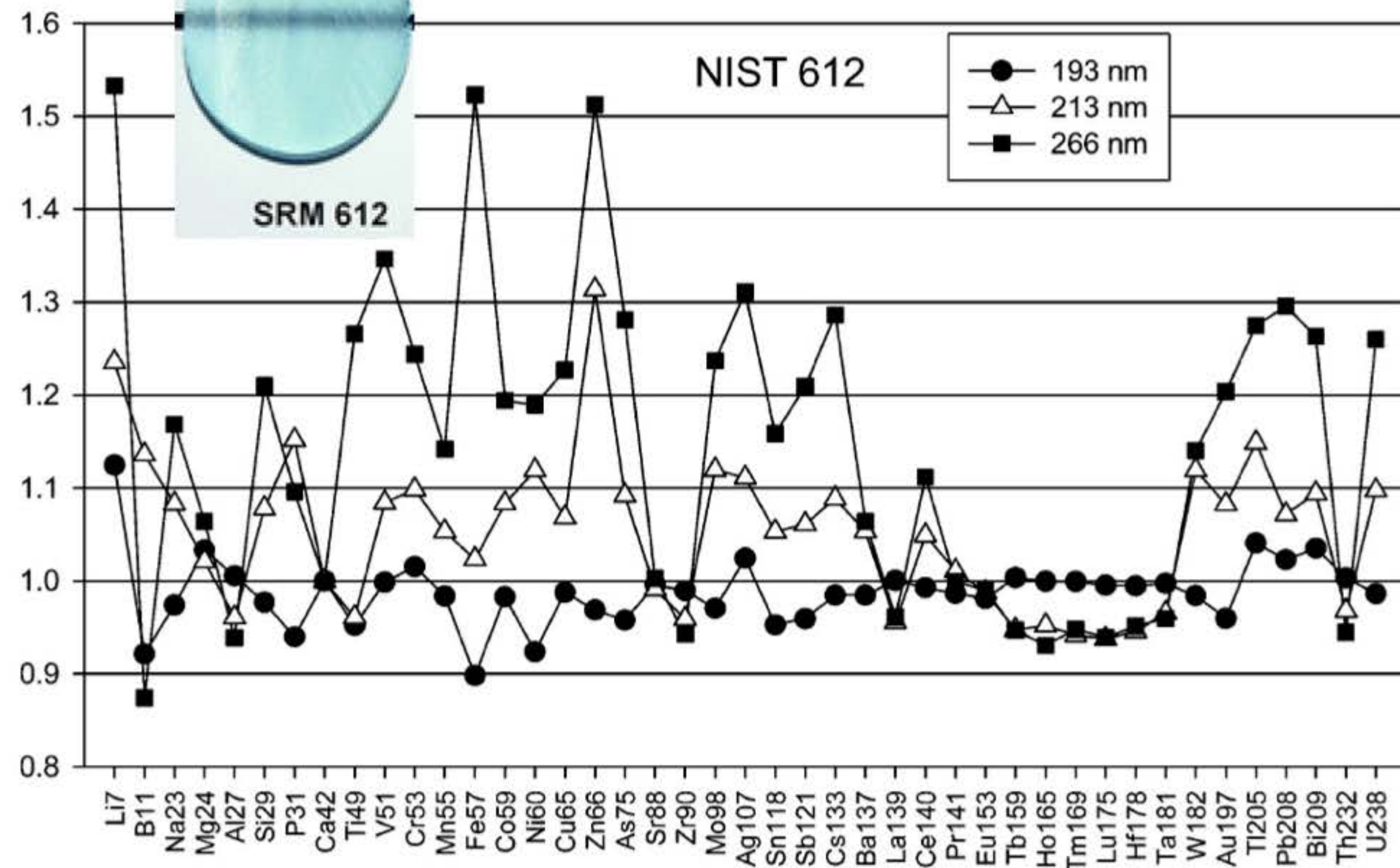
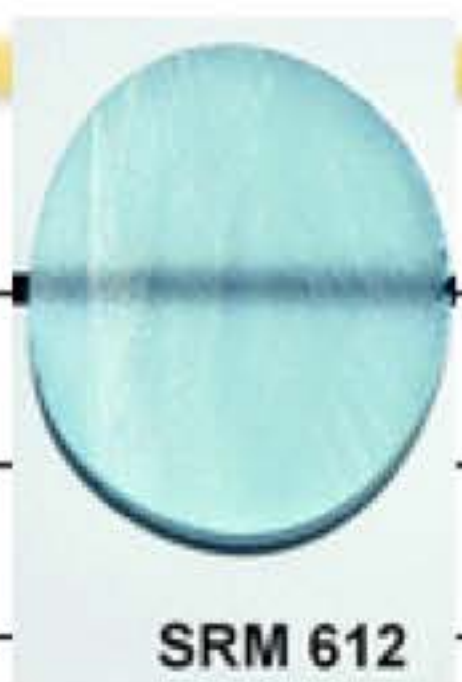
$$FI_{Pb/Ca} = \frac{\langle Pb \rangle_{\text{zone1}}}{\langle Ca \rangle_{\text{zone1}}} / \frac{\langle Pb \rangle_{\text{zone2}}}{\langle Ca \rangle_{\text{zone2}}}$$



The fractionation index depends on the sample...

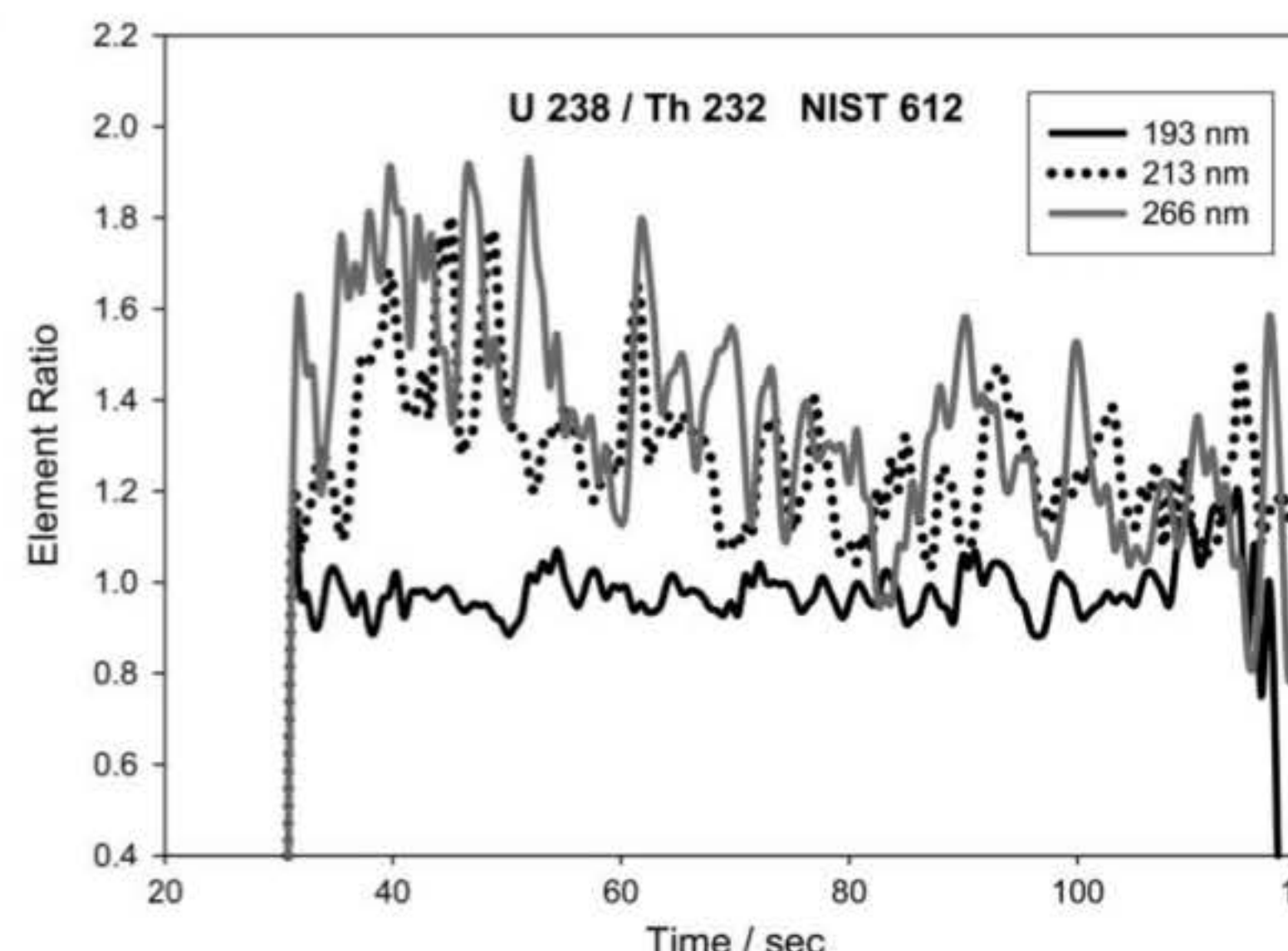


The fractionation index depends on the sample...



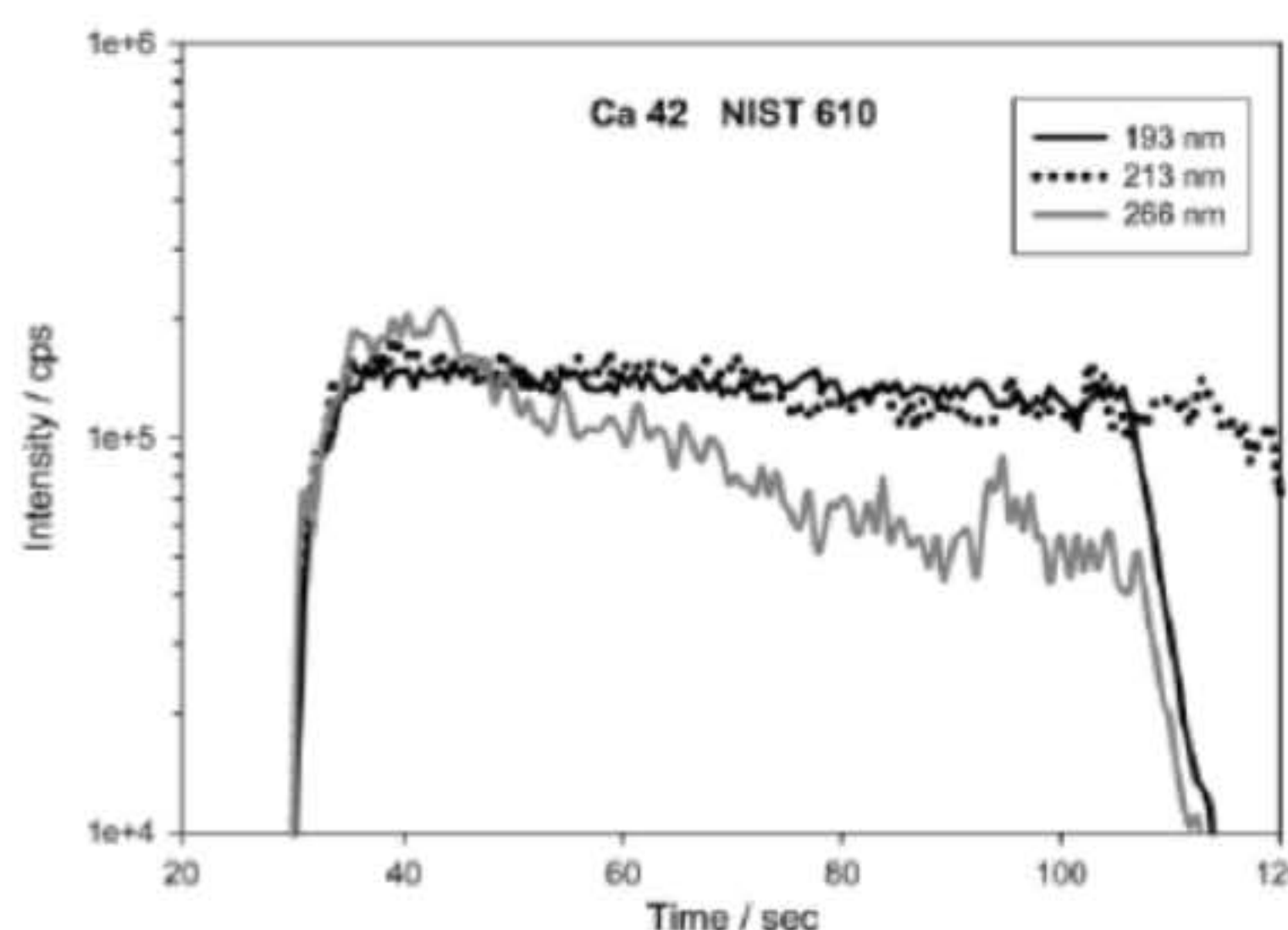
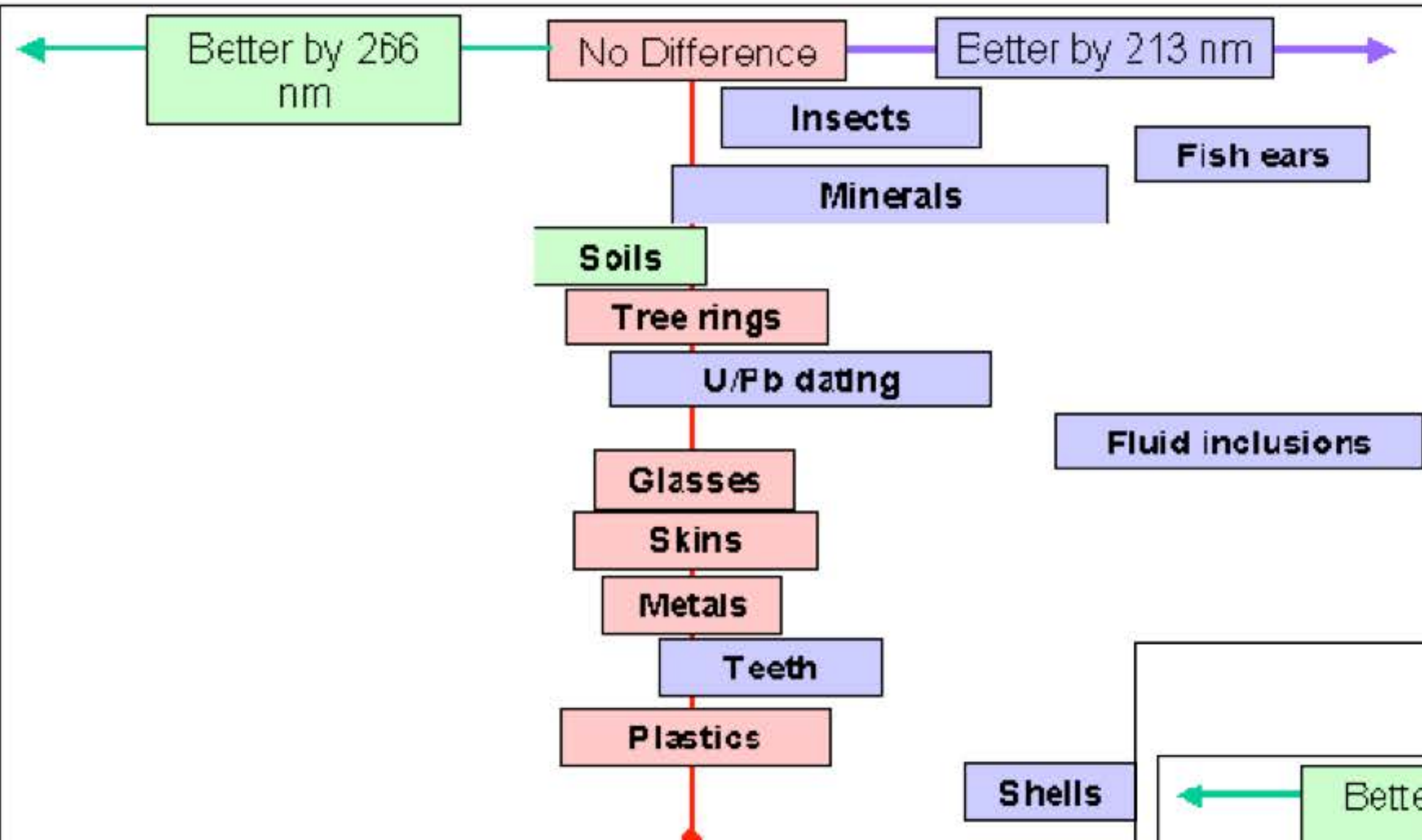
FI generally worse for transparent glasses

FI_{266nm} > FI_{213nm} > FI_{193nm}

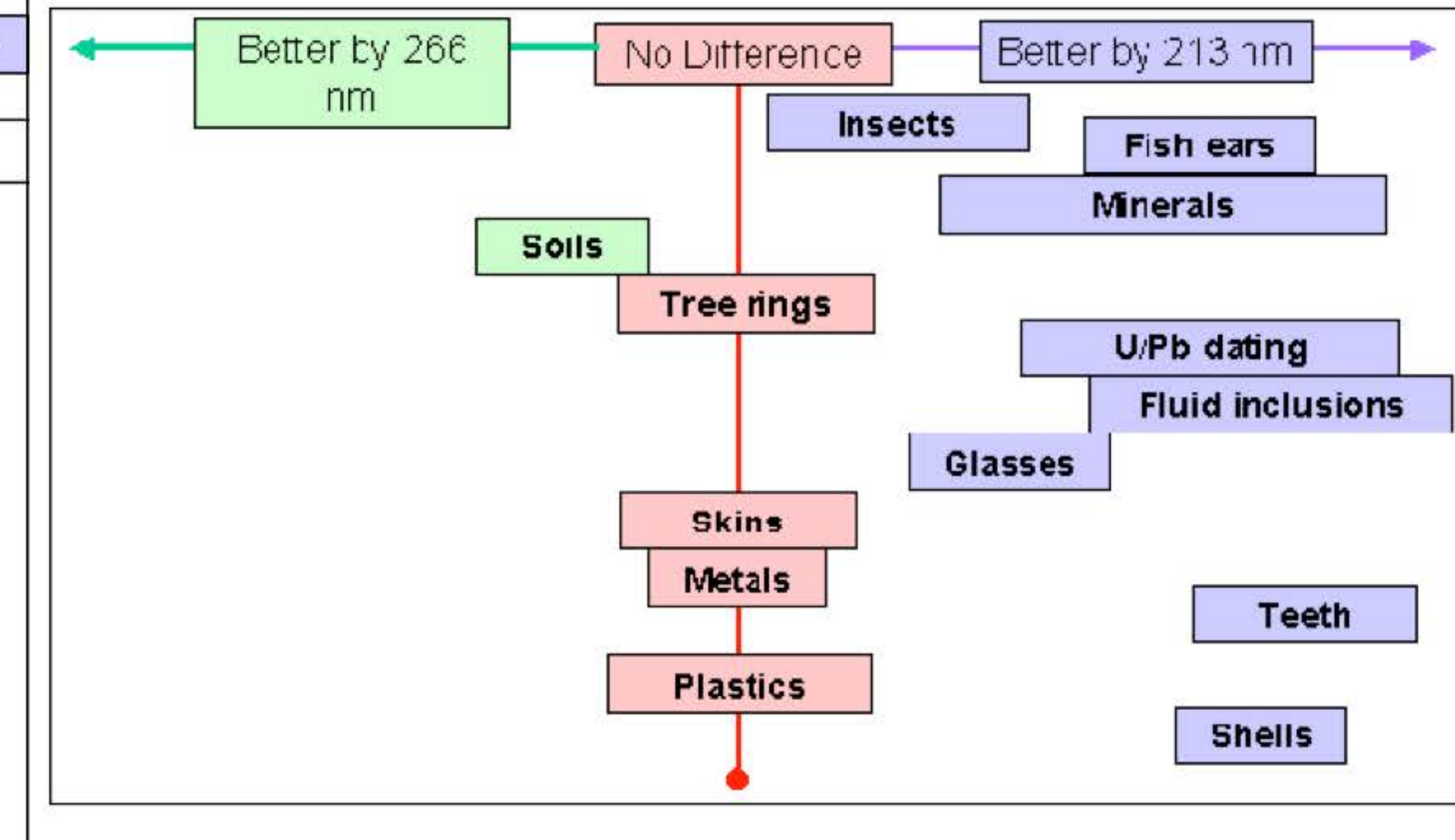


213 nm vs 266 nm lasers

Accuracy of 266nm vs 213nm



Precision of 266nm vs 213nm

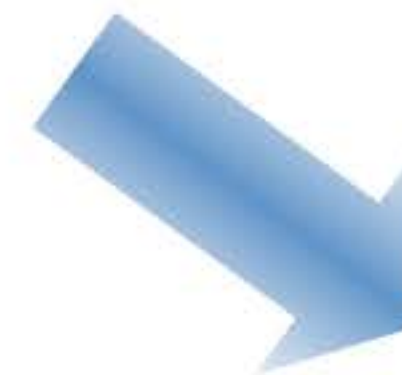
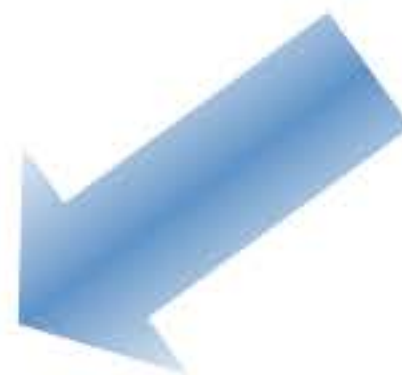


Solutions for elemental fractionation...

ELEMENTAL FRACTIONATION =

Non stoichiometric detection

Solution?



Matrix Matching using certified reference material

⇒ similar fractionation in the sample and the standard

Using less fractionating lasers

⇒ Deep UV,
⇒ Fluence
⇒ Power density,
⇒ Ultra short pulses (fs), Etc...

Tuning the LA/ICPMS

Tuning of the LAICPMS coupling :

- According to “normal” ICPMS recommendation in liquid configuration
- **Efficient particles atomization**

Use a NIST 612 glass sample and set the ICP parameters in order to get **$U/Th = 1 \pm 0,05$** (theoretical value $U/Th=1$).

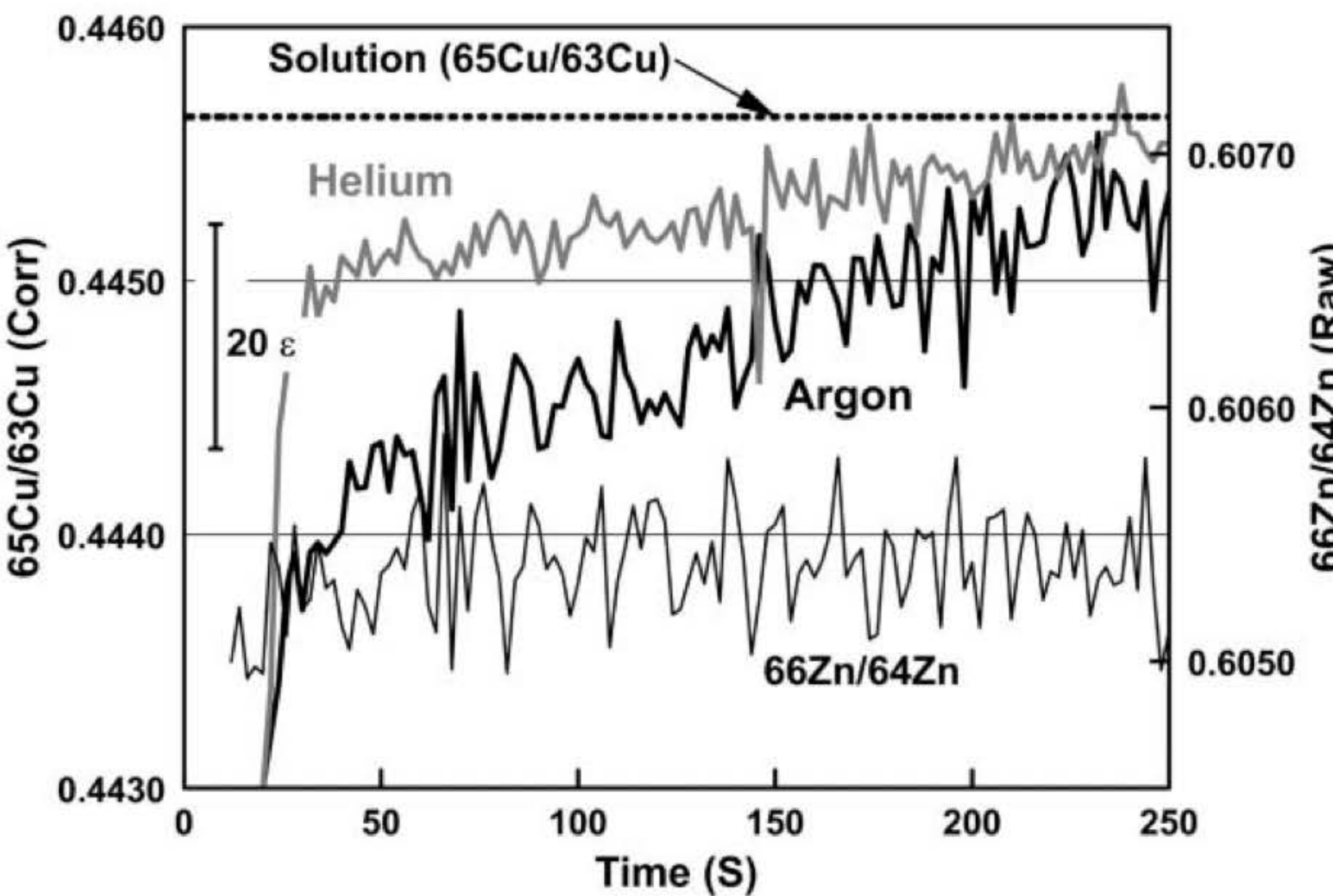
The U/Th ratios tend to be higher than 1 due to incomplete particles atomization.

Robust ICP conditions are mandatory to reach accuracy. They are very often obtained while sacrificing signal sensitivity, and vary from one instrument to the other :

- High power ($>1200W$)
- Reduced carrier gas flow (compared to the optimal signal sensitivity conditions)
- Reduced auxiliary gas

Isotope fractionation

nsLA/MC-ICPMS of chalcopyrite

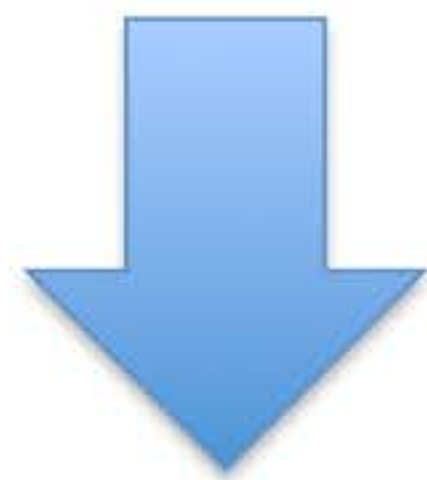


Like elemental fractionation, isotope fractionation occur also. It is mainly attributed to incomplete particles atomisation and faster diffusion of light isotopes...

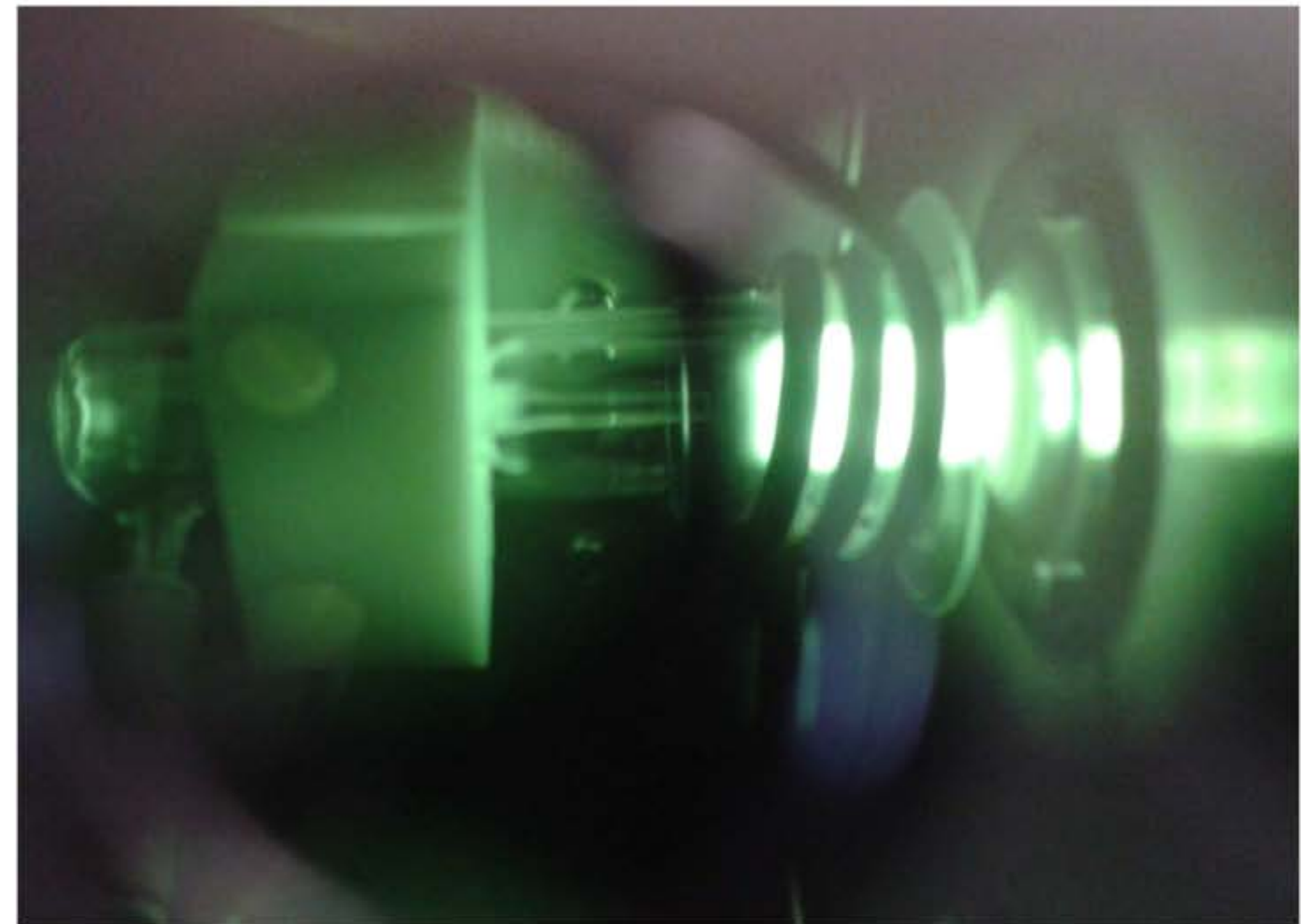
Fig. 1 Time resolved $^{65}\text{Cu}/^{63}\text{Cu}$ ratios, corrected for mass bias, for ablation of chalcopyrite using Ar (bold) and He (light) as ablation gases (ablation commenced at 20 s). The $^{65}\text{Cu}/^{63}\text{Cu}$ ratios gradually increased towards the value determined by solution-MC-ICP-MS analysis for the same chalcopyrite sample. The thin line shows the raw ratios for an Ar supported semi-dry Zn aerosol, produced by a desolvating nebulisation system, added to the carrier gas stream during the ablation of chalcopyrite in Ar. The constant $^{66}\text{Zn}/^{64}\text{Zn}$ ratio during ablation indicates that the increase in Cu isotope ratios was a laser-induced phenomenon. Data from Botfield (1999) and unpublished.

Plasma robustness...

- Only particles < 100-150 nm can be efficiently atomised into the ICP
- The ICP can tolerate a finite amount of particles (plasma loading)
- Specific desorption of the species at different places into the plasma

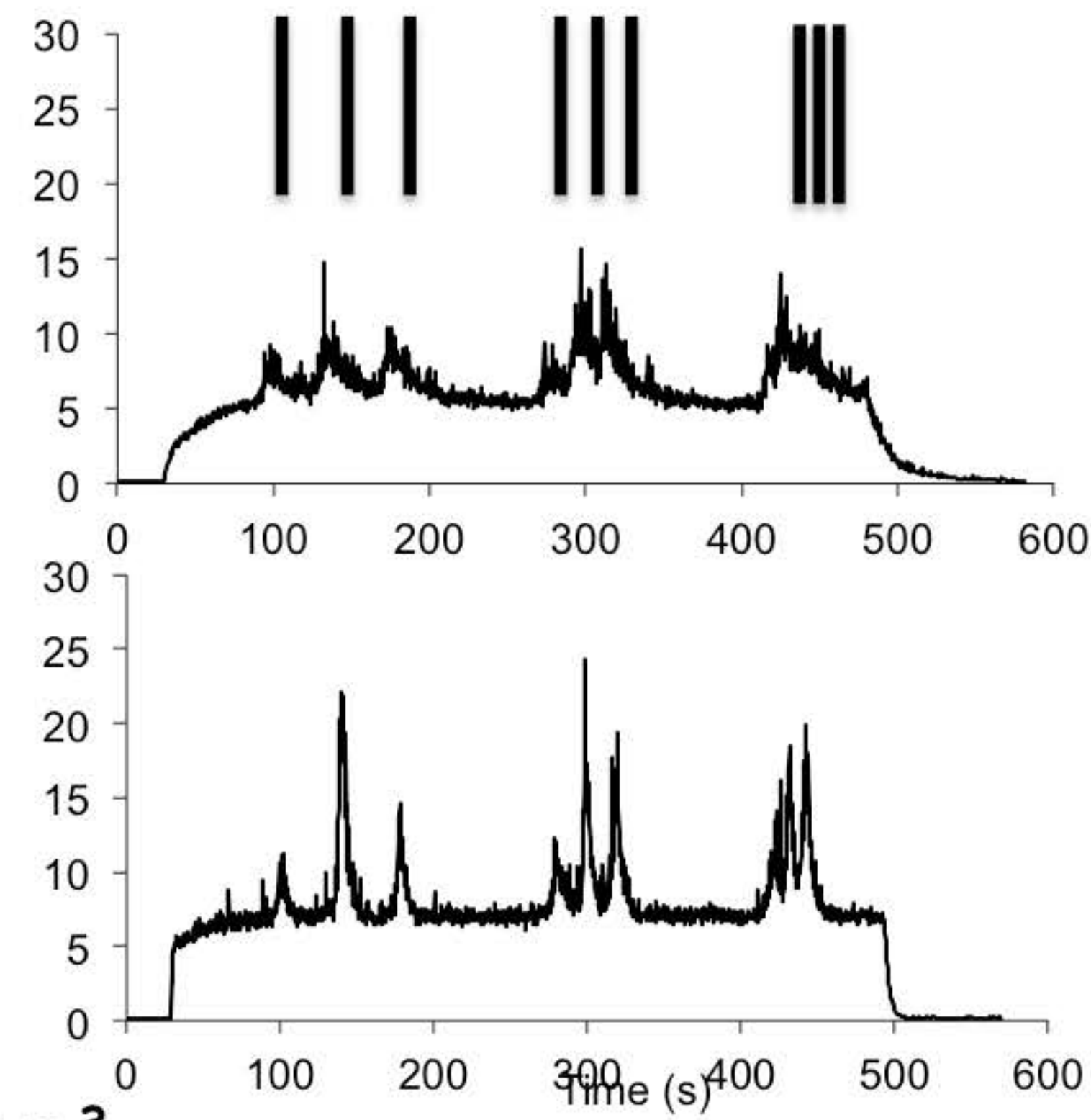
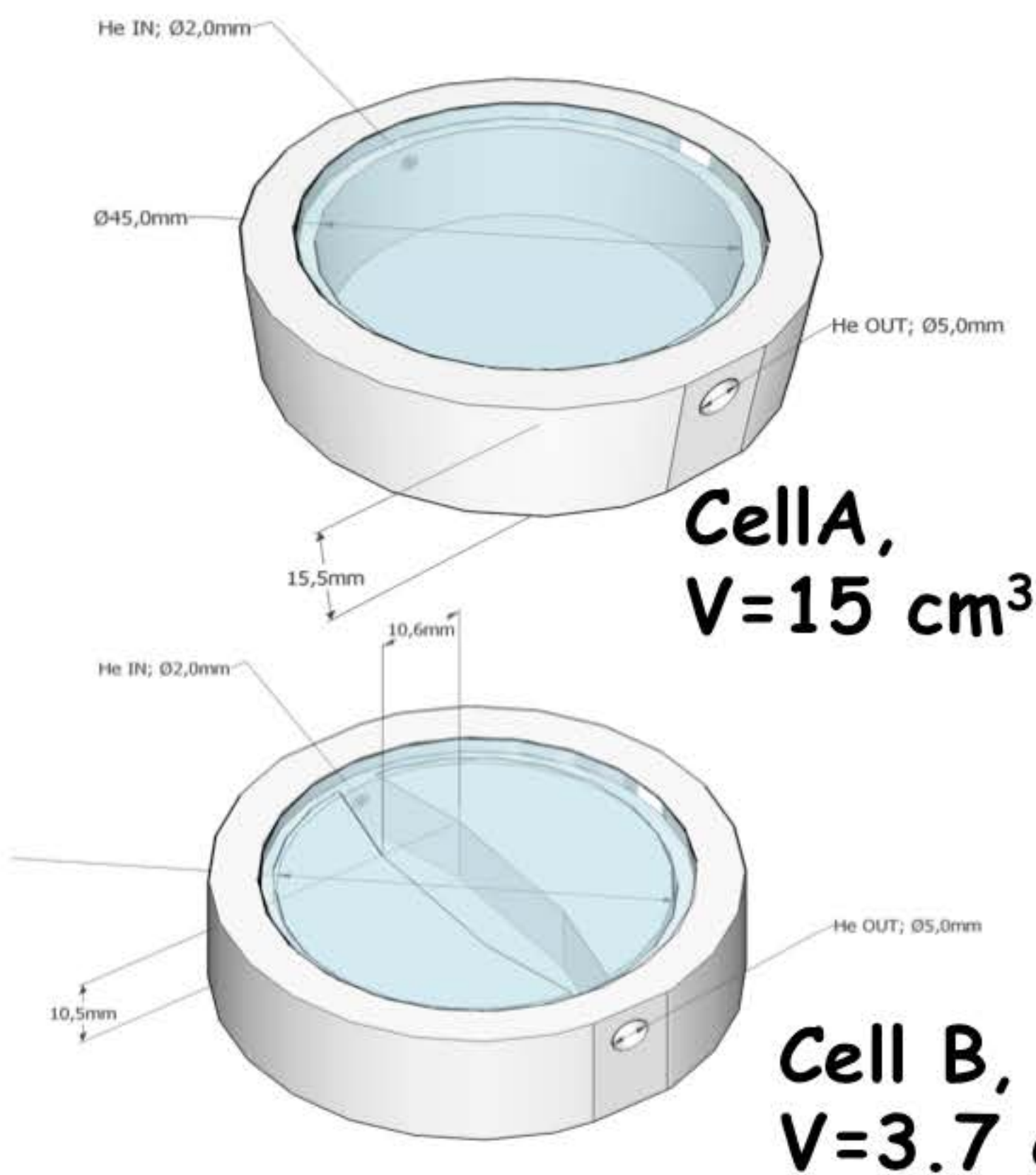


- Need for improving atomisation and ionisation efficiency
- Need for improving the plasma robustness.



Insights on the ablation cell

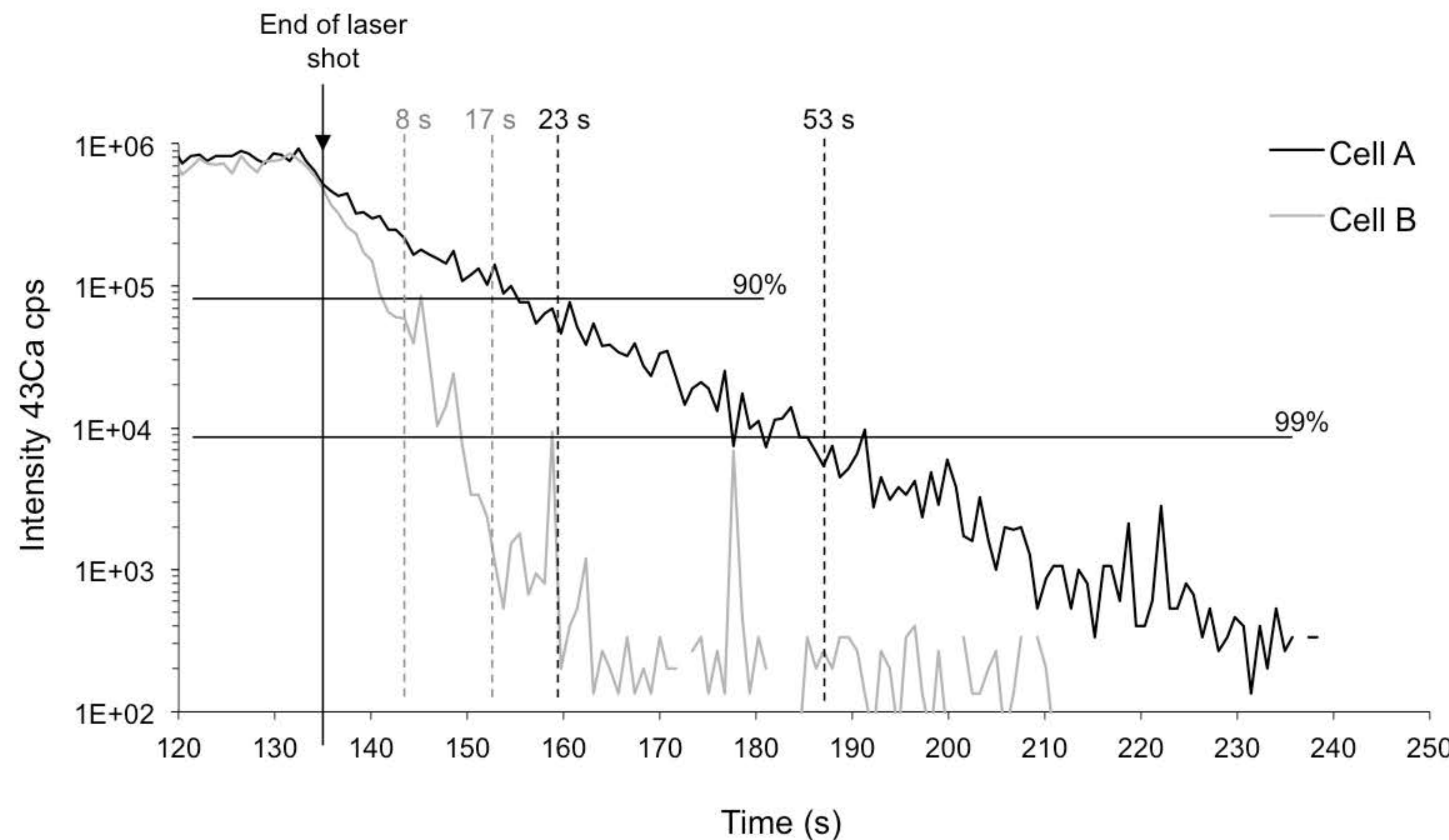
- => Aerosol transport efficiency affects sensitivity and accuracy
- => The finite size of the cell limits the size of the sample
- => Washout time : very important for keeping high spatial resolution (imaging).



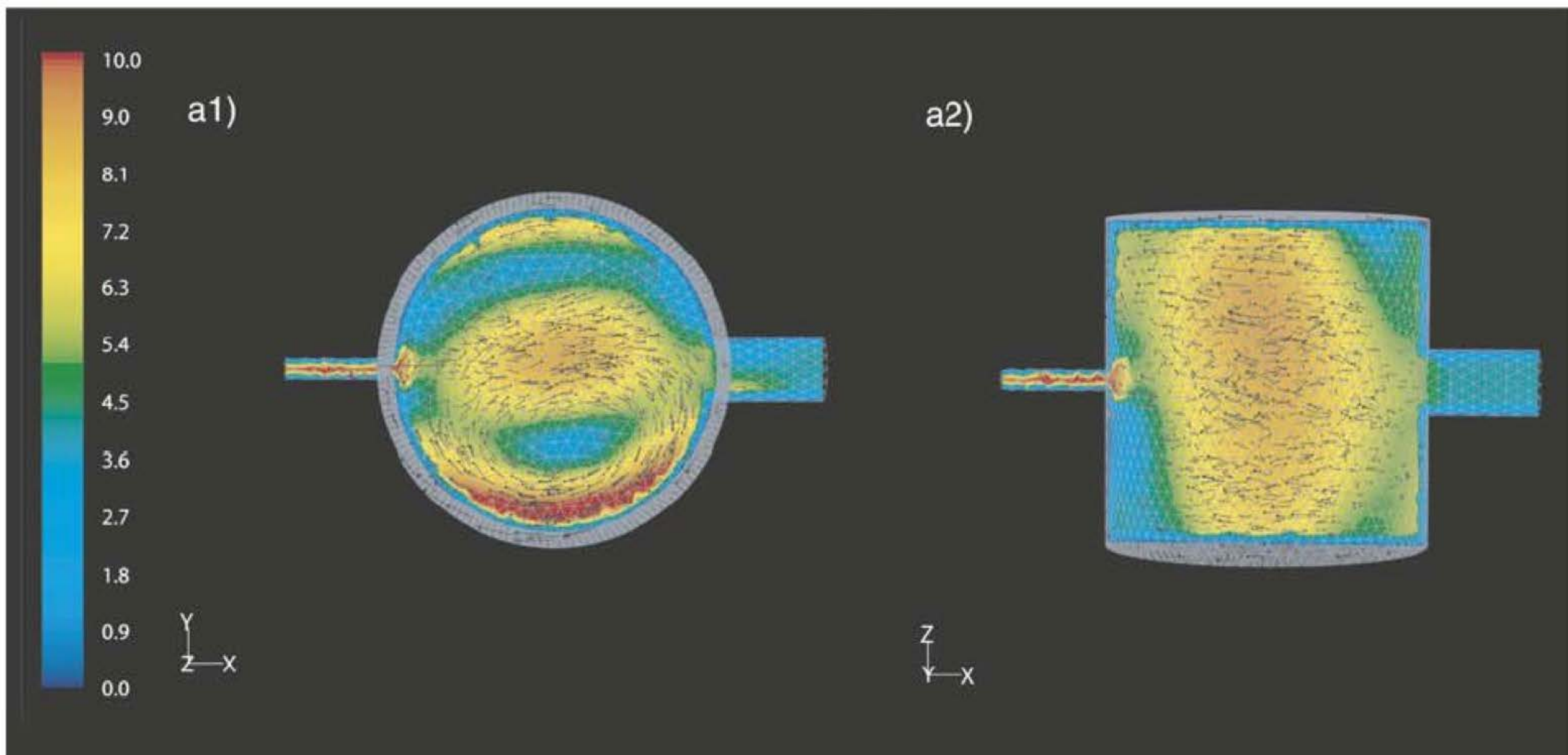
Insights on the ablation cell

The volume of the cell affects:

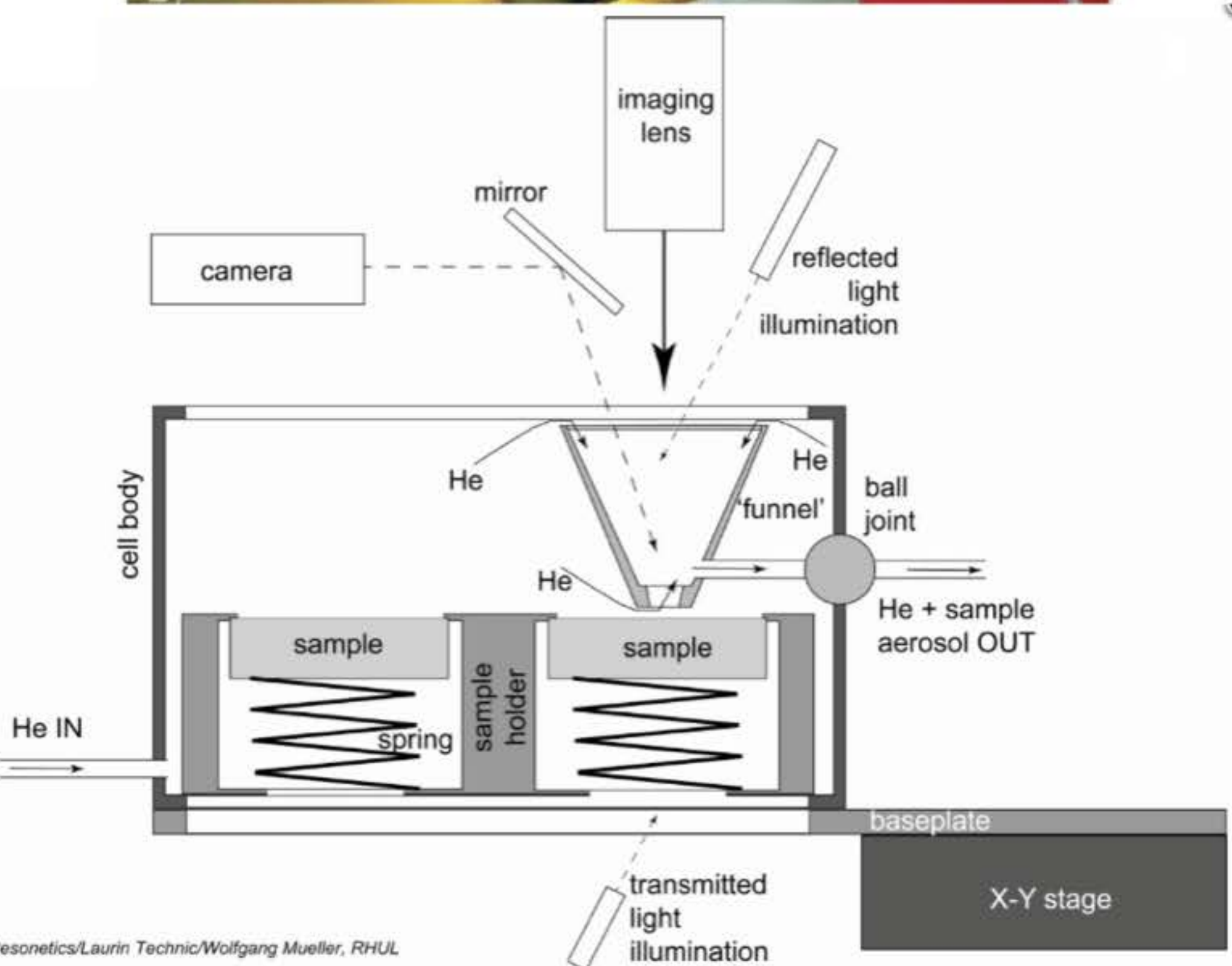
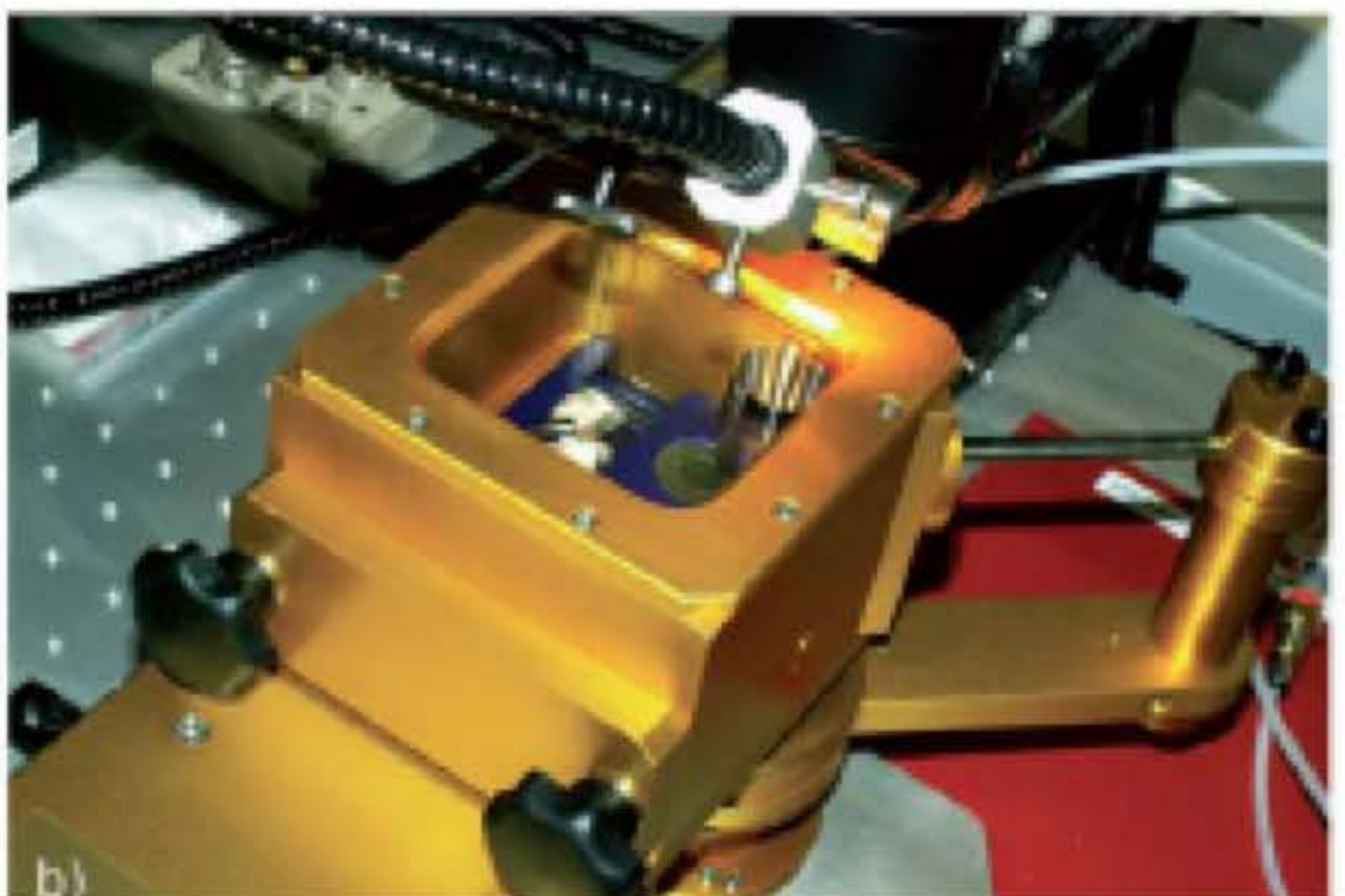
- spatial resolution in dynamic ablation (scans for instances)
- extraction efficiency and then signal intensity
- Washout time



Insights on the ablation cell



Towards mini cells for better washout time



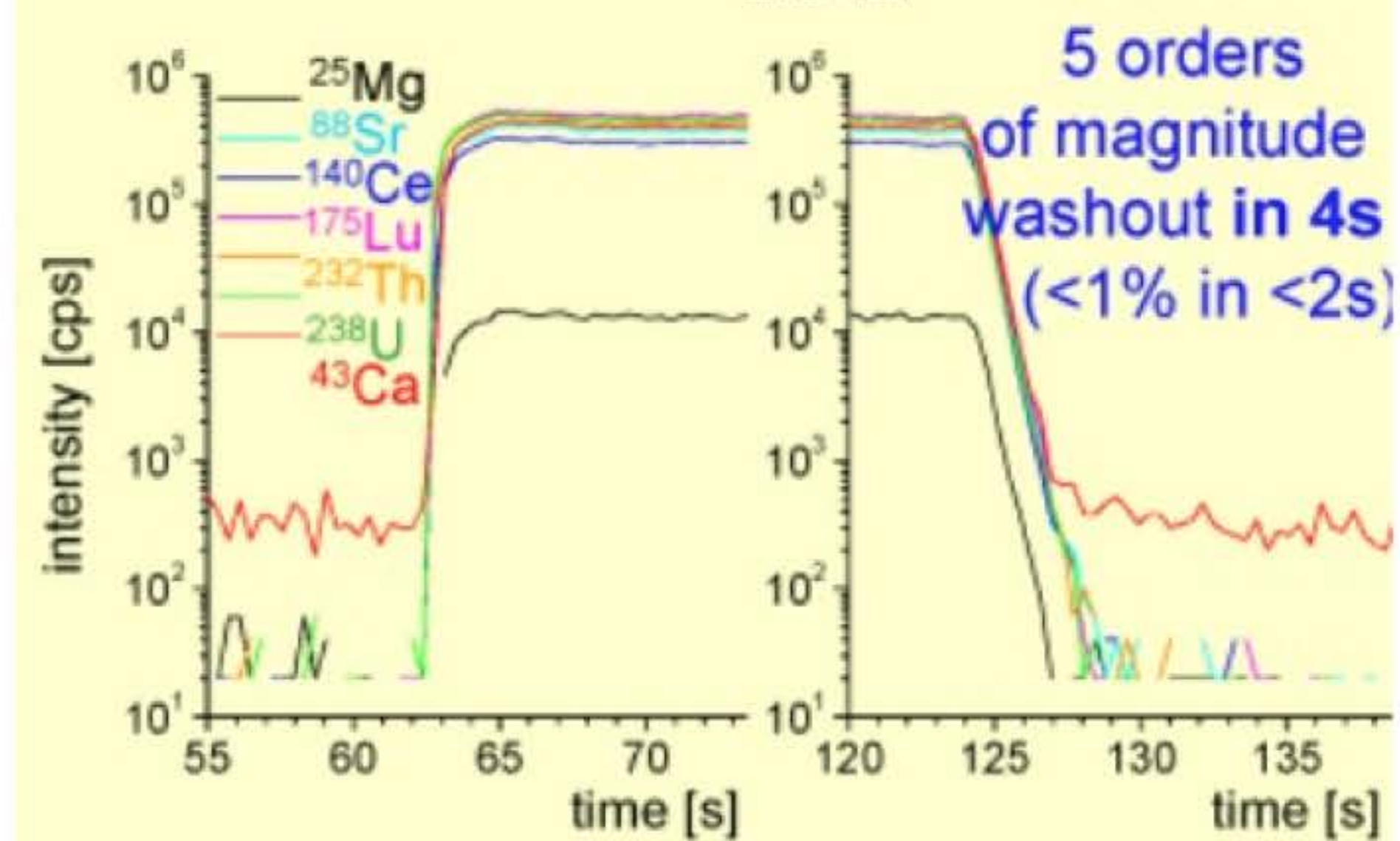
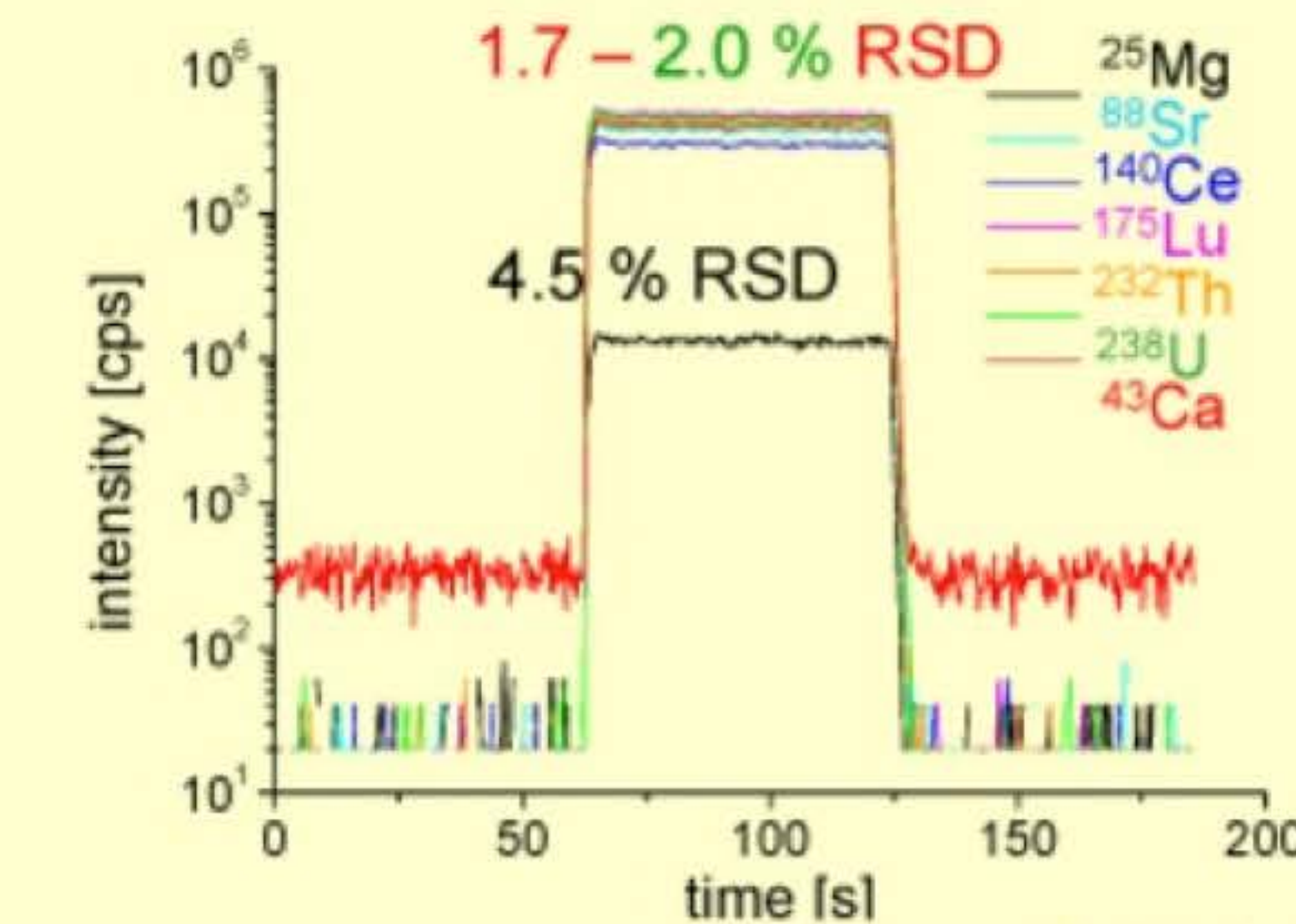
Resonetics/Laurin Technic/Wolfgang Mueller, RHUL

The dual-volume design is an integral part of the M50 and S155 ablation cell design.

193 nm excimer + 7500ce
74 μm , 10 Hz, He, 4 J/cm 2 , 1mm/min

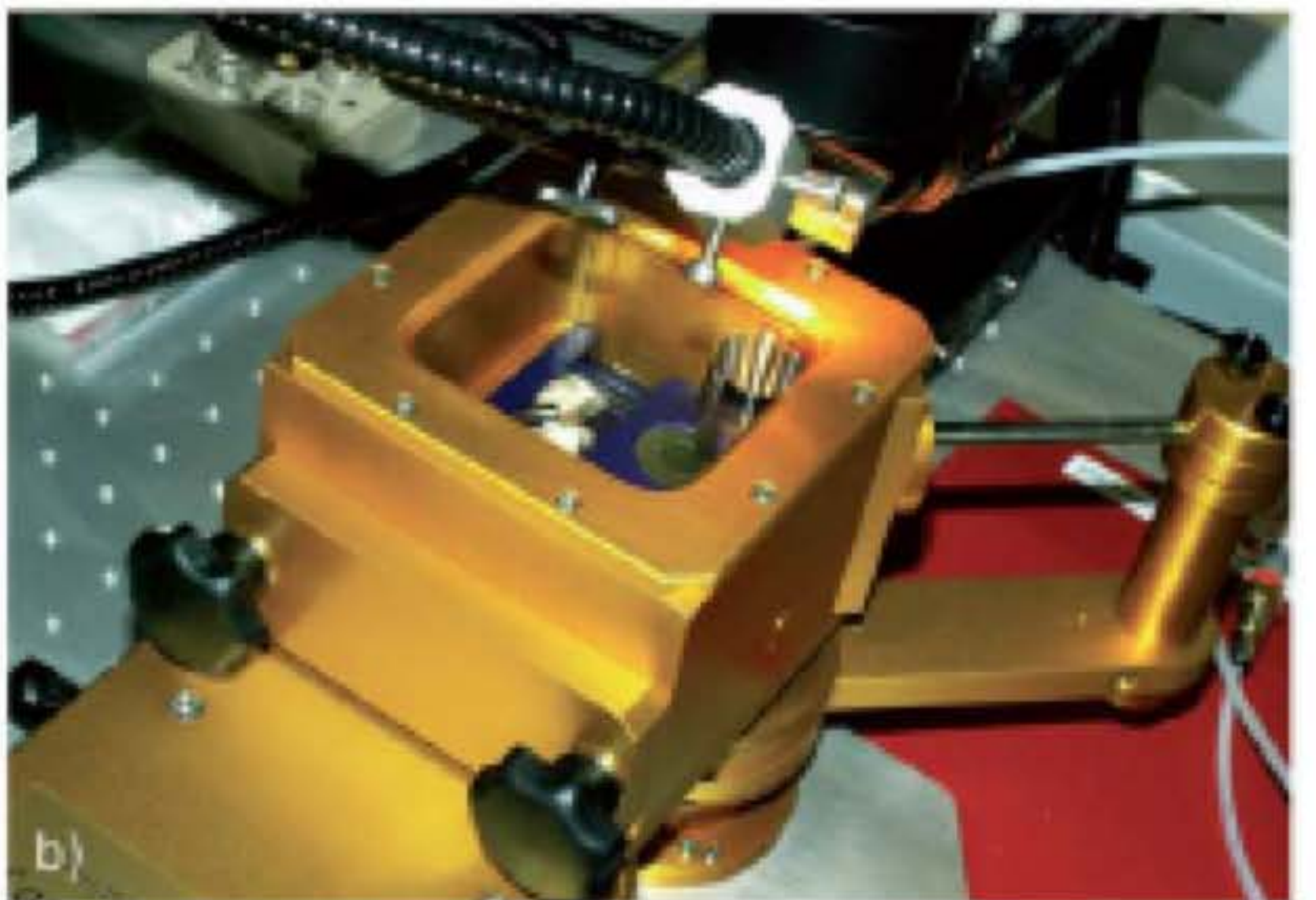
NIST 612

No 'squid' smoothing



Data Courtesy of W. Müller, RHUL

Towards mini cells for better washout time



Laurin cell 2: Resonetics, Cetac



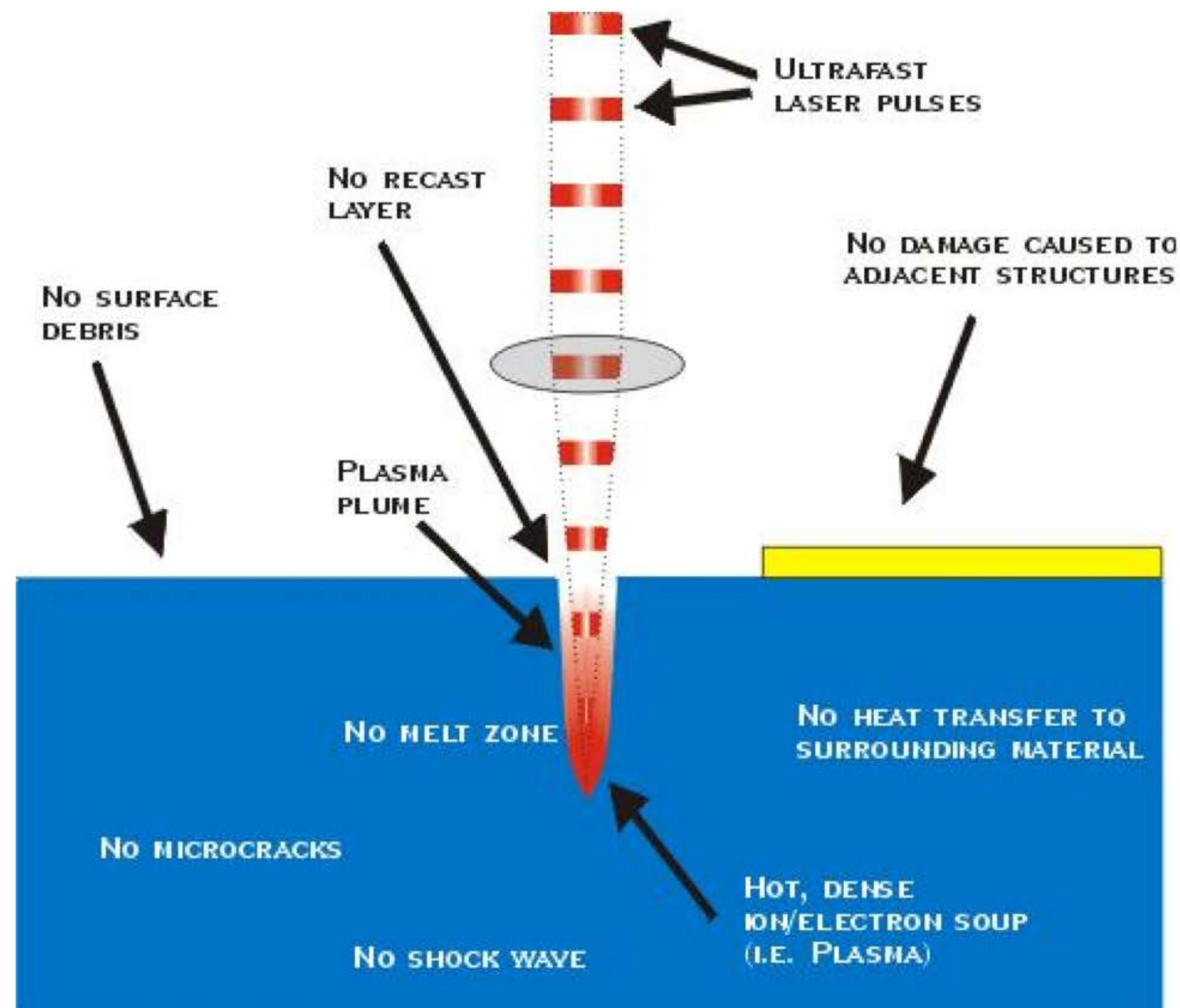
LFC, New Wave Research

New developments: ultrafast washout time : 30 ms! *Wang et al, anal. chem. 2013*



Supercell, New Wave Research

The femtosecond world...



Ultra short pulses : femtosecond lasers

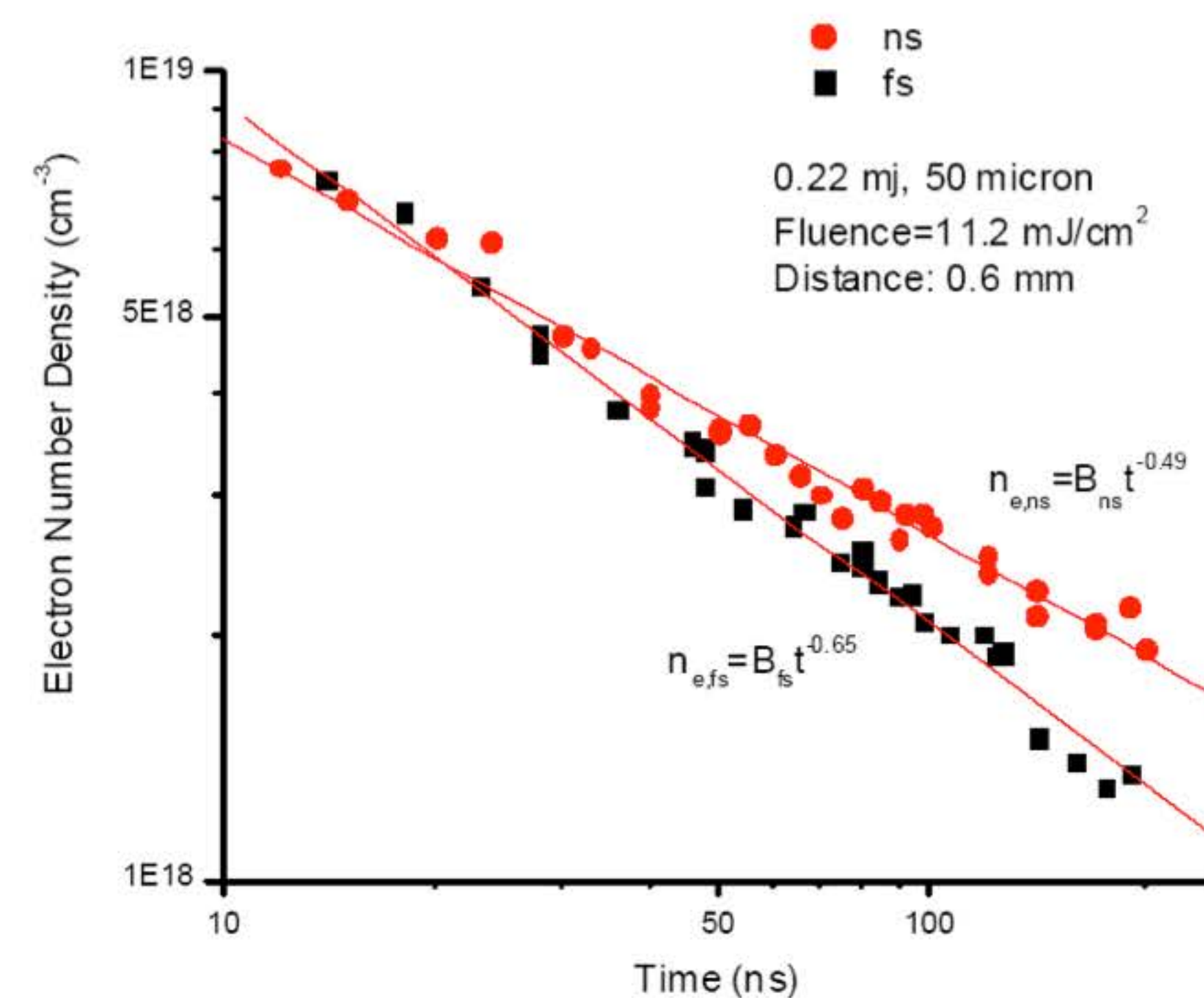
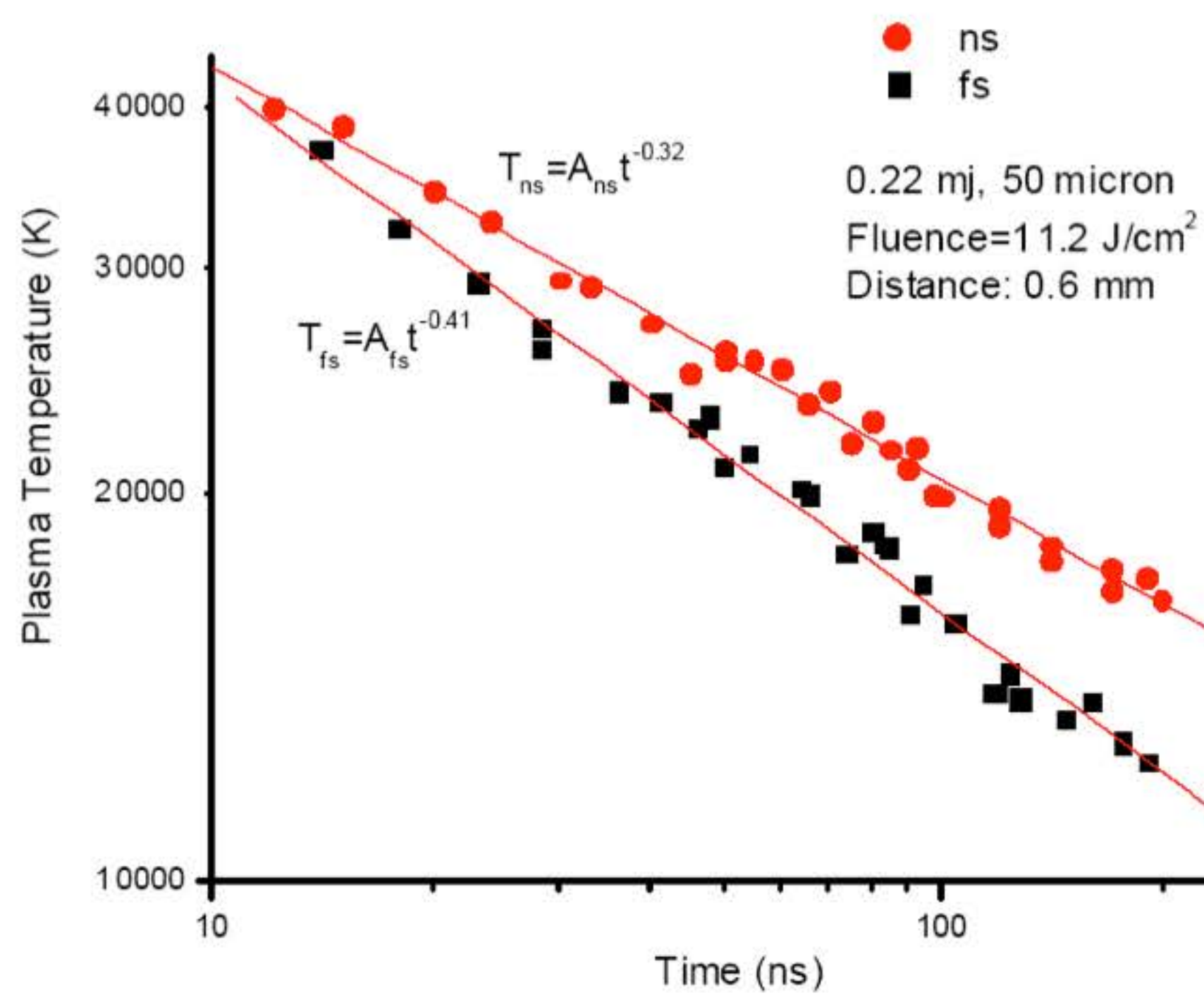
Nanosecond pulses:

Large heated zone
laser/plasma interaction
Large particle ejection due to melting

Femtosecond pulses:

The ablation process is confined in time
and spatially
No laser/plasma interaction
Very thin particles are produced

Less thermal effects



Short pulses versus ultra short pulses

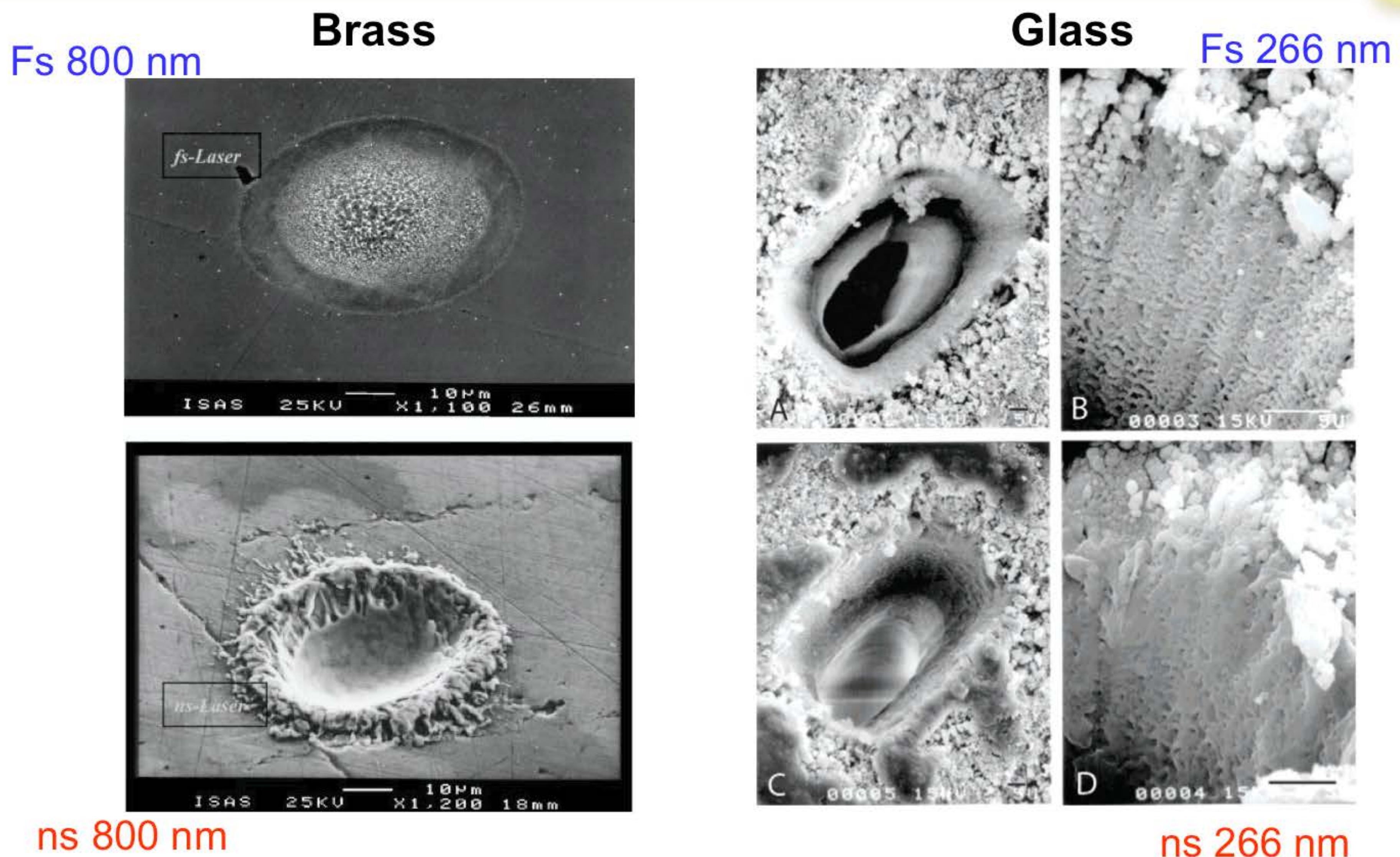


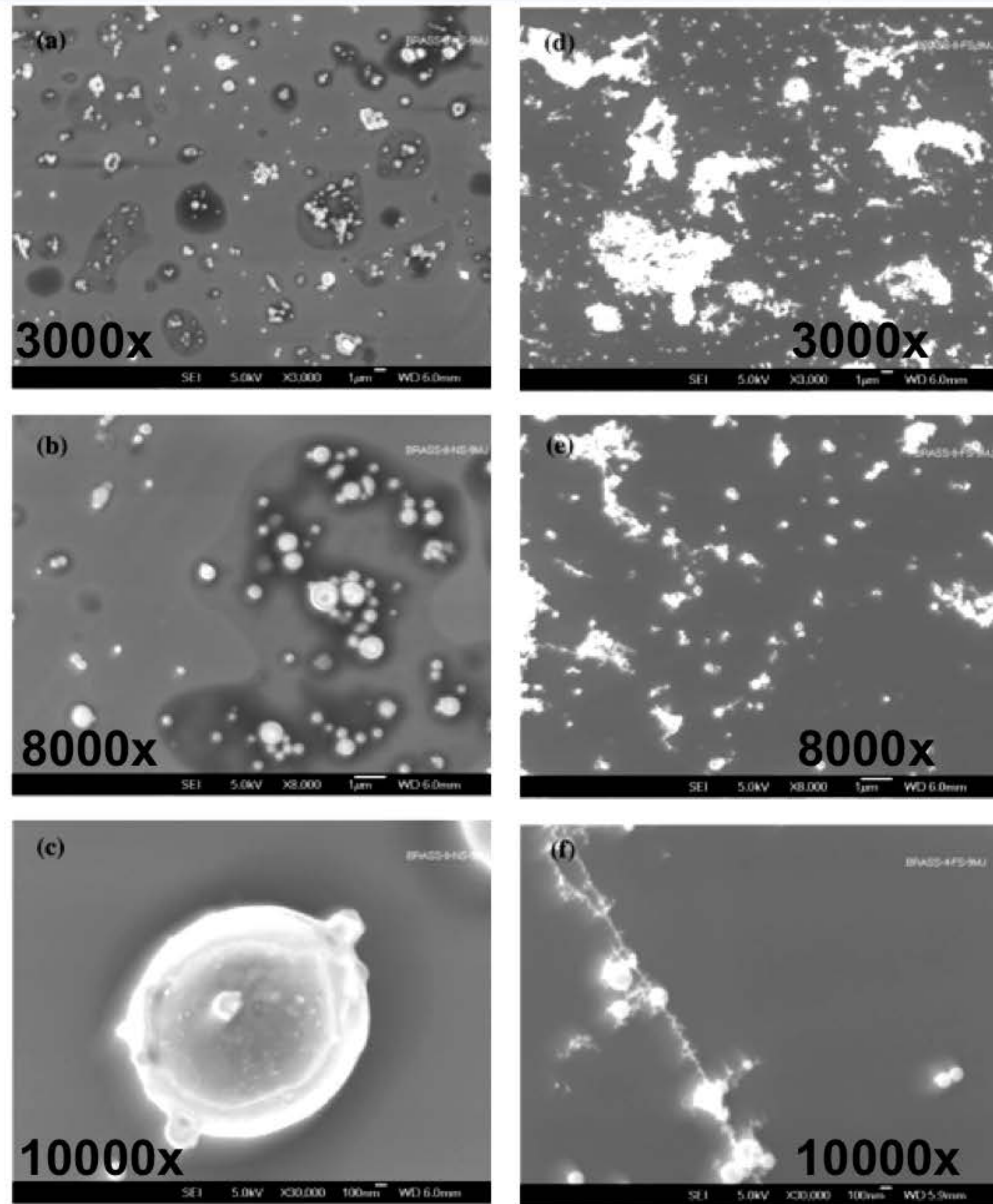
FIGURE 4. Fs- and ns-ablation of polished brass directly revealed different ablation mechanism. In both cases no beam shaping was used. Whereas the fs crater has a clean rim, the ns crater shows the typical pattern of melting. (Modified from Elsevier, Spectrochim. Acta B 55(2000)1771).

Poitras et al, Anal. Chem, 2003, 75, 6184-6190

Short pulses versus ultra short pulses

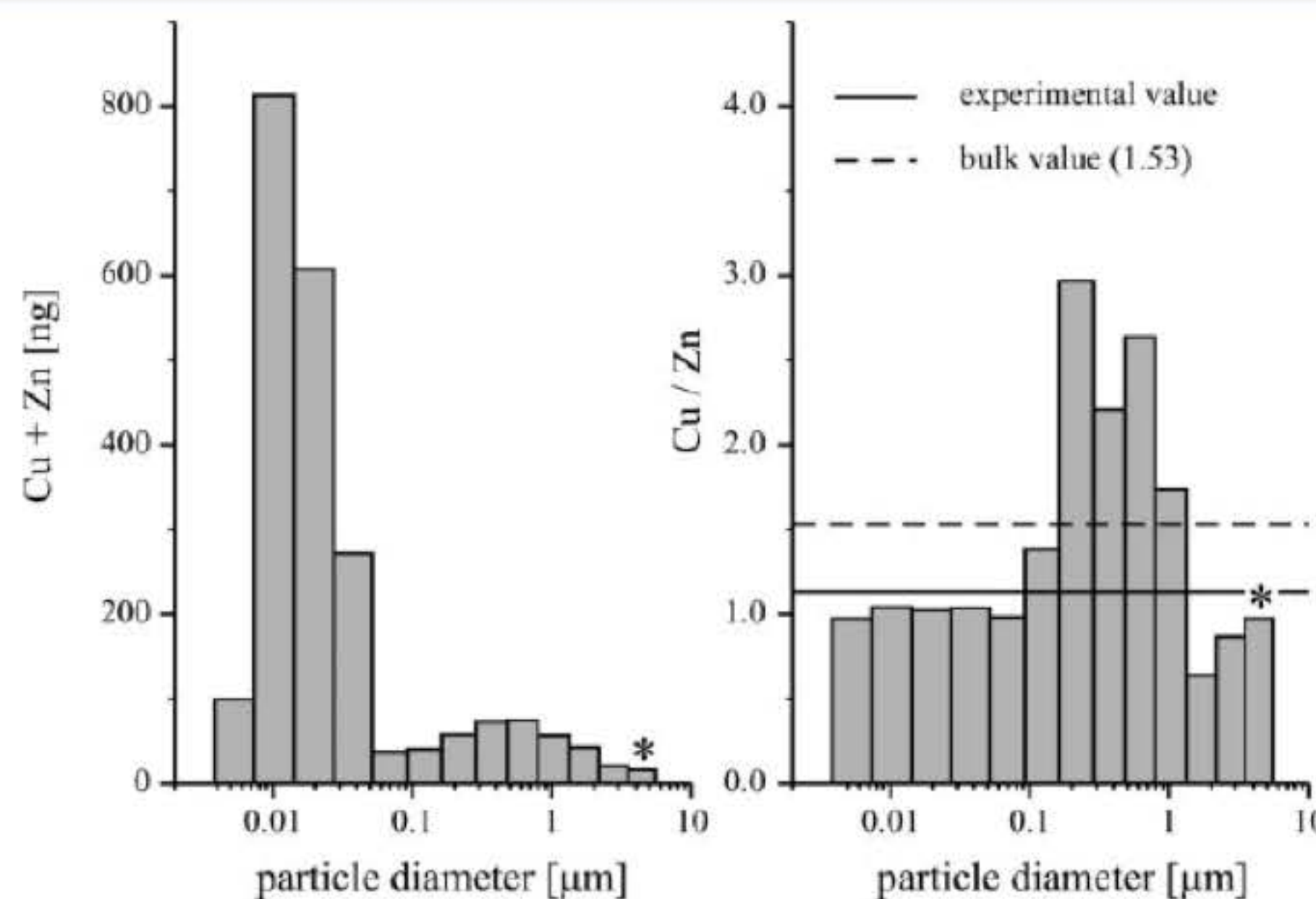
Brass

Nanosecond ablation 266 nm



Femtosecond ablation 266 nm

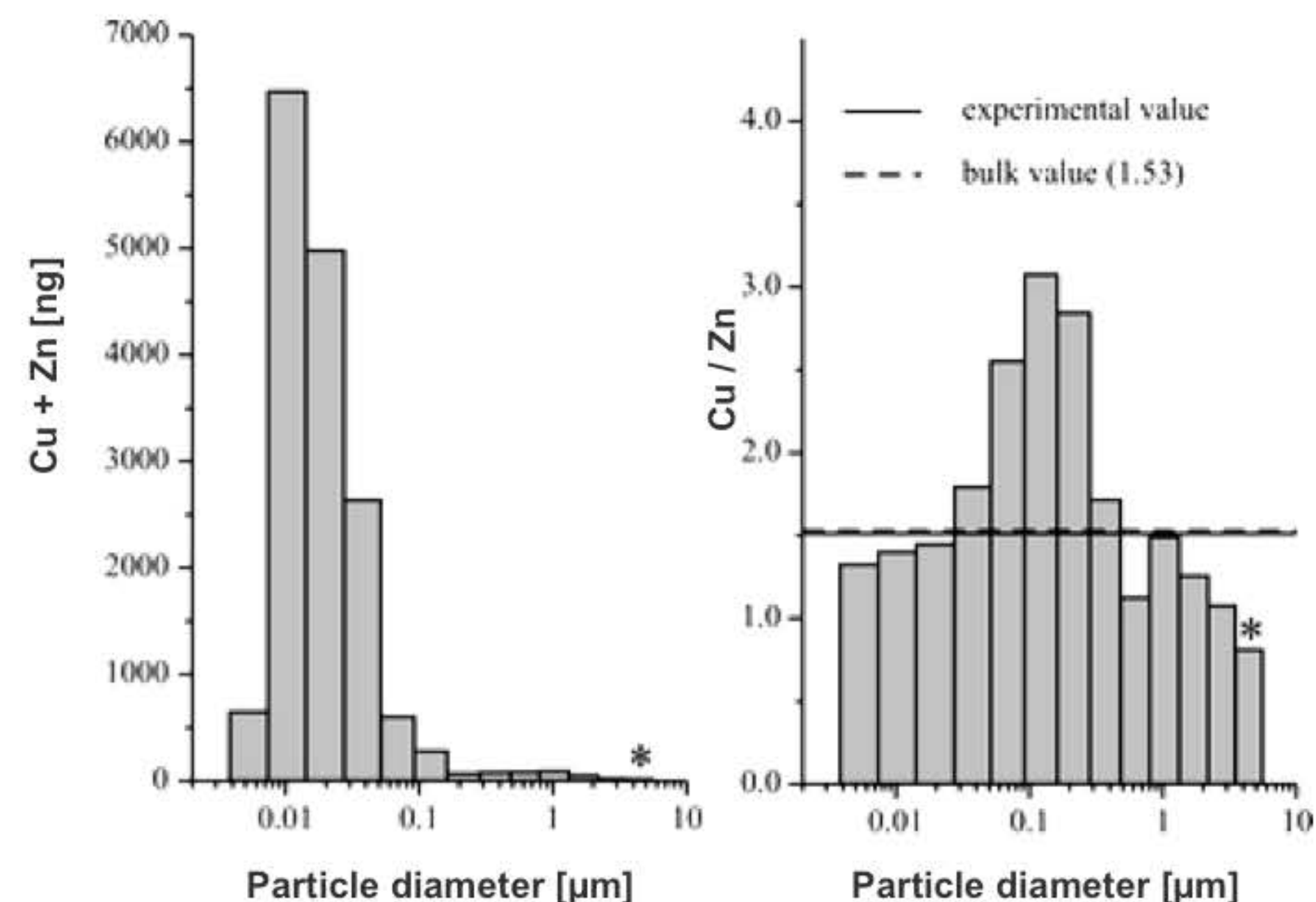
Short pulses versus ultra short pulses



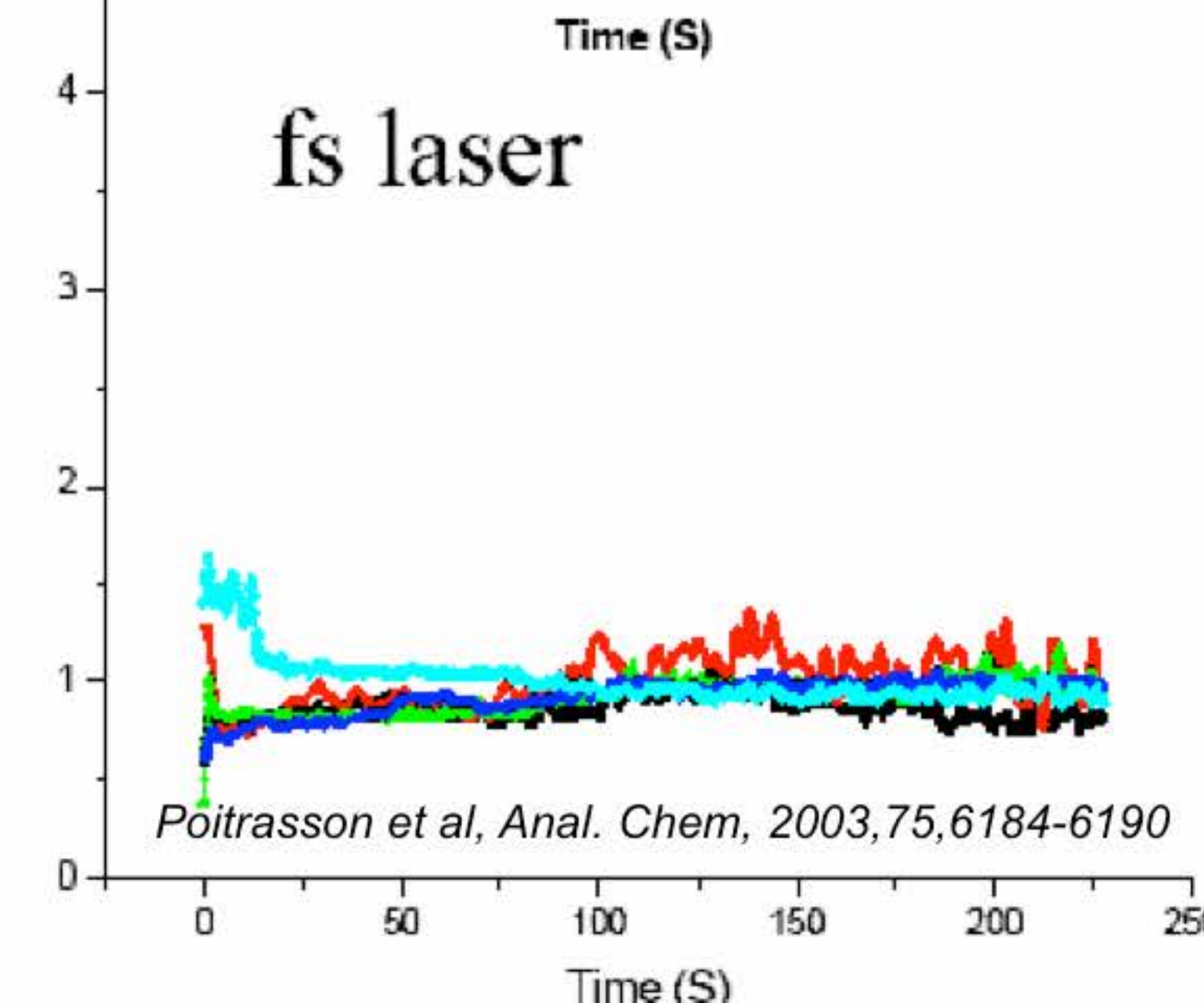
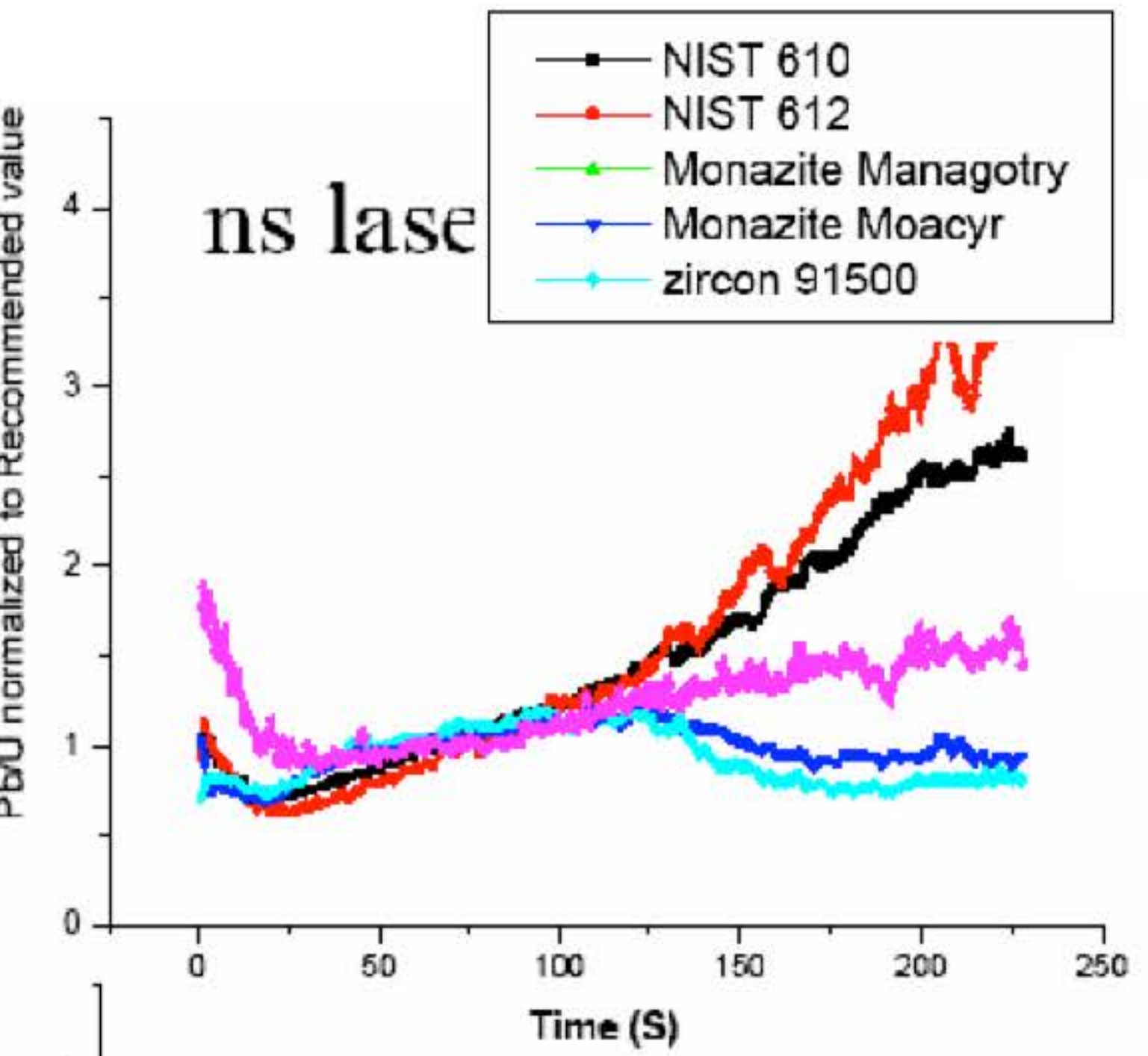
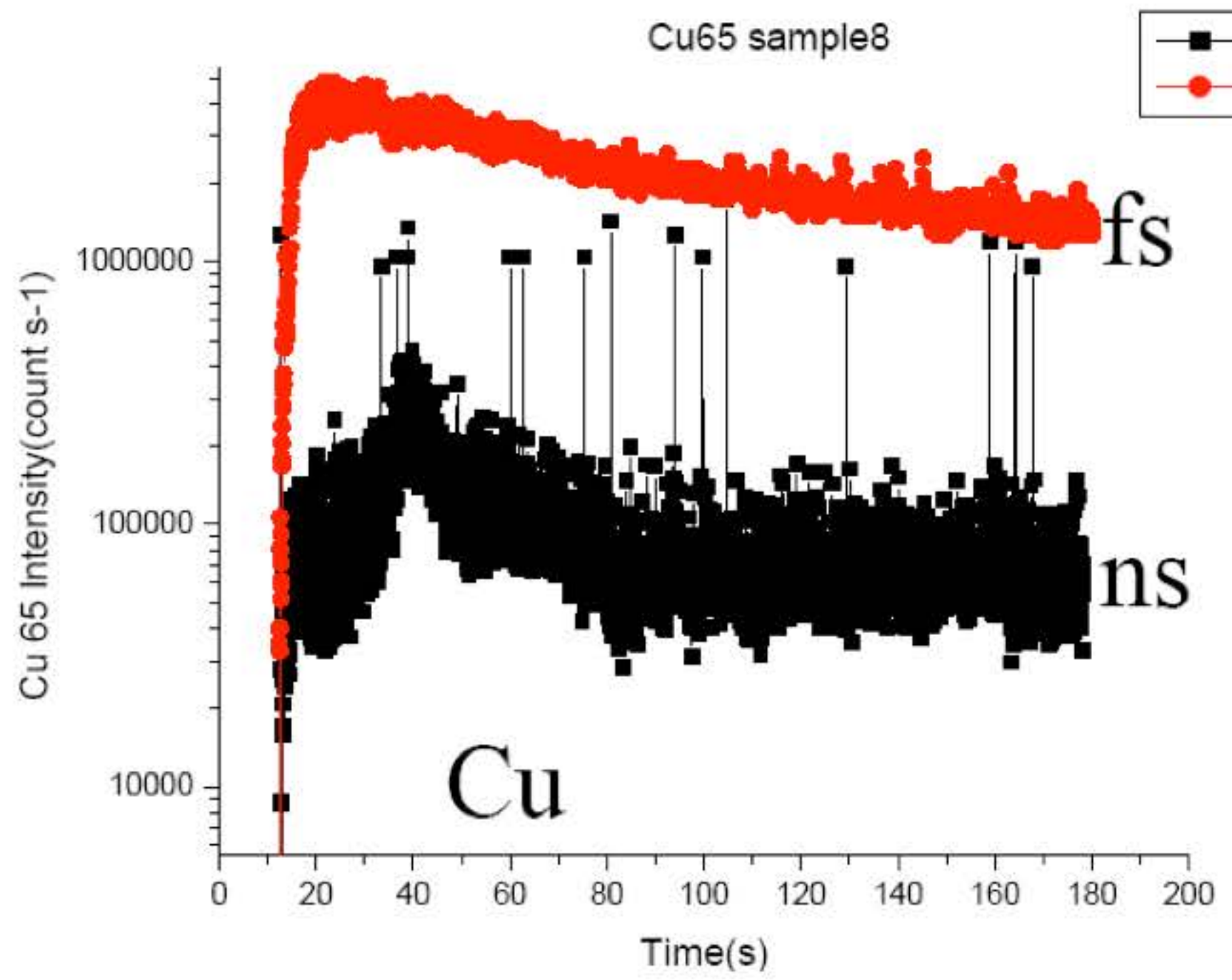
Particle size distributions

**800 nm femtosecond LA
He, fluence 2.5 J.cm²**

**800 nm nanosecond LA
He, fluence 2.5 J.cm²**



Short pulses versus ultra short pulses



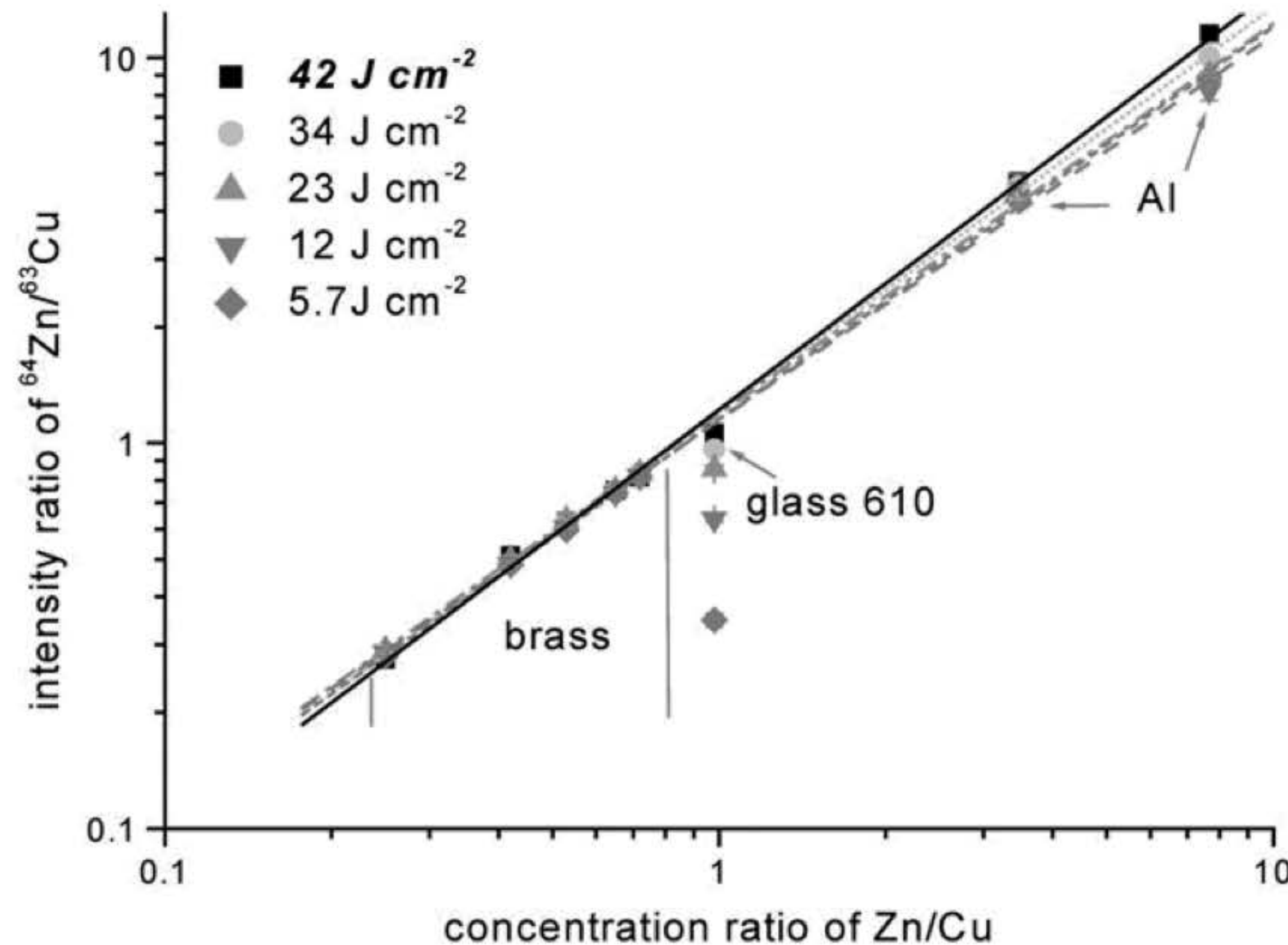
Very limited elemental fractionation due to:

- Very limited thermal effect (no preferential evaporation)
- production of thin particles easily atomised in the ICP
- Augmentation du signal d'un facteur 10

Stability improvement

Sensitivity improvement (mostly on metals)

Is non matrix match calibration possible?

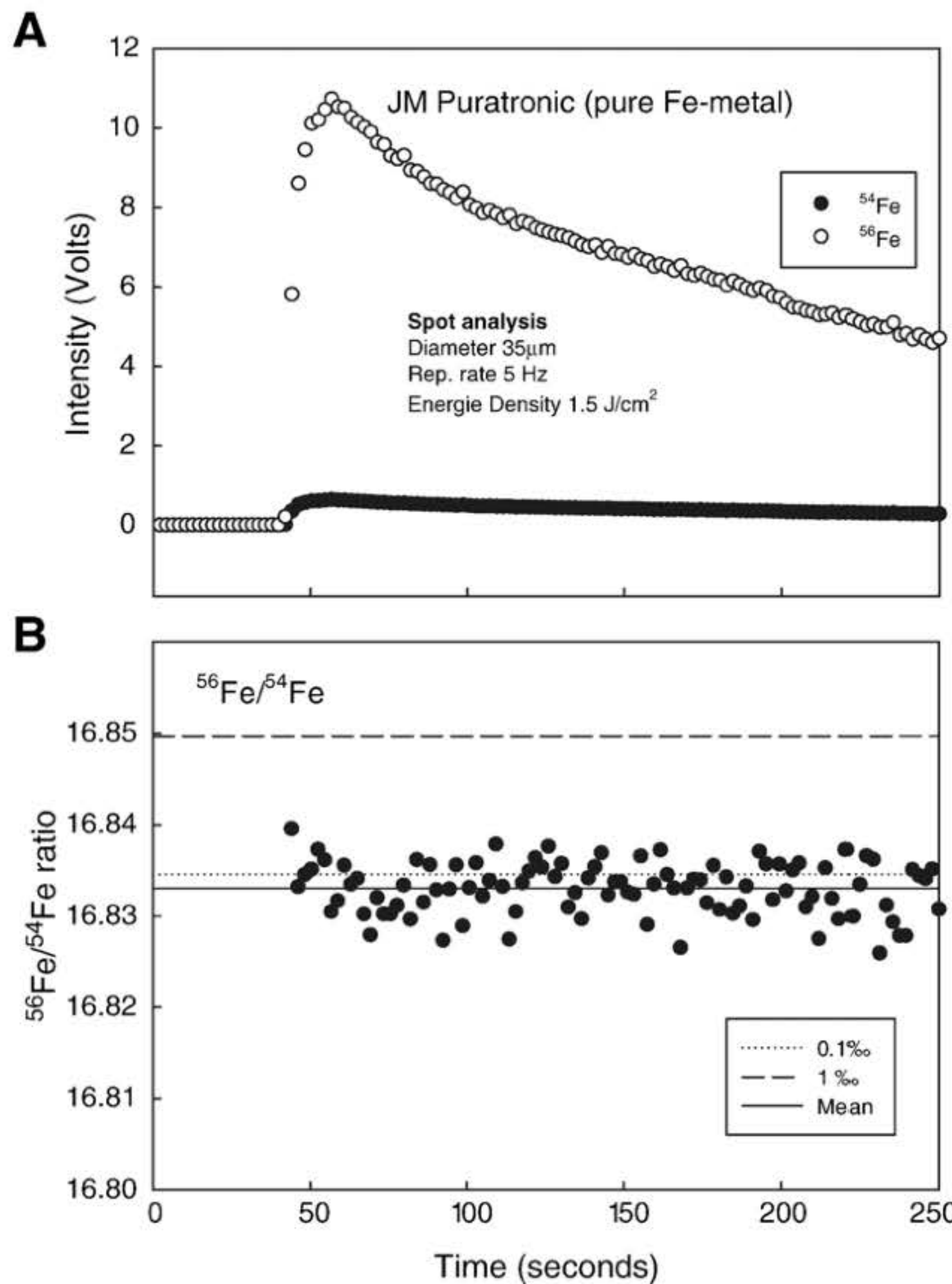


Non-matrix matched calibration

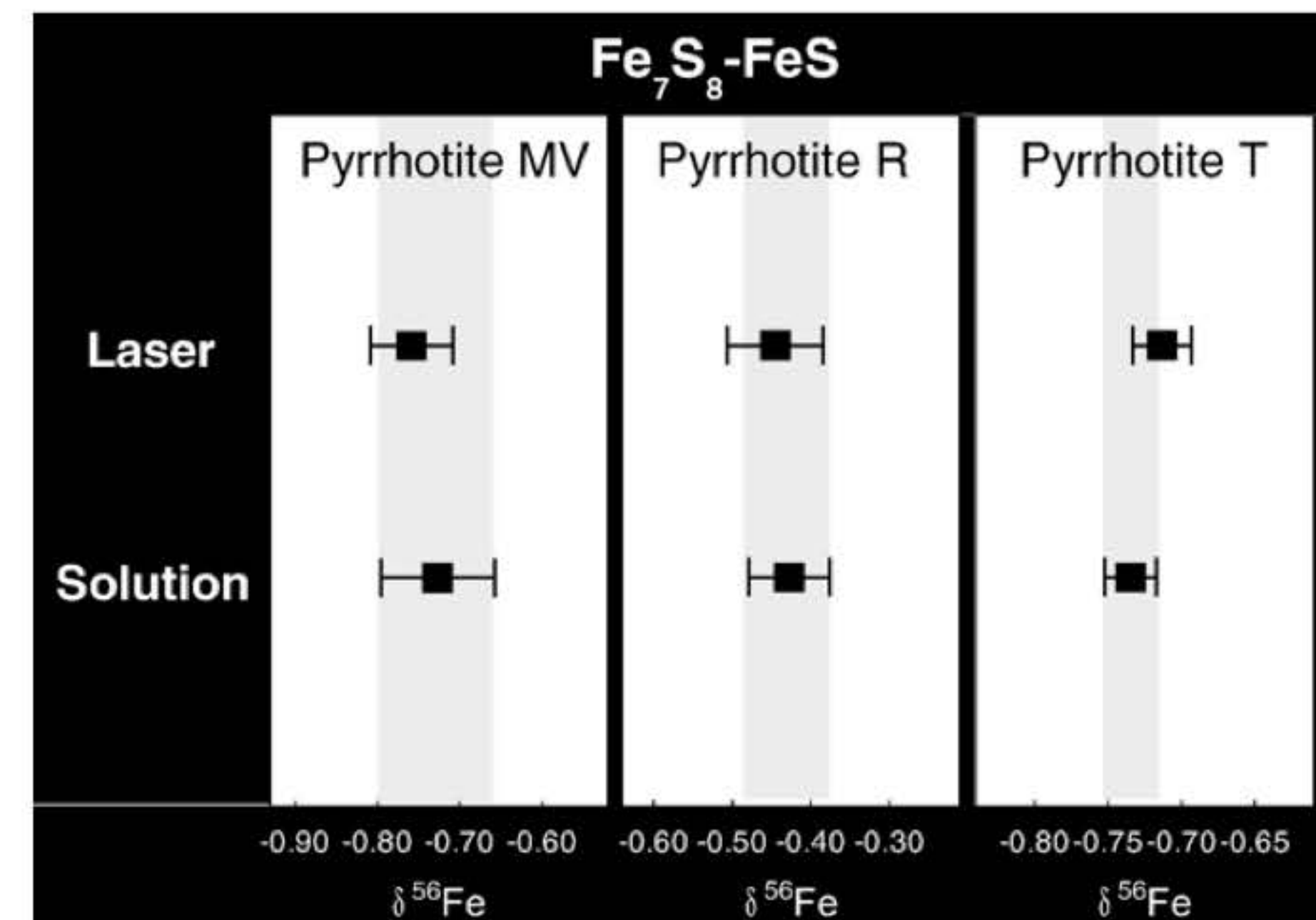
- High fluence for glass sample
- Low fluence for high thermal conductivity and low melting point sample (Al)

Fig. 3 The experimental $^{64}\text{Zn}/^{63}\text{Cu}$ ratio against the certified ratios for five brass, two aluminium and one glass sample measured with different fluences. The straight lines represent fits to the measured data (full line 42 J cm^2 ; dotted line 34 J cm^2 ; dashed-dotted line 23 J cm^2 ; dashed line 12 J cm^2 ; short dashed line 5.7 J cm^2). The data for 42 J cm^2 were recorded with a tighter focused beam while the fluence of the other measurements was varied by attenuation of the laser beam.

Isotopic fractionation?

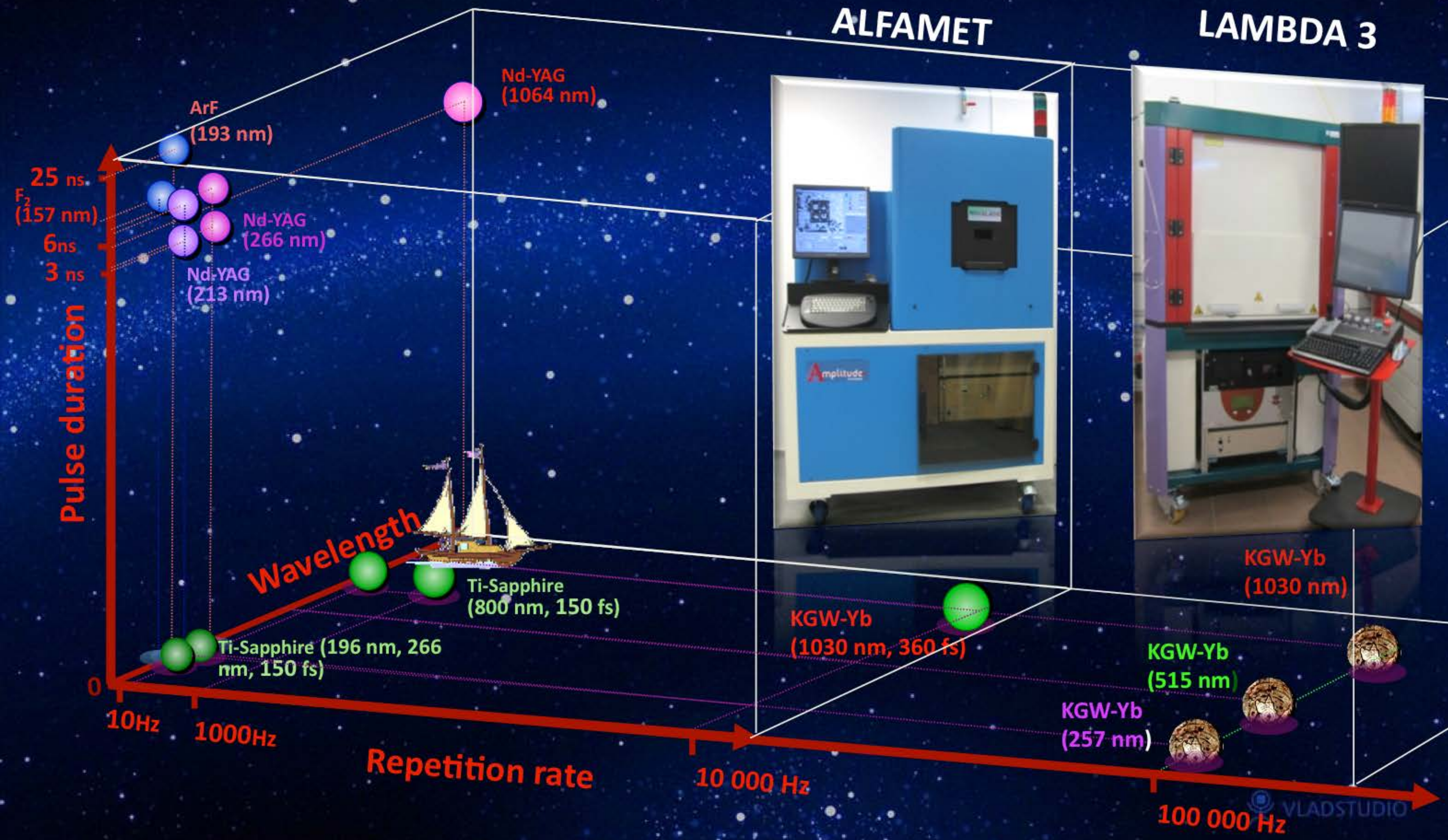


196 nm Fs LA/MCICPMS



No apparent isotopic fractionation

More wavelengths, higher repetition rate...



High repetition rate femtosecond laser...

s-Pulse oscillator/amplifier femtosecond laser

- Low energy (less than 2 mJ)
- High repetition rate (<100 kHz)
- pulse duration = 360 fs
- Crystal : KGW doped with Yb , 1030 nm in the fundamental



- Diode pumped laser
 - Compact
 - Robust

<10 kHz
E < 0,1 mJ



<100 kHz
E < 2mJ

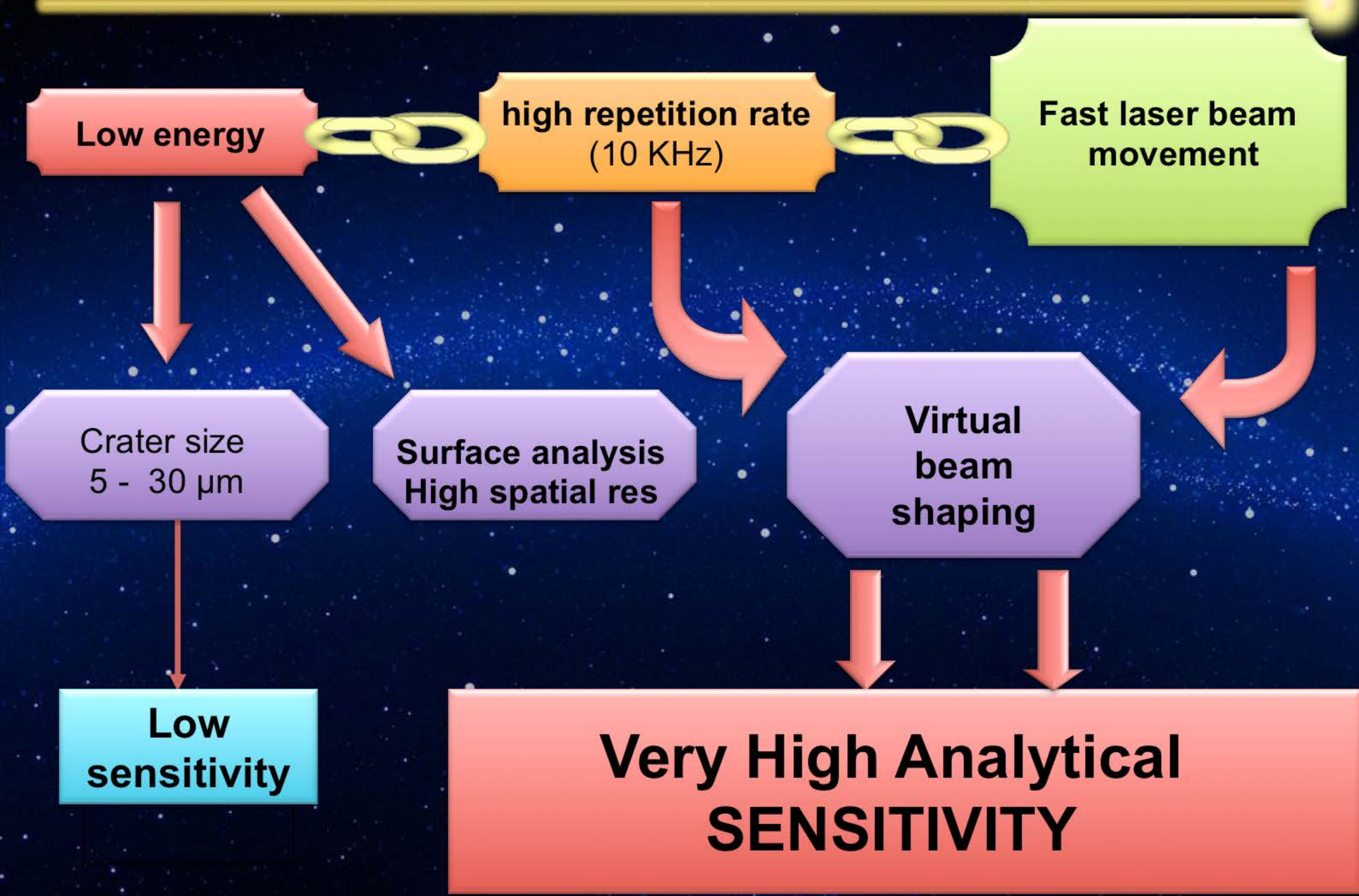
First High repetition rate femto-ICPMS...

Alfamet : developed by LCABIE - Amplitude - Novalase

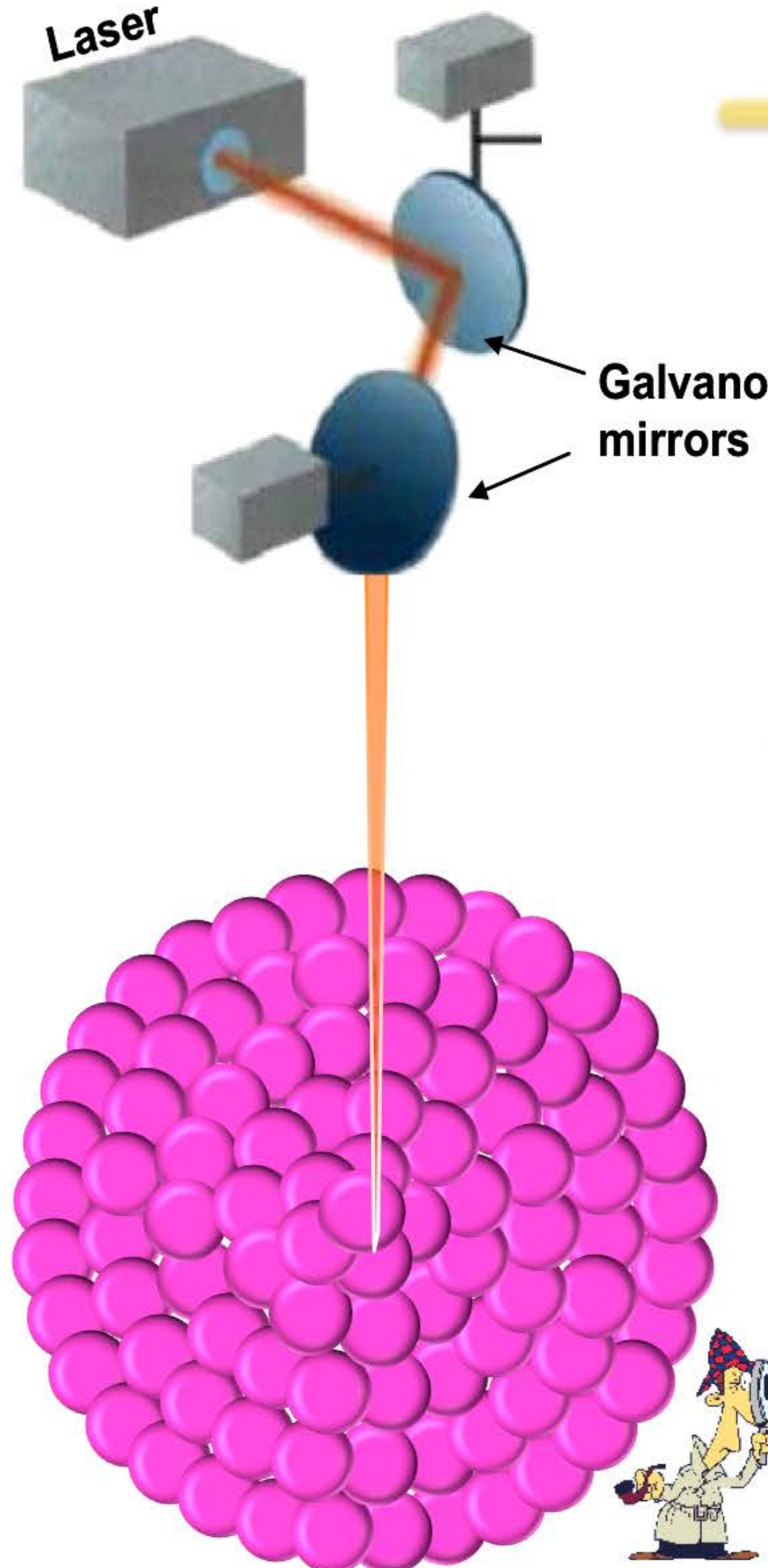


- Fs pulses
- Compact
- Mobile
- Fully integrated
- Automated
- High spatial resolution
- Precise energie control
- High analytical performances
- Low energy
- High repetition rate

First High repetition rate femto-ICPMS...



Virtual beam shaping



High repetition rate (<100 kHz)

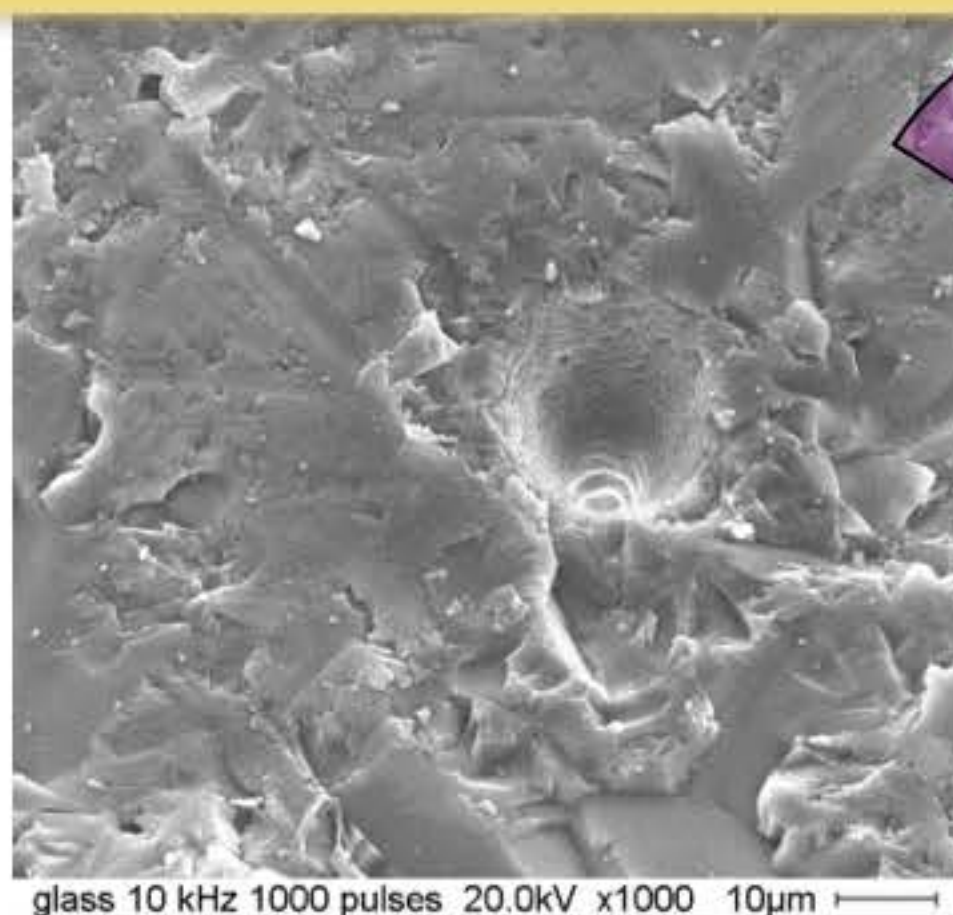
Small crater
($\approx 10 \mu\text{m}$)

Fast beam scanning
(<2 m/s)

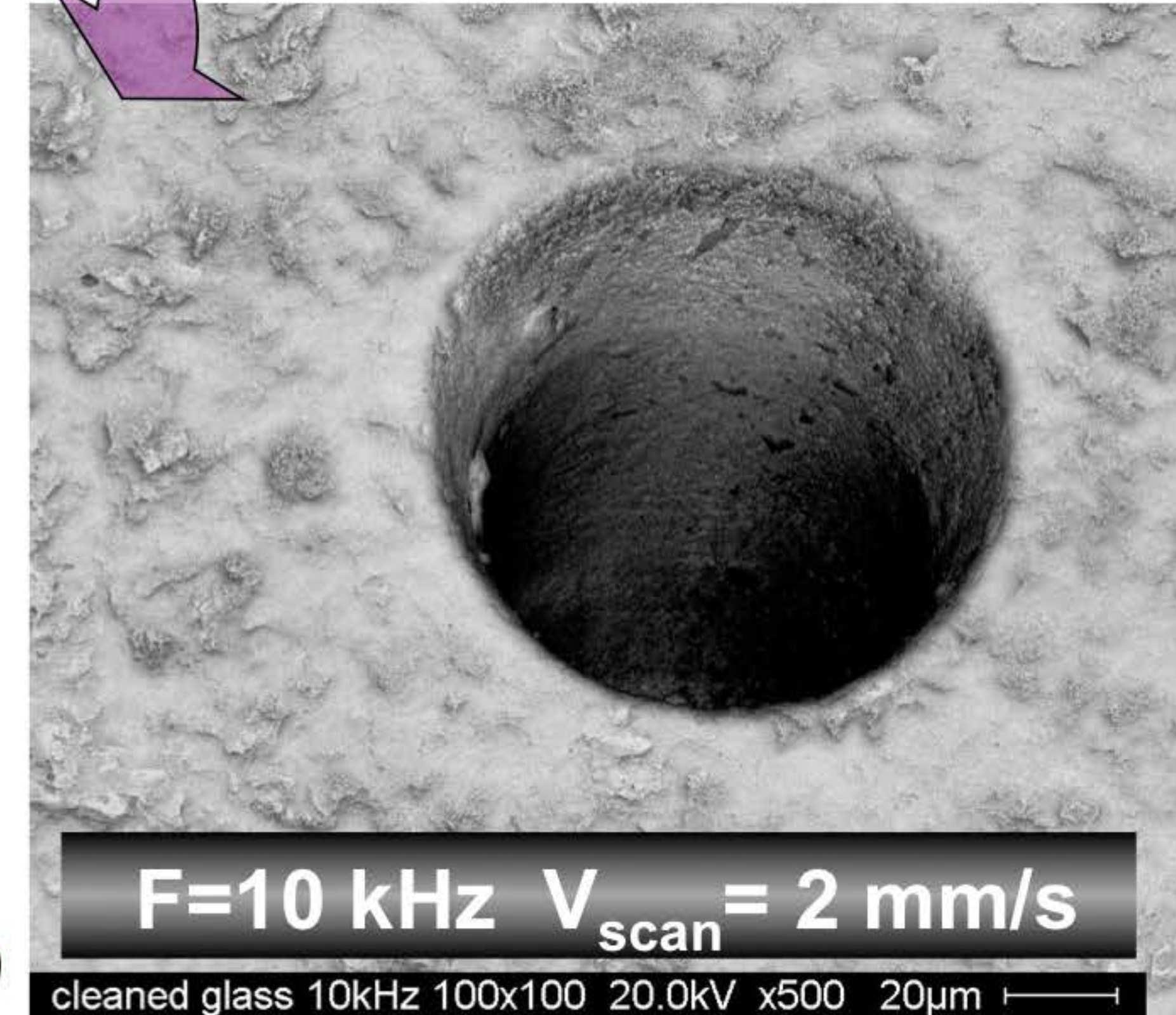
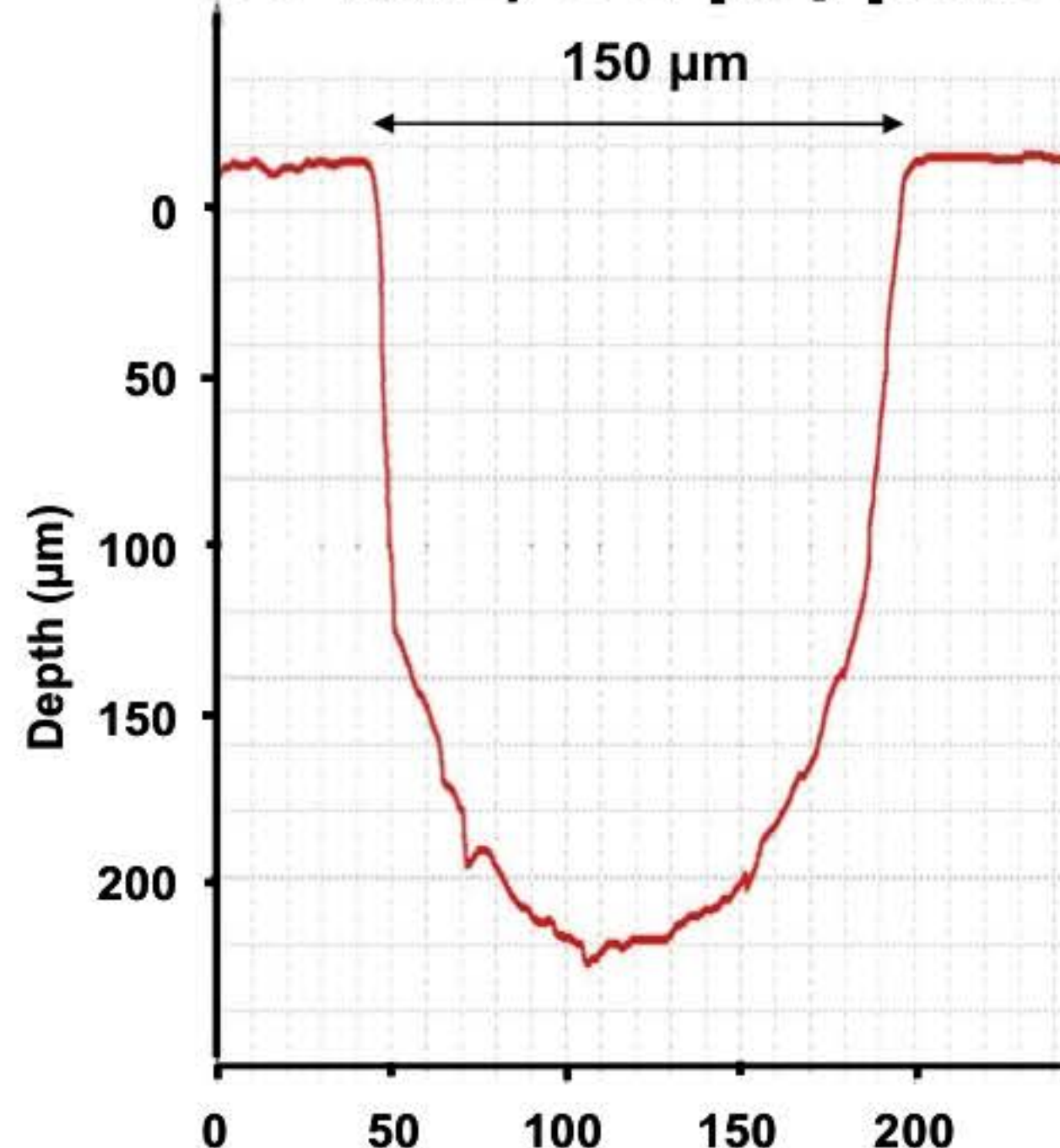
We can virtually adjust the apparent beam shape and size

The virtual beam shape is achieved in few ms

Virtual beam shaping for flash ablation

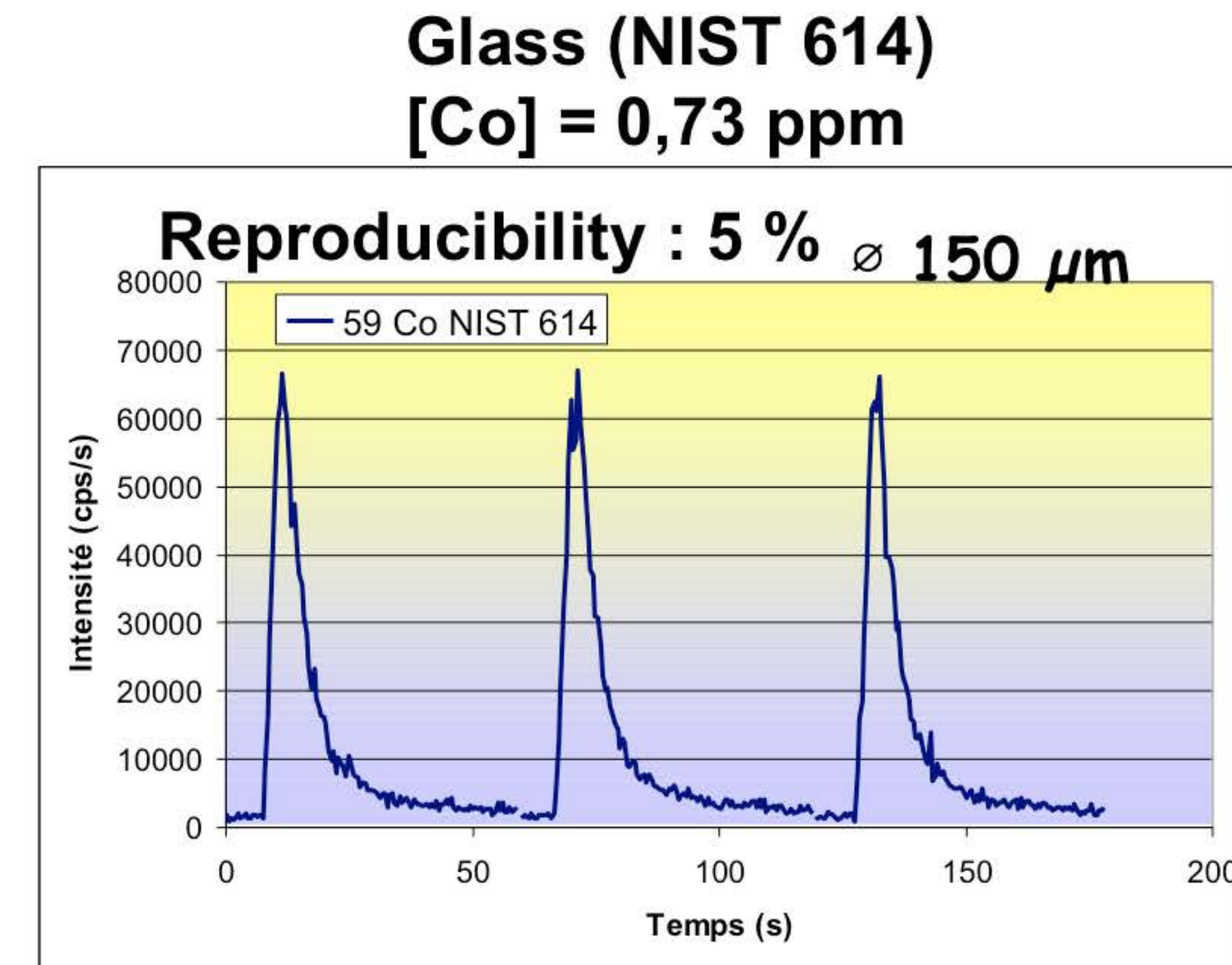
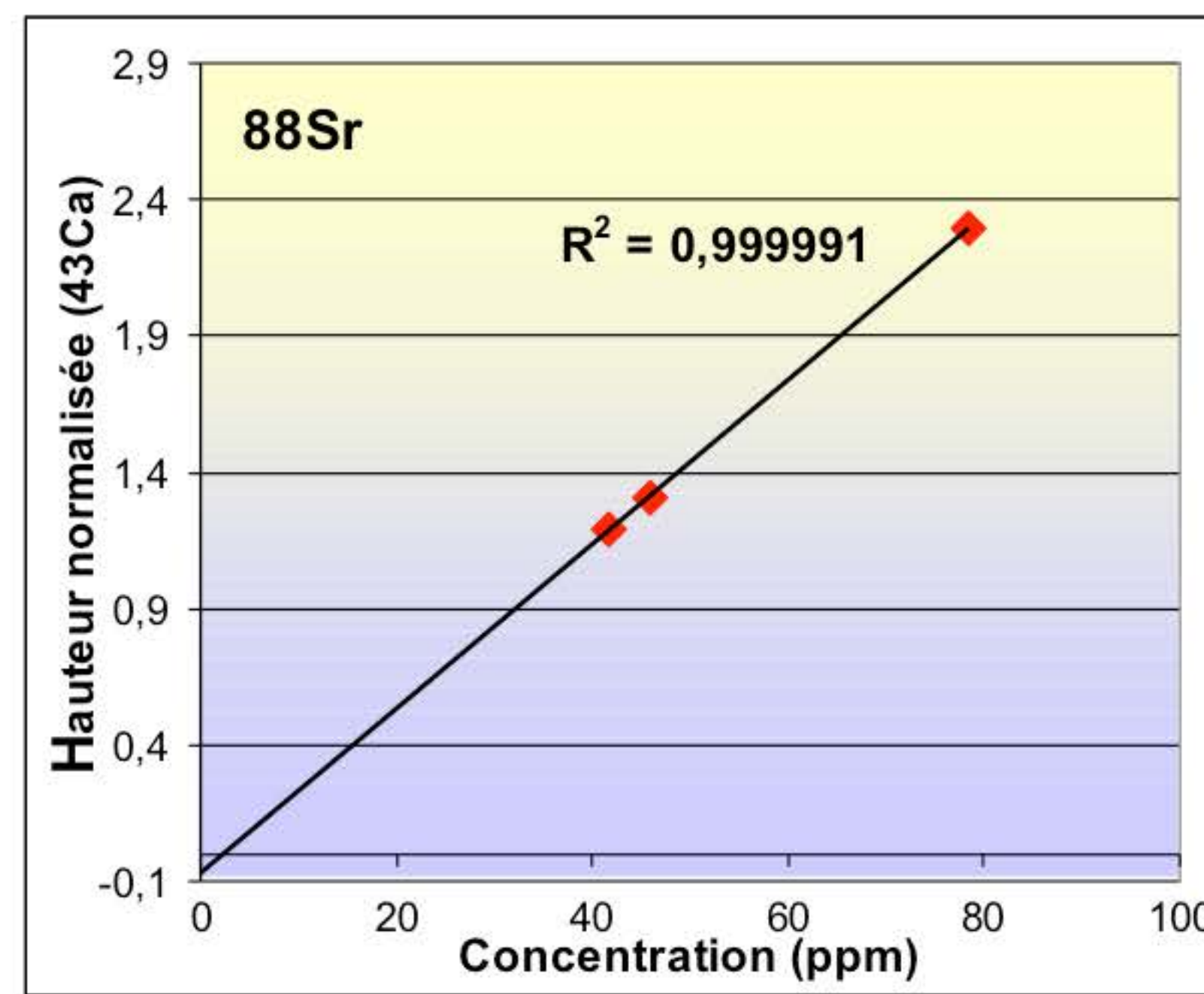
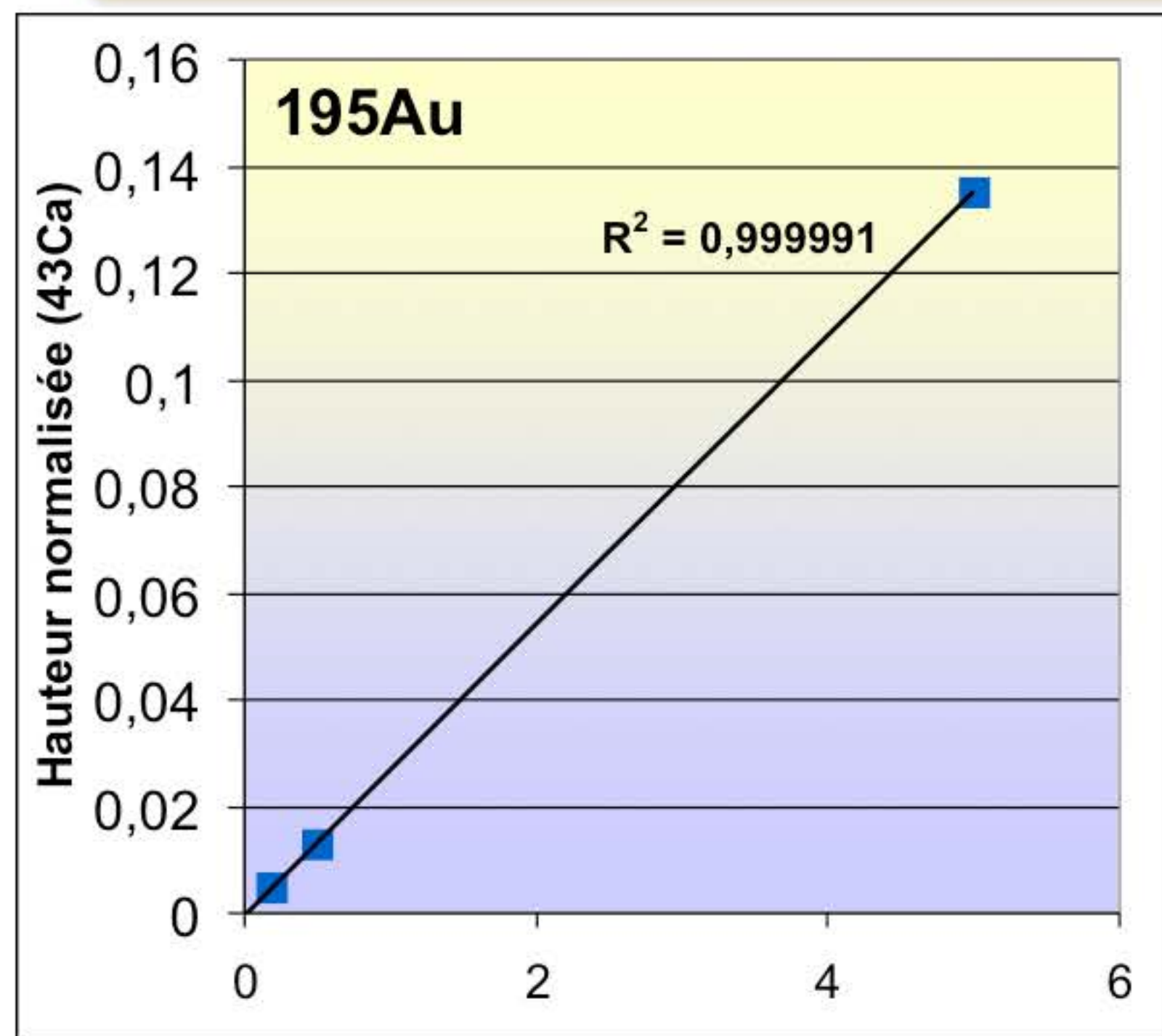


**Crater profile
10 kHz, 31 μJ/pulse**



6 concentric circles
4710 craters in 0.47 s X 100 times
 $\Delta x = 0.2 \mu\text{m}$
Overlapping area = 99 %

Virtual beam shaping for flash ablation



Max energy (here 0,5 uJ) @ 10 KHz

Virtual beam shaping for flash ablation : LOD

Using a Thermo X7 quad ICPMS

Femtosecond (360 fs)
flash ablation

@ 150 µm

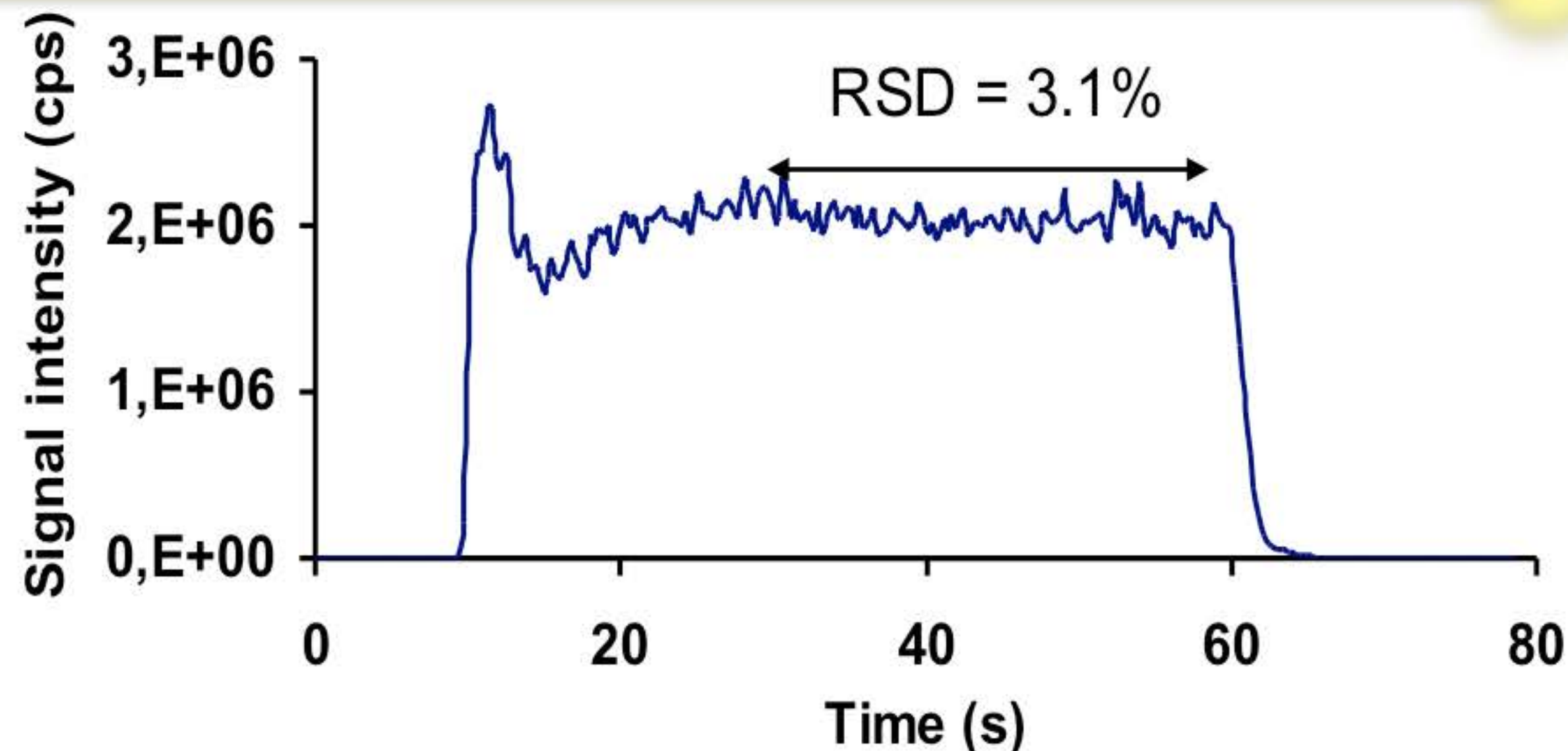
Nanosecond (8 ns)
UV 266 nm, 20 Hz, 2mJ

Limites de détection (ng/g)	(nist 612) Femtoseconde	Improvement factor compared to 266 nm ns laser
^{59}Co	14,1	x 25
^{65}Cu	38,6	x 12
^{88}Sr	3,3	x 26
^{107}Ag	1,10	x 8
^{111}Cd	7,83	
^{197}Au	0,73	x 10
^{205}Tl	0,42	x 13
^{208}Pb	1,10	x 11
^{232}Th	0,15	x 41
^{238}U	0,13	x 16

Signal stability

Femtosecond IR 1030 nm

Energy : 75 μ J/pulse
Repetition rate : 500 Hz
Ablated width : 100 μ m;
Stage speed: 10 μ m/s

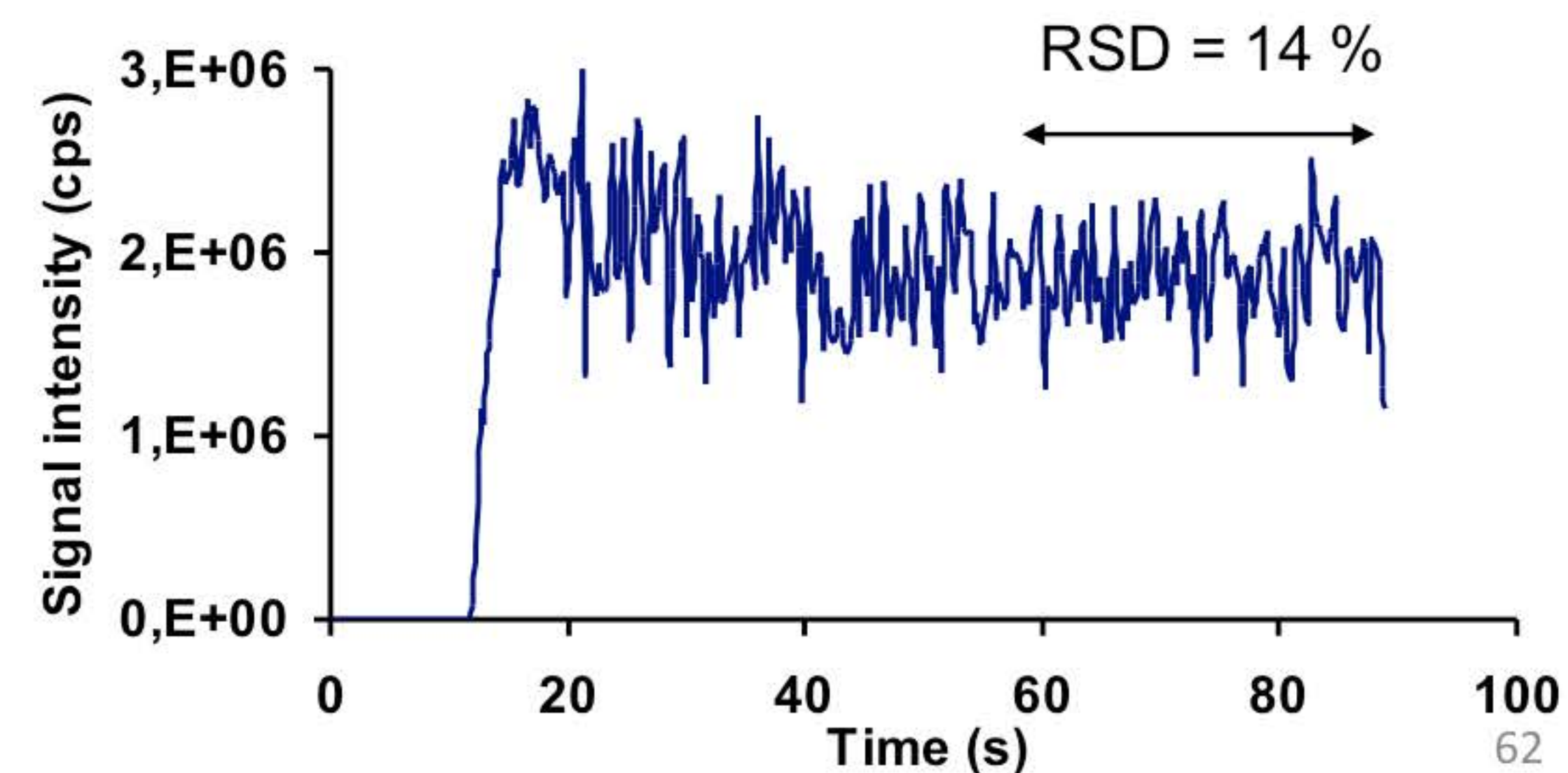


Single line scanning ablation mode

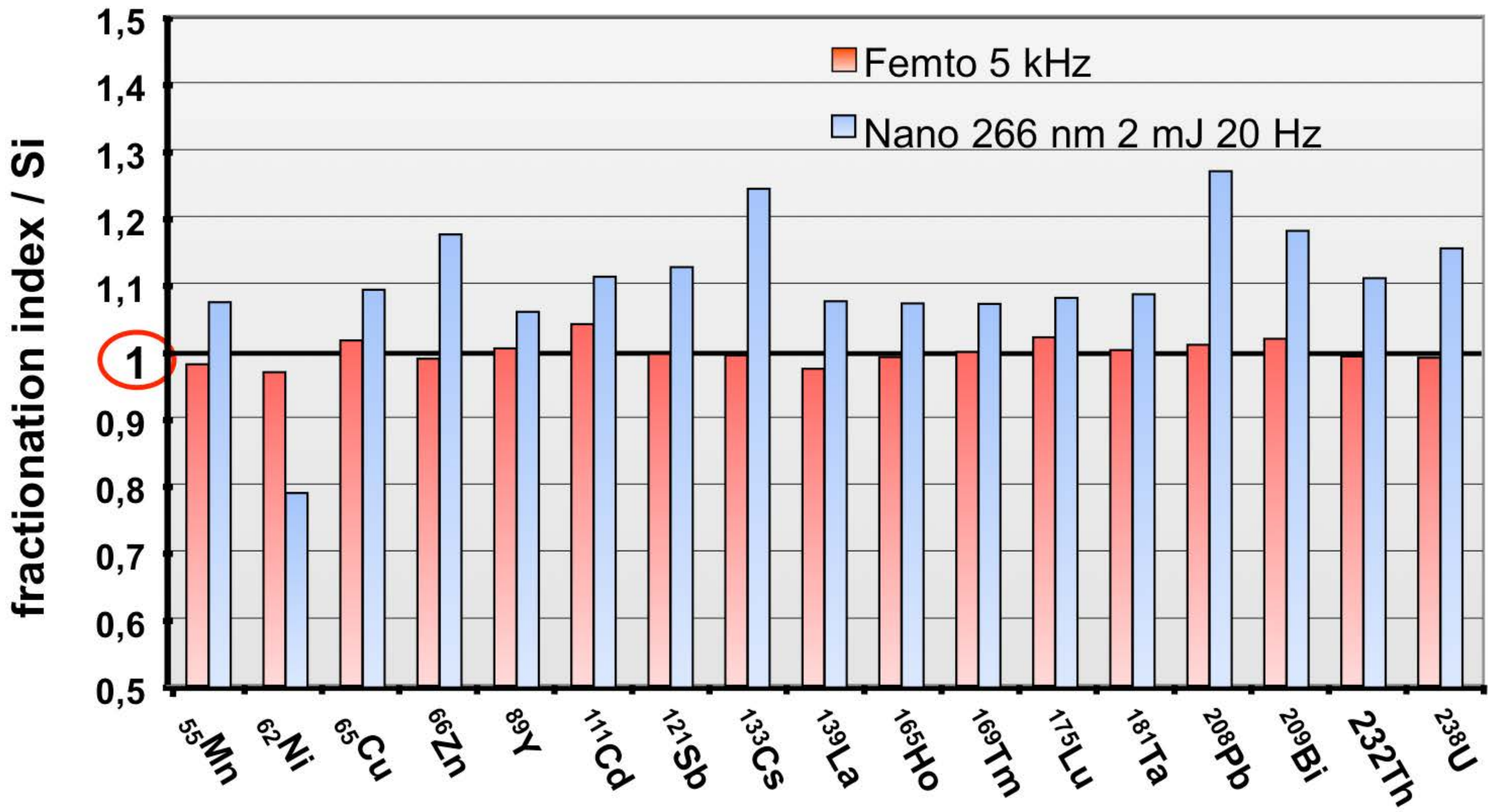
Ablation of a certified glass sample (NIST 612) Indium

Nanosecond UV 266 nm

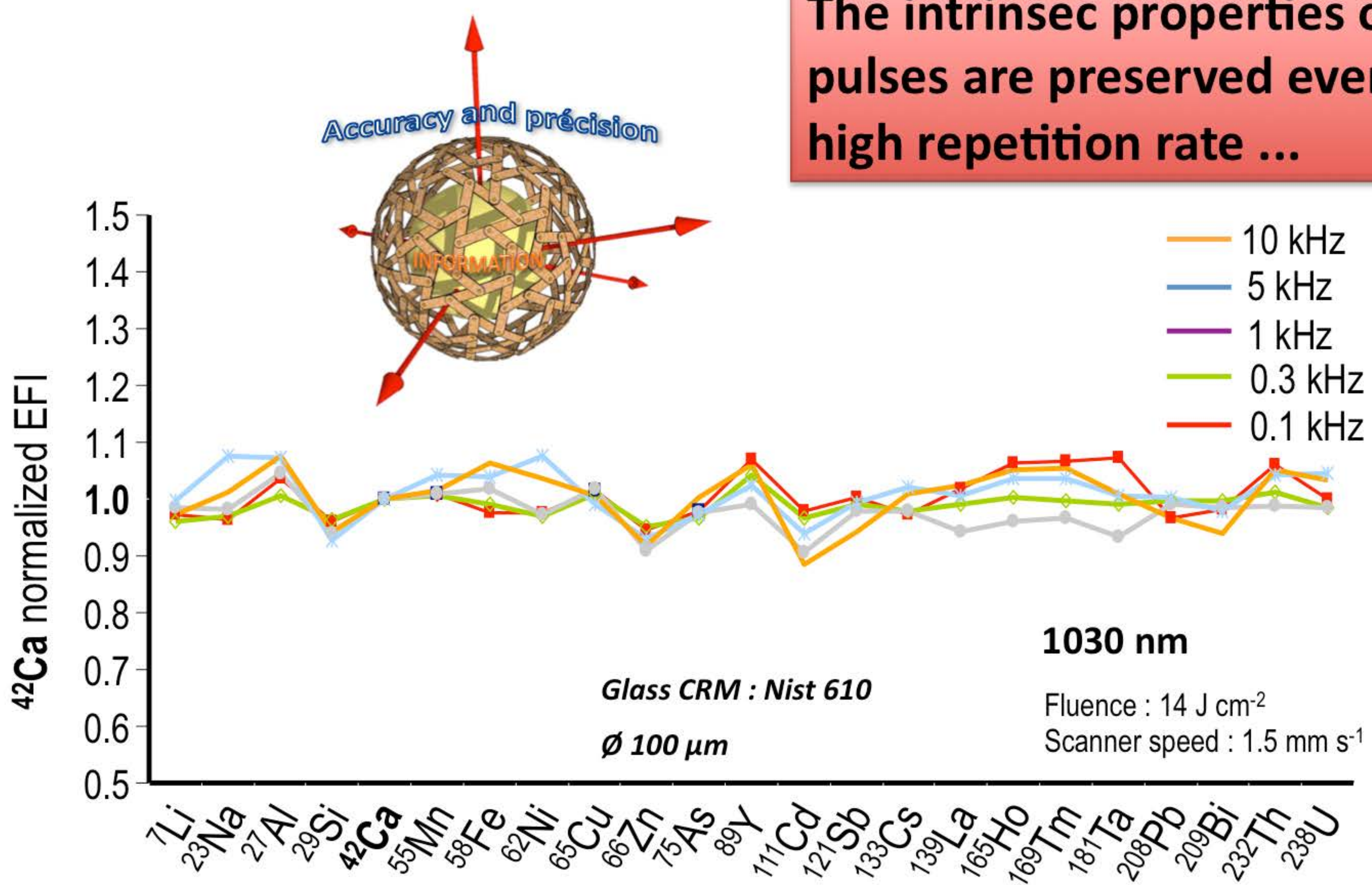
Energy : 1.3 mJ μ J/pulse
Repetition rate : 20 Hz
Ablated width : 100 μ m;
Stage speed: 10 μ m/s



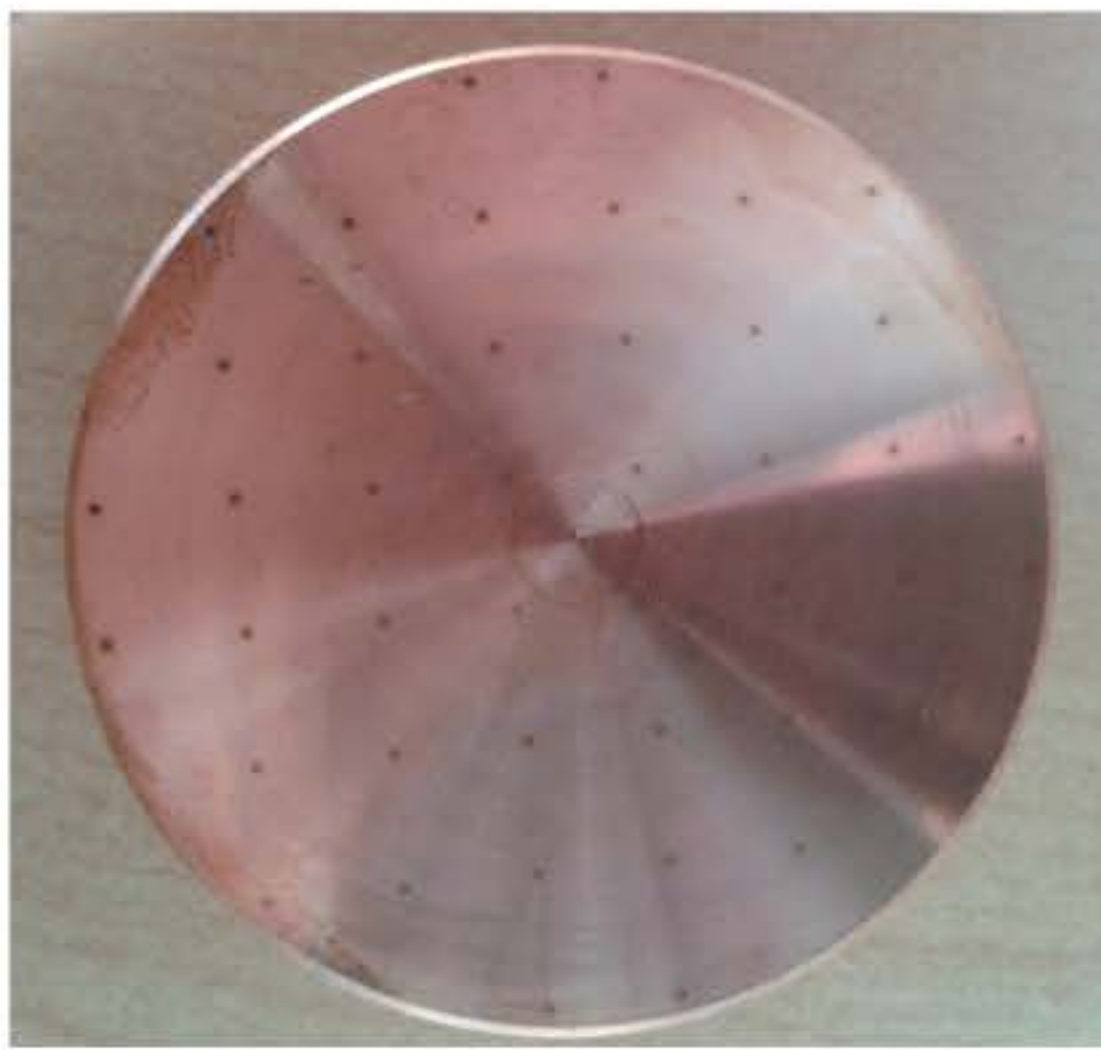
Elemental fractionation



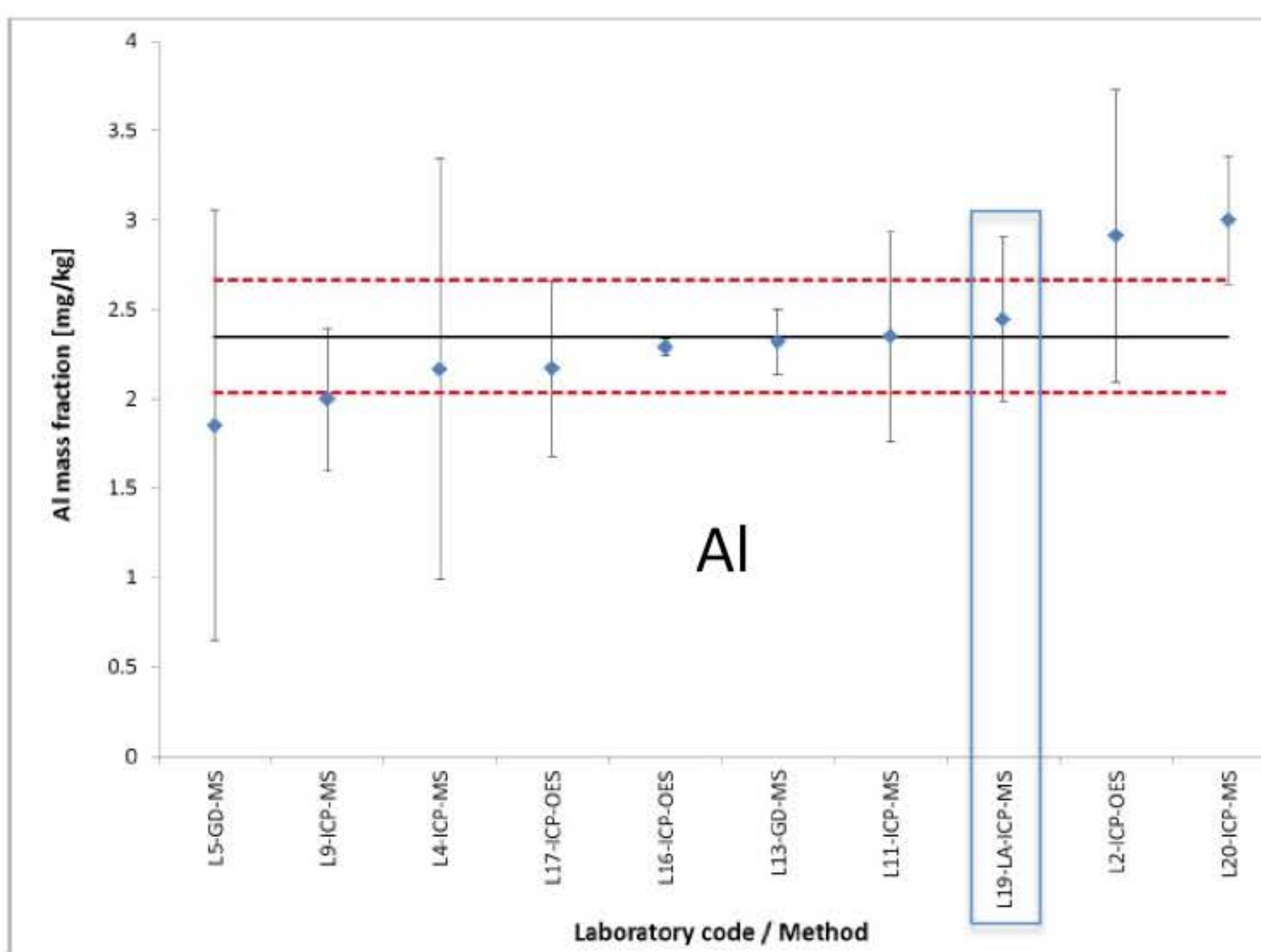
Elemental fractionation



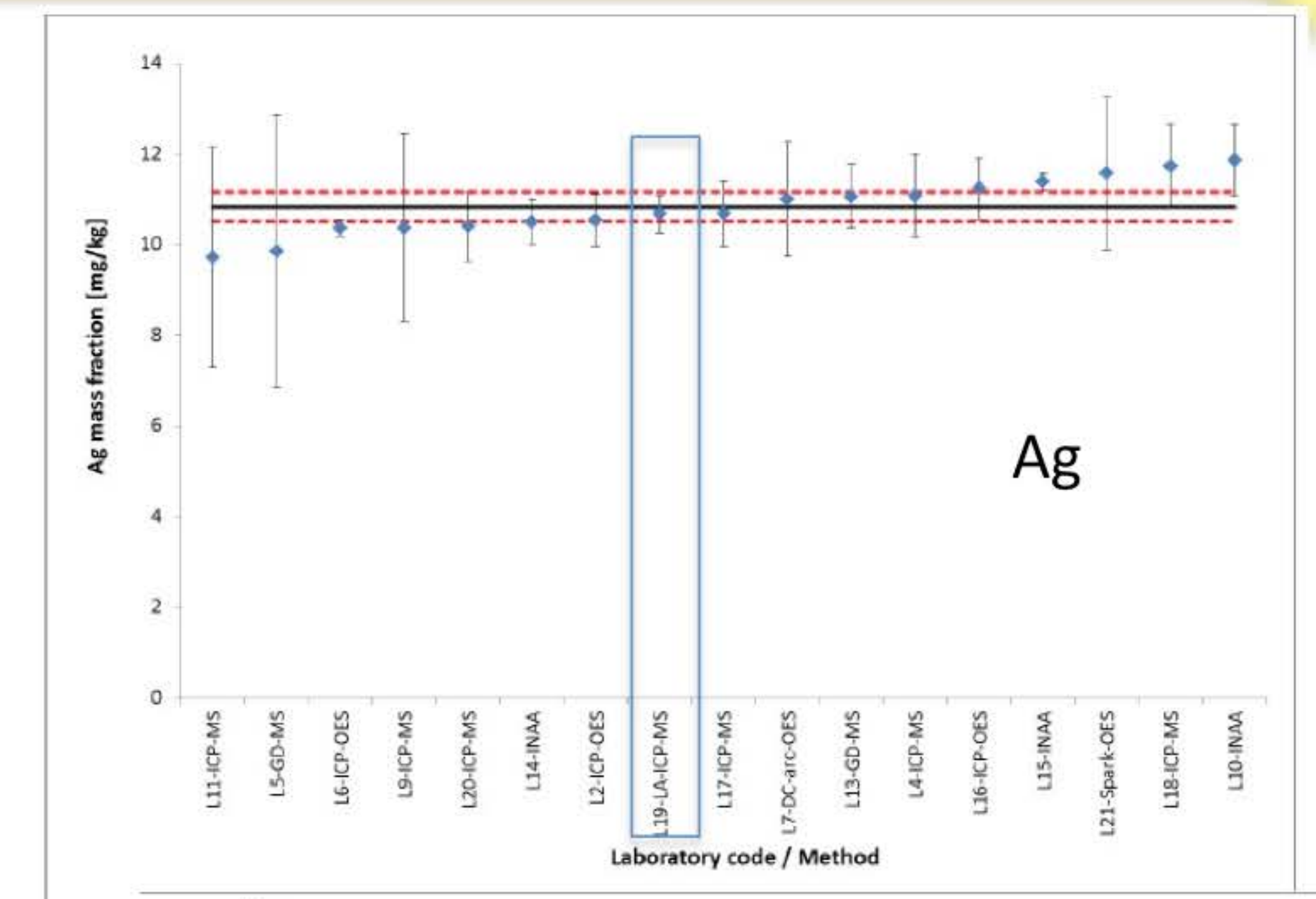
Trace elements in copper – Round Robin



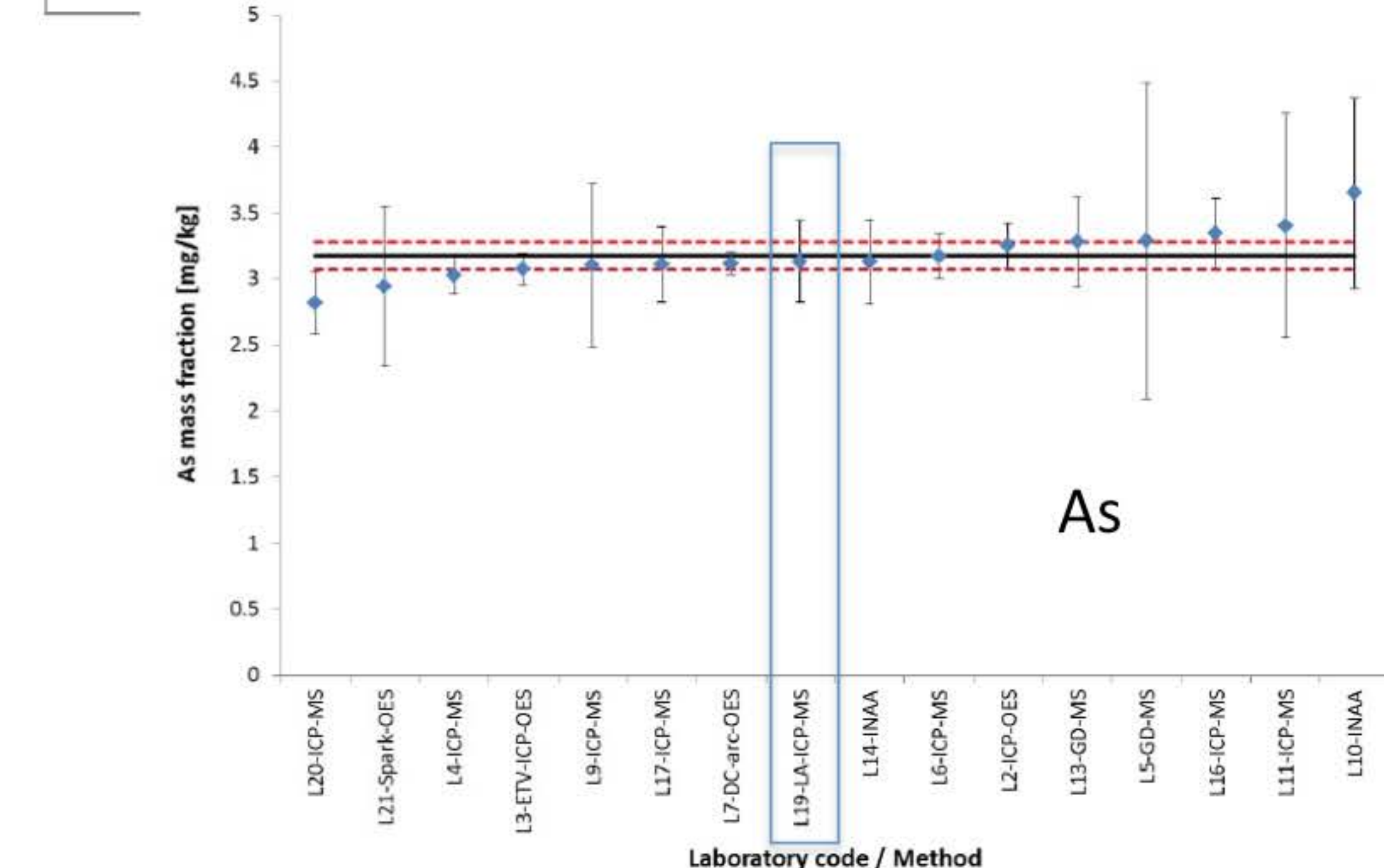
ICPMS
ETV-ICPOES
GDMS
ICPMS
ICPAES
SPARK OES
etc...
and fsLA-ICPMS



Al



Ag

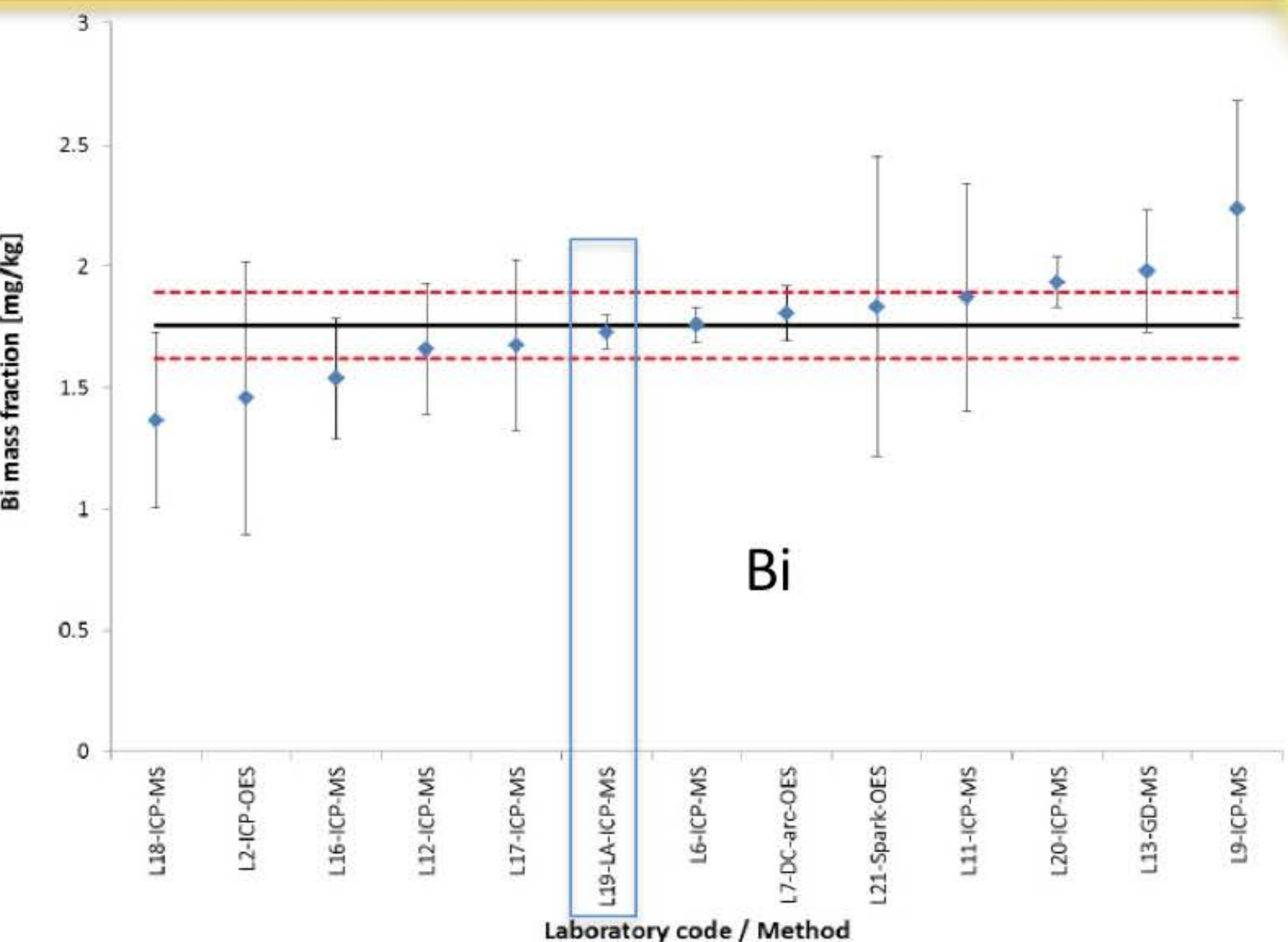
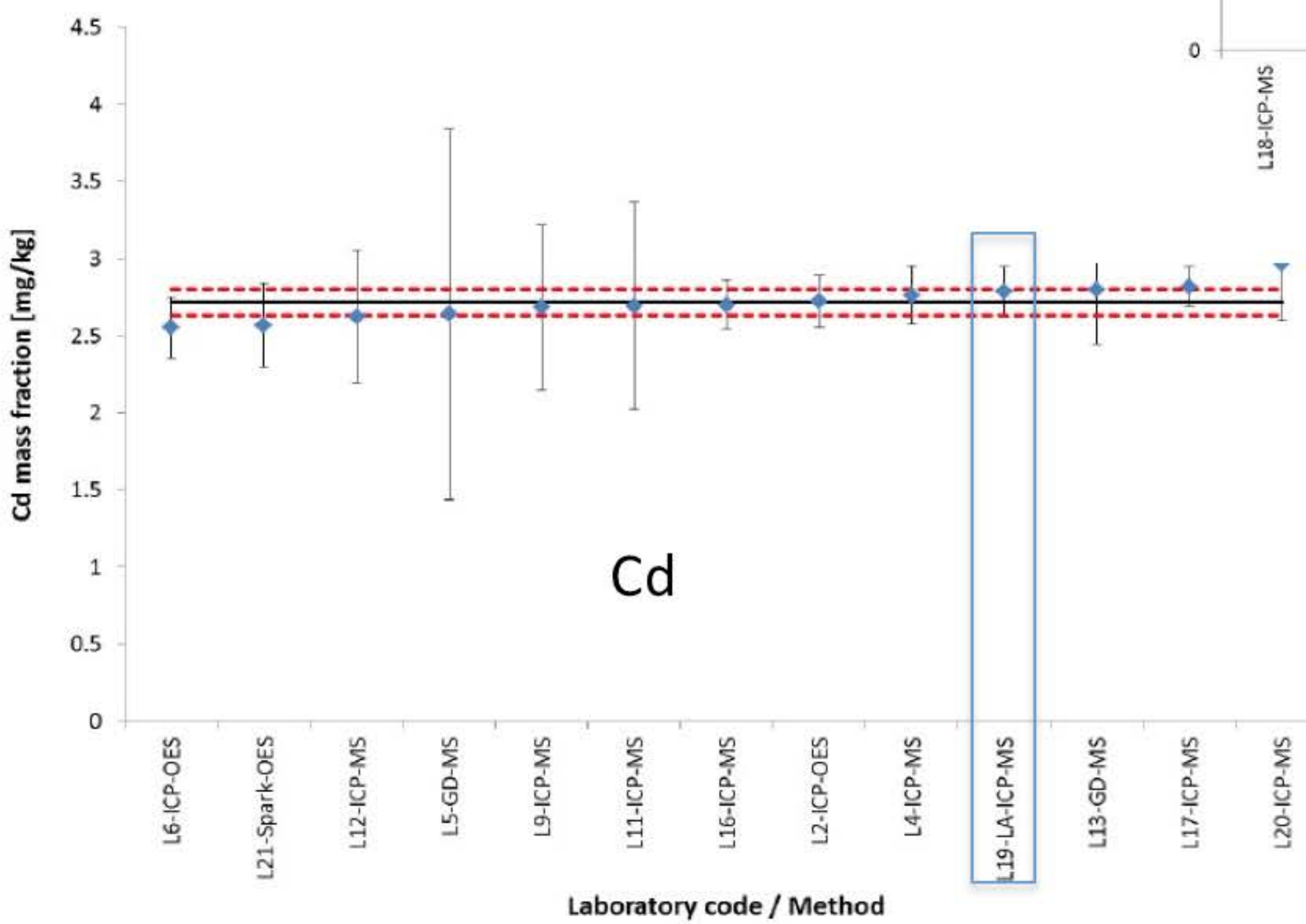


As

Trace elements in copper – Round Robin

Femtosecond laser ablation provides good precision and accuracy.

Note that due to the high thermal conductivity of Cu, laser ablation is not a priori the best indicated approach.

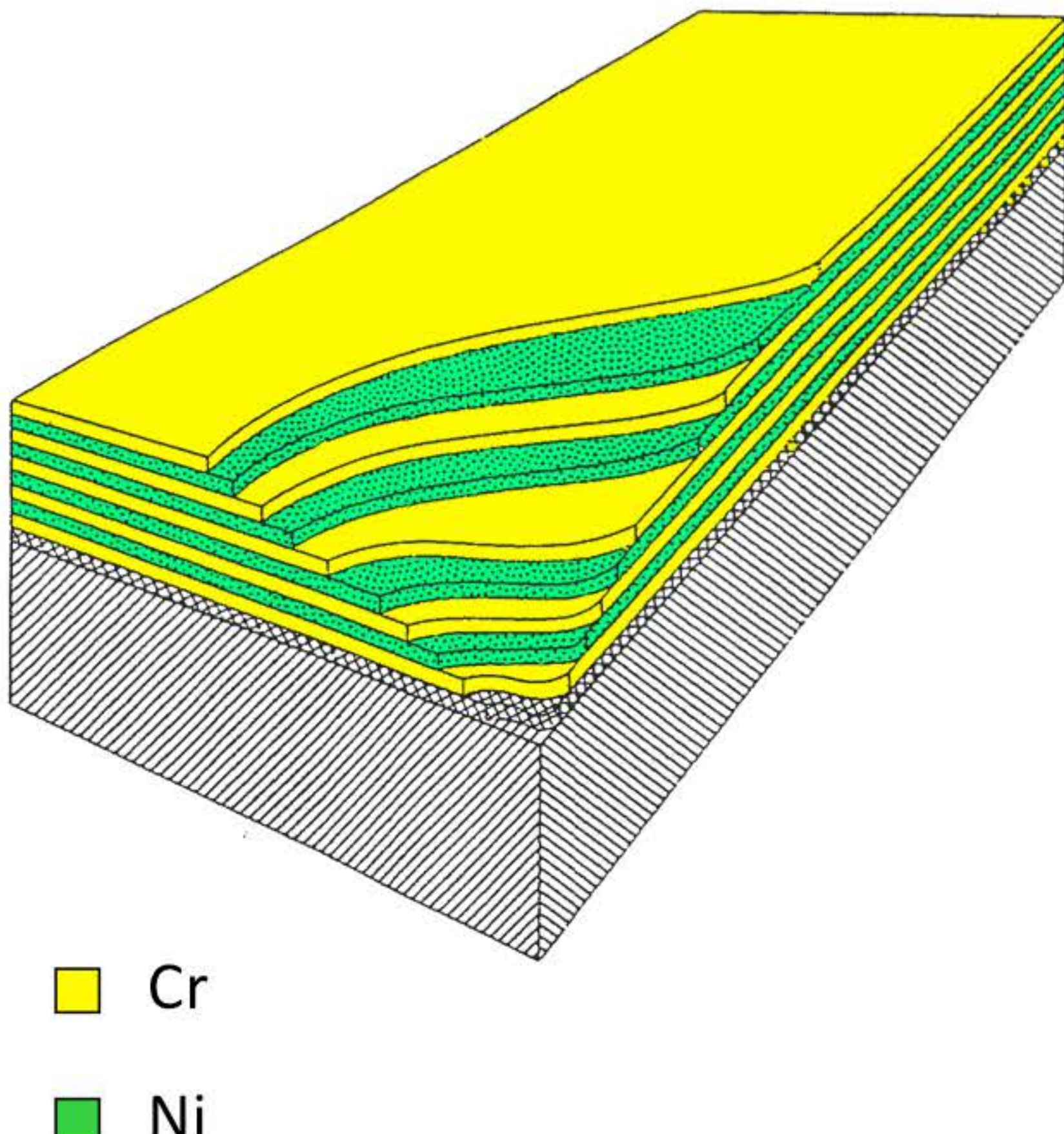


In depth profiling with fs pulses

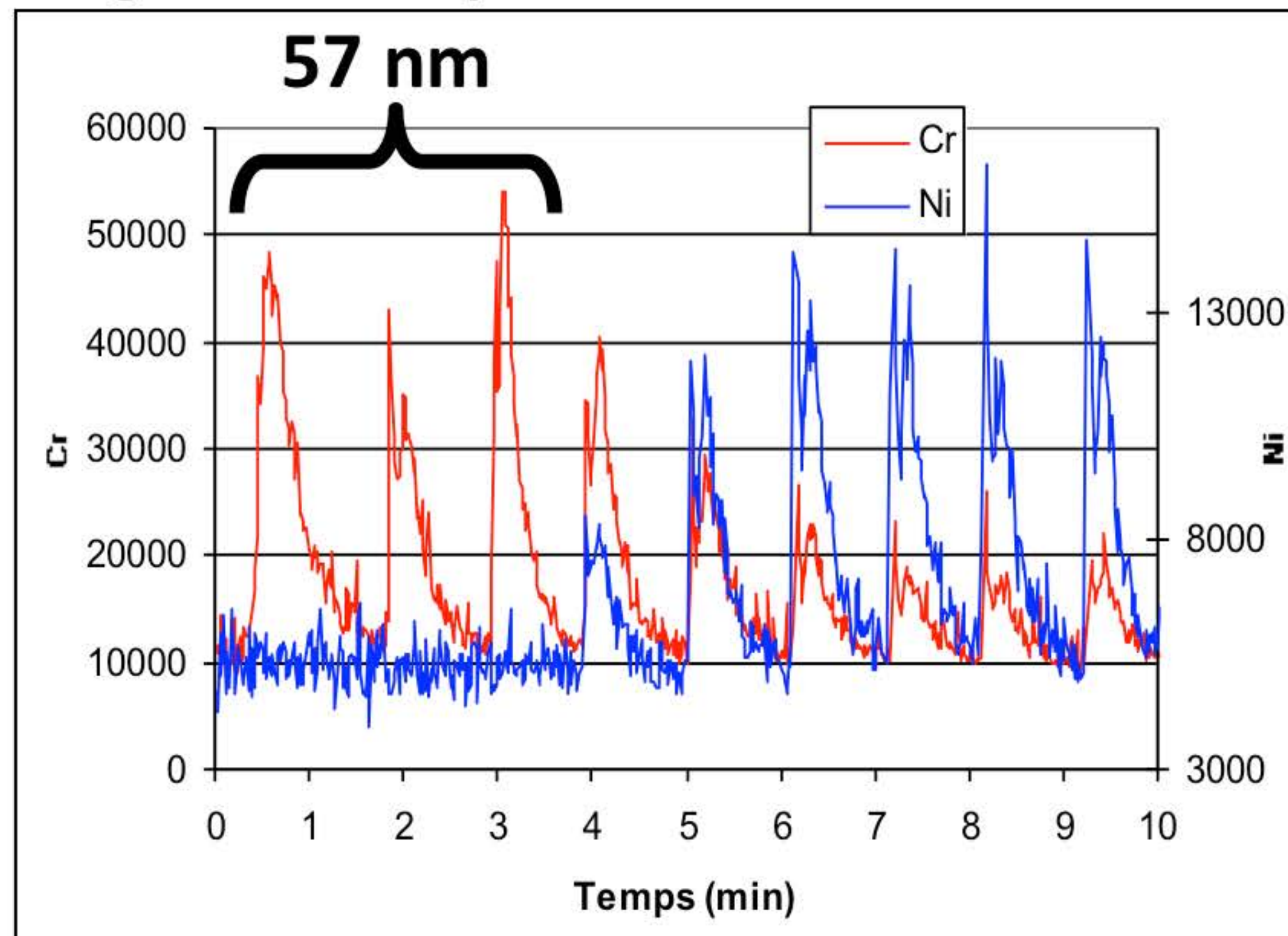
CRM: NIST 2135c

Multi layer material

Cr (57 nm) and Ni (56 nm)

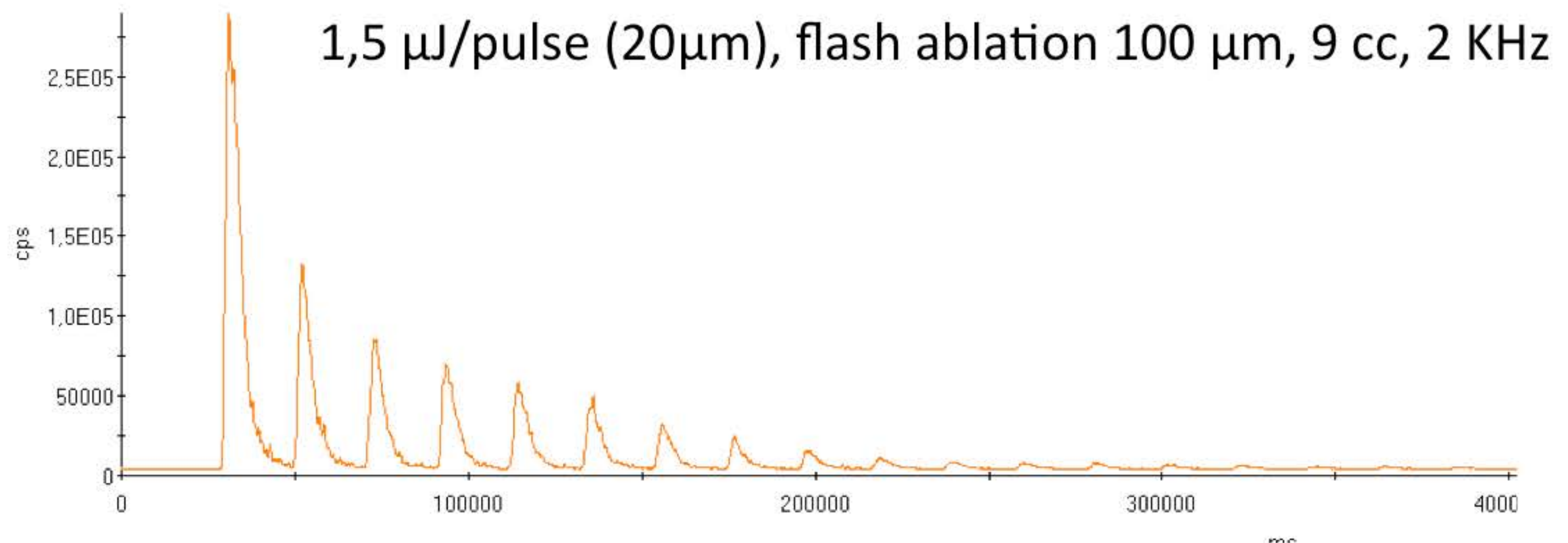
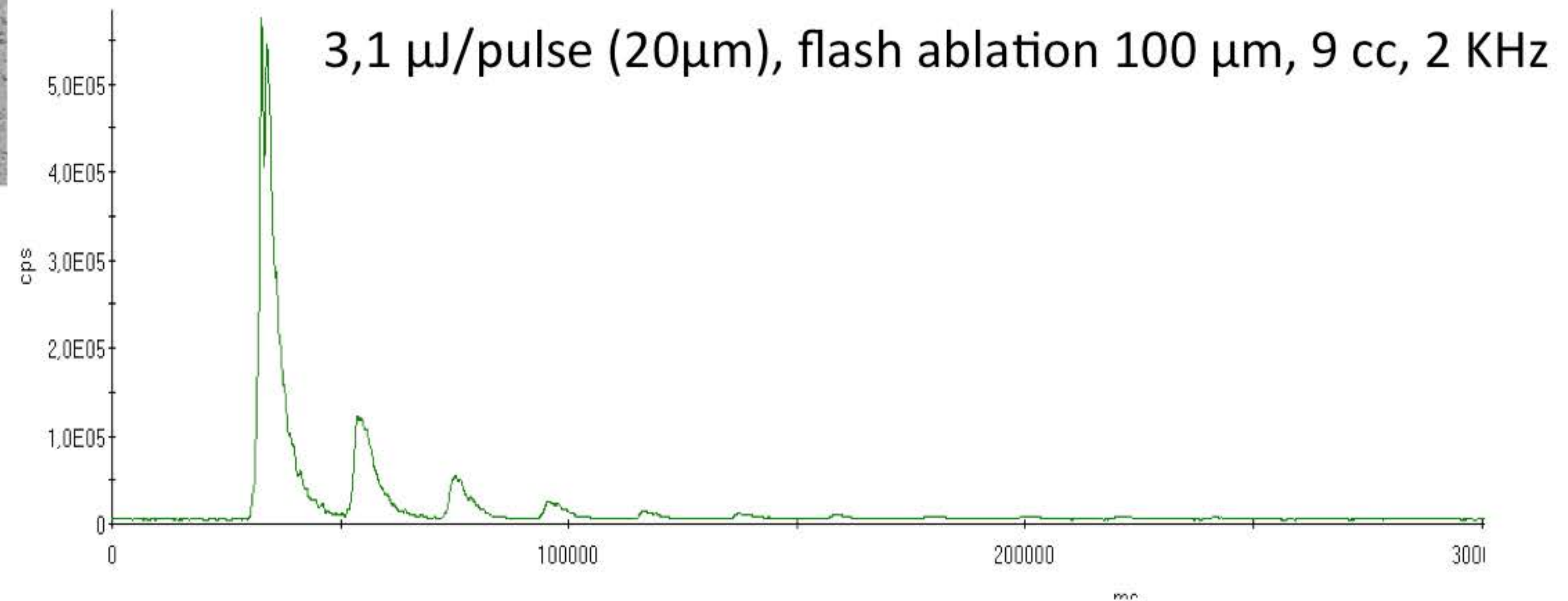


- ⇒ In depth resolution of about 20 nm per pulse...
- ⇒ The energy level should be adjusted close to the ablation threshold.
- ⇒ resolution though by the laser beam gaussian shape



In-depth profiling with fs pulses

In depth profile of Phosphorus in a P-doped concrete



⇒ Low energy
for better in depth
resolution

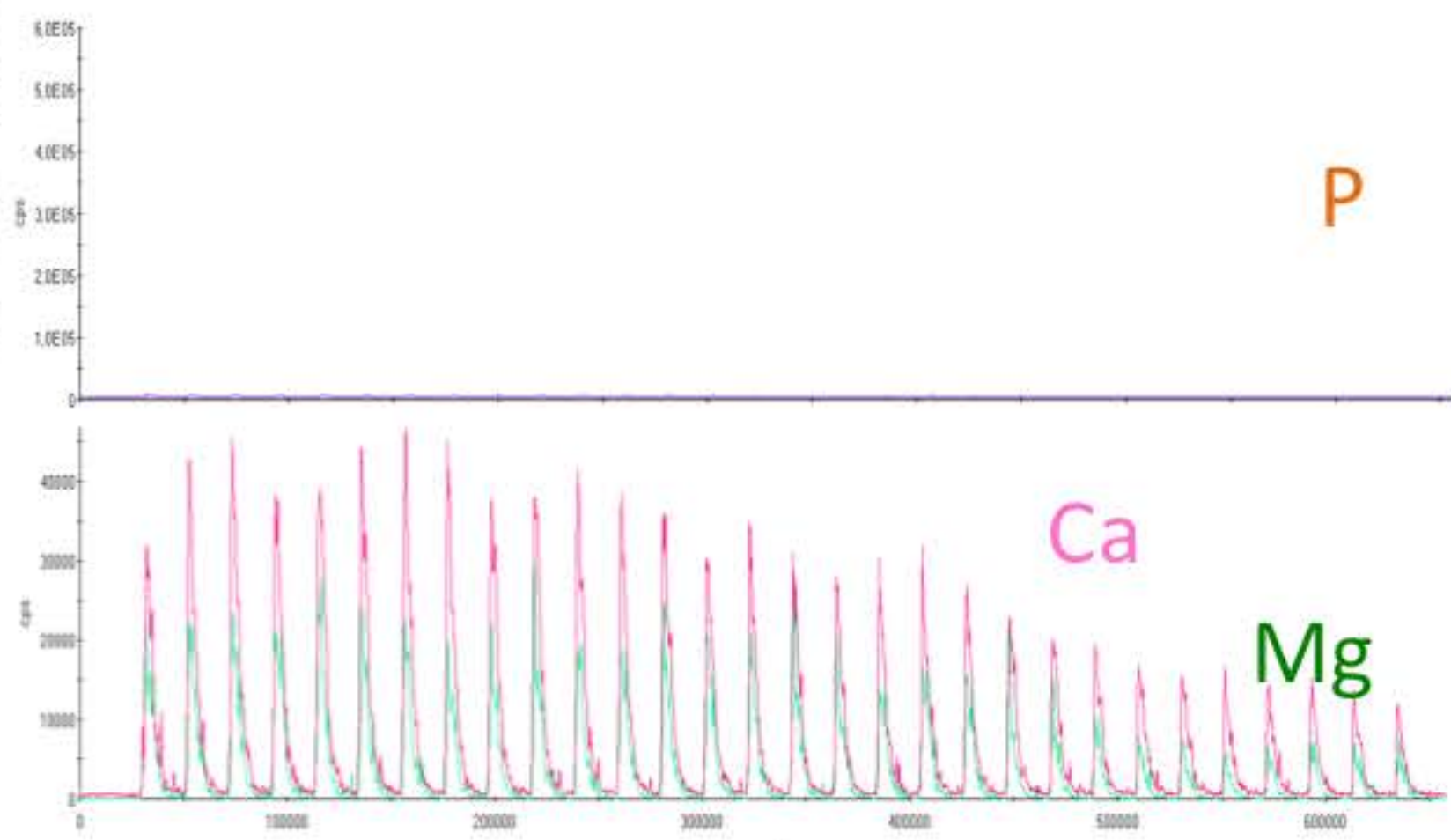
In-depth profiling with fs pulses

In depth profile of Phosphorus in a P-doped concrete

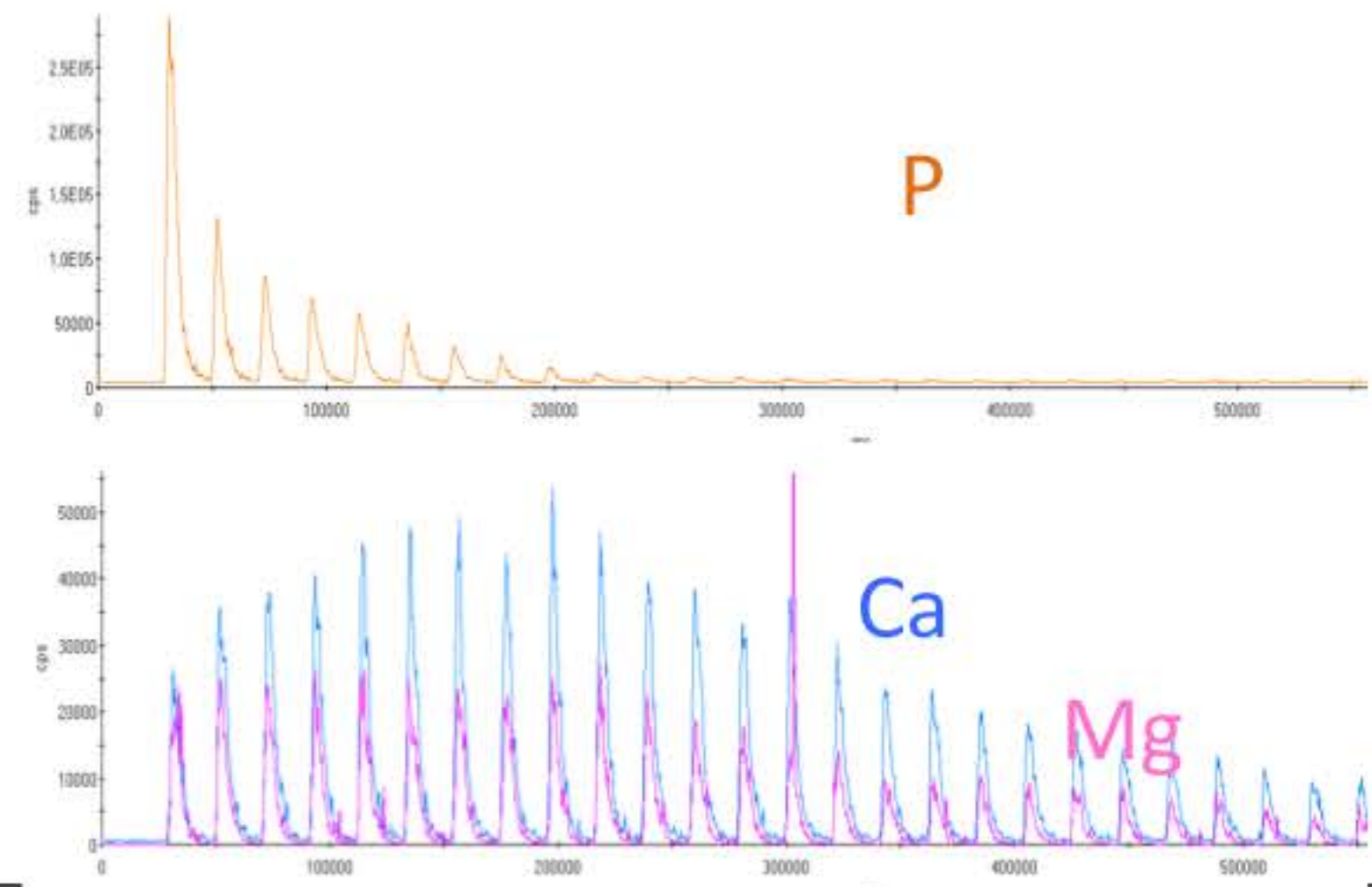


⇒ Internal
normalisation (Ca
or Mg)

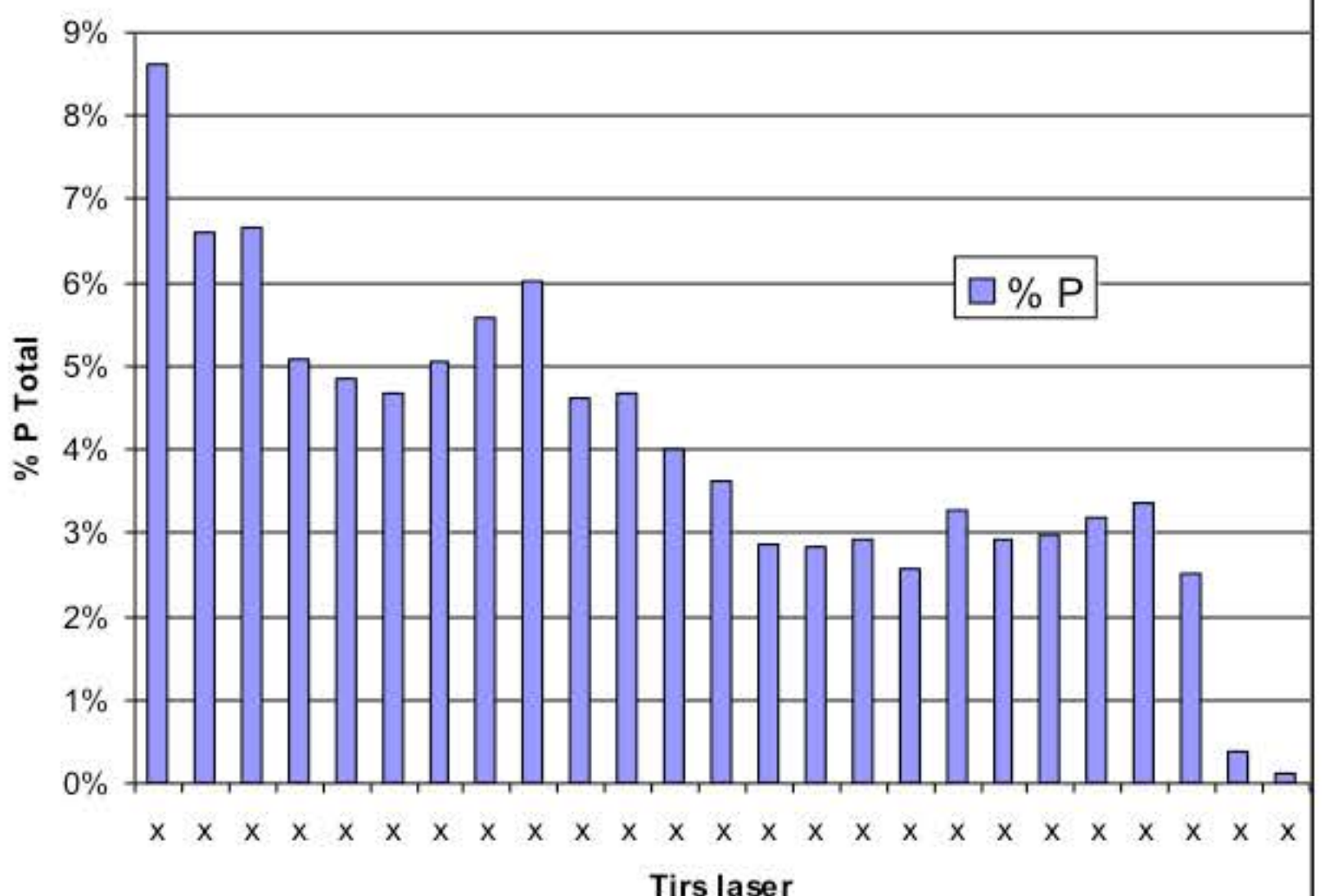
Reference concrete



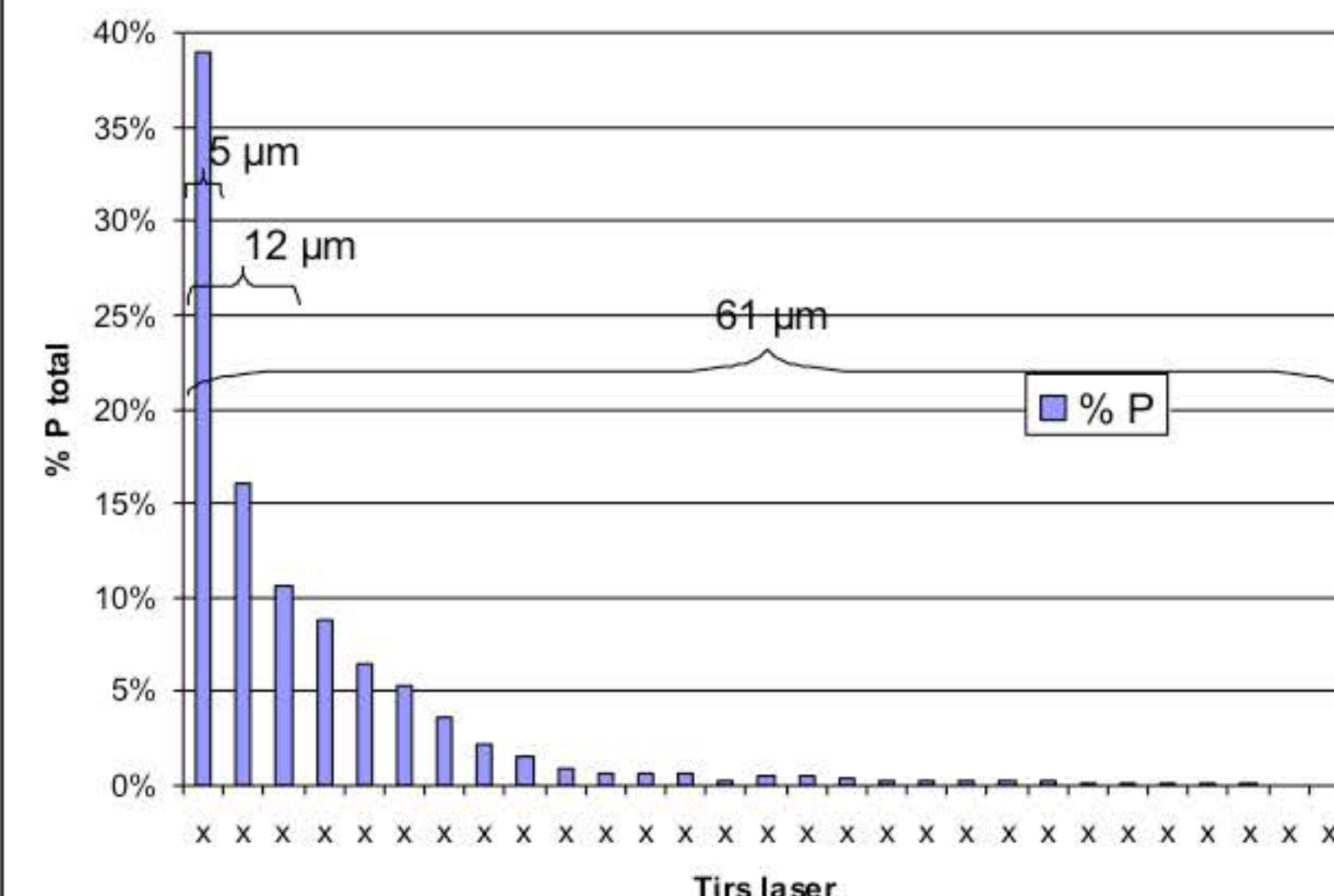
P-Doped concrete



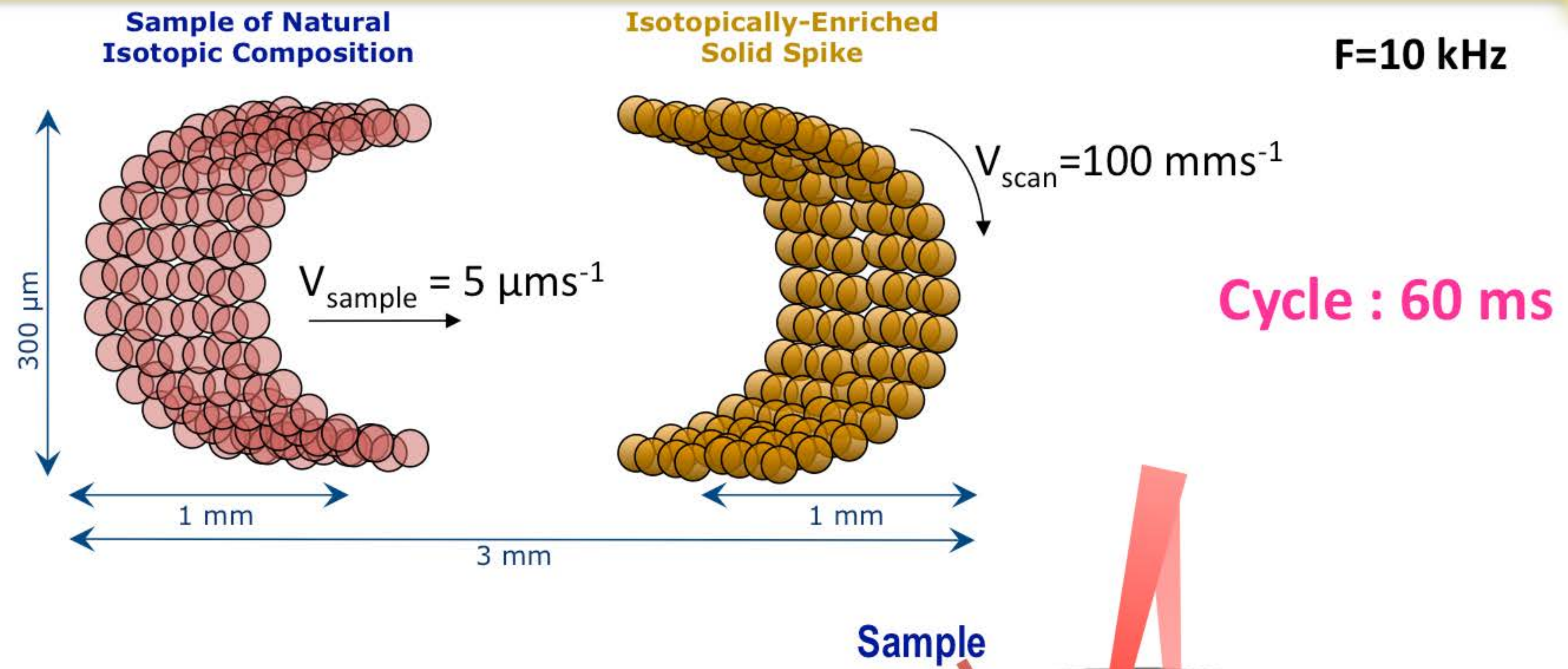
1,5 µJ -Béton de référence 1



1,5 µJ - Béton 2

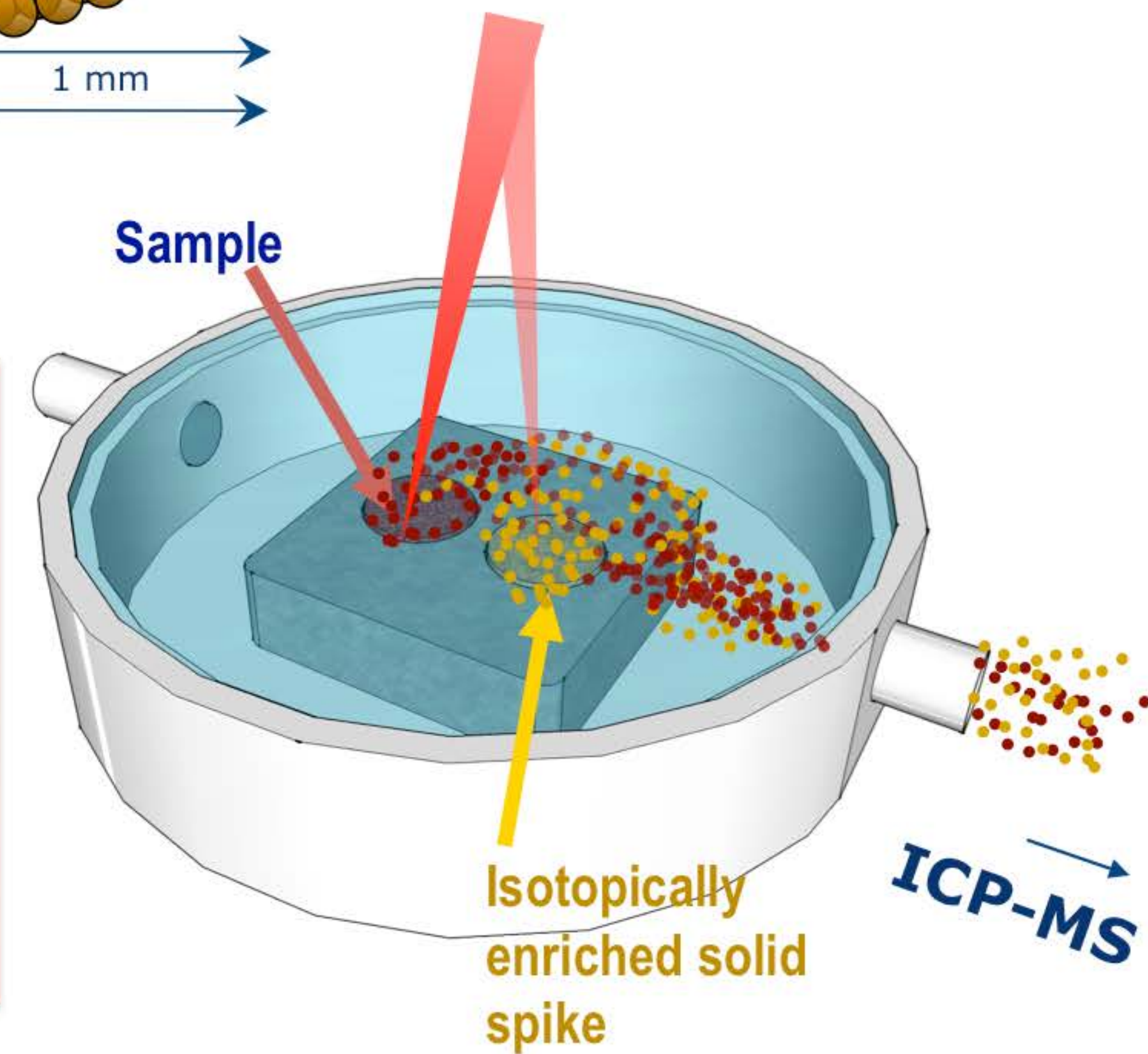


Direct in-cell Isotope Dilution analysis



Simulating a split beam...

- => The laser beam is virtually at two places simultaneously
 - ⇒ the laser ablates simultaneously the sample and an isotopically enriched sample
 - ⇒ the 2 aerosols are mixed into the cell
 - ⇒ then the isotope dilution takes place into the cell



Direct in-cell Isotope Dilution analysis

Paramètres laser

pulse

ALFAMET

360 fs

Wavelength

1030 nm

Repetition rate

1000 Hz

Energy

45 μ J

Scanner speed (ablation)

1 mm.s⁻¹

Scanner jump

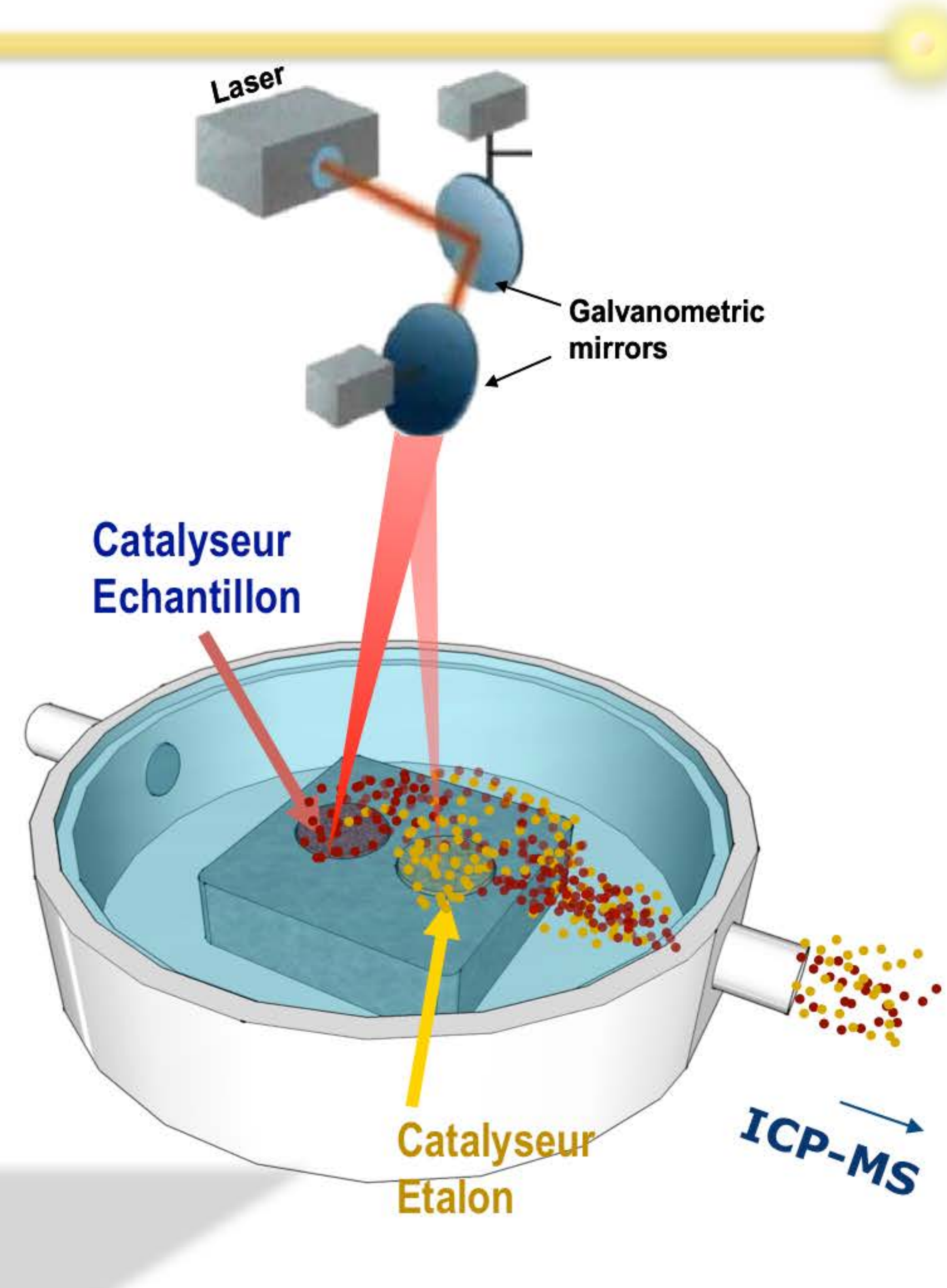
100 mm.s⁻¹

virtual beam shape

150 μ m

Distance between 2 pellets

1 mm

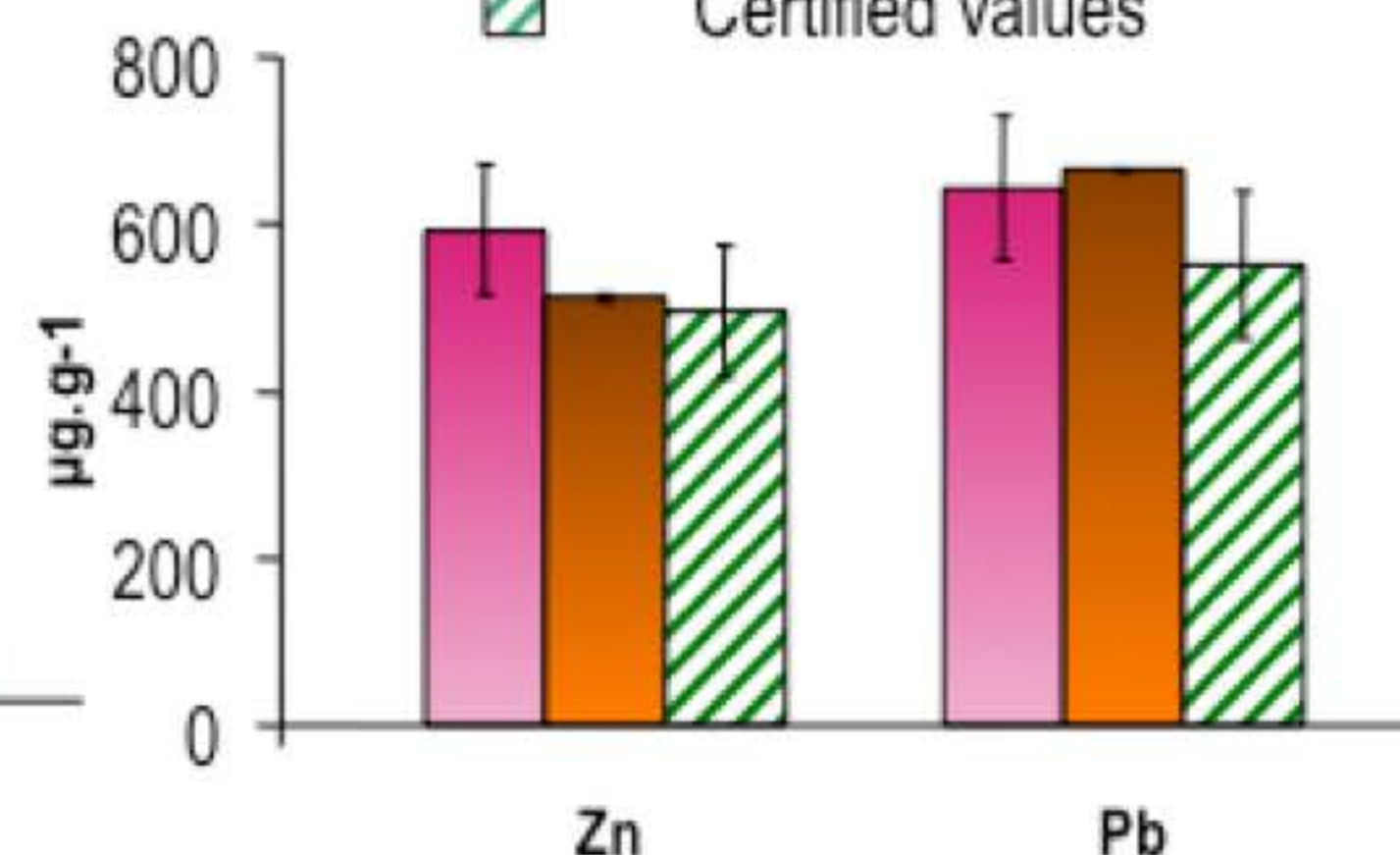
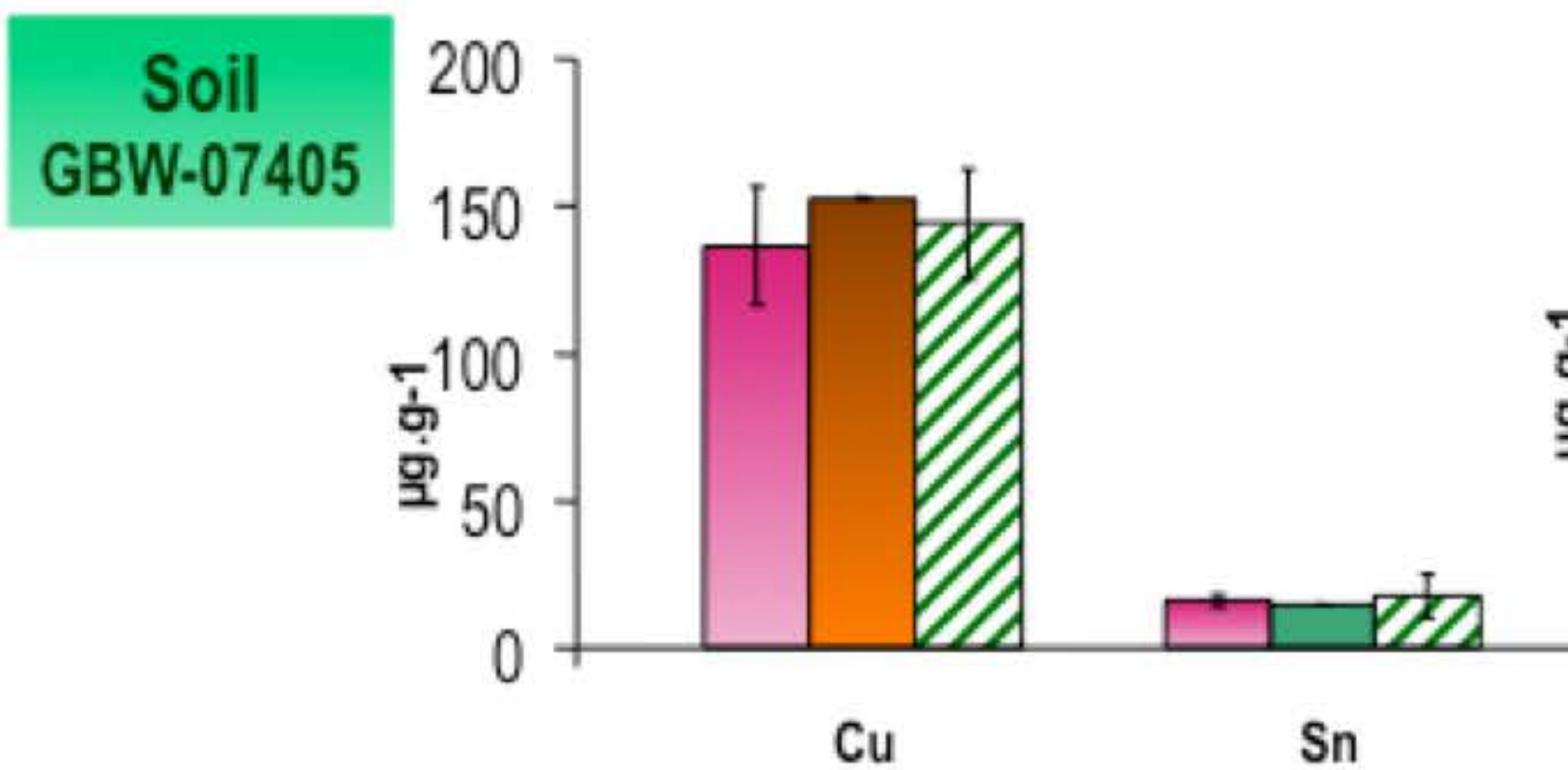


Direct In-cell isotope dilution

In-cell ID/ICPMS
< 6 min

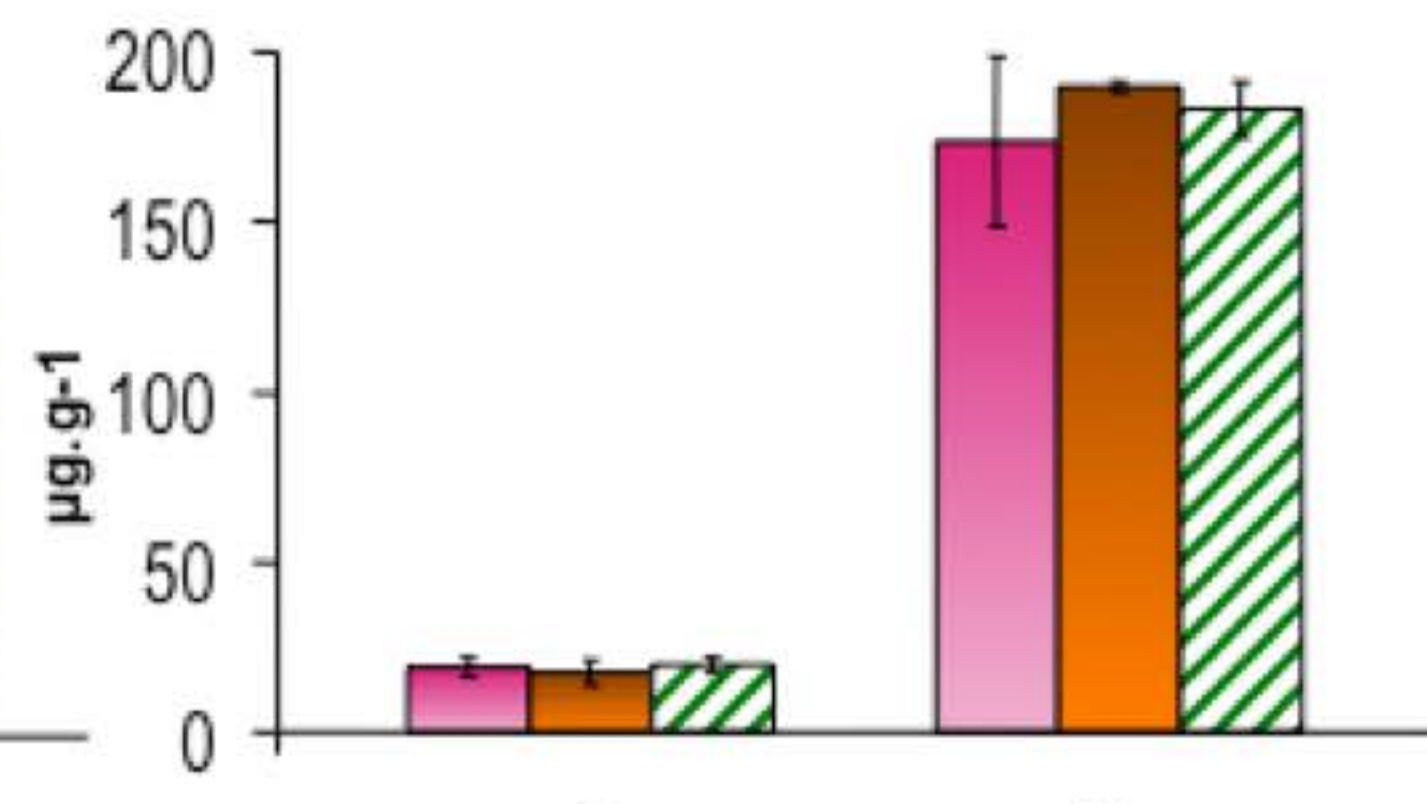
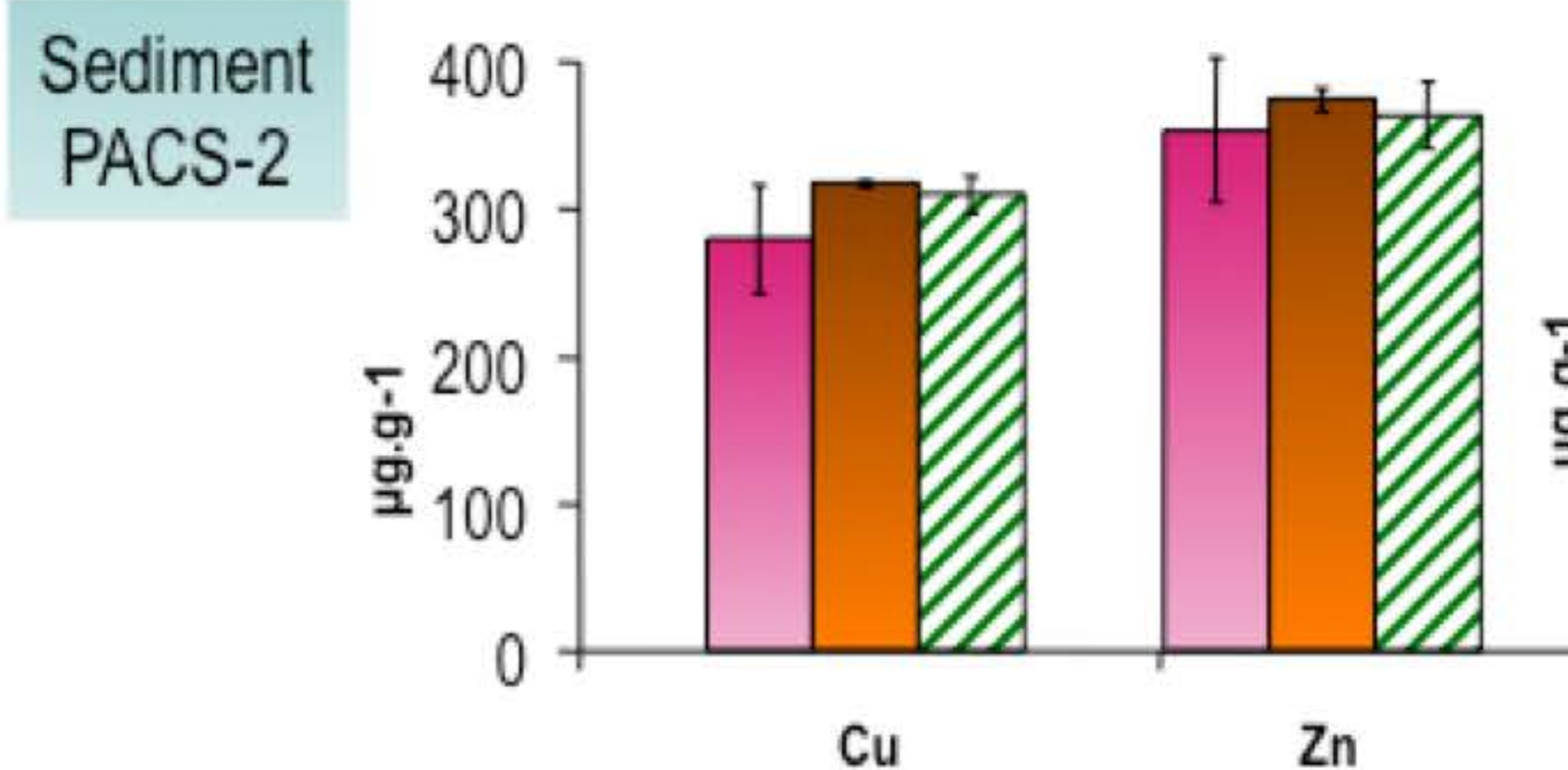
Conventional ID/ICPMS
6 Hours

- In-cell / Fs-LA-ICP-IDMS
- Digestion / ICP-IDMS
- Certified values



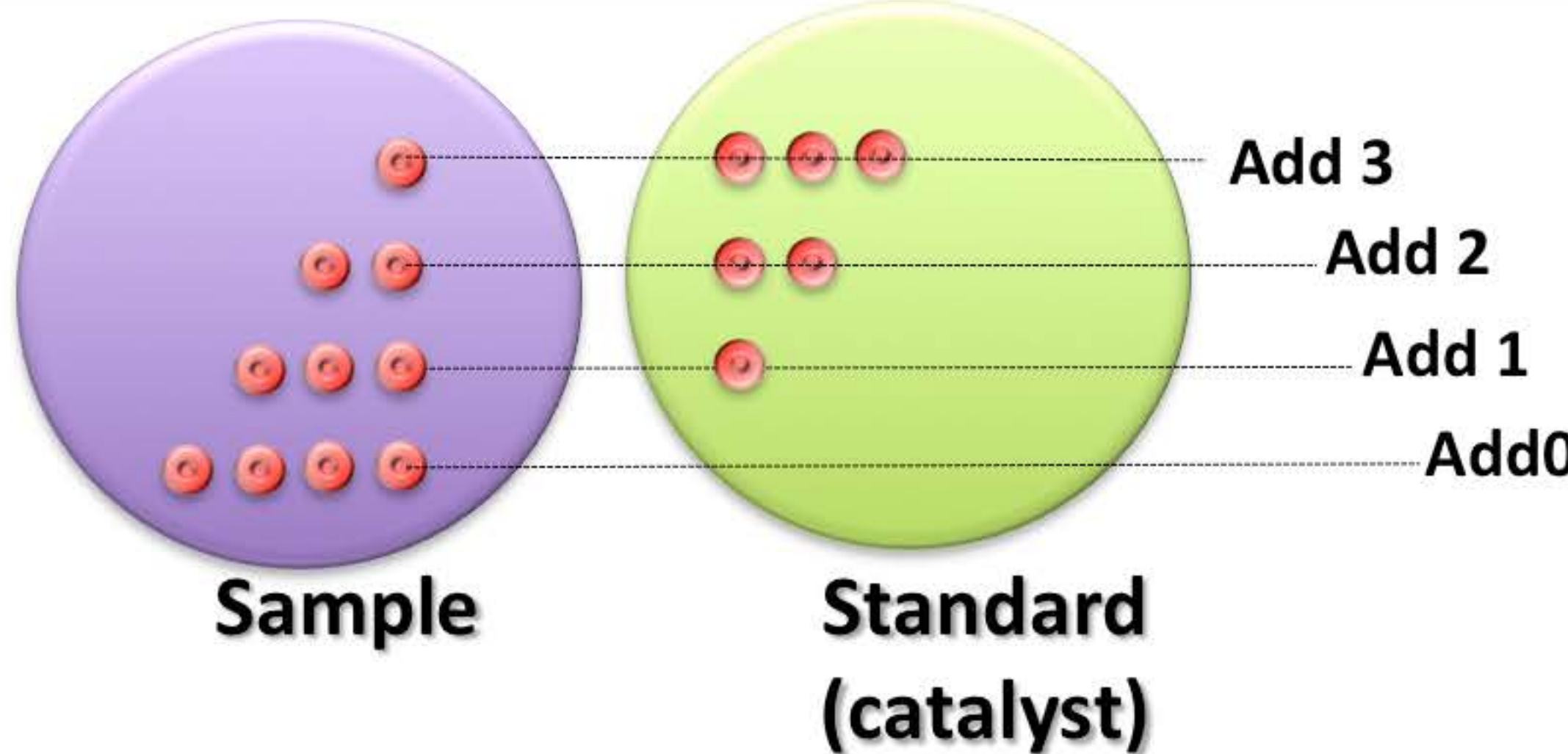
APPLICATION TO
SOILS AND
SEDIMENTS
ANALYSIS

⇒ in 6 min vs 6
hours

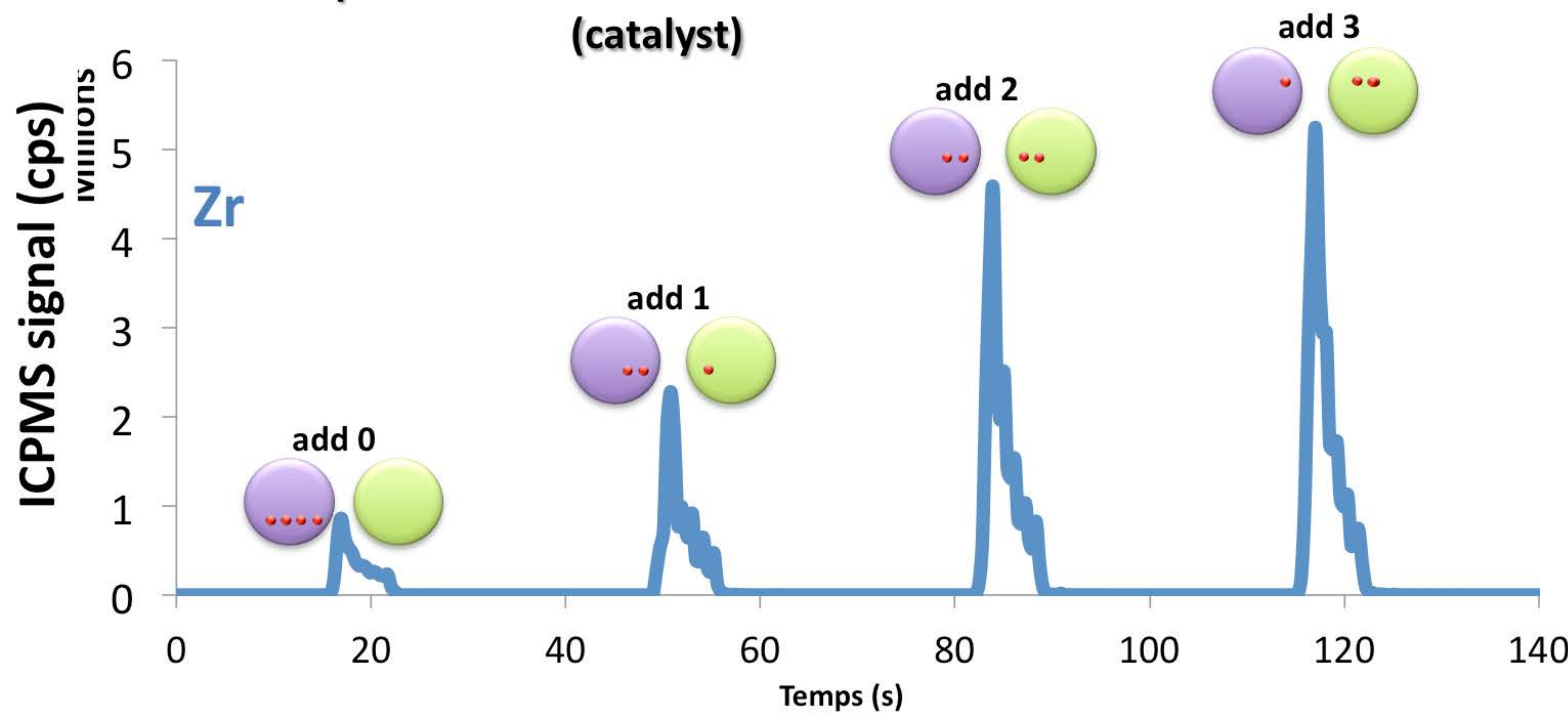


⇒ limitations due to
sample
inhomogeneity

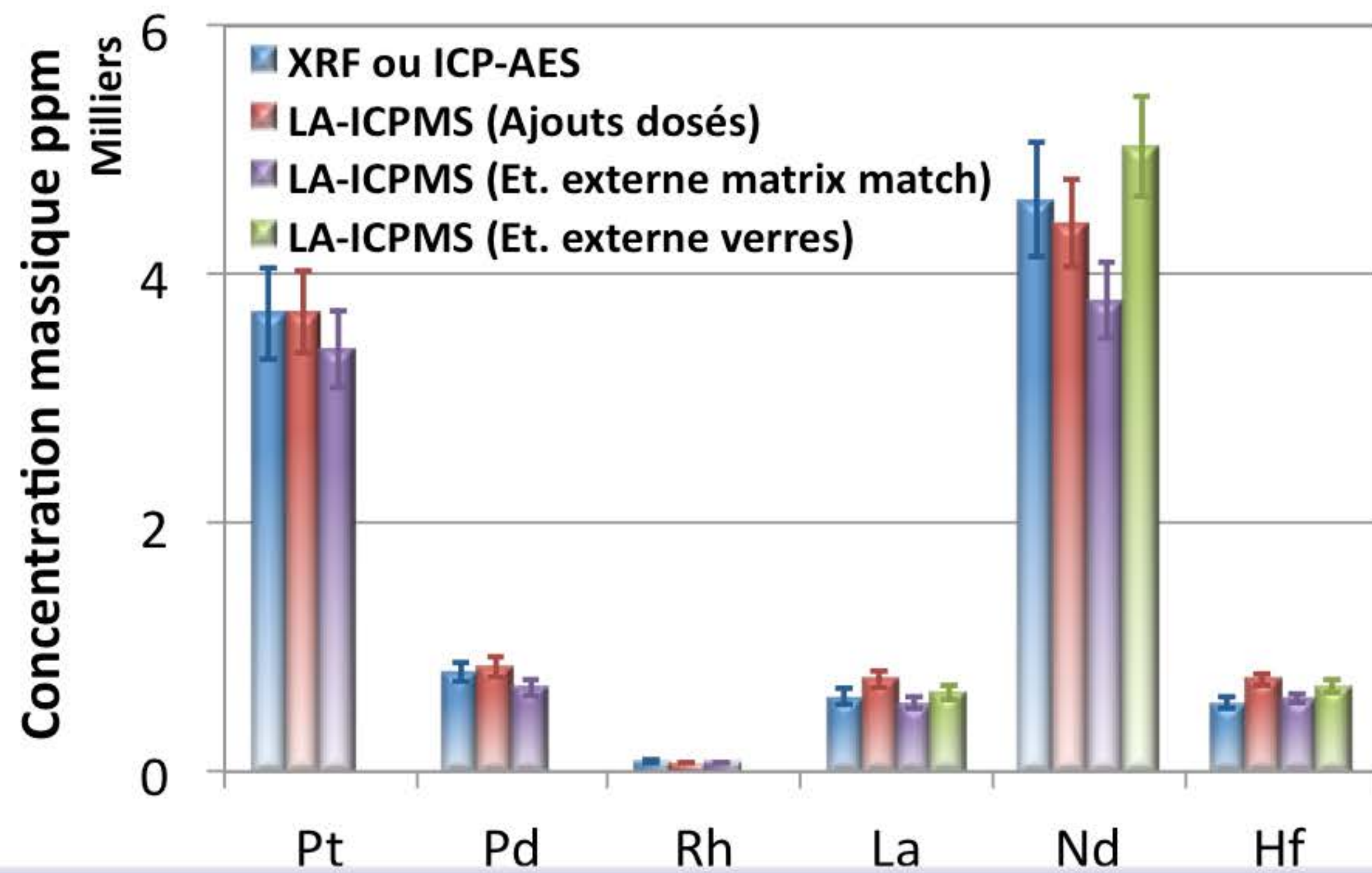
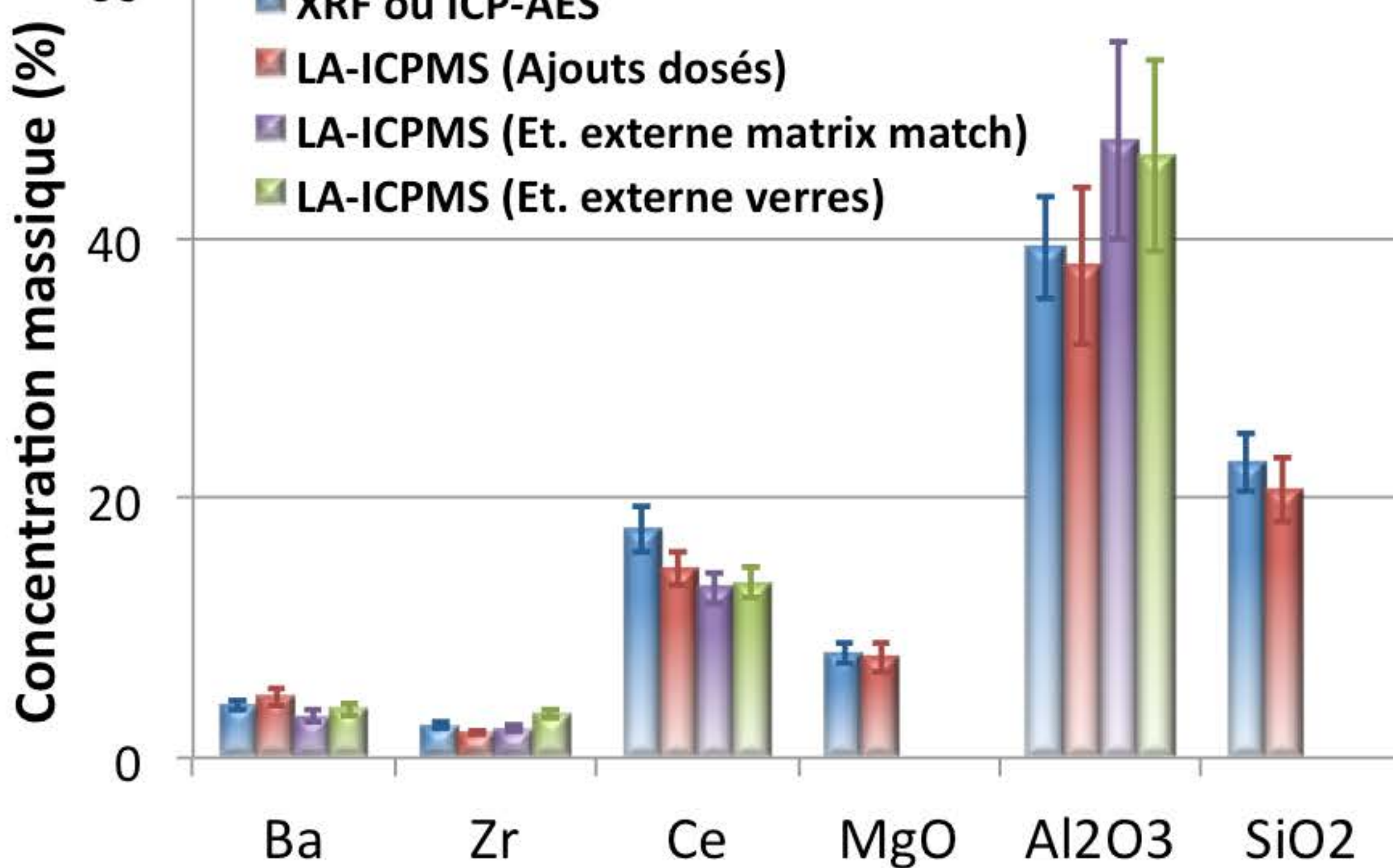
Direct In-cell standard addition



- Constant nb of shots
- Identical ablation yield from one pellet to the other



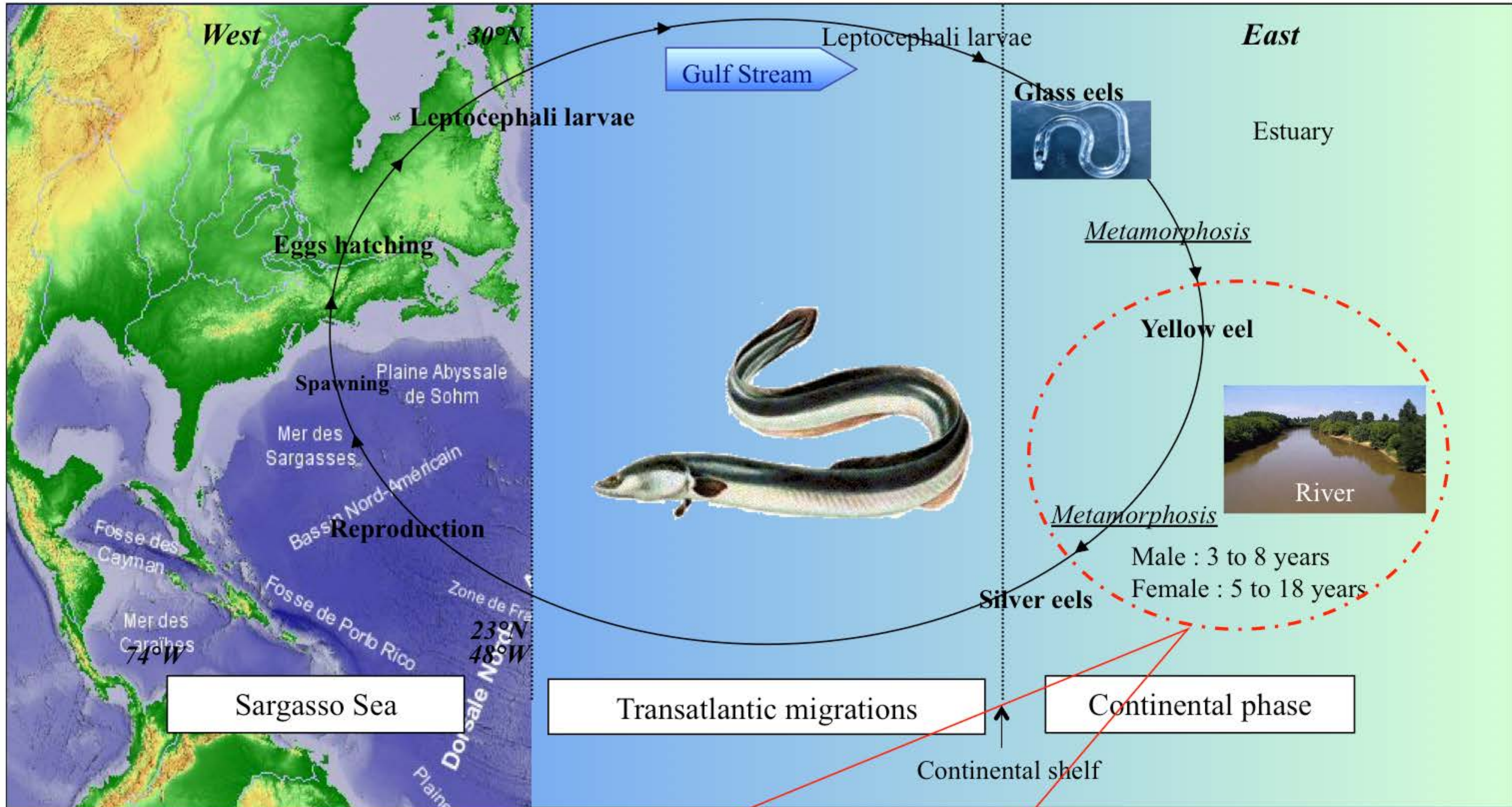
Validation



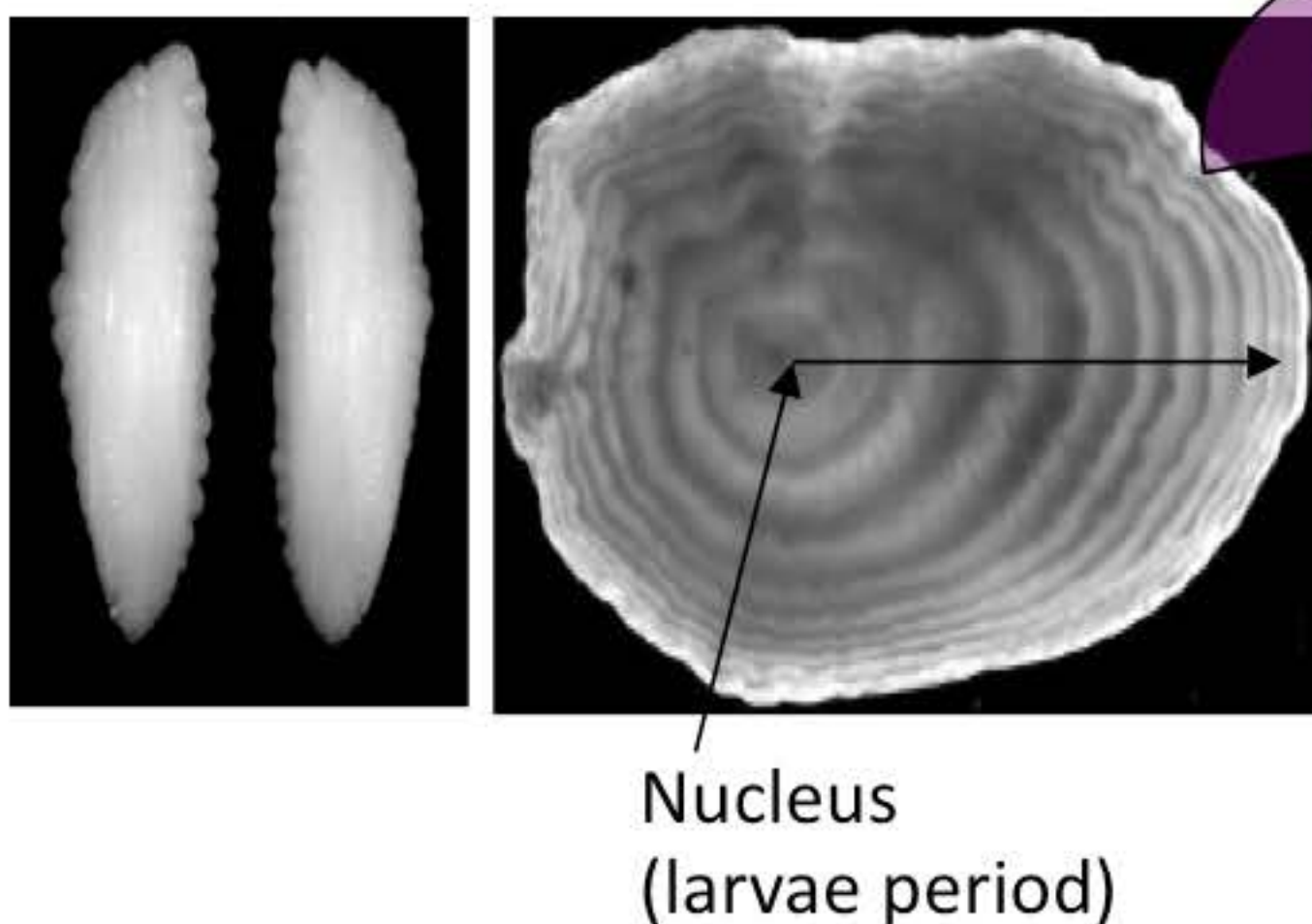
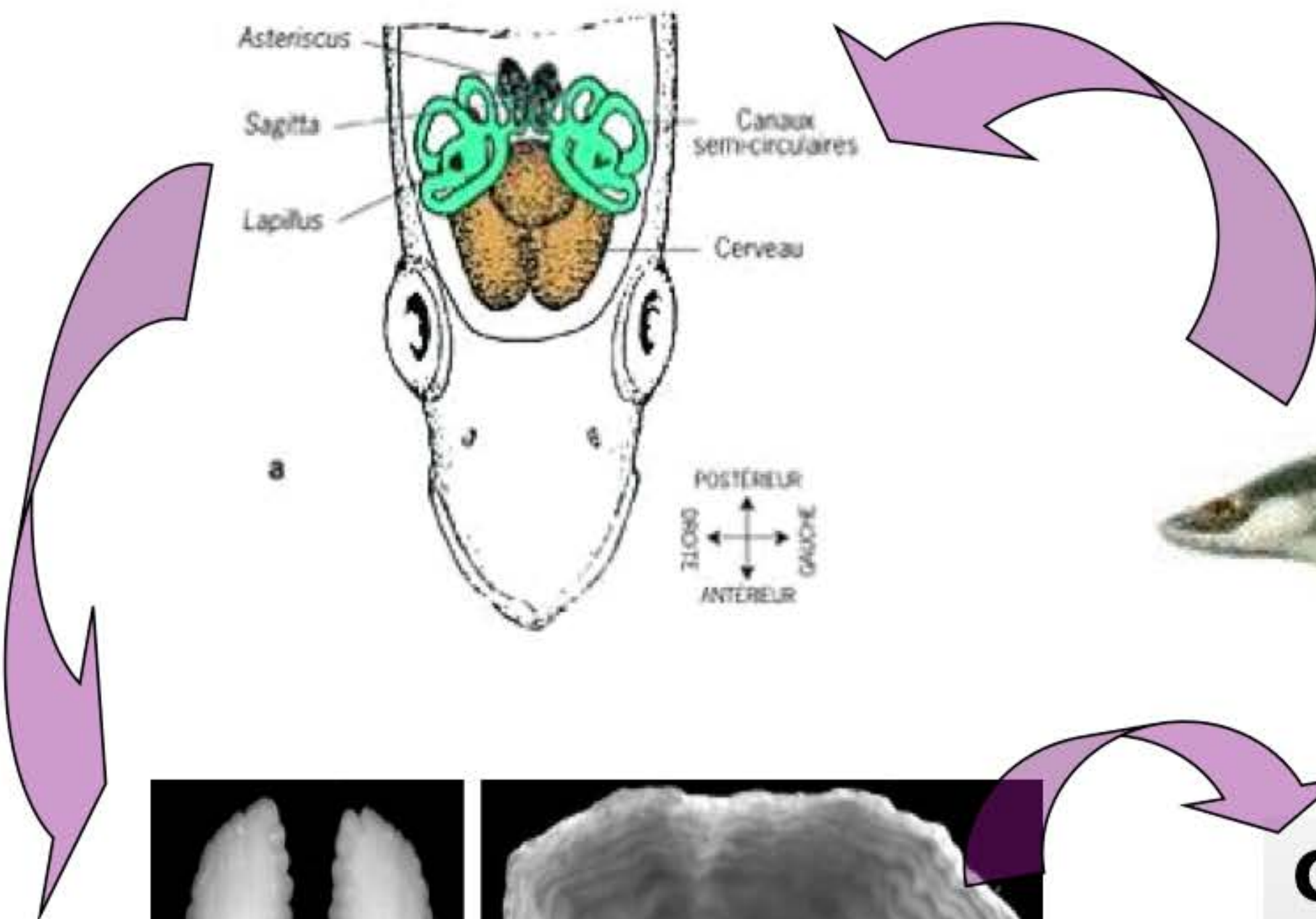
Application of the virtual beam shaping to biocarbonate analysis

European eel *Anguilla anguilla* : biological cycle

- Ubiquitous declining species with great local and european economical stakes
- Long live predator, high fat content, high resistance to physico-chemical conditions.



Anthropogenic activity influence on the Adour ecosystem : eel as a model
Markers of physico-chemical condition : from the molecular response level to the reconstruction of the individual history through the otolith



Growing striae (aragonite)
=> time scale

Analysis of trace element in eels
otoliths as a tracer of migration

High spatial resolution and
sensitive analytical technique LA-
ICPMS

Trace element and isotope microchemistry



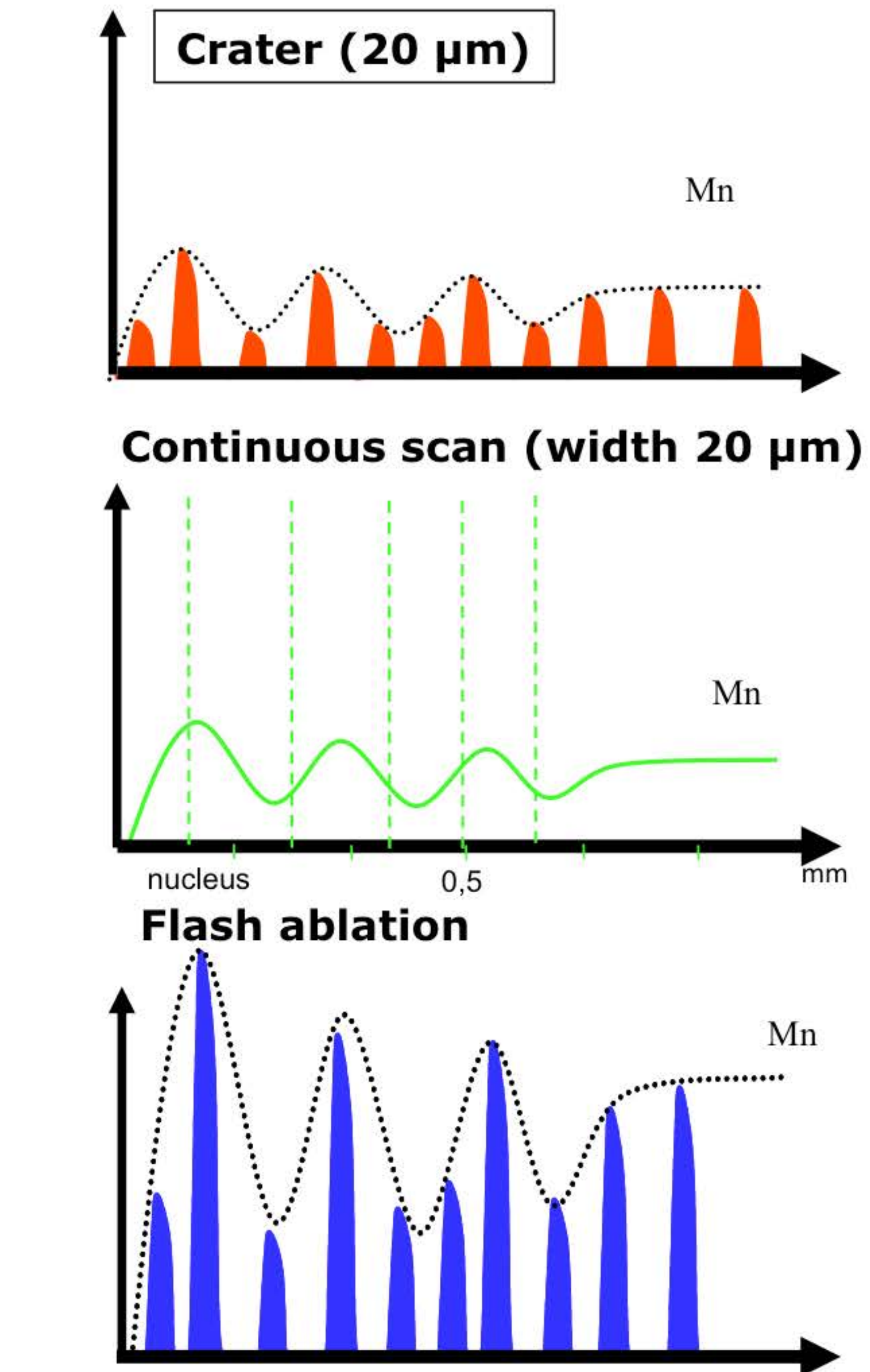
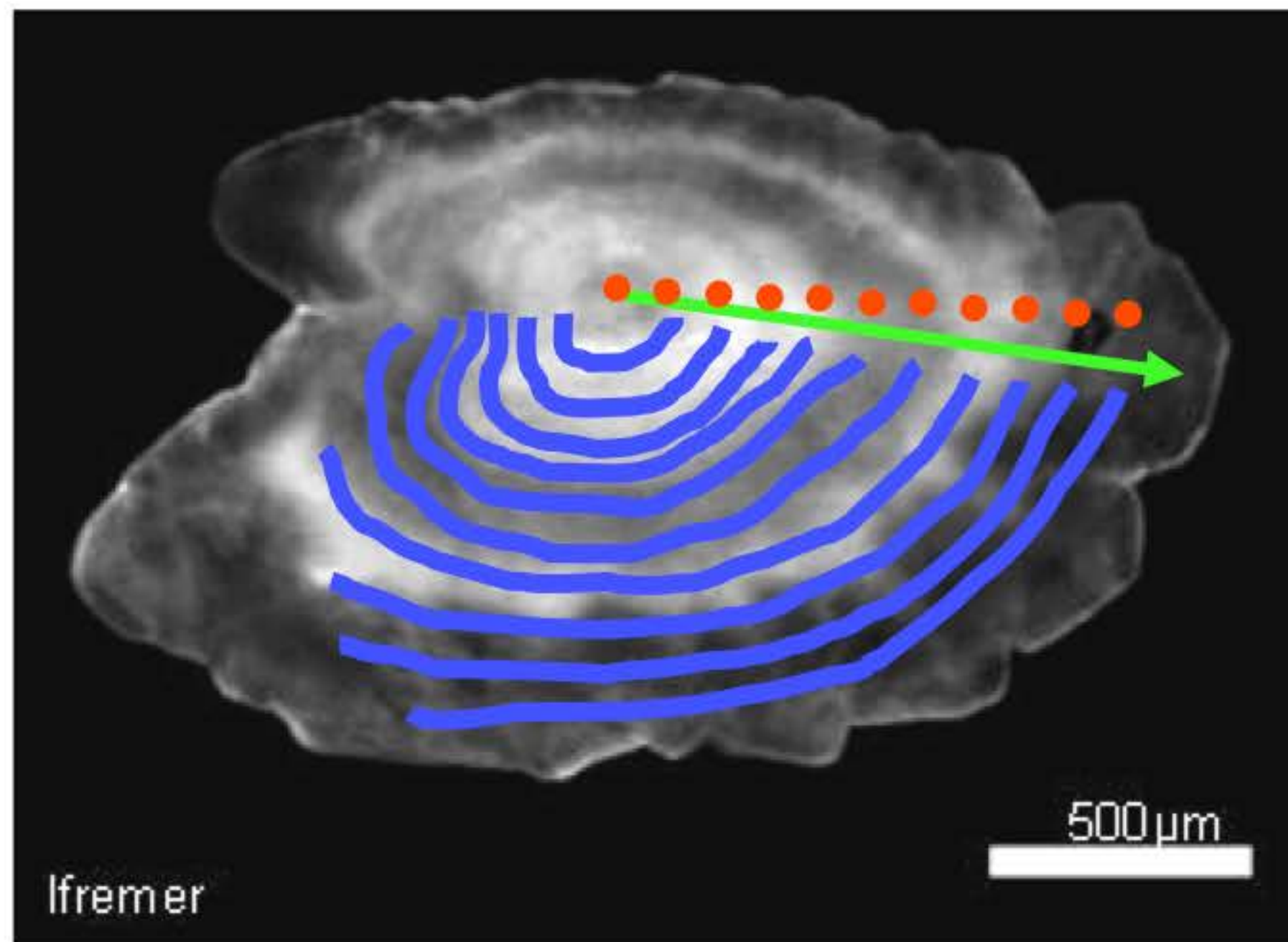
Ba, Sr, Mg,
Mn, Zn, Cd,
Pb, Li, Ca...

$^{87}\text{Sr}/^{86}\text{Sr}$

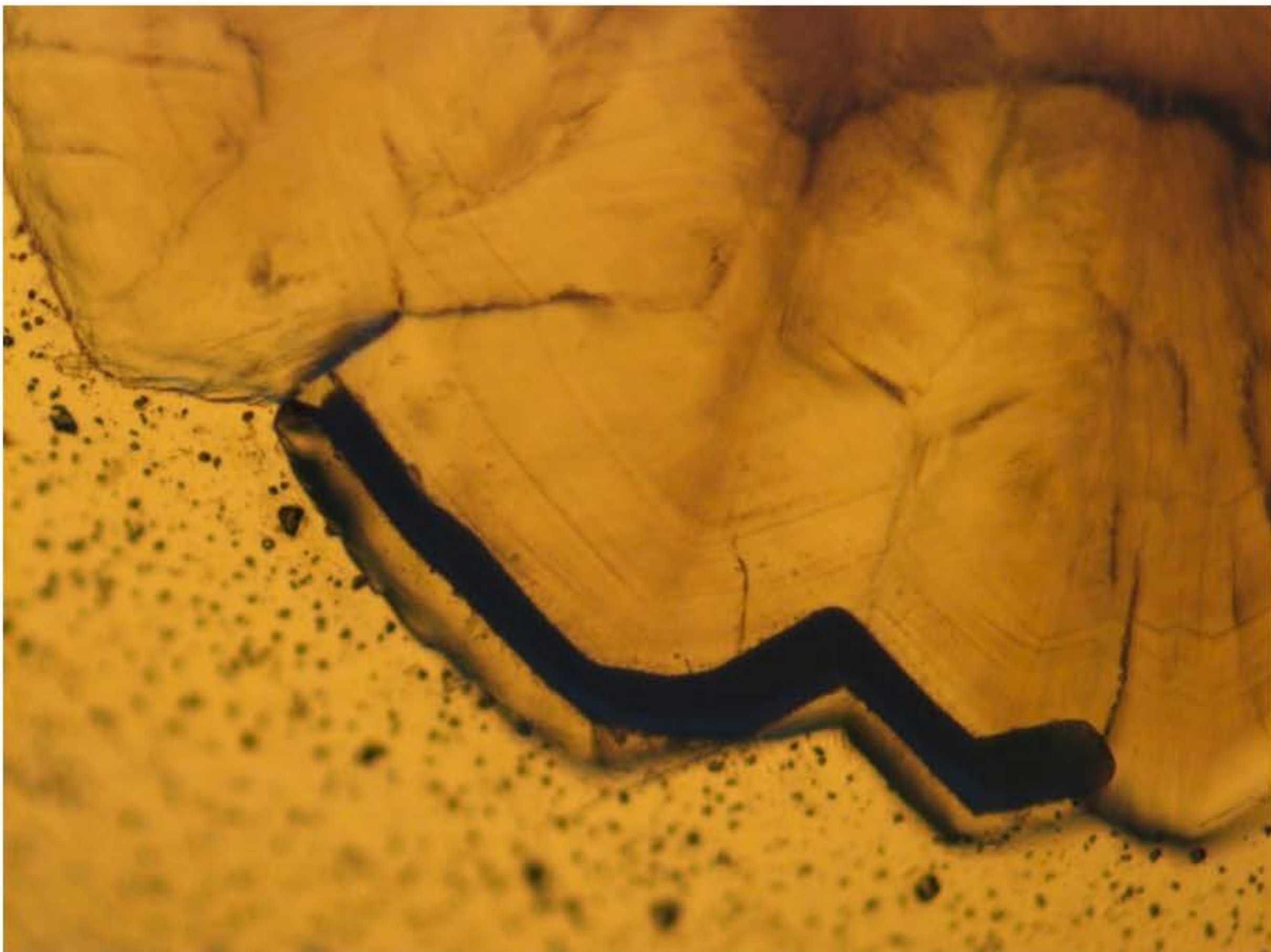


Virtual beam shaping

Increasing the ablation rate to improve the signal to noise ratio...

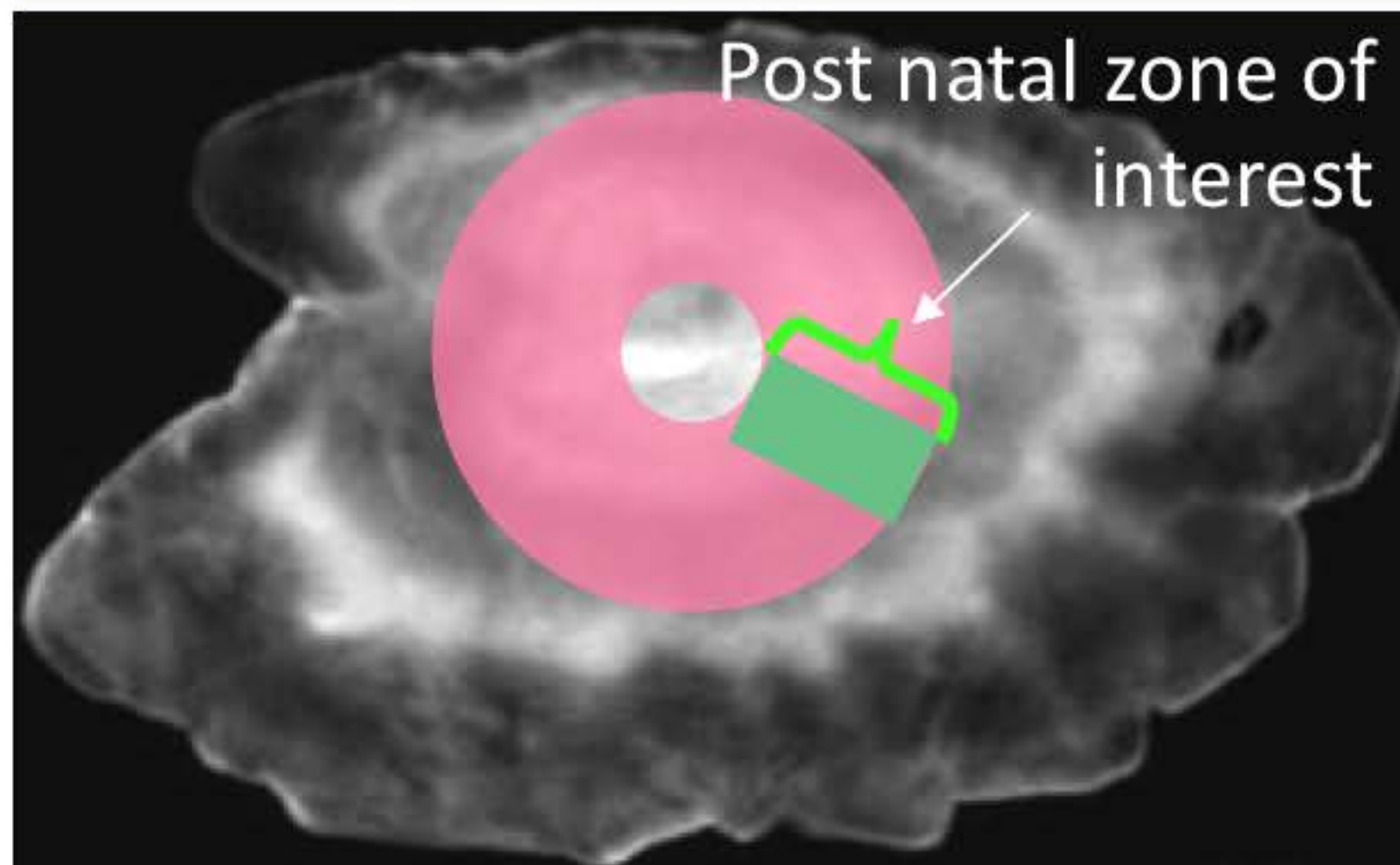


Flash ablation to understand a given life-time history



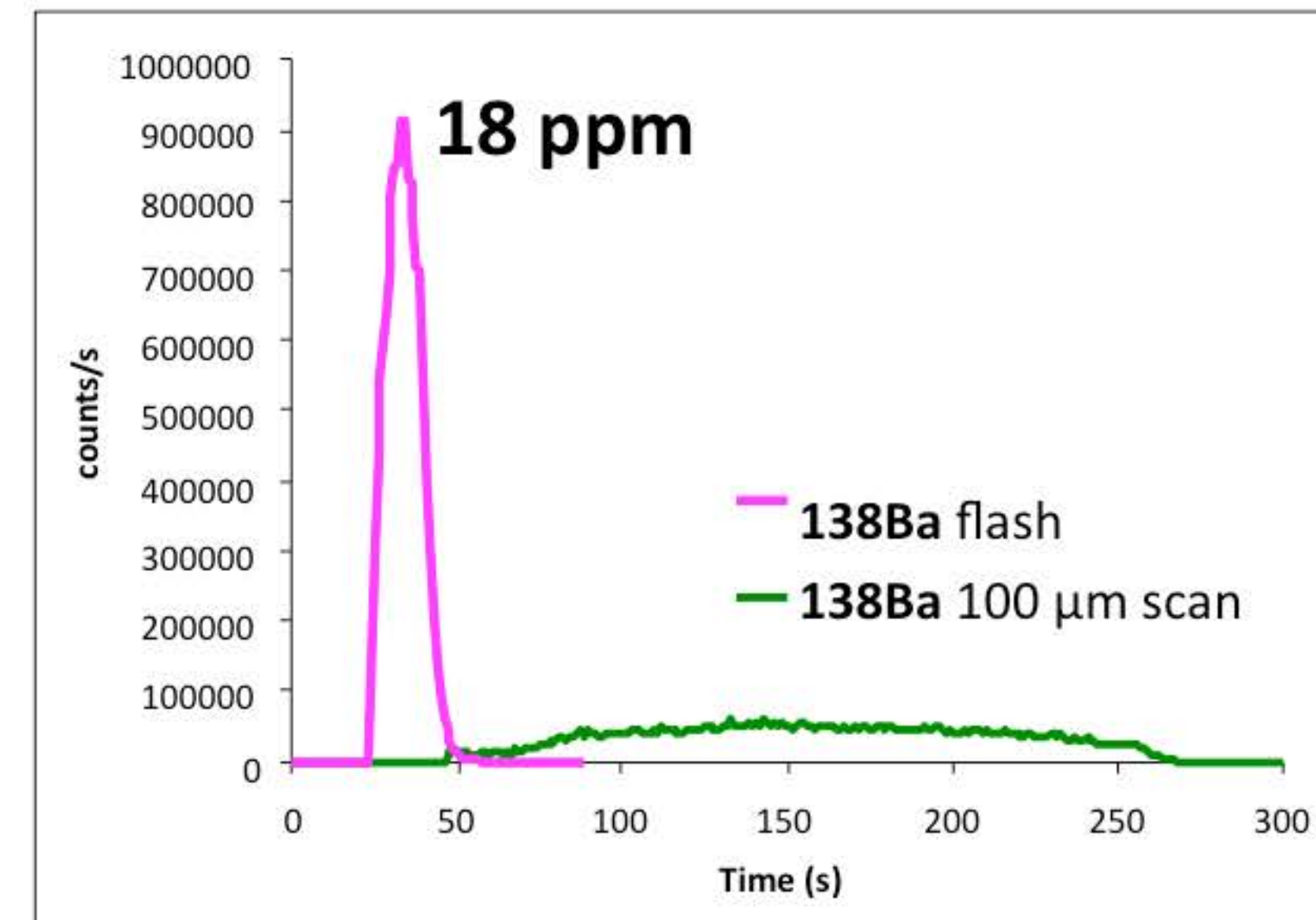
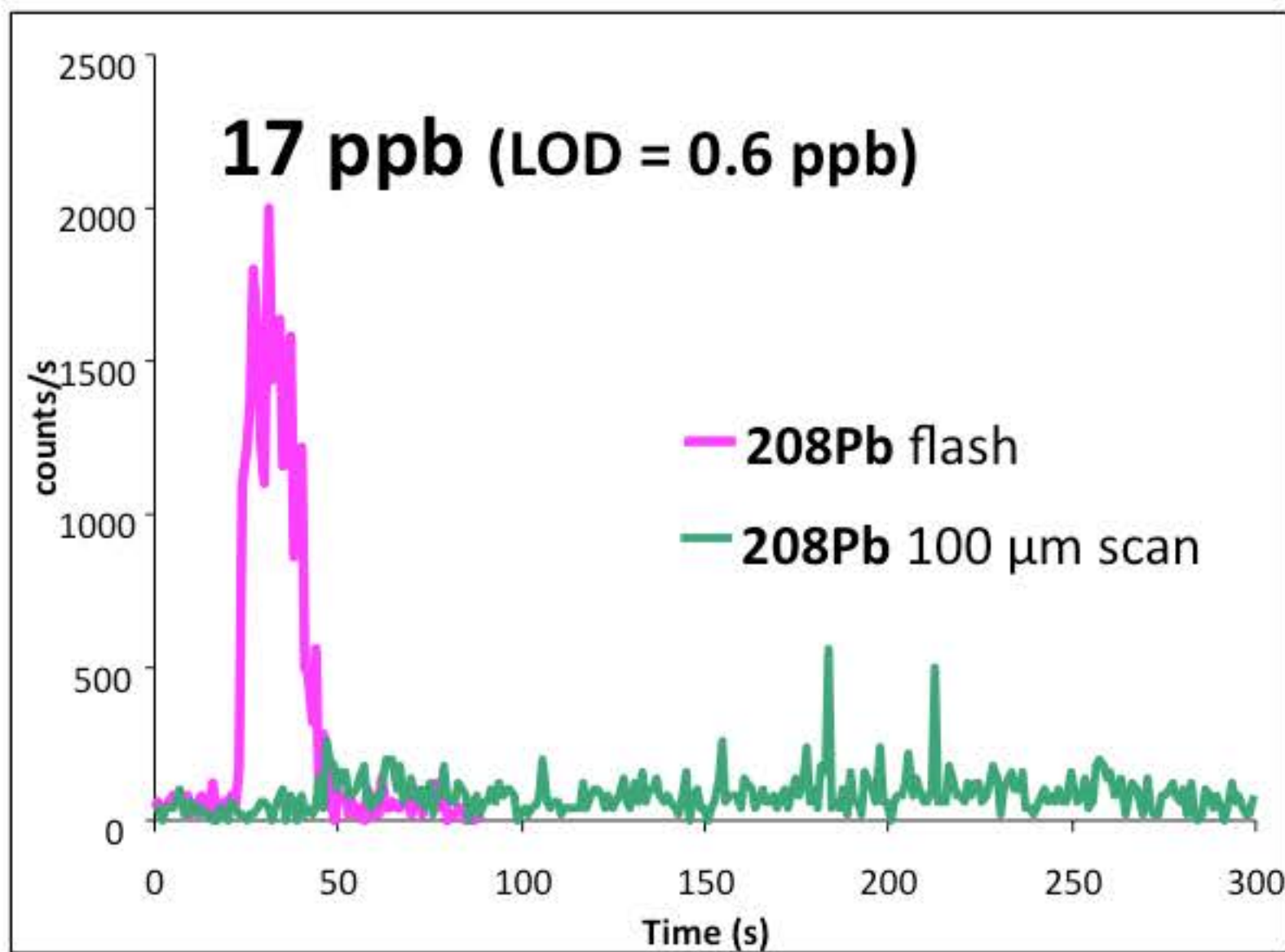
Otolith border
= sampling place

Flash ablation to understand a given life-time history



Flash ablation of the post natal growing zone for high sensitivity...

$$\text{Ablation rate}_{\text{flash}} = 20 \times \text{Ablation rate}_{\text{scan}}$$

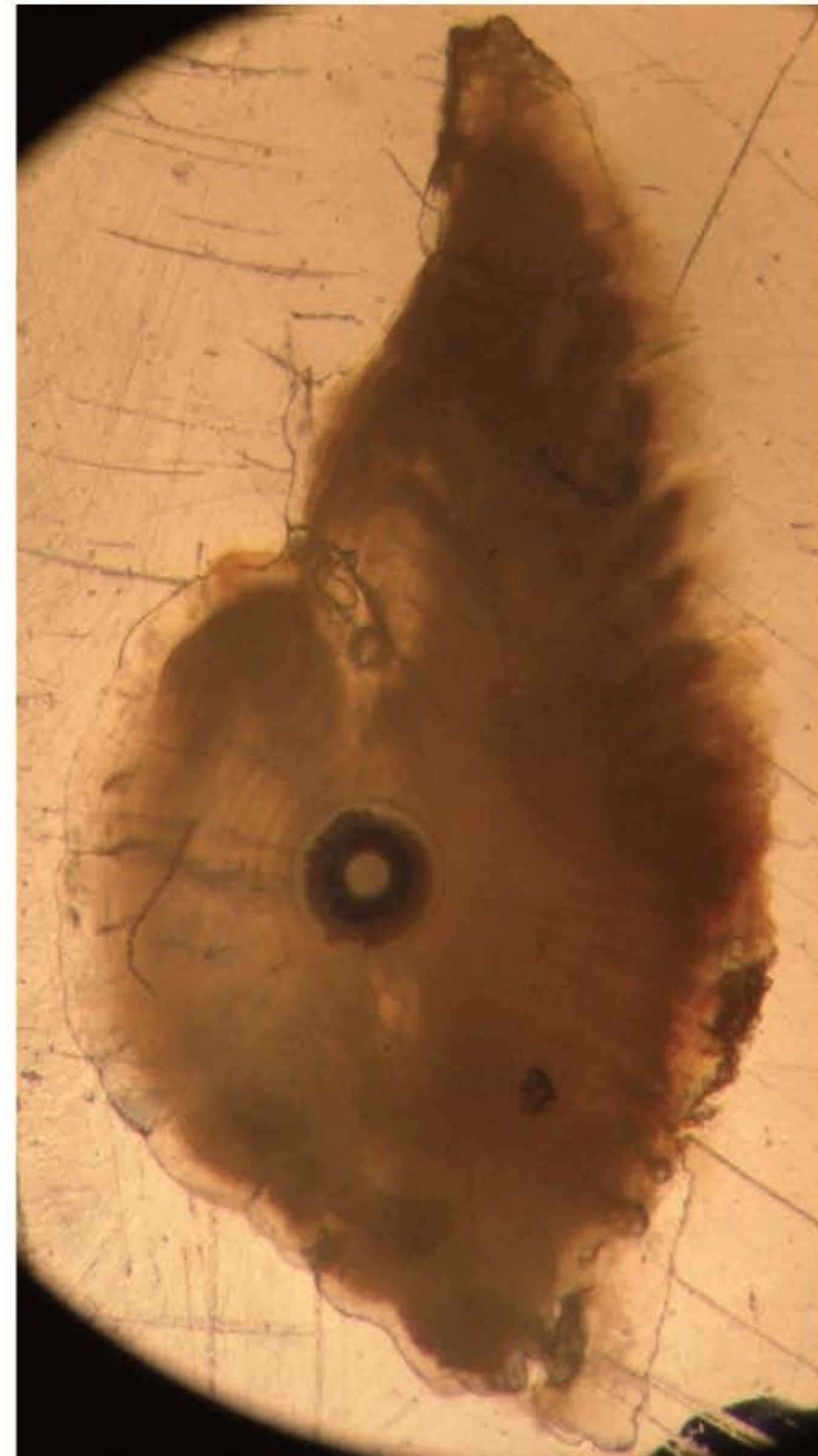


Simulating a corona-shape laser beam

Perrier et al, Can. J. Fish. Aquat. Sci. 68: 977–987 (2011)



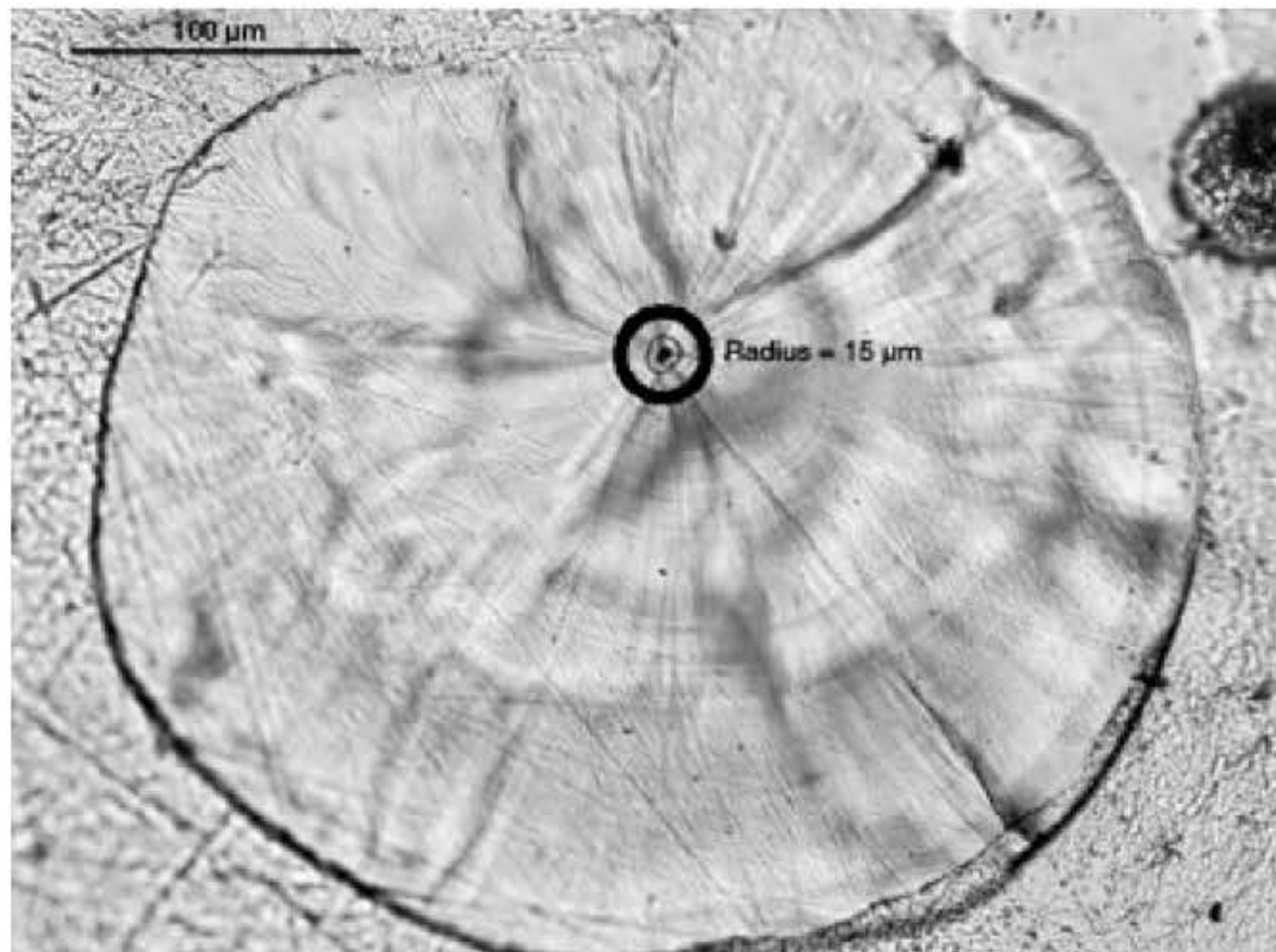
a



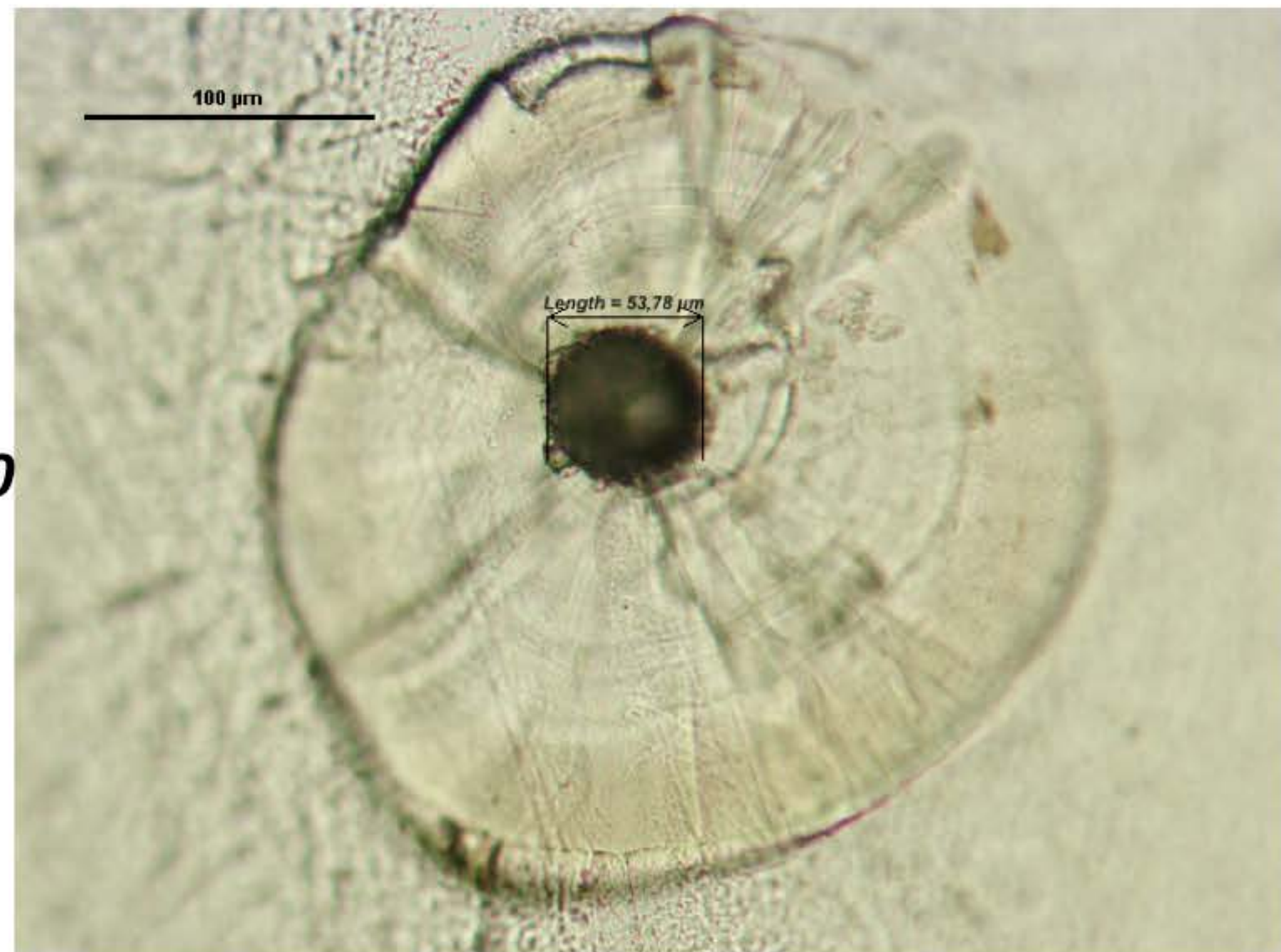
b

Fig. 2. Pictures of (a) juvenile and (b) adult Atlantic salmon otoliths showing the area ablated by the laser prior to inductively coupled plasma mass spectrometry analysis. The annulus ablated is 200–600 µm, is centered on the primordium, and corresponds to the juvenile period of growth only.

Simulating a corona-shape laser beam



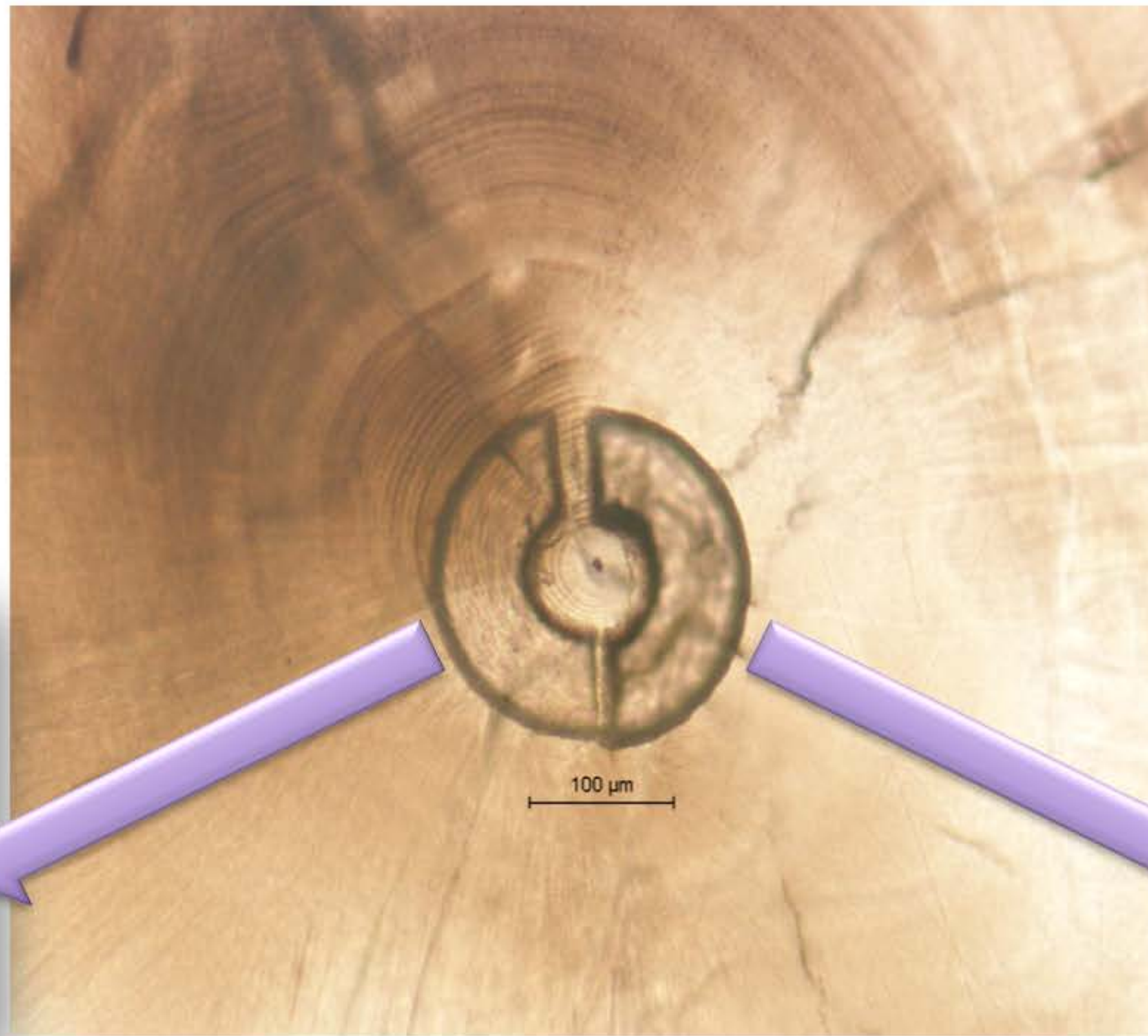
Corona ablation around the nucleus to avoid the mother's signature => place of birth



Martin et al, Ecology of Freshwater Fish, 2010

Fig. 3. Representative otolith image with an annular ablation trajectory along the first feeding mark (15 µm away from the primordium) - *Eel*.

Simulating a semi corona-shape laser beam



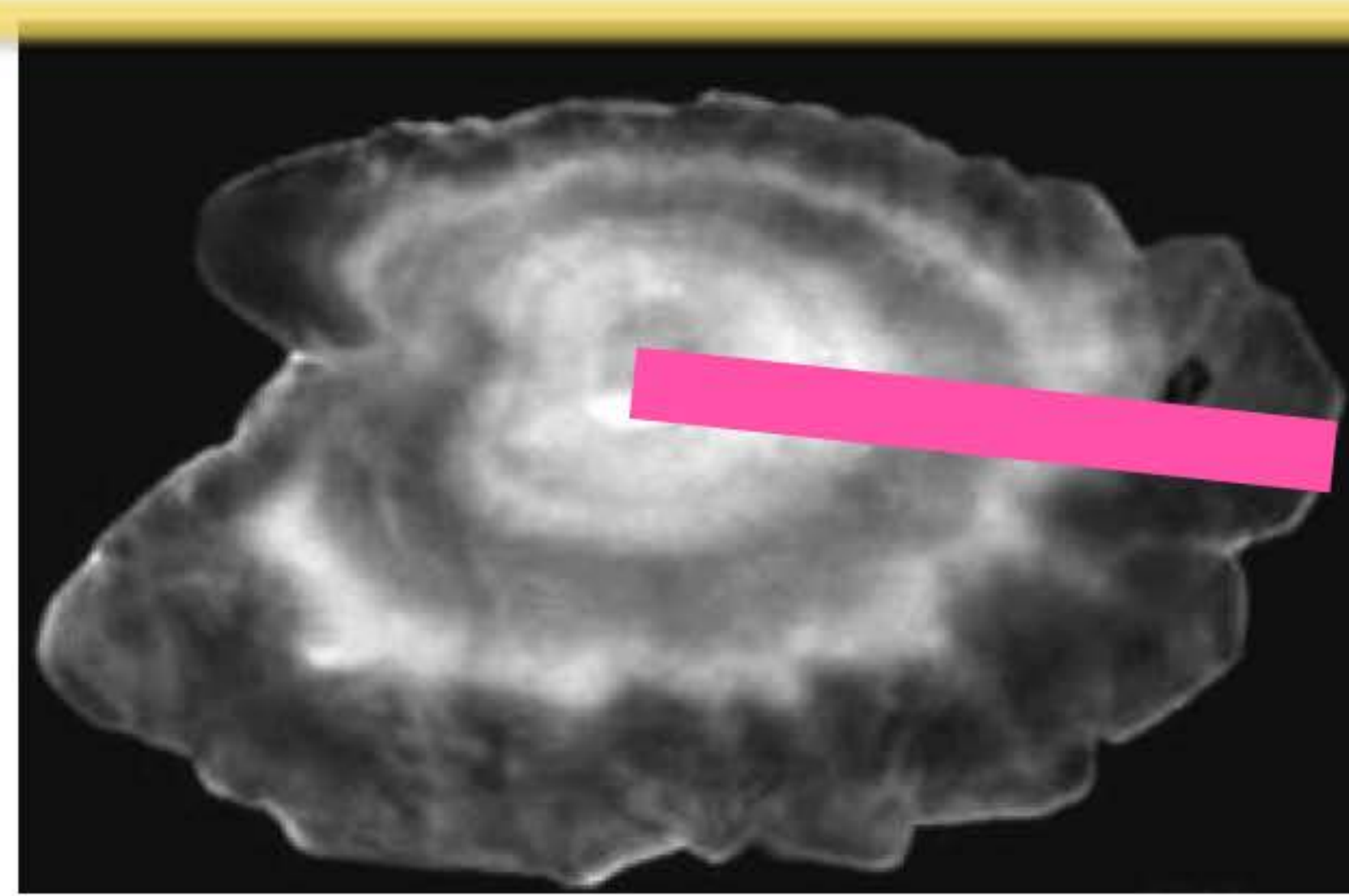
Alosa



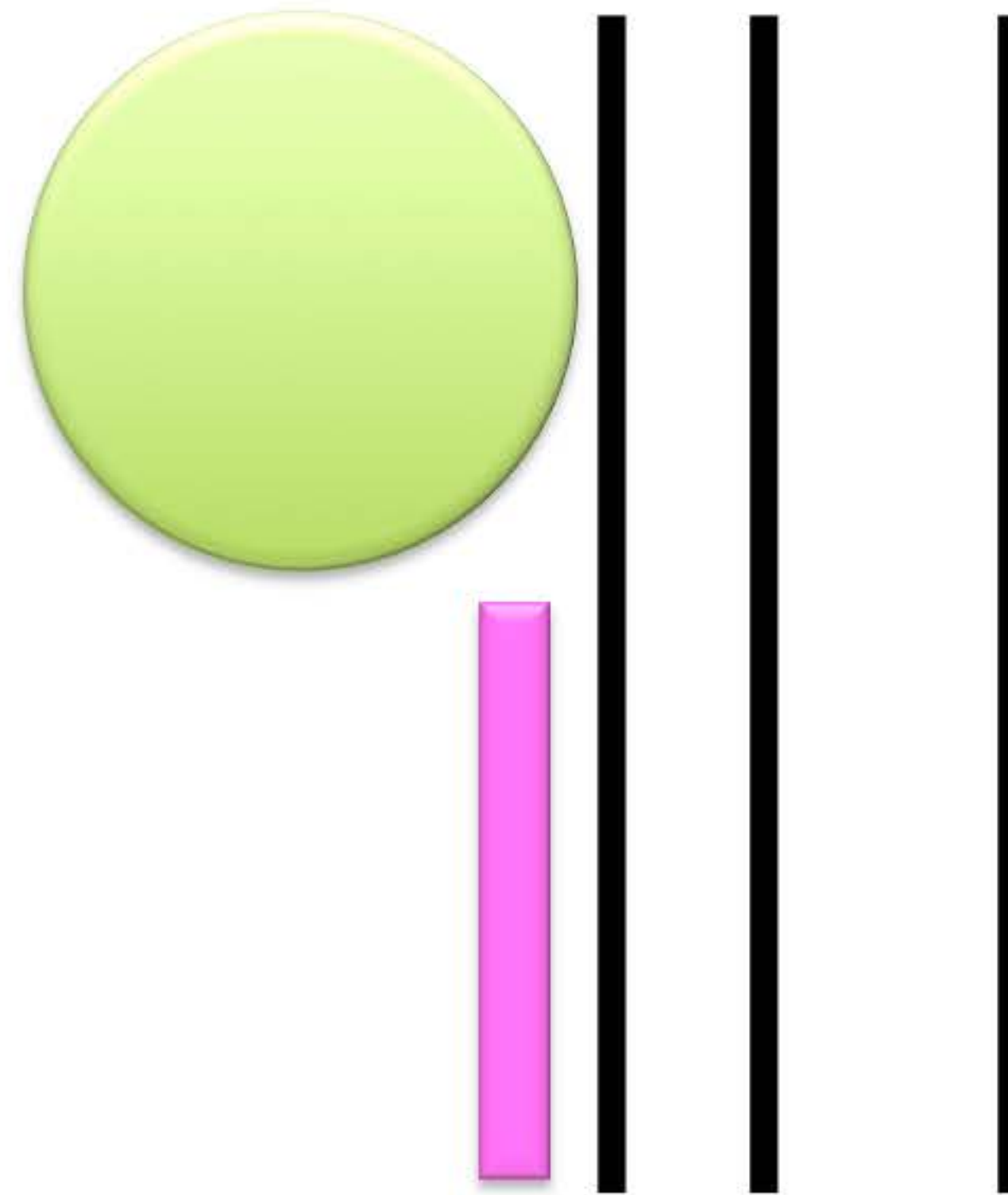
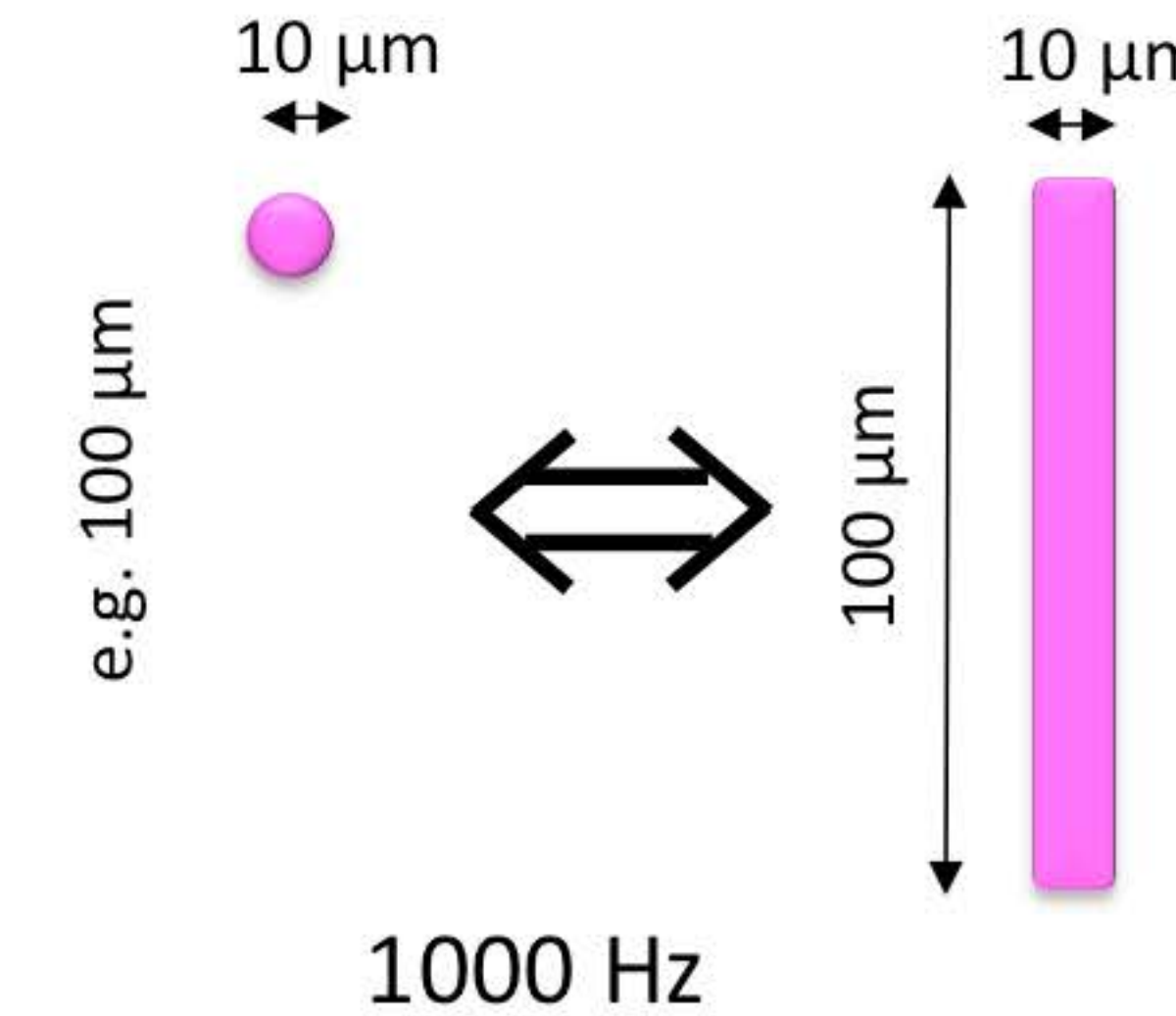
Trace metal analysis
Ba, Sr, Mg, Mn, Zn, Cd,
Pb, Li, Ca...

**Isotope
distribution**
 $^{87}\text{Sr}/^{86}\text{Sr}$, ...

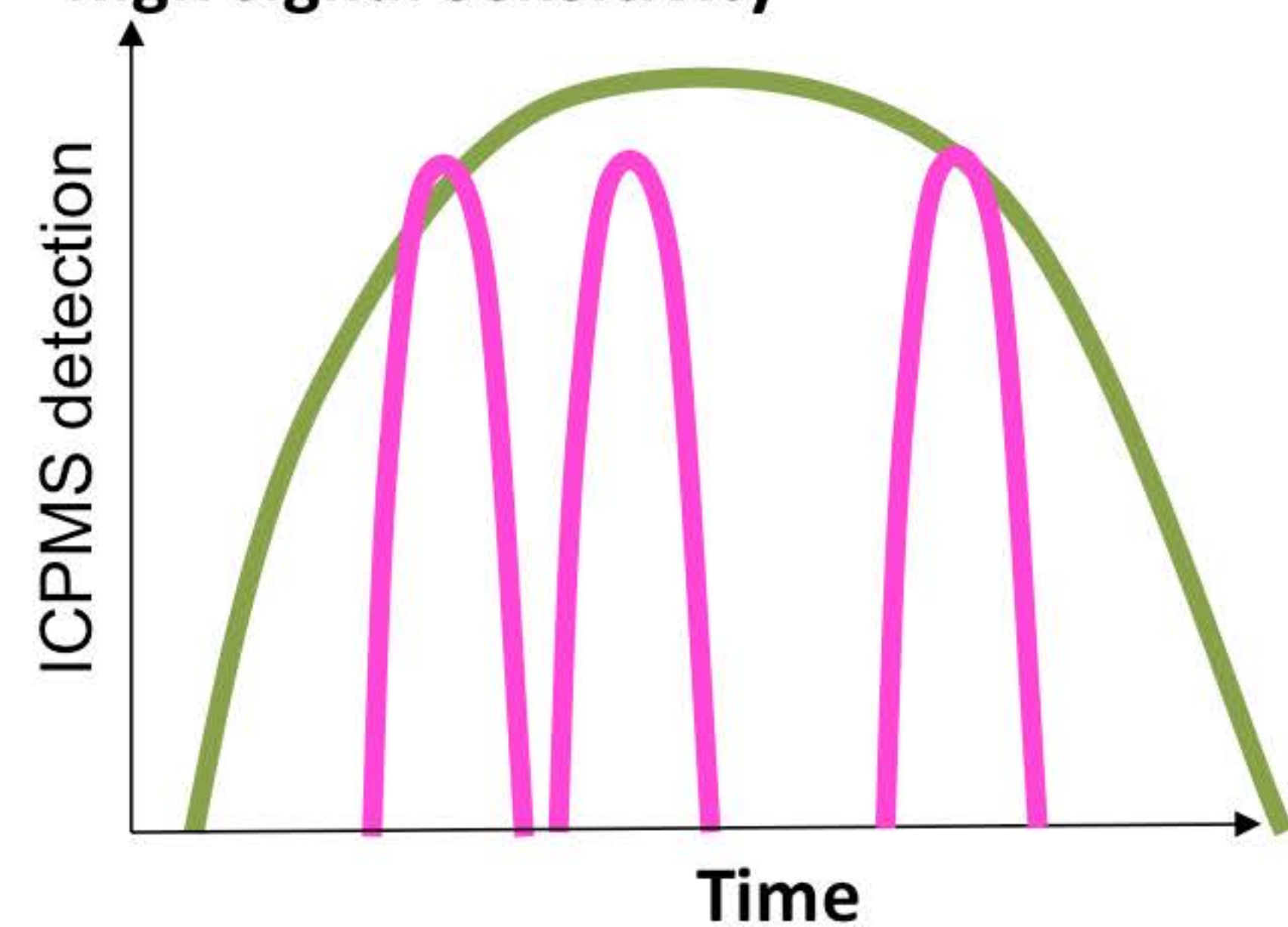
Simulating a sharp blade laser beam



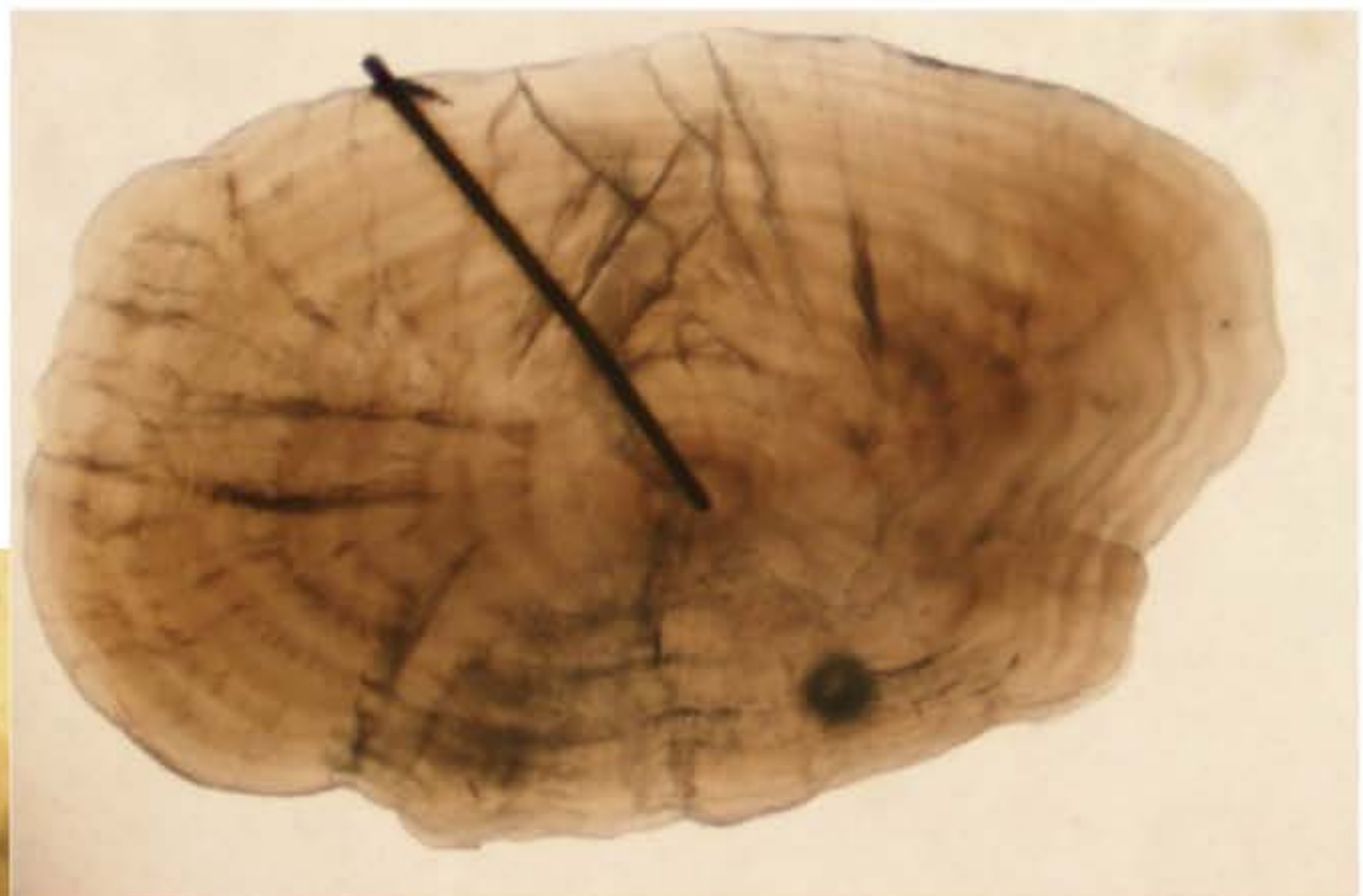
Scanning with a virtual sharp blade...



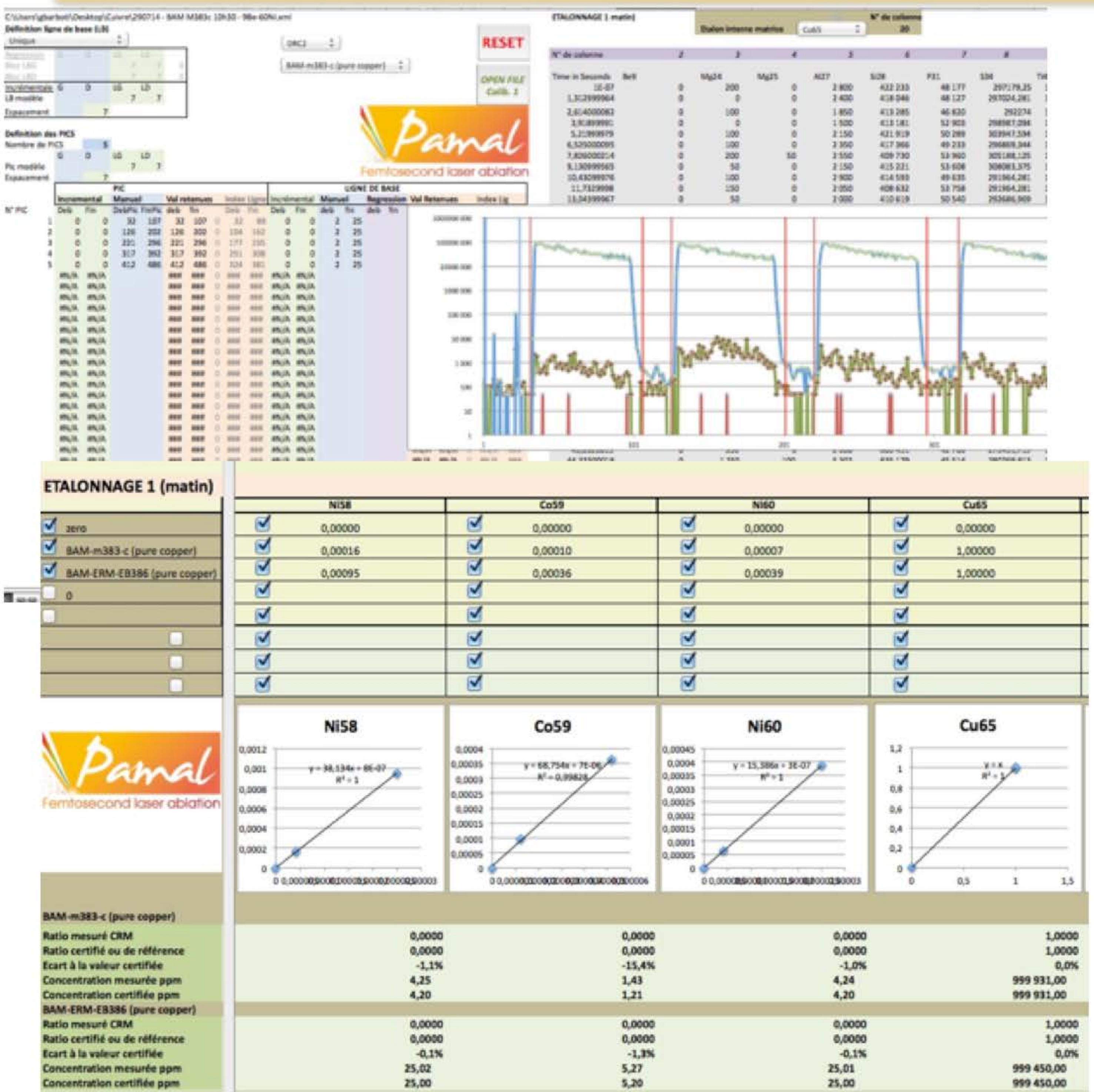
Large spot vs sharp blade ablation :
-> better spatial resolution while keeping
high signal sensitivity



Sharp blade ablation scan, growing axis, life history



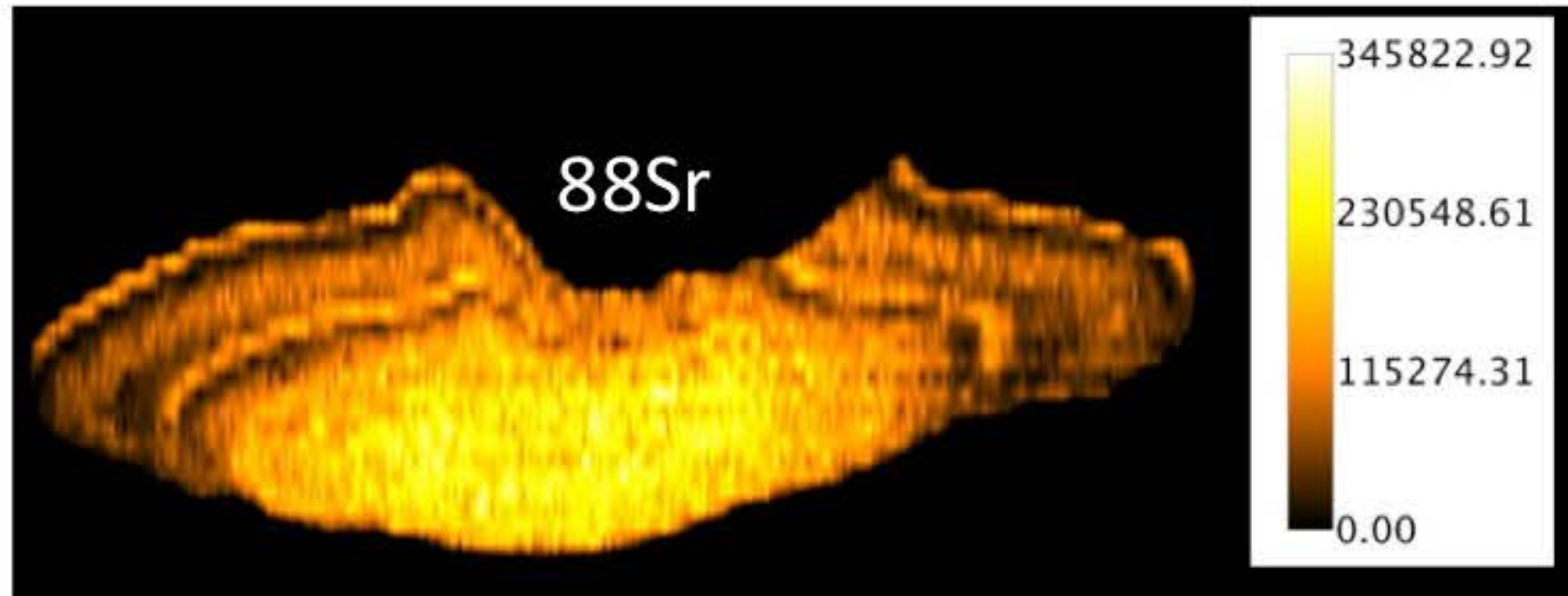
Quantitation and quality control



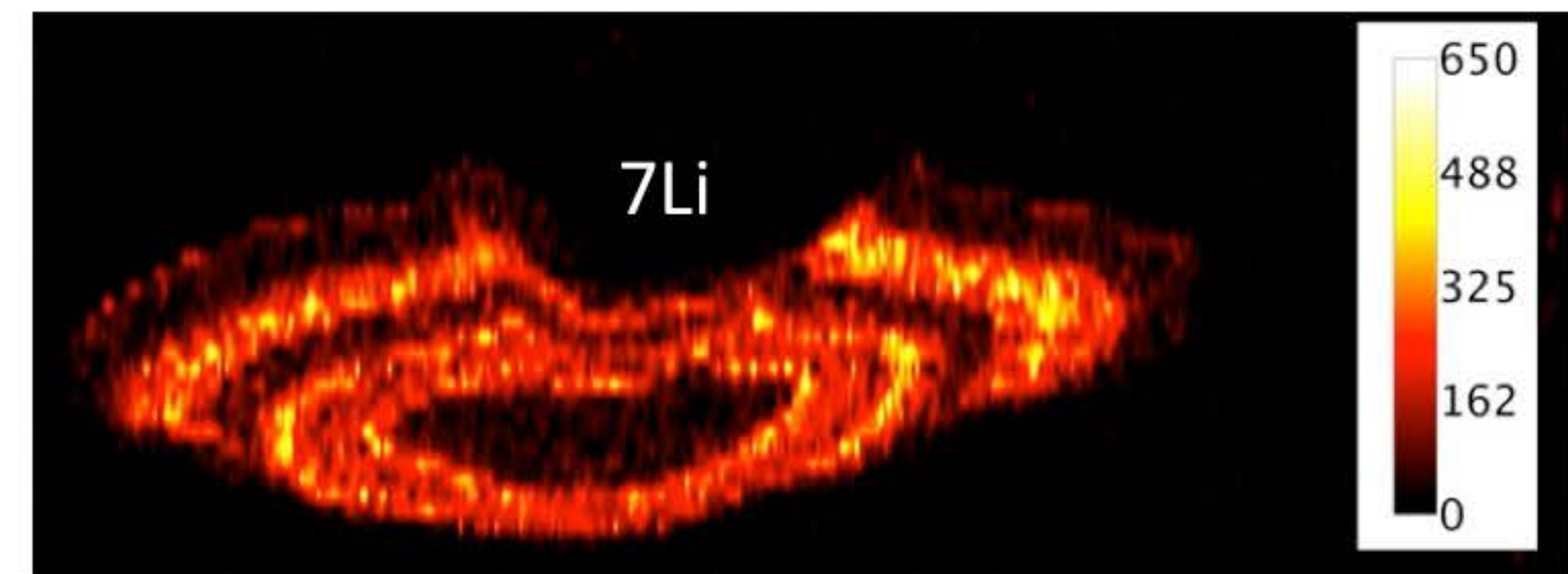
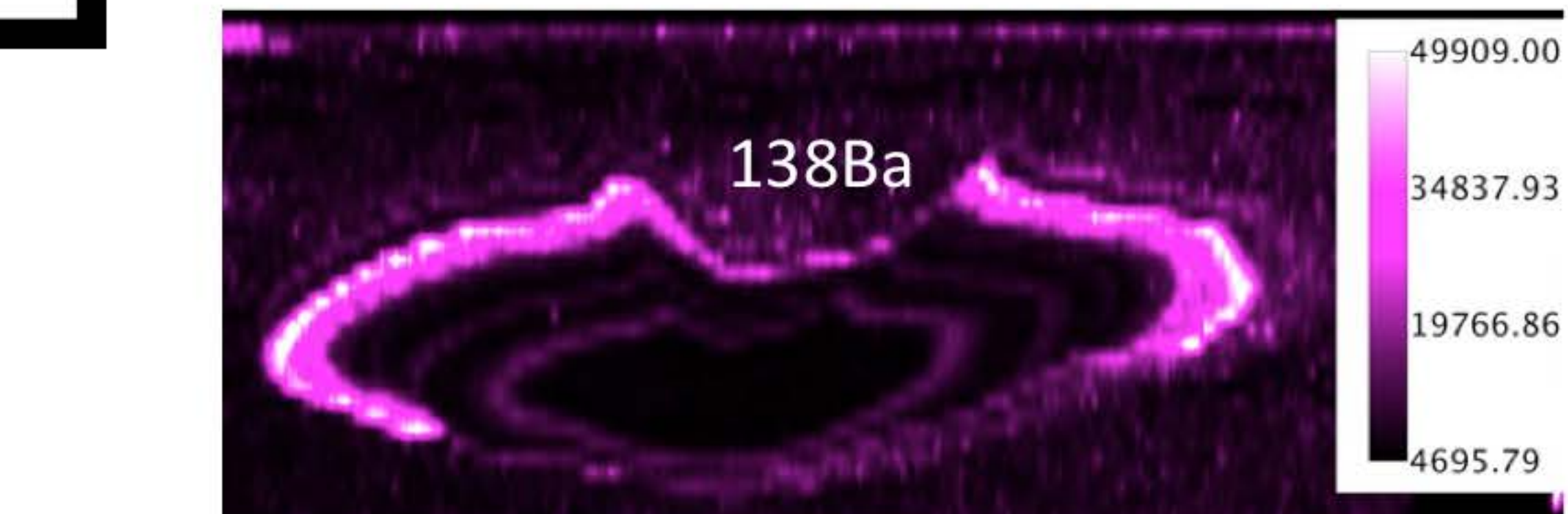
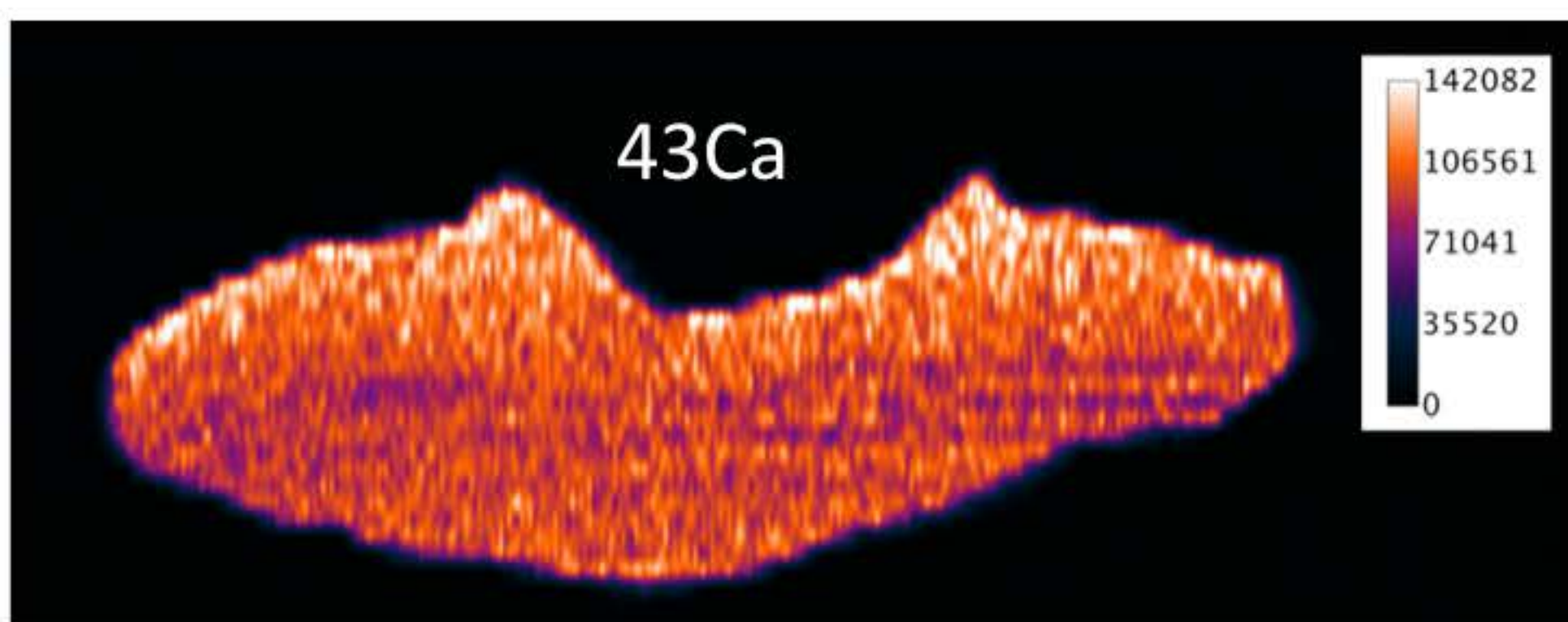
We have developed our own VBA Macro working with Excel (FOCAL series) for data processing and quantification. FOCAL series allows rapid quantification with quality control tools for the various laser ablation approaches : ablation lines (continuous scan across a sample, spot ablation, rasters for imaging).

When images are required, the processed data are imported with ImageJ for easy handling.

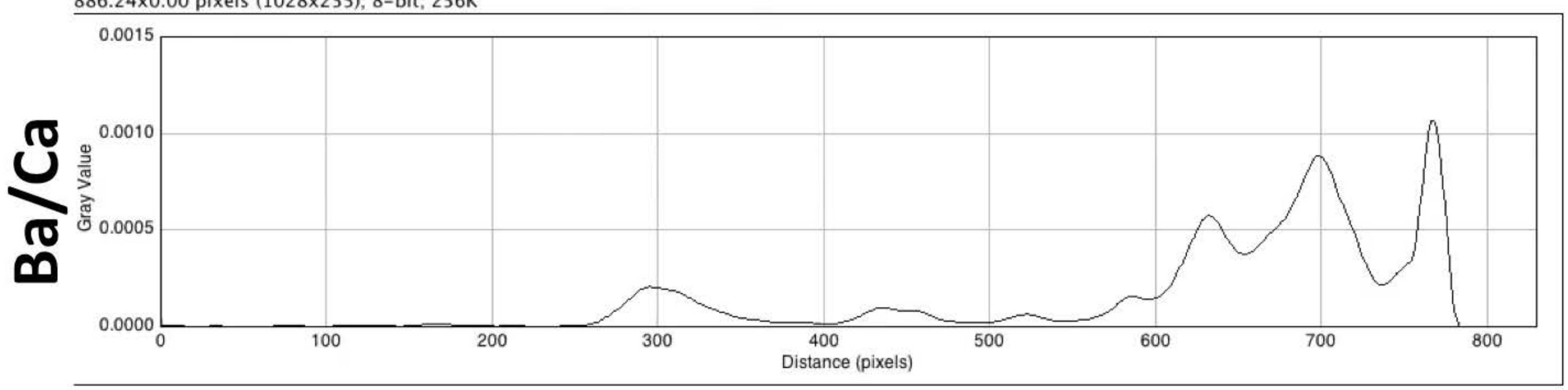
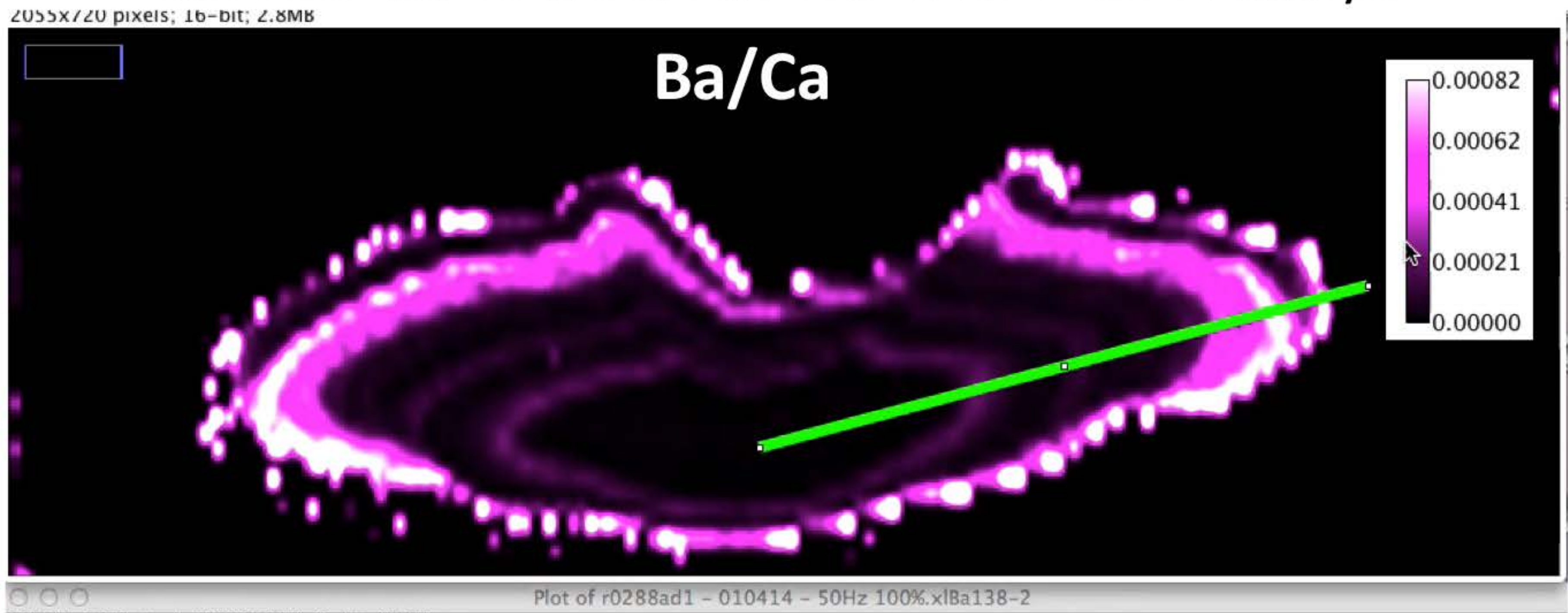
The sharp-blade shape allows real square pixels and better resolution.



Once the image is acquired, select the desired axis for the plot profile



Otolith imaging as a decision tool to select the best ablation scan direction for routine analysis



Simultaneous isotopic and trace element information

LAMBDA 3
360 Fs
1Hz-100 000 Hz
257 nm



Using the same laser trace....

Element XR (Jet Interface)

- High sensitivity (HRICPMS)

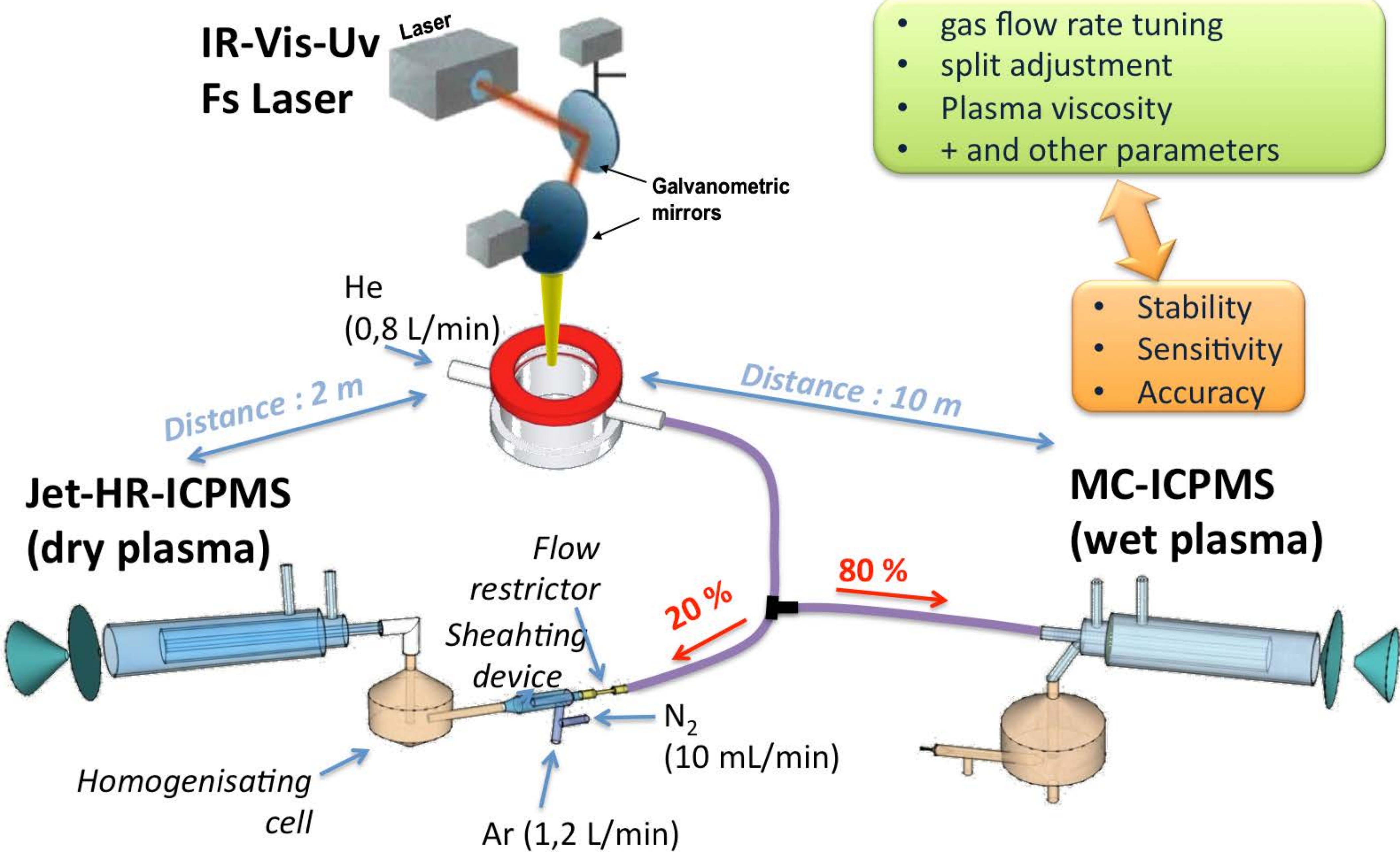


Nu Plasma HR

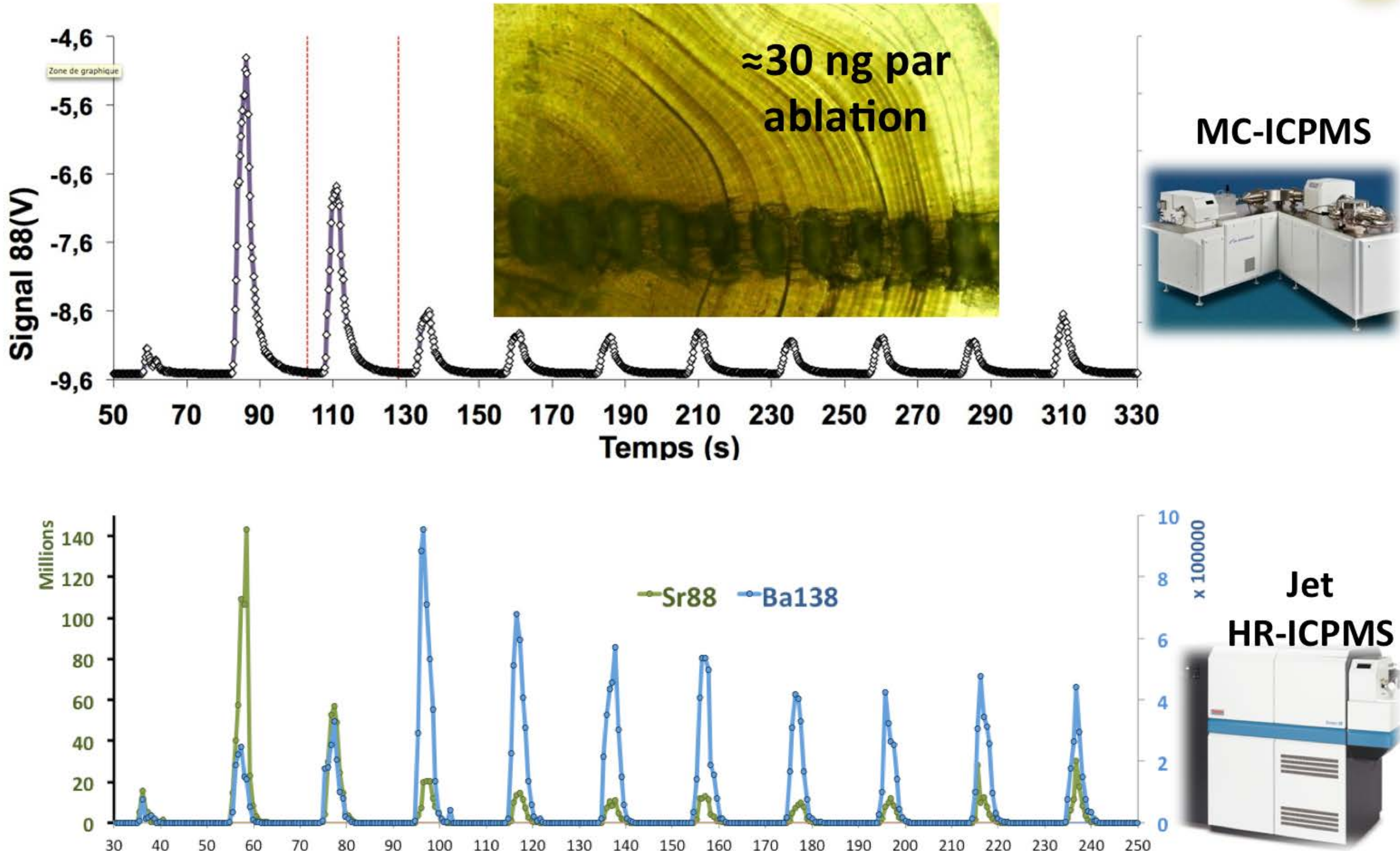
High isotopic precision (MCICPMS)



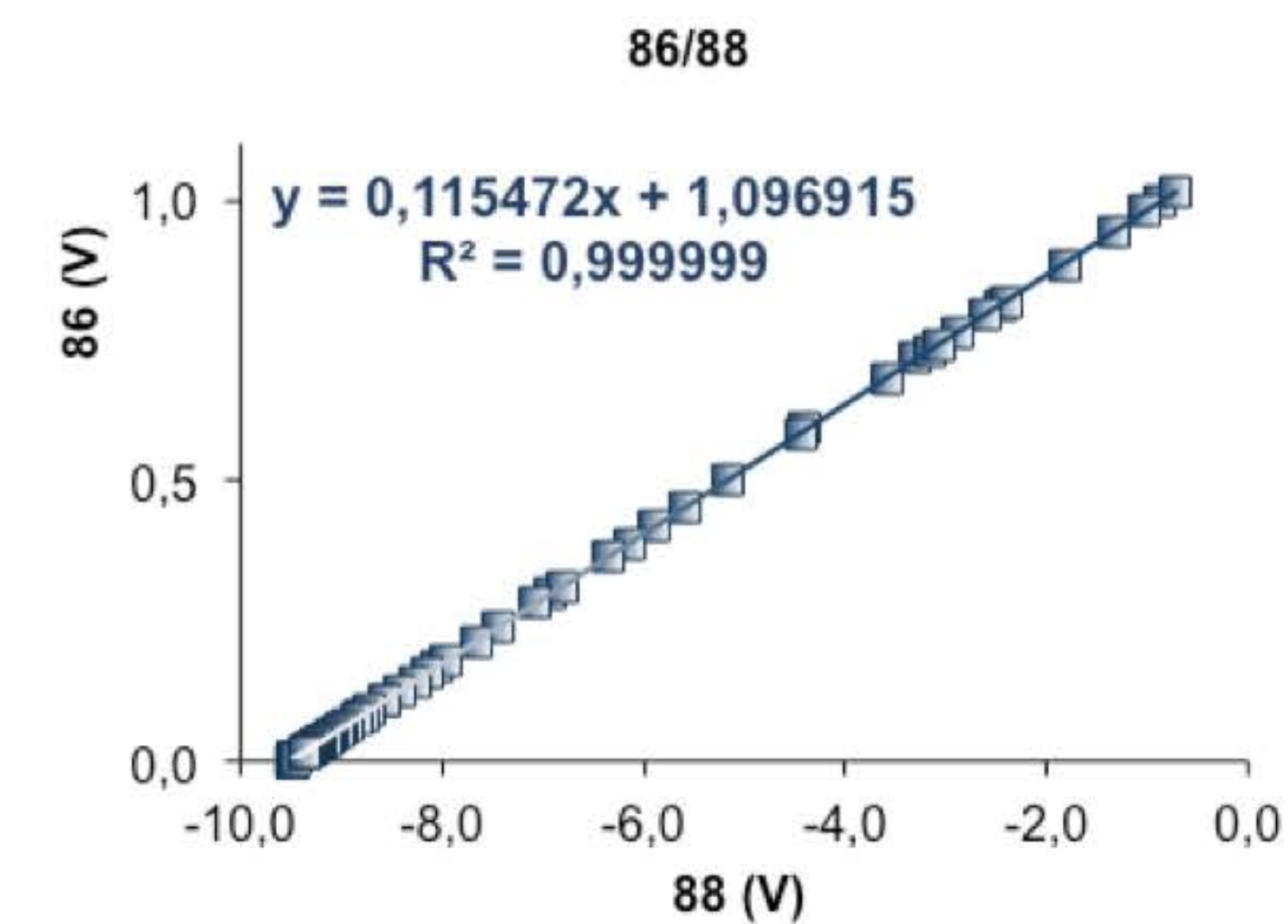
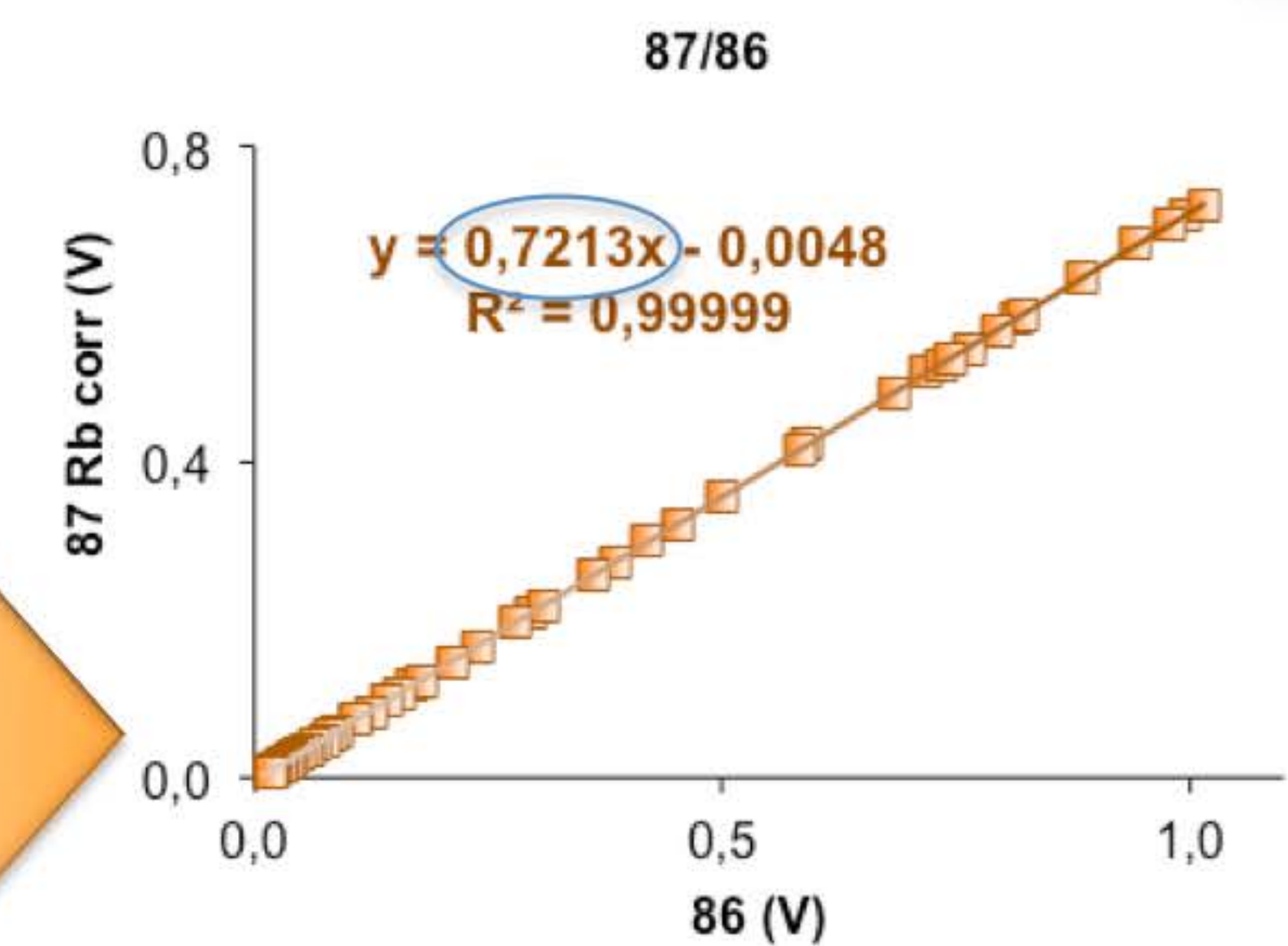
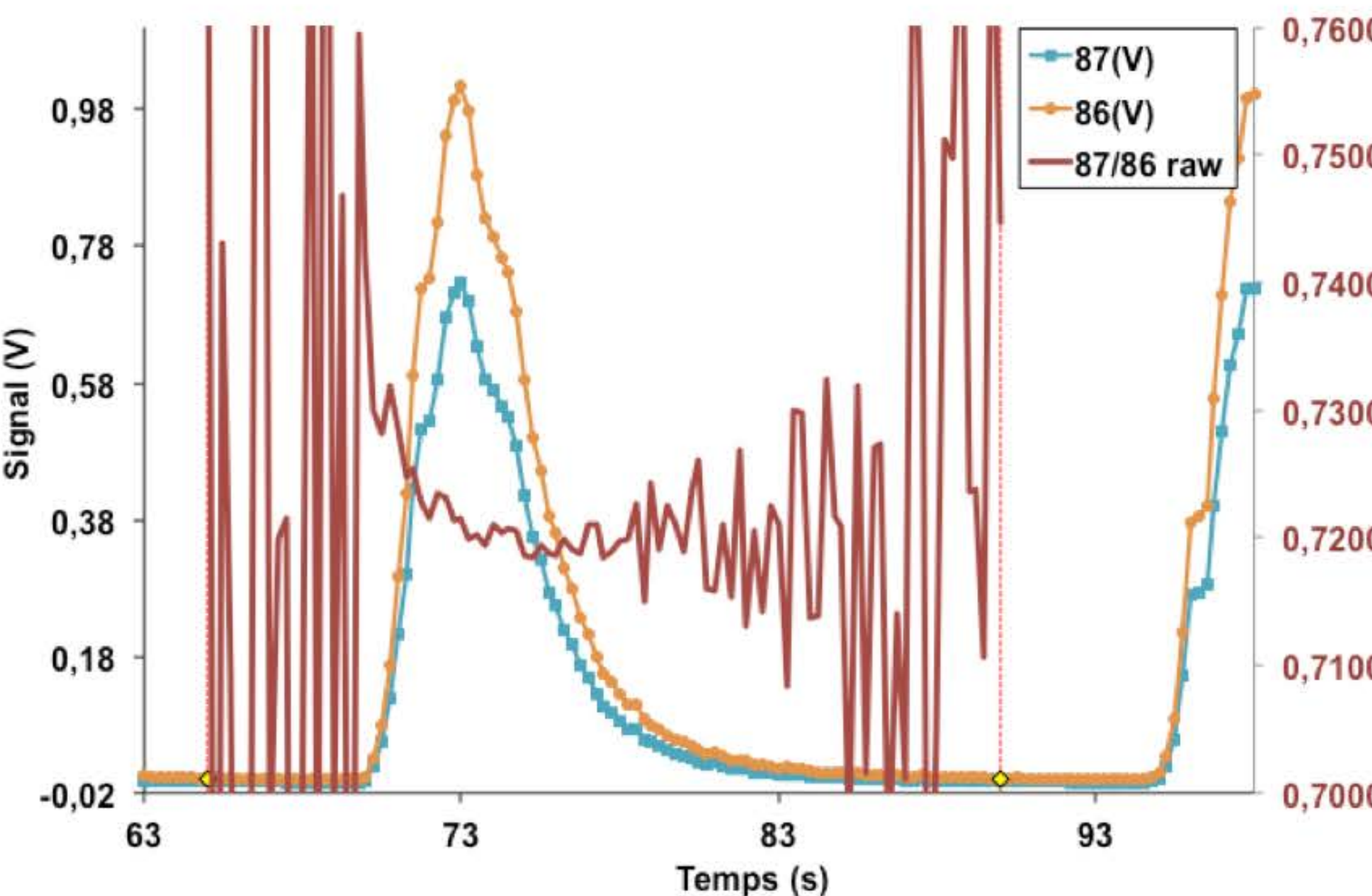
Simultaneous isotopic and trace element information



FsLA- 2D-SF-ICPMS : Simultaneous isotopic and trace element information



Isotopic data reduction for fast transient signal using an innovative Linear Regression Slope approach



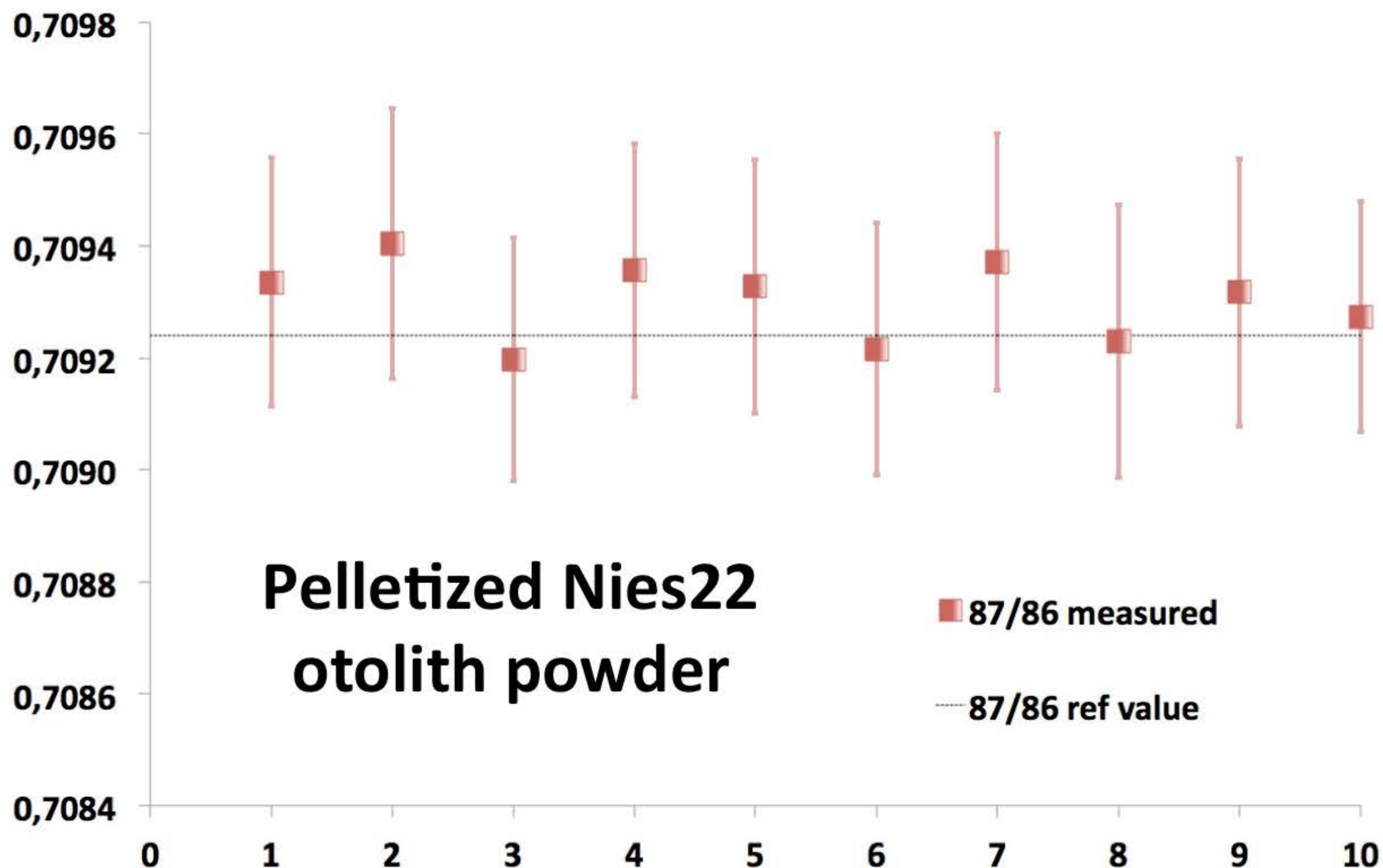
- Very easy
- Natural weighting of the statistic
- precision improved by $\times 10$ (minimum)
- mass bias correction using $^{88}\text{Sr}/^{86}\text{Sr}$

- Fietzke et al.(2008), JAAS, Sr by LA/MCICPMS
- Epov et al.(2010), Anal. Chem: Hg by GC / MCICPMS
- Sanabria et al (2012), Anal.Chem; Pb by GC/MCICPMS
- Resano et al (2012), JAAS, Cu by LA/MCICPMS

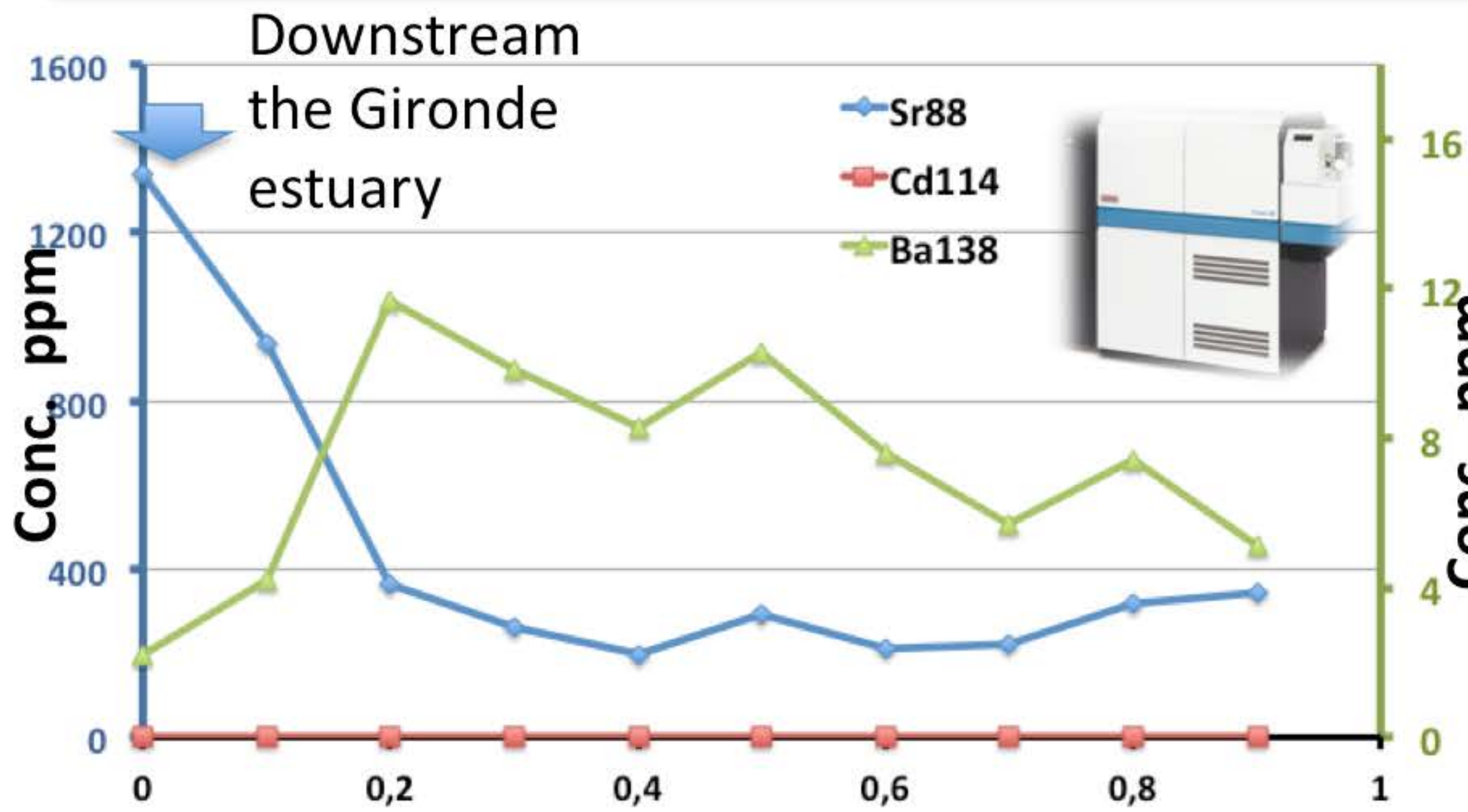
LCABIE

Precision on fast transient signal using the Linear Regression Slope approach

External Precision (2xRSD) n=10 : 200 ppm i.e. (0,02 %)
Internal precision (2xRSE): 600 ppm, (i.e. 0,06%)

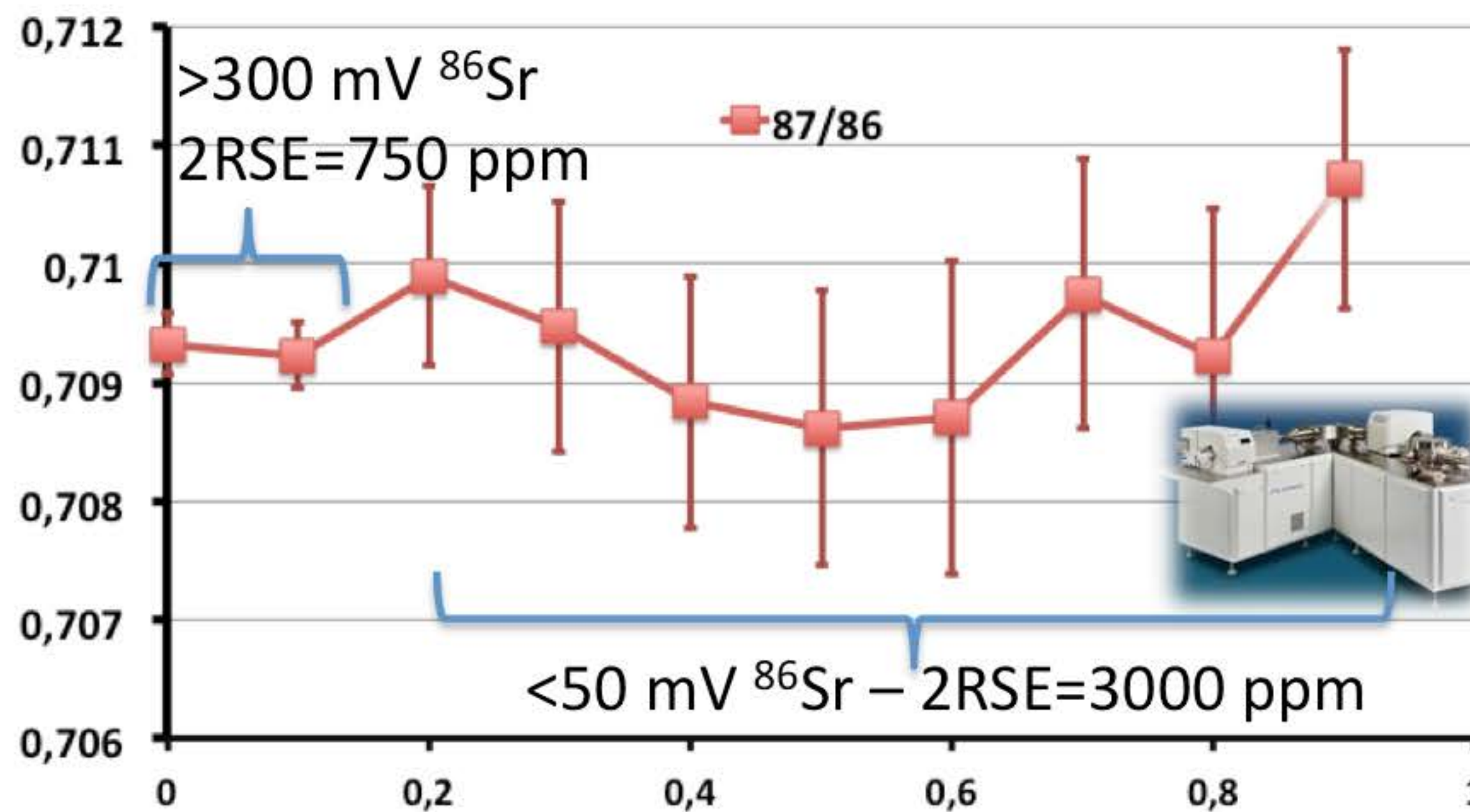


Simultaneous isotopic and trace element information



Typical LODs with fsLA/Jet-HRICPMS

Sr = 40 ppb *i.e. 1,2 femtograms*
 Ba = 6 ppb *i.e. 180 attograms*
 Cd = 4 ppb *i.e. 120 attograms*



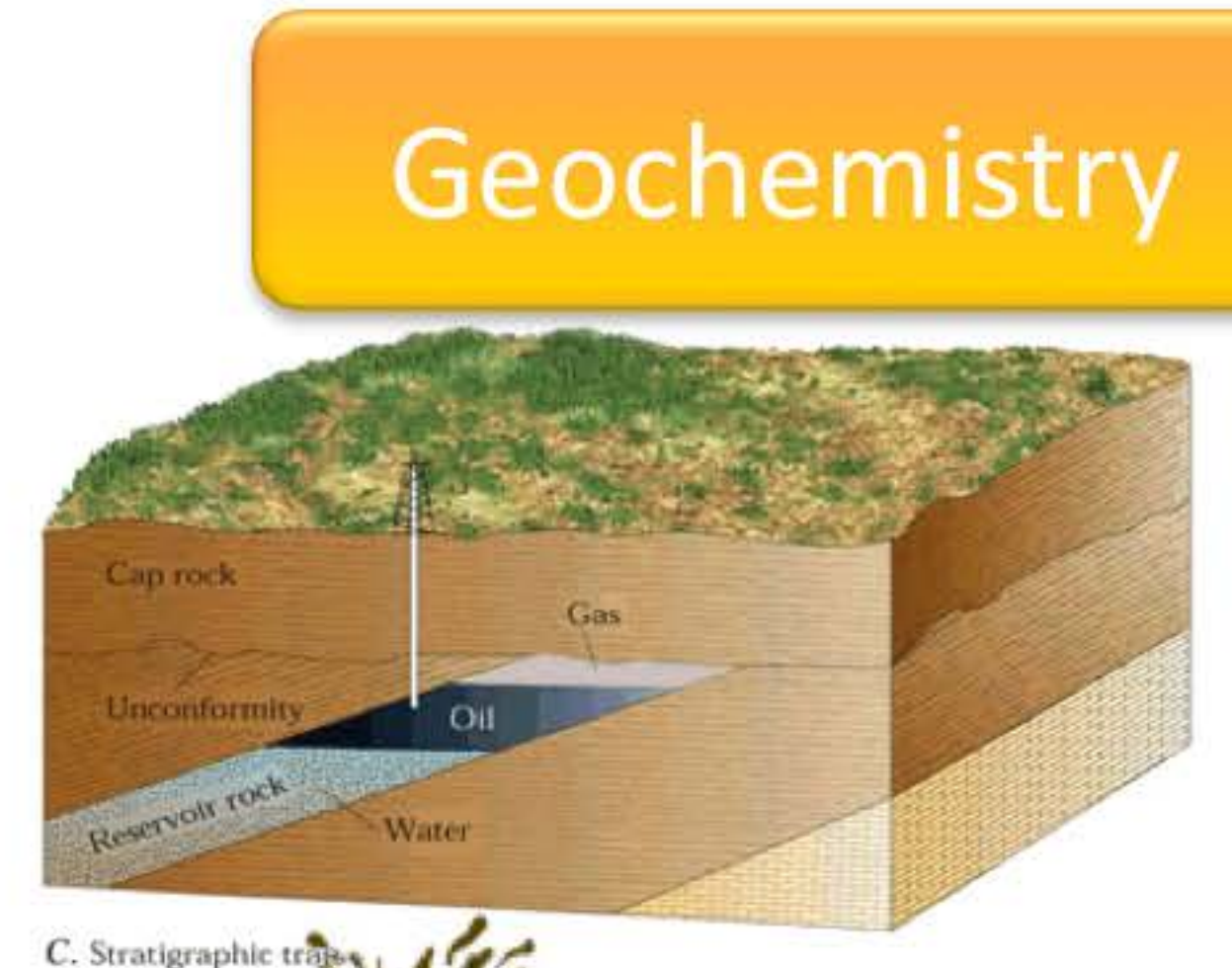
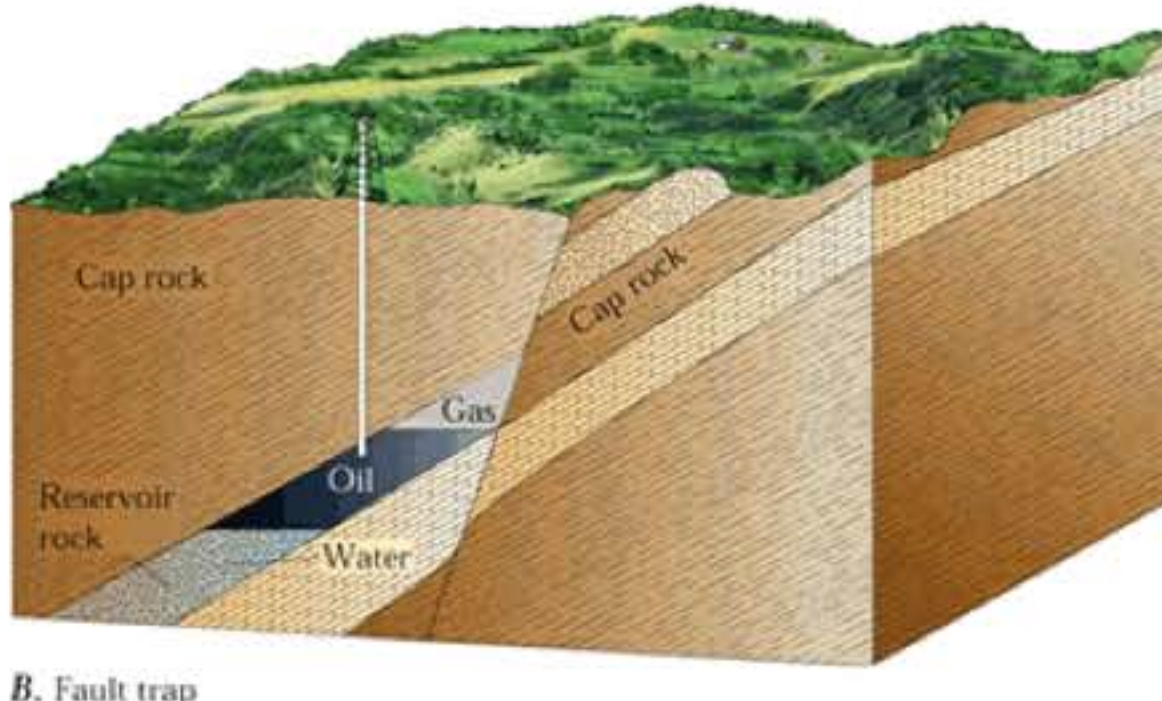
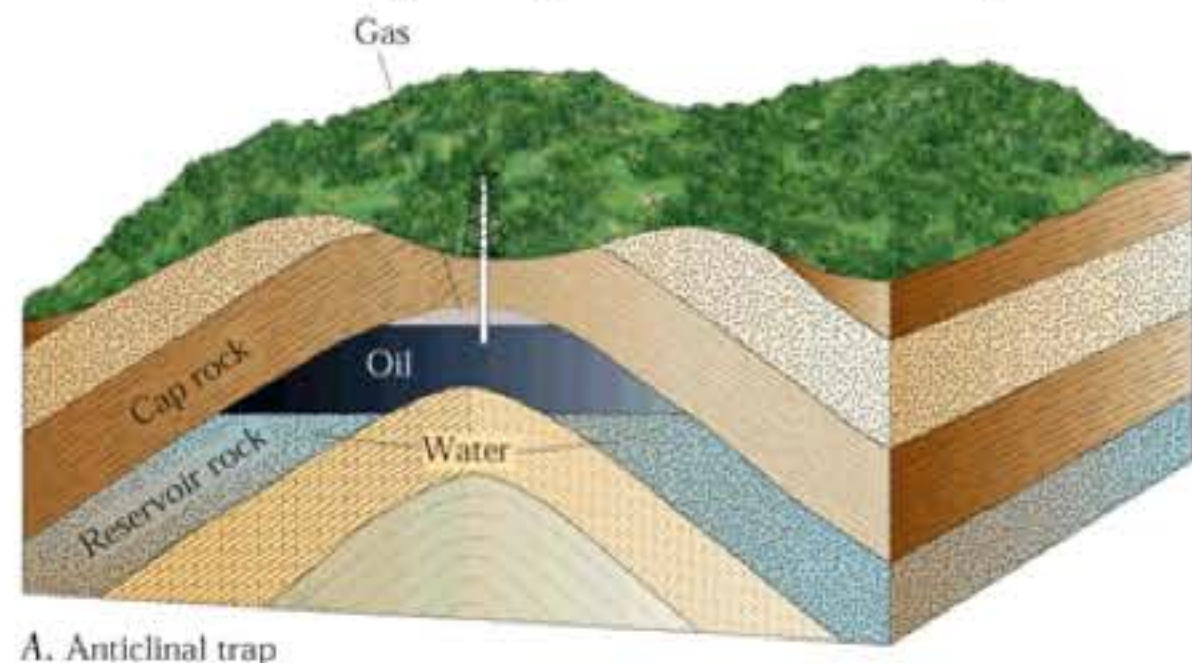
Versatile approach with complementary information.
 Relevant when some geochemical signatures are not significantly pronounced (here 87/86Sr)

Application of the virtual beam shaping to crude oil



Direct analysis of trace metals in petroleum product

Better understanding in petroleum reservoir => upstream
(Exploration).



Geochemistry

- Oil-Oil correlation
- Oil-source rock correlation
- Deposits conditions
- Oil maturity
- Oil migration
- Degrees of biodegradation



Analytical challenge

Organic product analysis still not easy in ICPMS :

- high sample dilution (crude oil)
- O₂ feeding
- Mineralisation



Trace element analysis in crude oil by FsLA- ICPMS :

Laser Ablation

- Direct analysis



- Very limited sample preparation

- No sample dilution

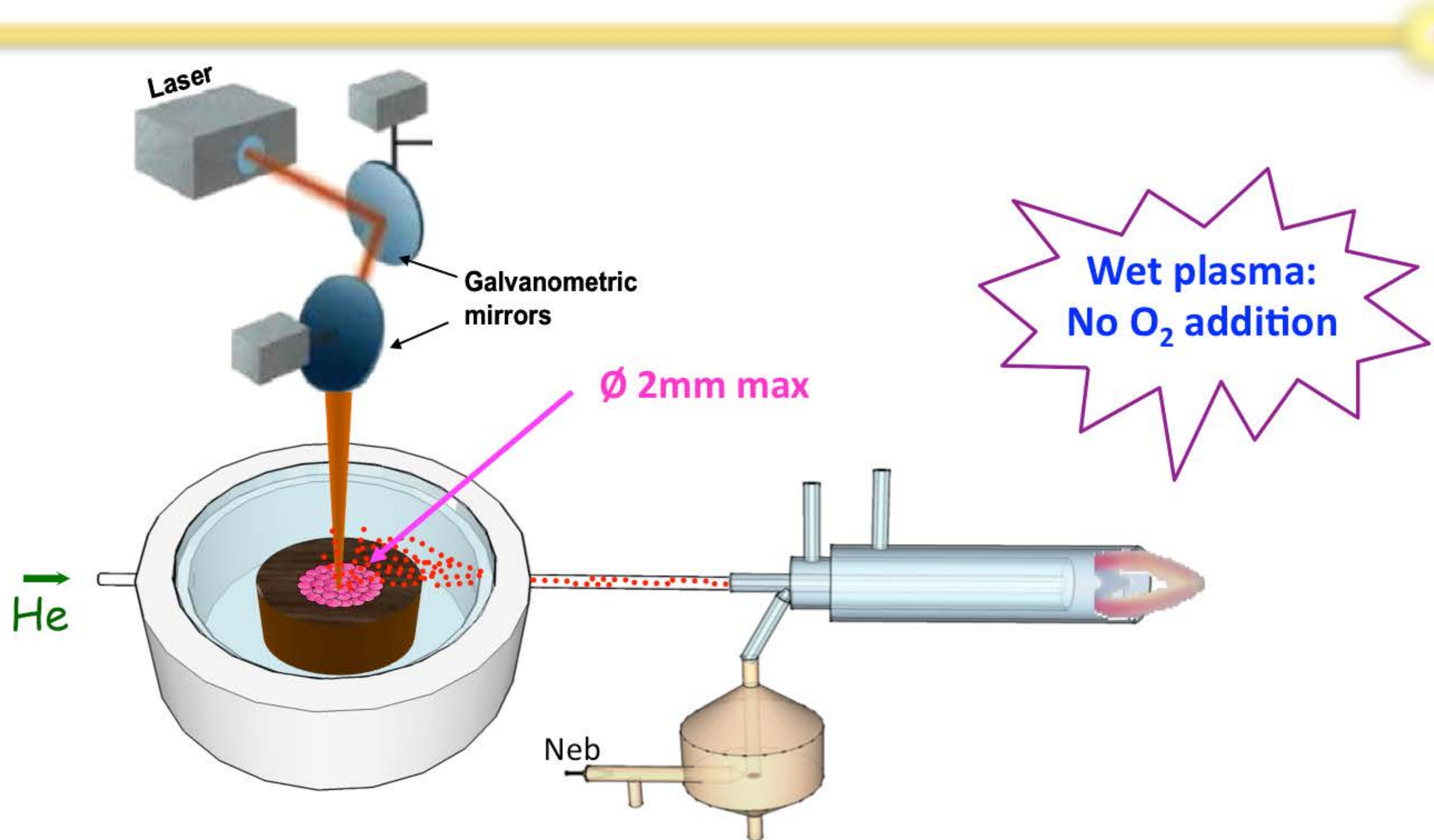
- Low organic sample introduction (~20 µg/min)
⇒ better plasma tolerance
⇒ No need for oxygen feeding

High repetition rate FsLA/ ICPMS coupling



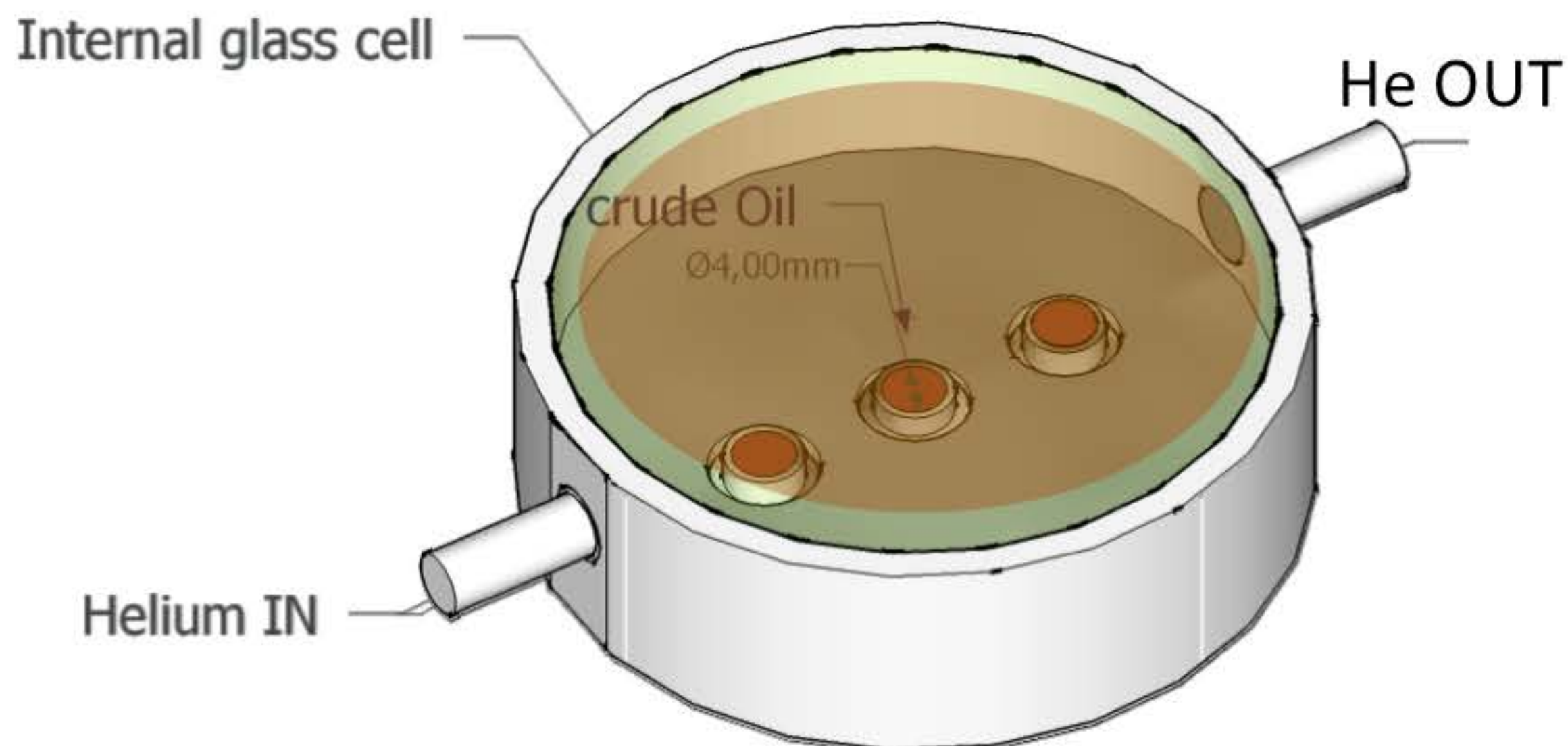
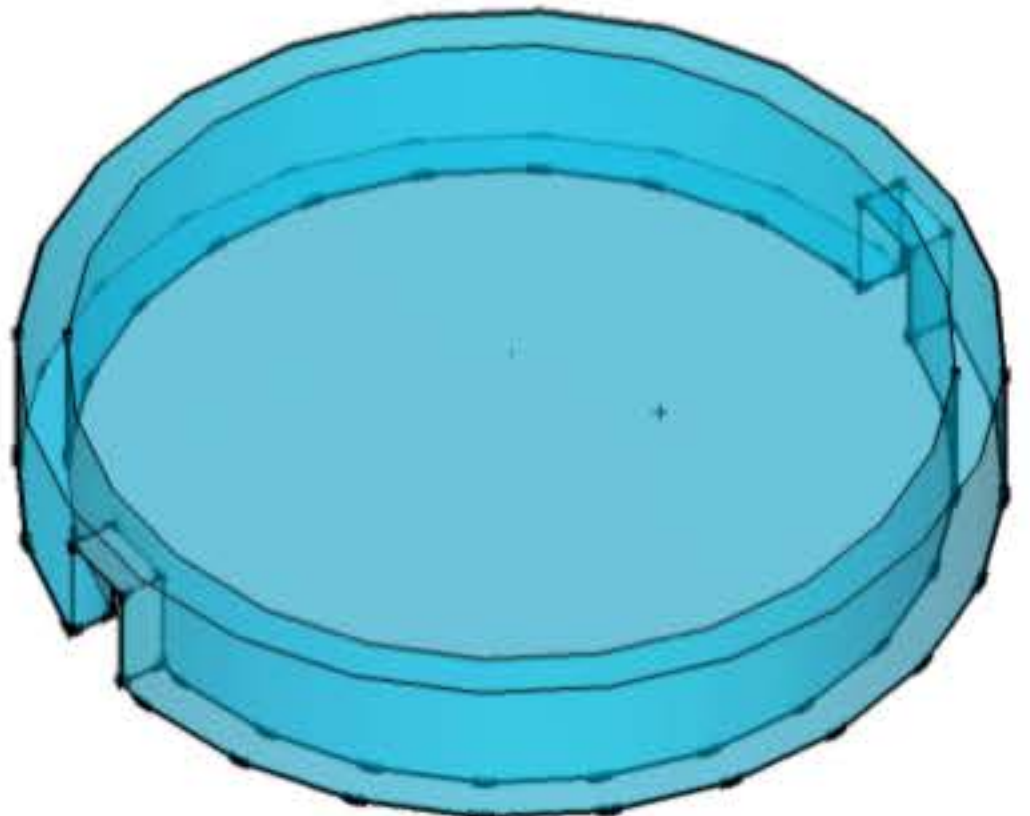
- Fast analysis (< 2 min compared to 20 min in conventional nebulisation)

Trace element analysis in crude oil by FsLA- ICPMS :



- Wavelength : 1 030 nm,
 - Pulse duration : 360 fs,
 - 17 μm laser beam
 - Repetition rate : up to 10 000 Hz
 - Fast 2D laser ablation trajectories (up to 280 mm.s⁻¹)
- } High sensitivity

Trace element analysis in crude oil by FsLA- ICPMS :



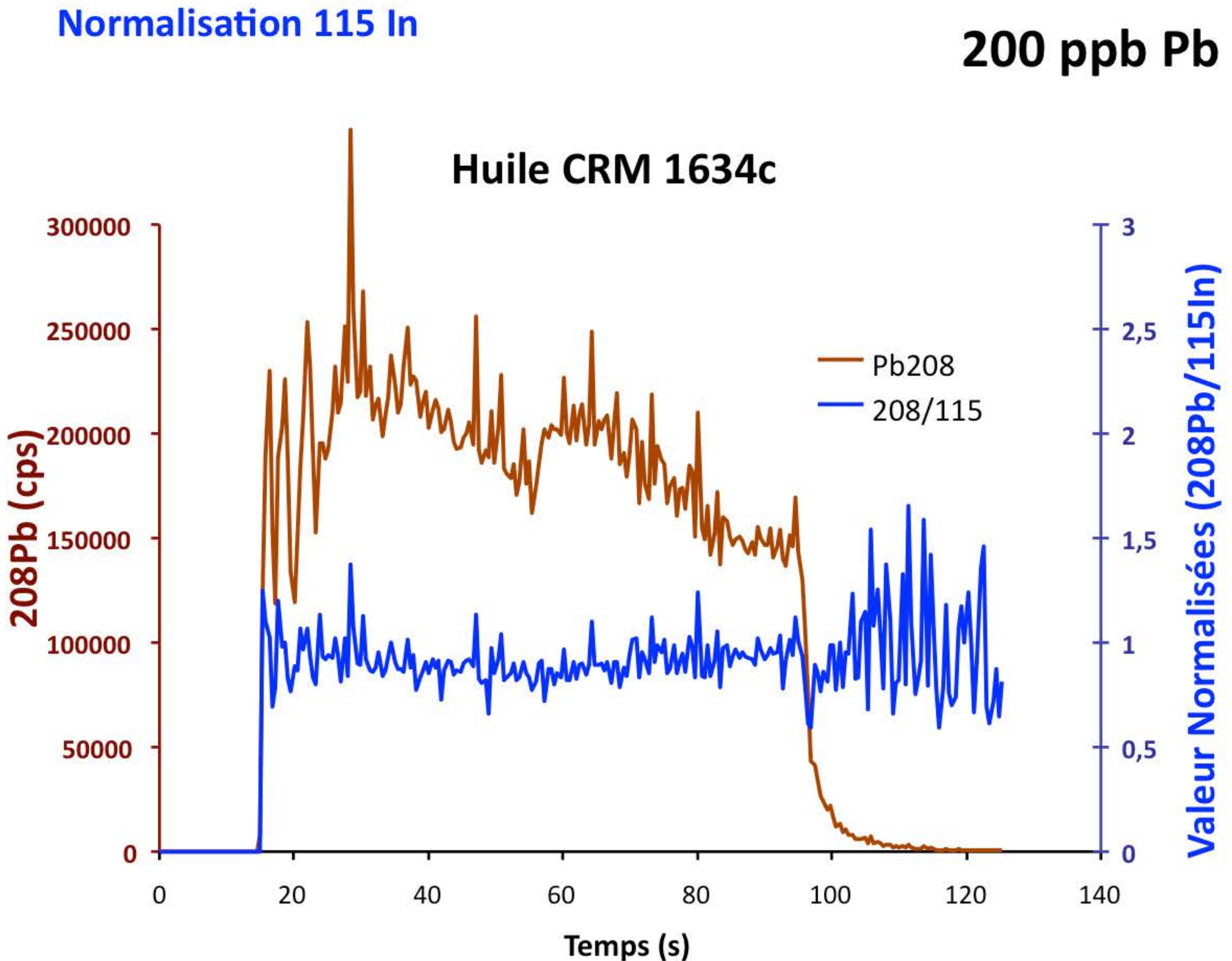
Substantial splashing effects:

- ⇒ Contamination
- ⇒ Cell window alteration
- ⇒ Objective alteration

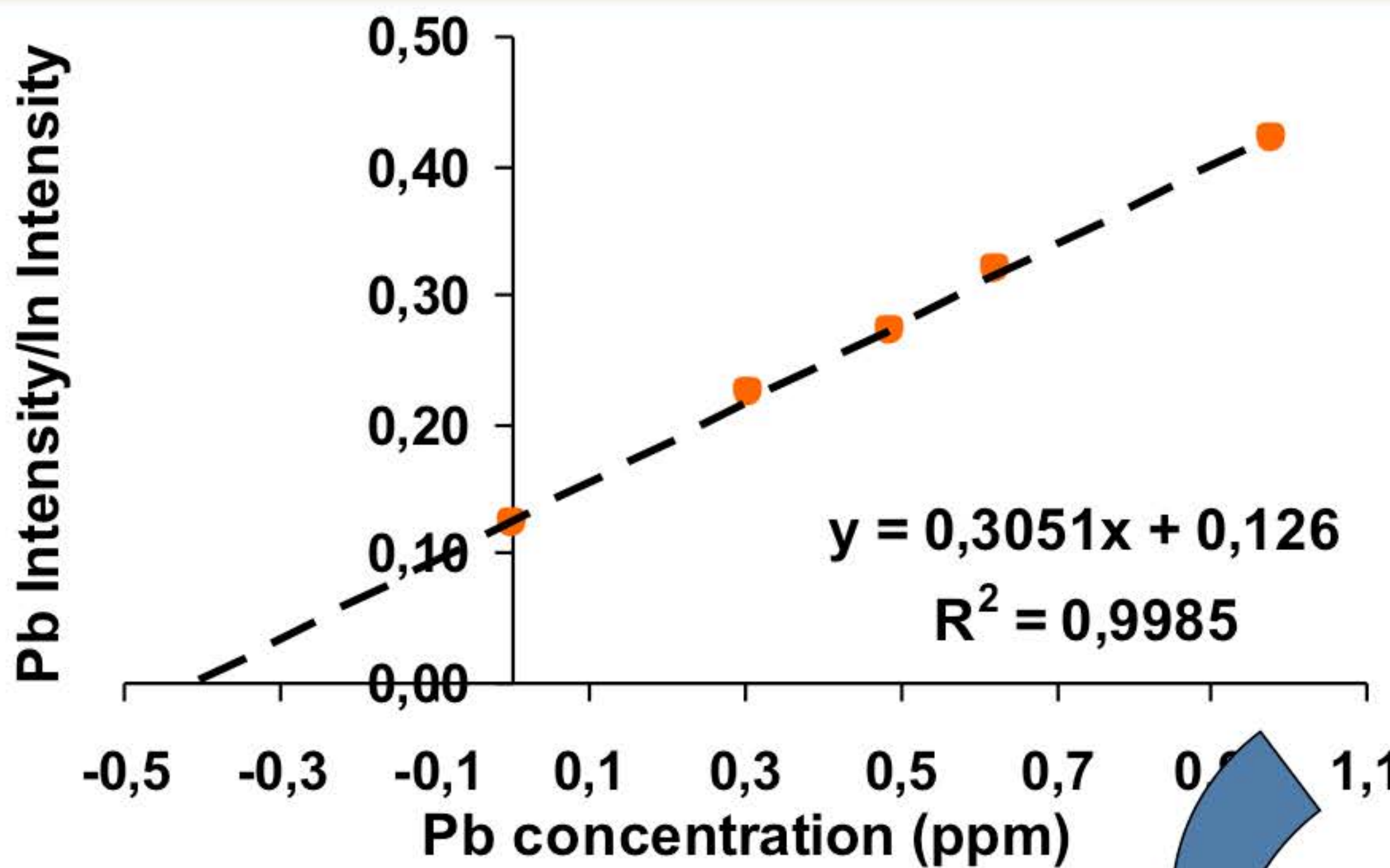
The internal cell **4 mm** above the samples acts as an impaction stage to:

- ⇒ Preserve the cell window
- ⇒ Stop splashes (large particles and droplets) just after ejection
- ⇒ Limit contamination

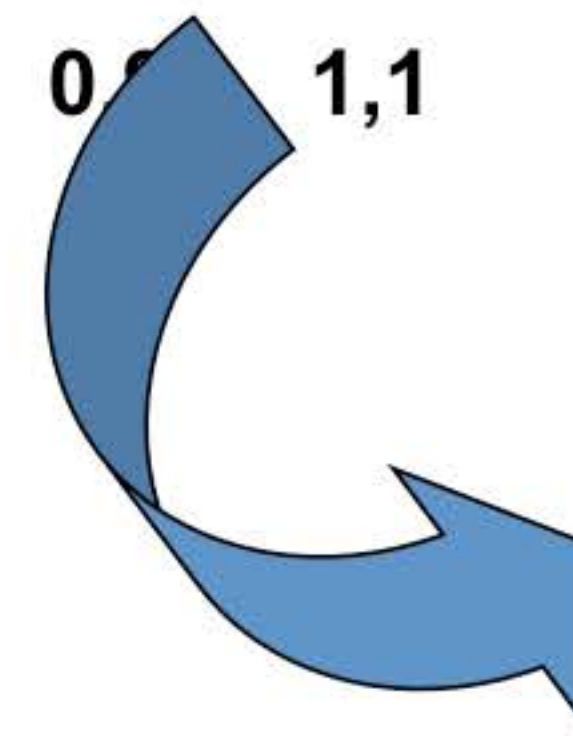
Trace element analysis in crude oil by FsLA- ICPMS :



Trace element analysis in crude oil by FsLA- ICPMS :



Optimal conditions: 1 KHz,
100 mm.s⁻¹, 30 J.cm⁻²,
=> transport efficiency ~ 30 %



	LOD ($\mu\text{g/g}$)
51 V	0.005
60 Ni	0.008
59 Co	0.001
75 As	0.007
98 Mo	0.002
208 Pb	0.0006

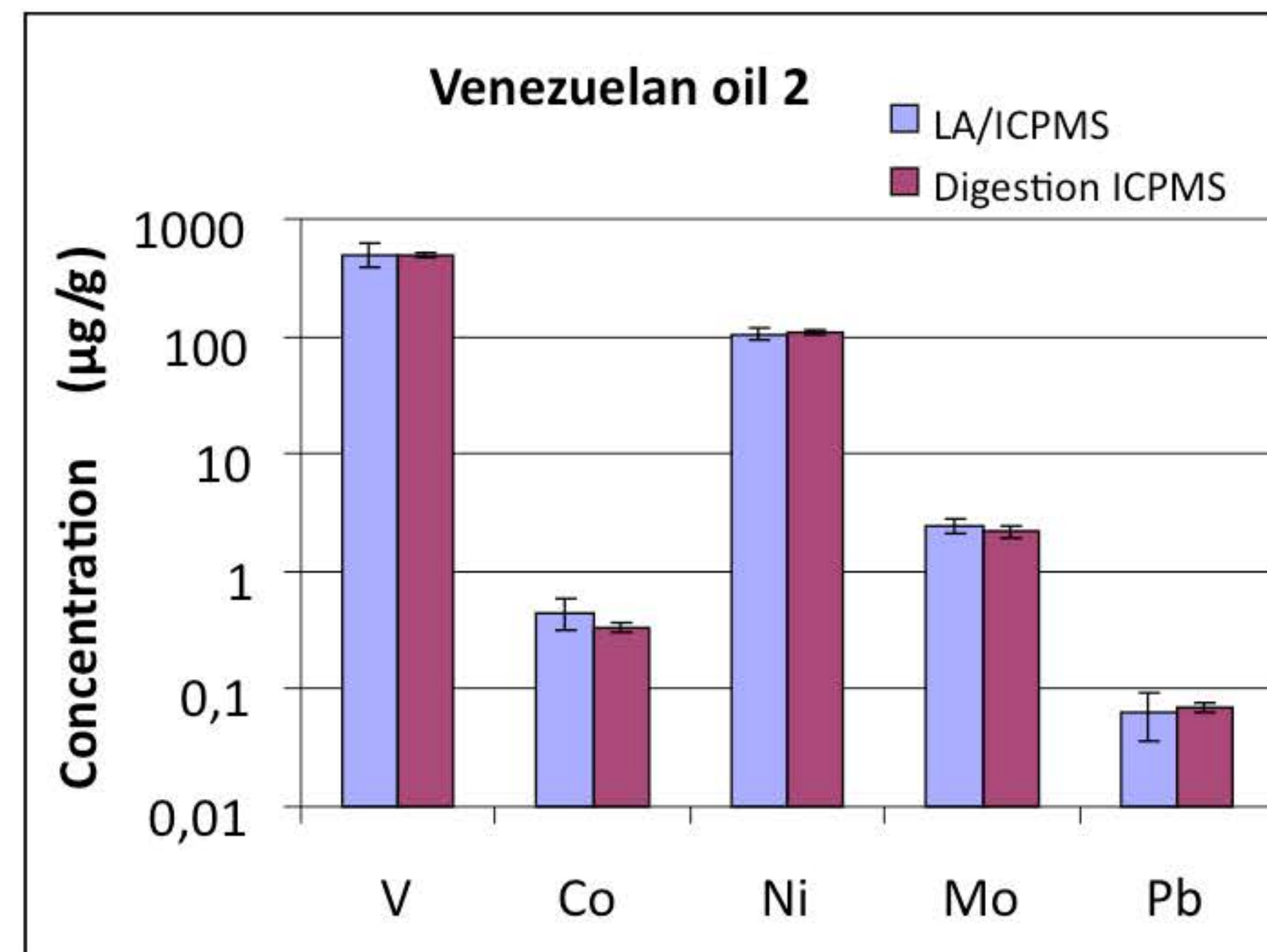
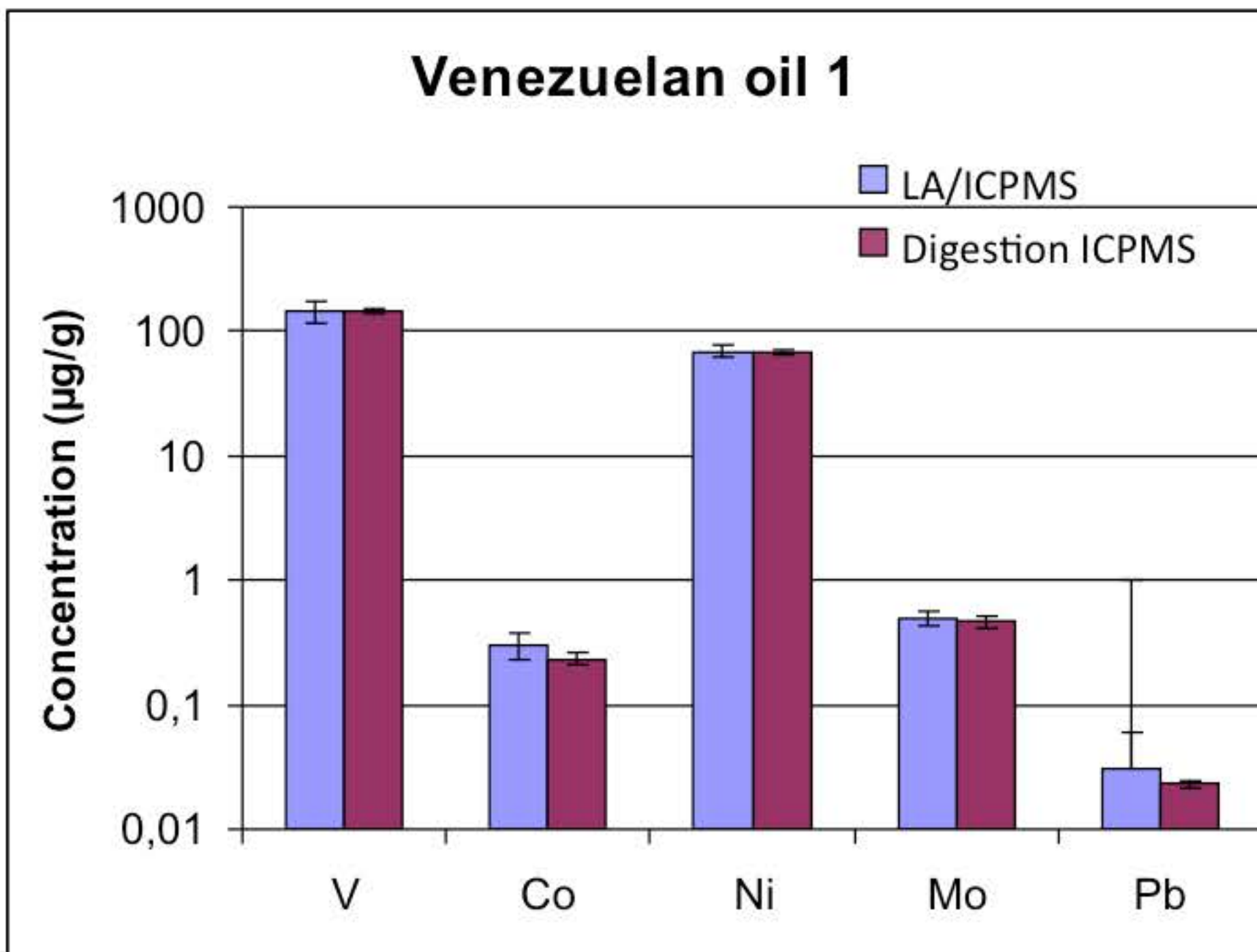
Sample preparation:

- Indium (internal standard) + Xylene (dilution 2 to 5)
- Evaporation under Nitrogen stream

Trace element analysis in crude oil by FsLA- ICPMS :

External calibration with NIST 1634c

=> Fast (2 min) and accurate...



In press in ABC

Forensic applications

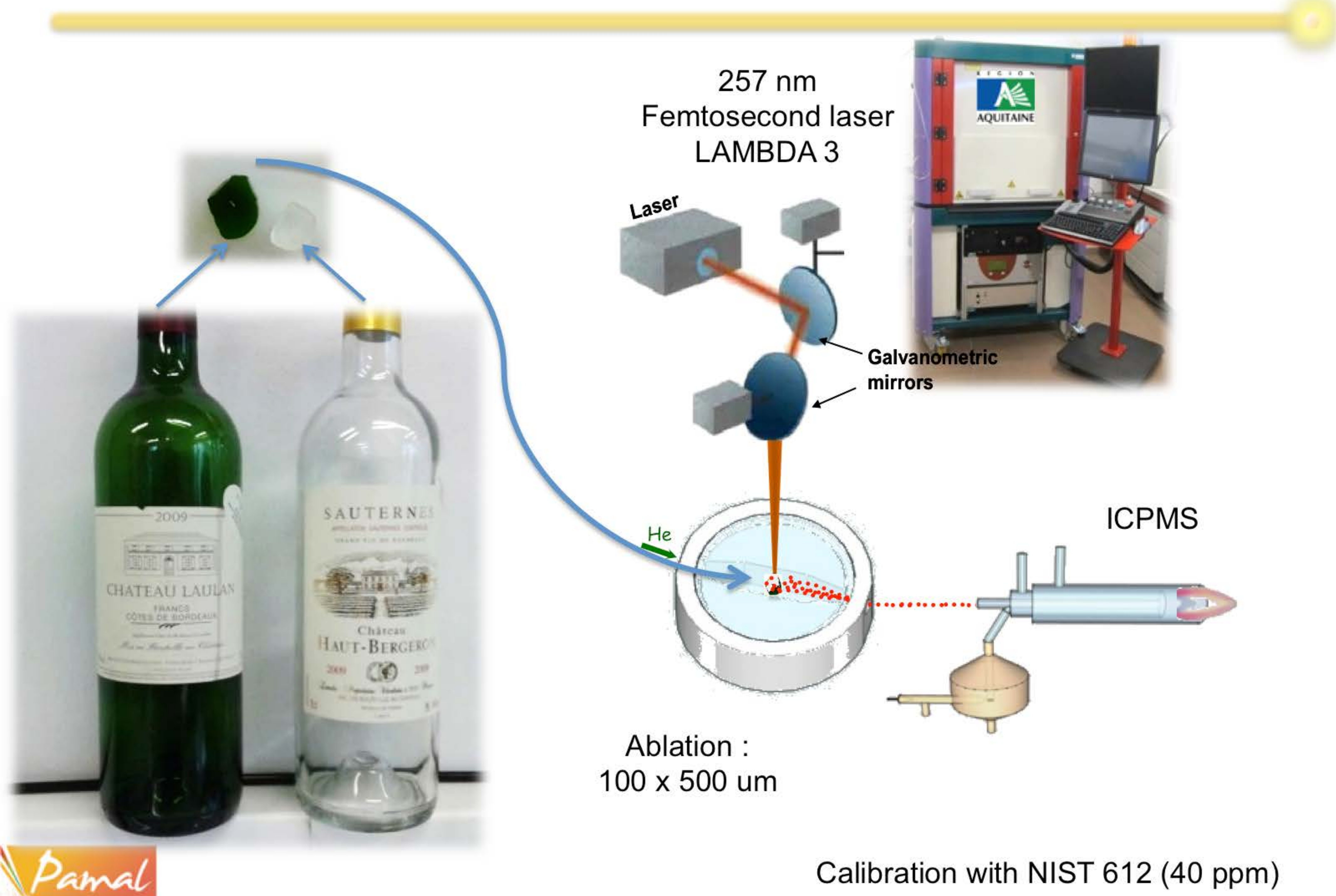


Fighting against Wine counterfeiting



- Is this bottle counterfeited?
- Where is it from (country)?
- Who did it?

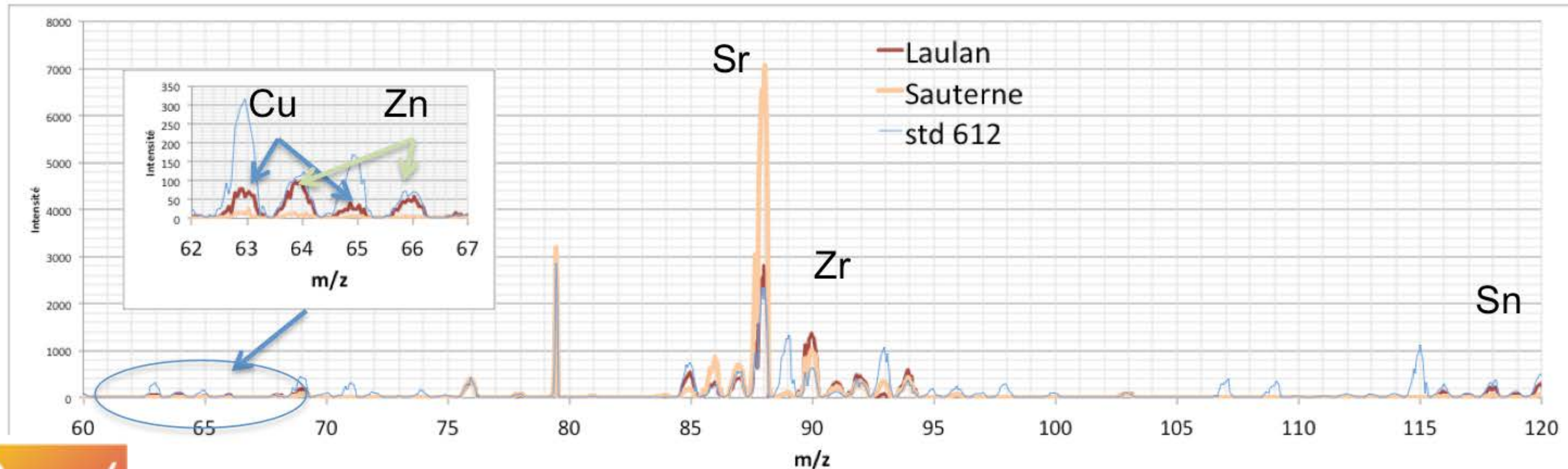
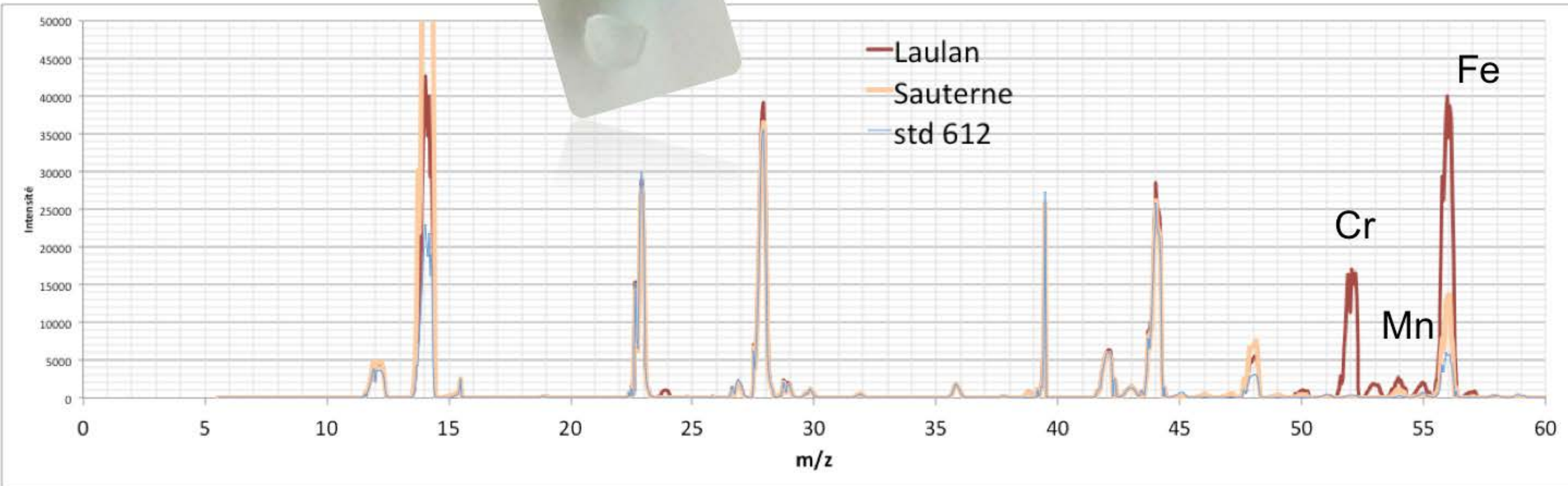
Trace element analysis in glass FsLA- ICPMS :



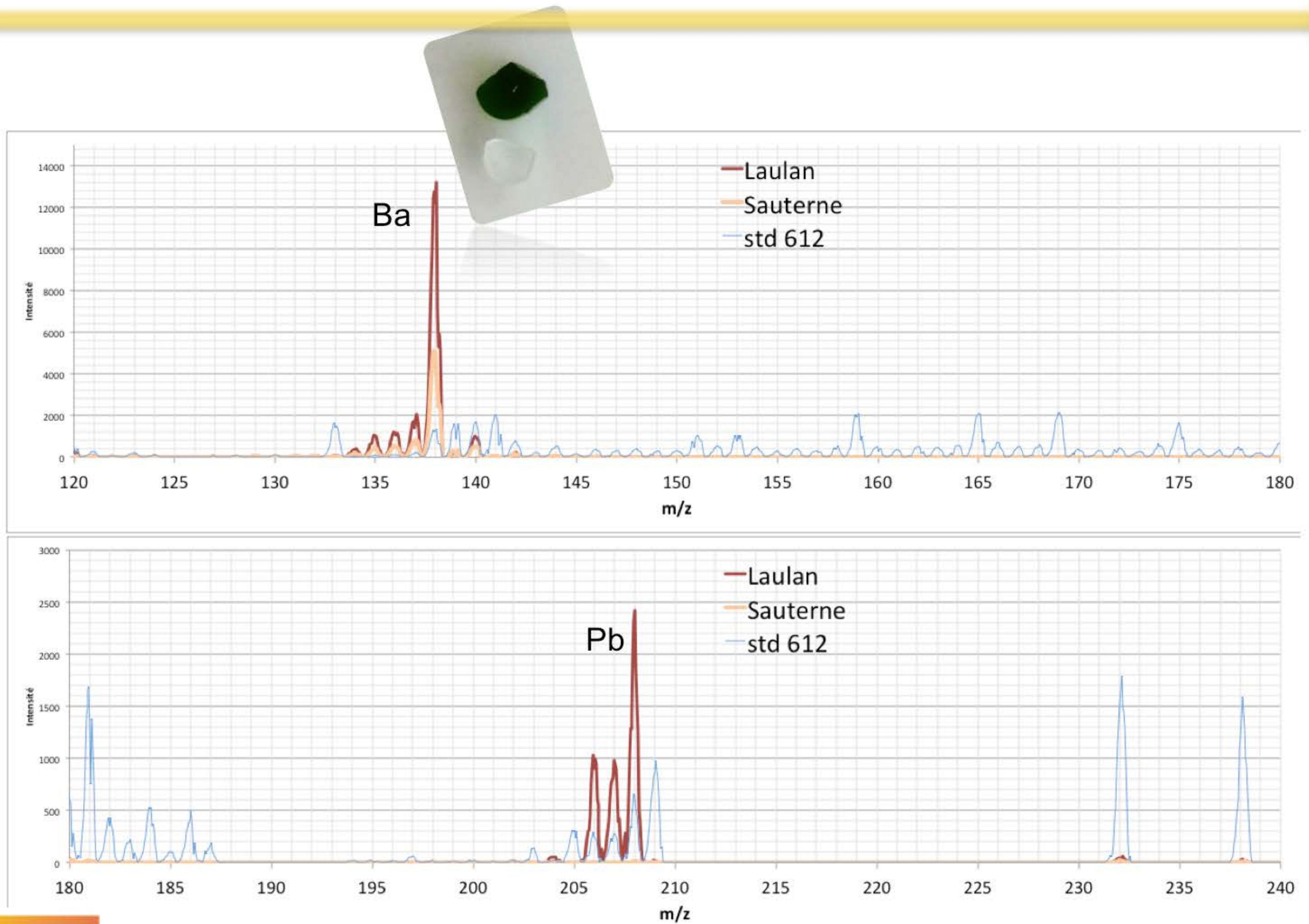
Trace element analysis in glass FsLA- ICPMS :



Semiquantitative analysis



Trace element analysis in glass FsLA- ICPMS :



75 elements analysed by UVfs/HRICPMS

4 bottles of de Pauillac + 4 suspect bottles (Asia)
+ 1 copy of Pomerol (Asia)

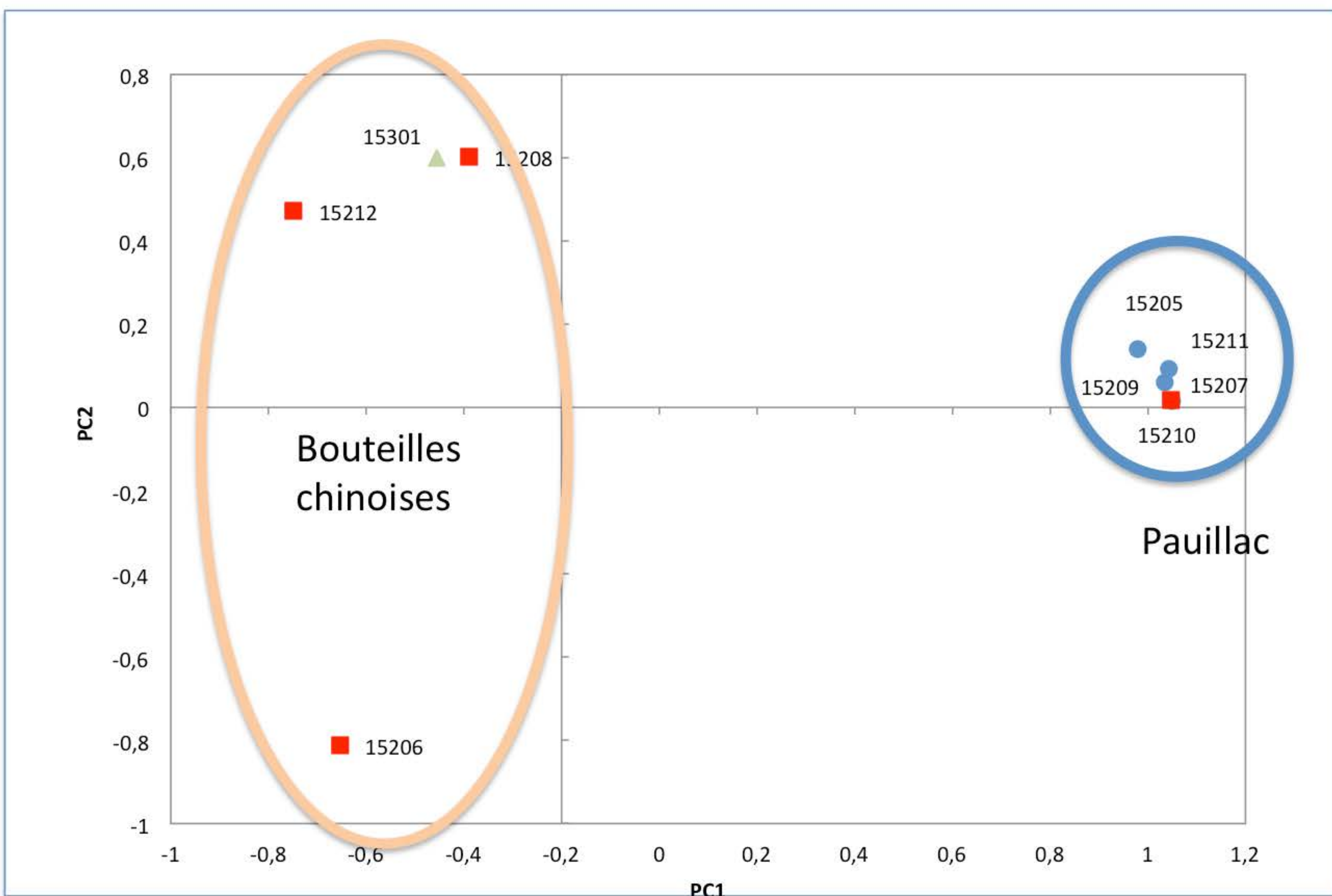
Li7	Ti47	Rb85	Sn118	Tb159	Ir193
Be9	V51	Sr88	Sb121	Dy163	Pt195
B11	Cr52		Y89	Te125	Ho165
Na23		Mn55	Zr90	I127	Er166
Mg24		Fe56	Nb93	Cs133	Tm169
Al27	Co59		Ba138	Yb172	Pb208
Si28	Ni60	Mo98	La139	Lu175	Bi209
P31	Cu63		Ru101	Ce140	Hf178
S32	Zn66		Rh103	Pr141	Hf179
Cl35	Ga69		Pd105	Nd146	Ta181
K39	Ge72		Ag107	Sm147	W182
Ca44		As75	Cd111	Eu153	Re185
Sc45		Se78	In115	Gd157	Os189

Very discriminating
Discriminating
Poorly discriminating

⇒ LOD: 0,06 ng/g (Pr) – 2 ng/g (Pb) - 20 ng/g (Sn) all analyzed in medium resolution
(so with only 10% transmission)

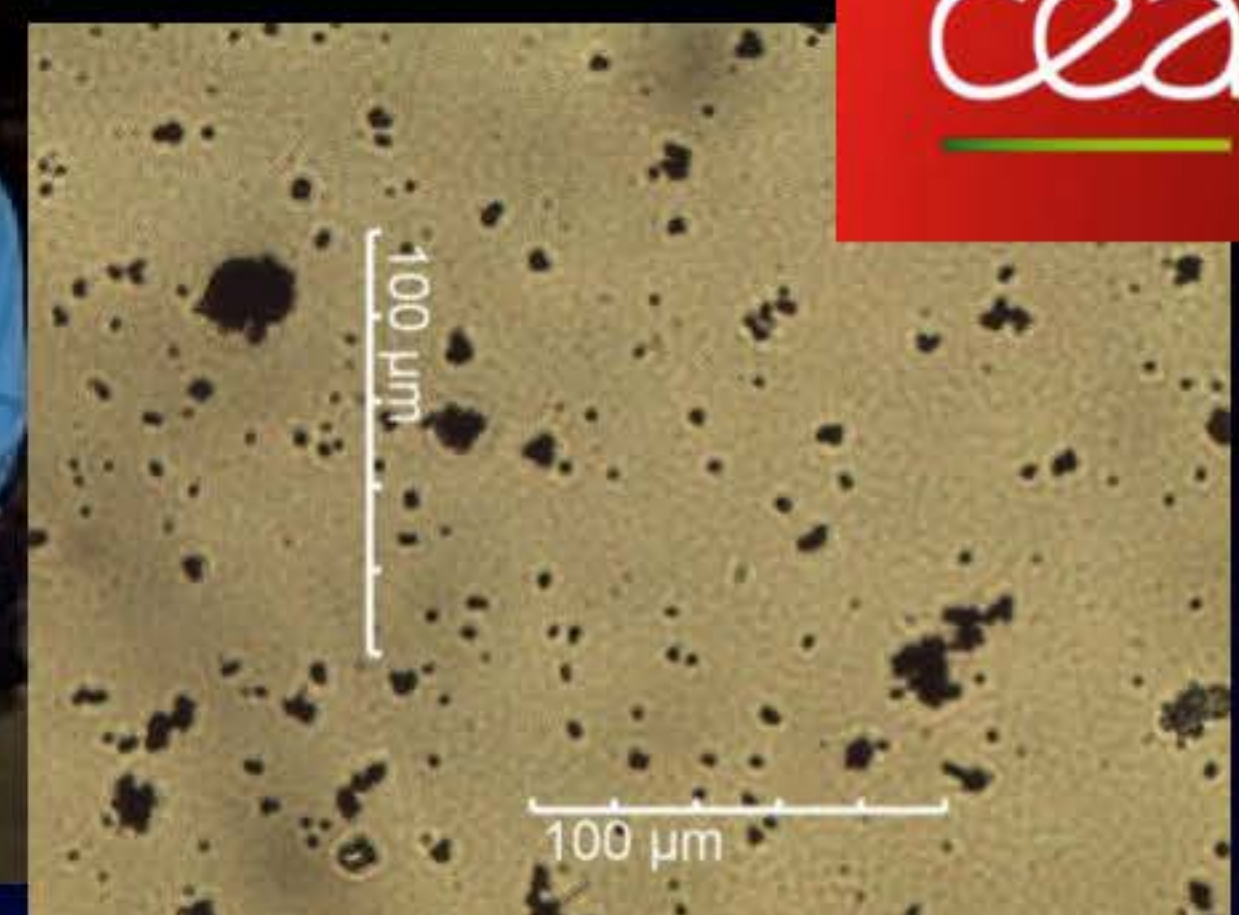
=> 20 discriminating elements with 9 highly discriminating

Unambiguous authentication using PCA



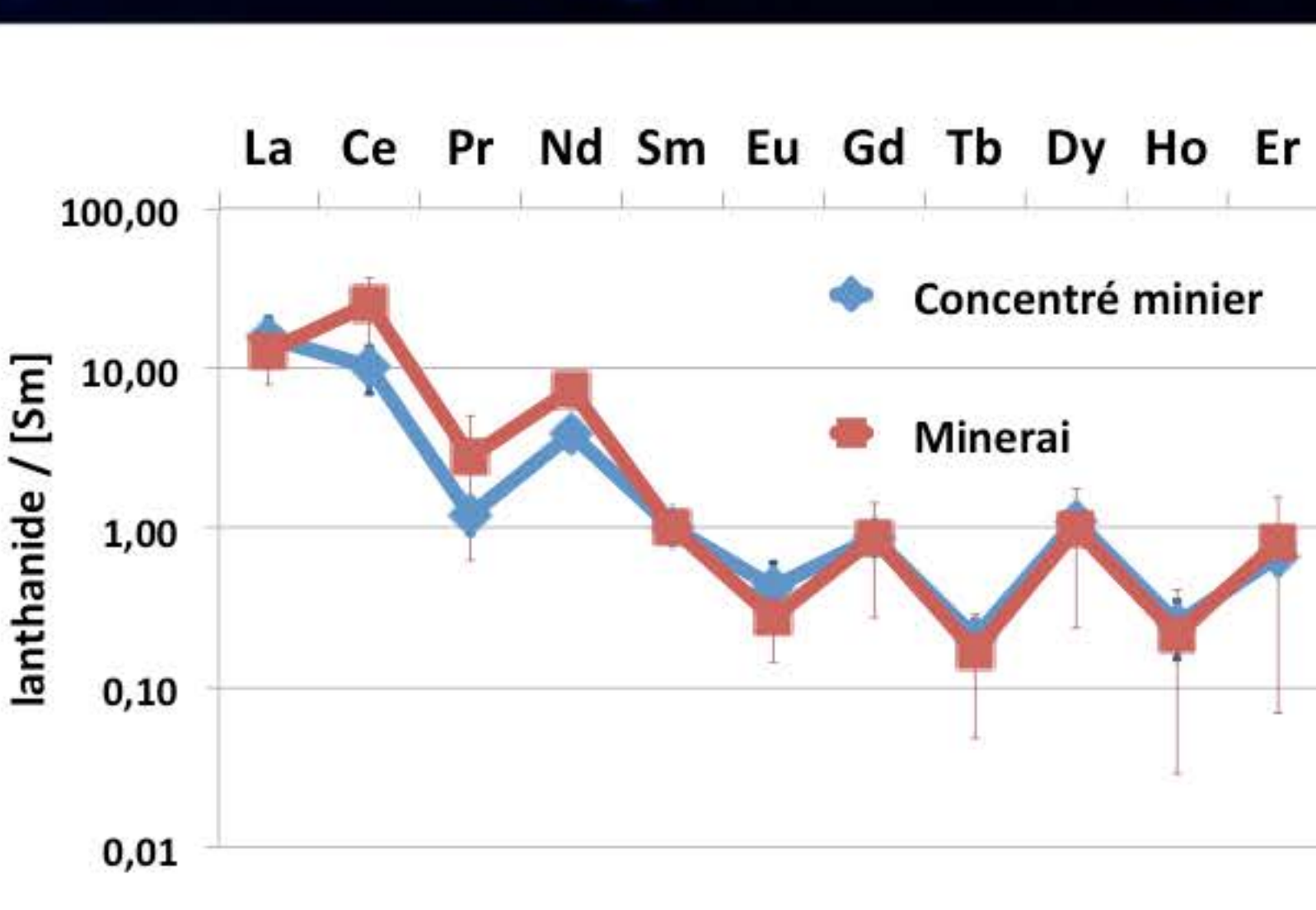
Le millésime 2006 suspect est en fait un vrai Pauillac

Forensic sciences at the particle size

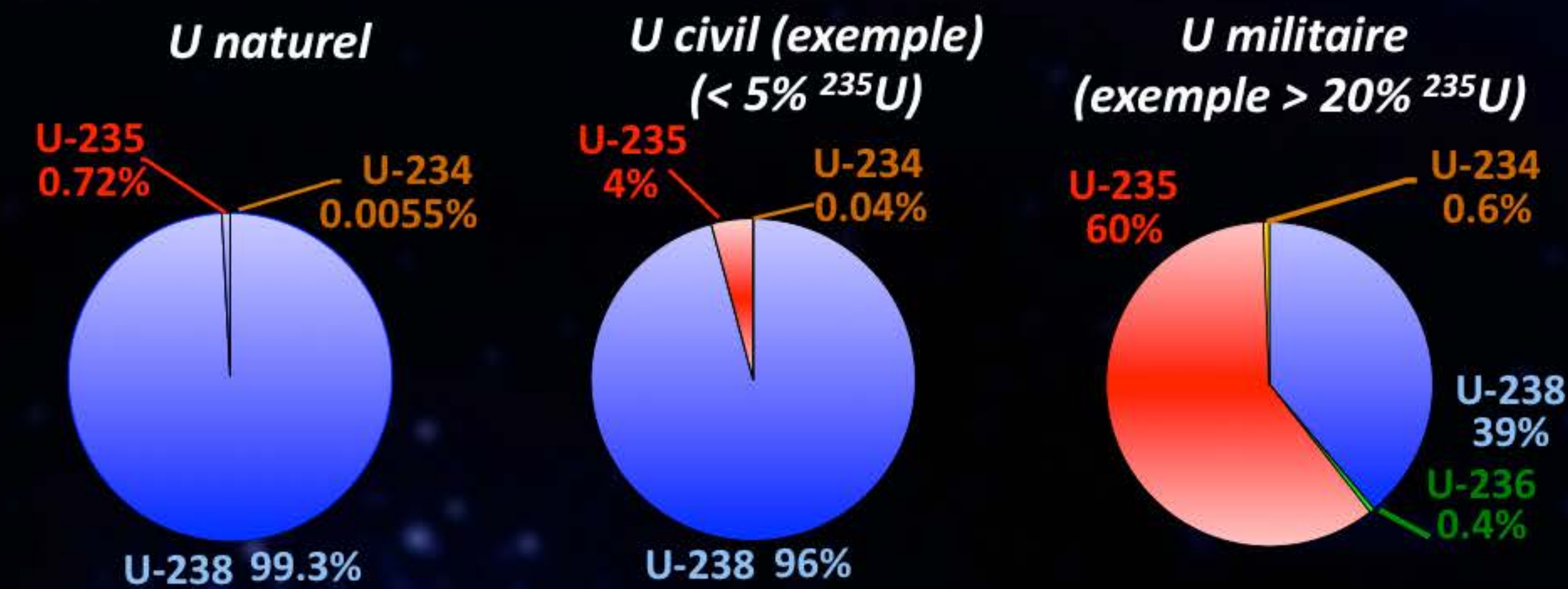


particles of few nanograms => detection of few pico, femto and even attograms

ORIGIN



USE



Uranium isotopic composition of micrometric particles

In the framework of the Non Proliferation Treaty (NPT, 1968), whose aim is to avoid spreading of nuclear weapons, the

International Atomic Energy Agency (IAEA) is in charge of controlling the nuclear installations worldwide in the countries that established safeguard agreements with the IAEA (183 countries have signed the treaty, 50 operated nuclear facilities).



IRAK, 1991: due to the discover of a clandestine nuclear enrichment program (**not detected by regular inspections**), the IAEA became



aware of the limitations of the controls previously carried out, only on **nuclear materials declared and accessible to the inspectors in declared facilities**.

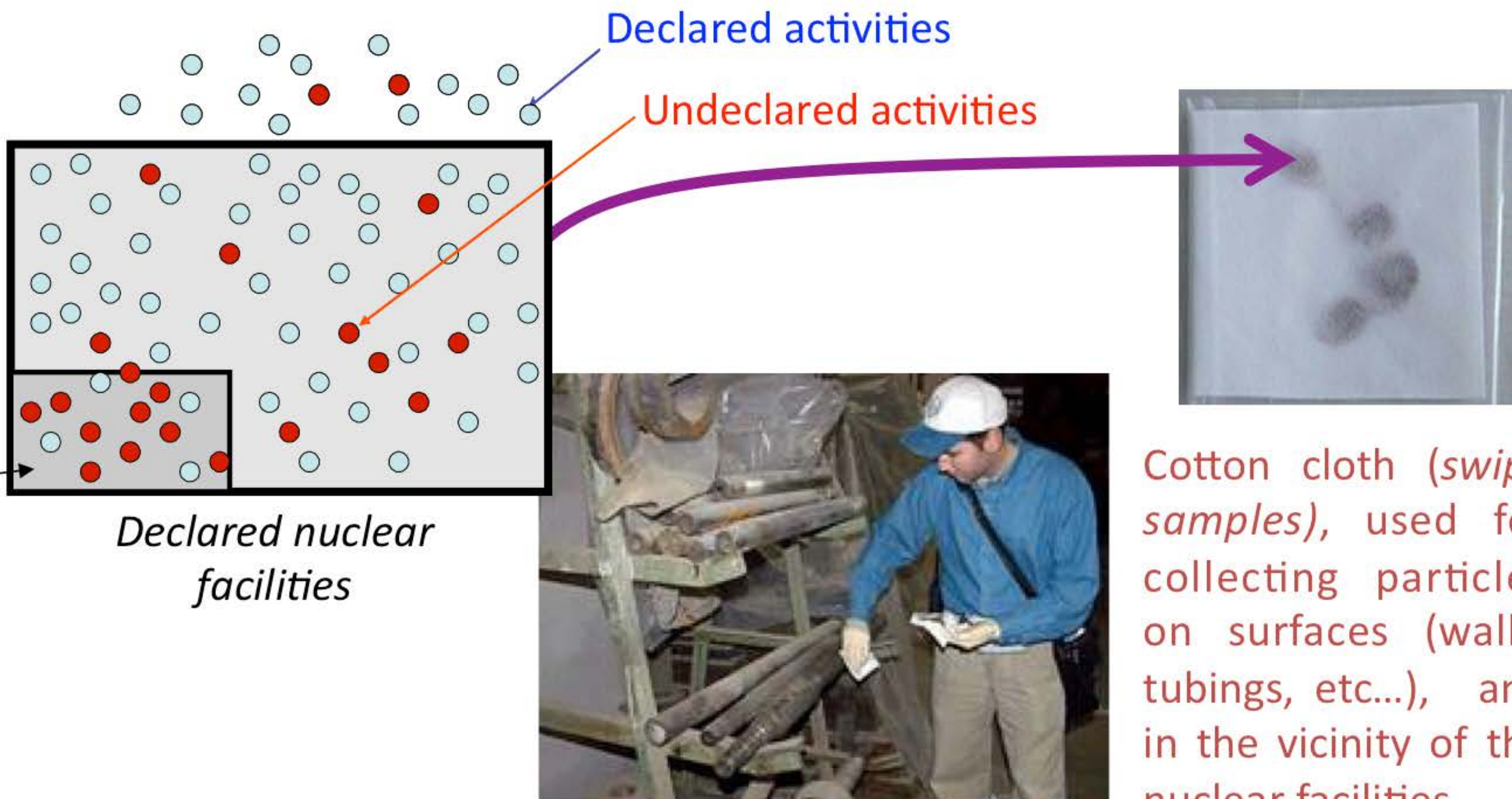
- ▶ Undeclared facilities => no control
- ▶ Undeclared nuclear material => not collected by inspectors

Urgent need to reinforce legal protocols and analytical methods

Uranium isotopic composition of micrometric particles

The challenge is to detect and characterize nuclear materials (uranium, plutonium) present in a nuclear facility, without access to these materials

Physico-chemical processes applied to a material, or even the displacement itself of a material release some very thin particles ($< \mu\text{m}$ to few μm) that will spread in the nuclear facilities or around.

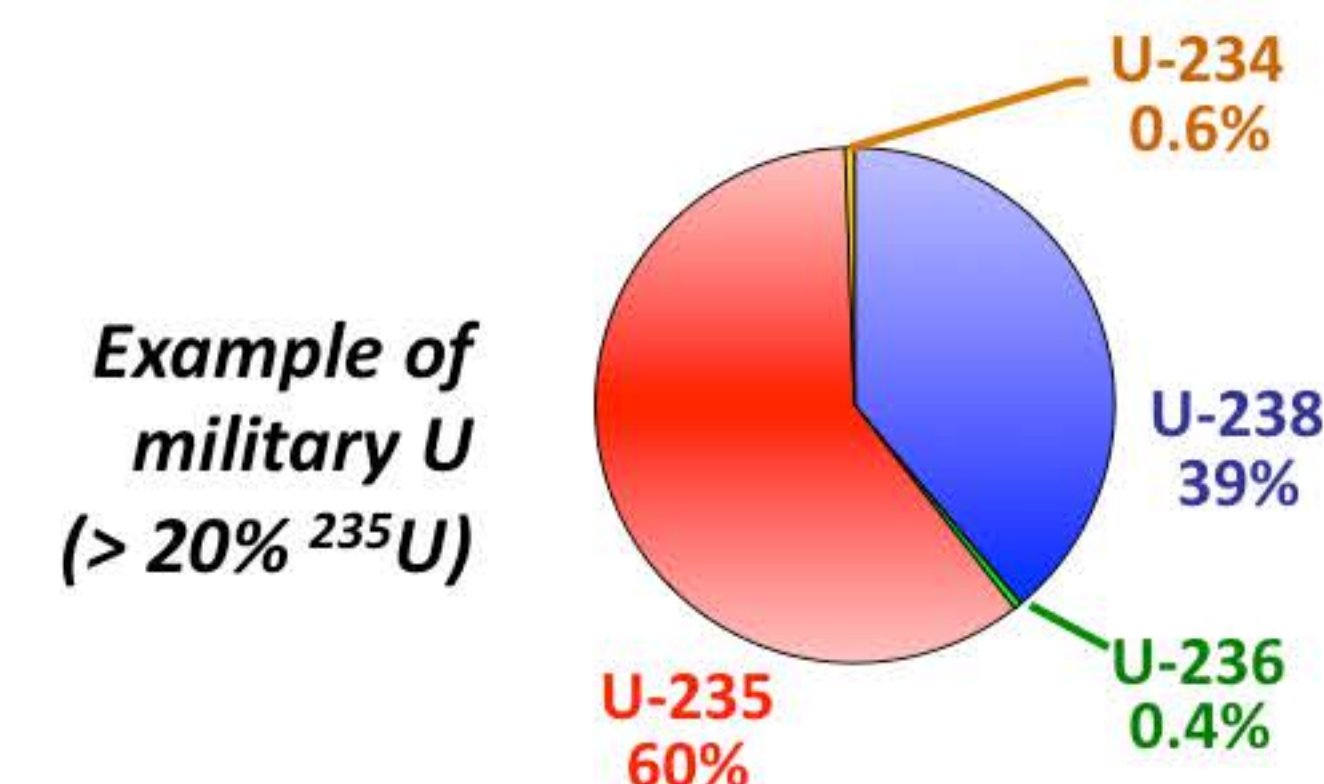
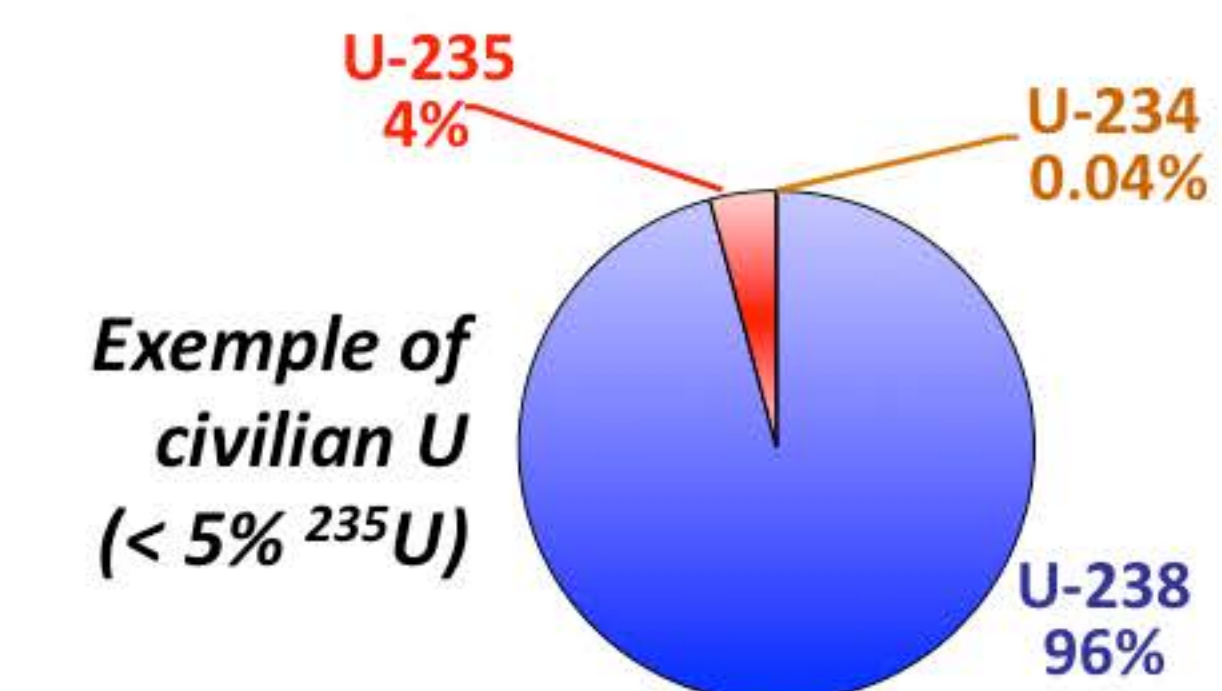
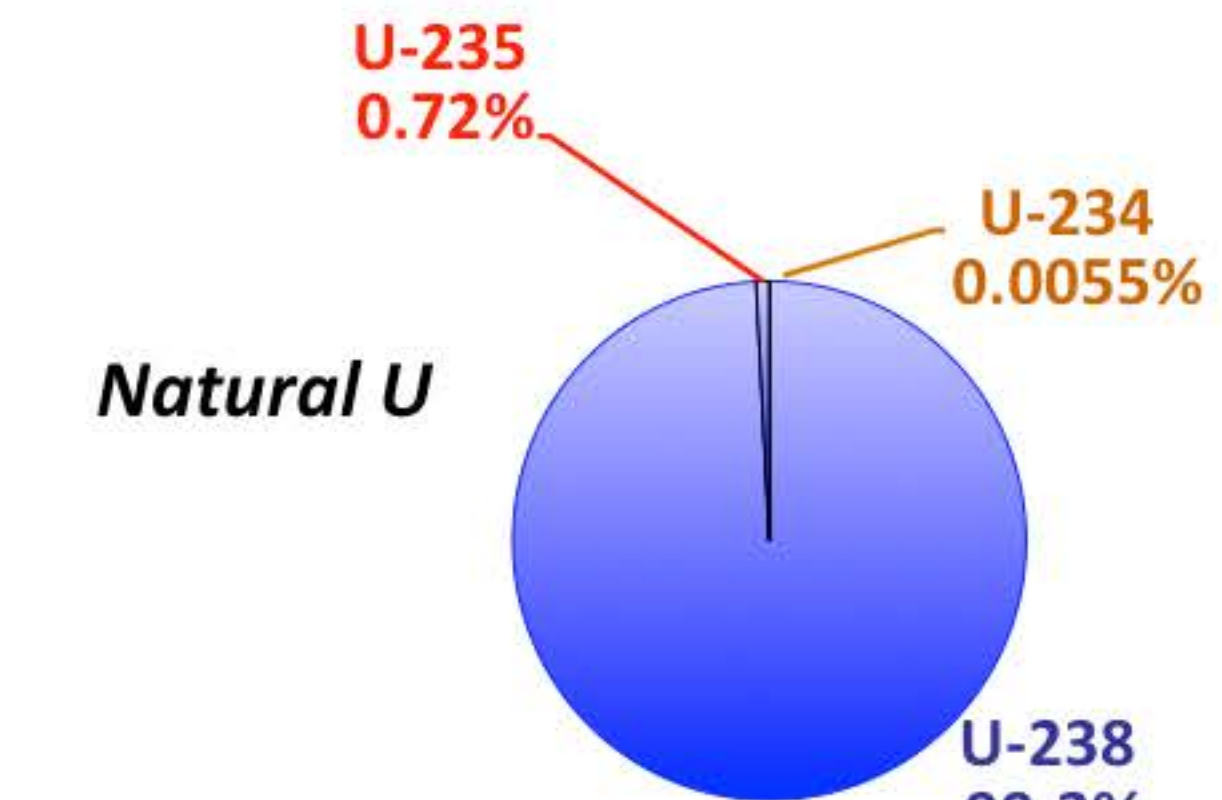


Uranium isotopic composition of micrometric particles

► **Aim:** determine the **use** (military, civilian, natural,...) and, if possible the **associated treatment** (irradiation, purification, enrichment process, ...) and the **origin** of the nuclear material.

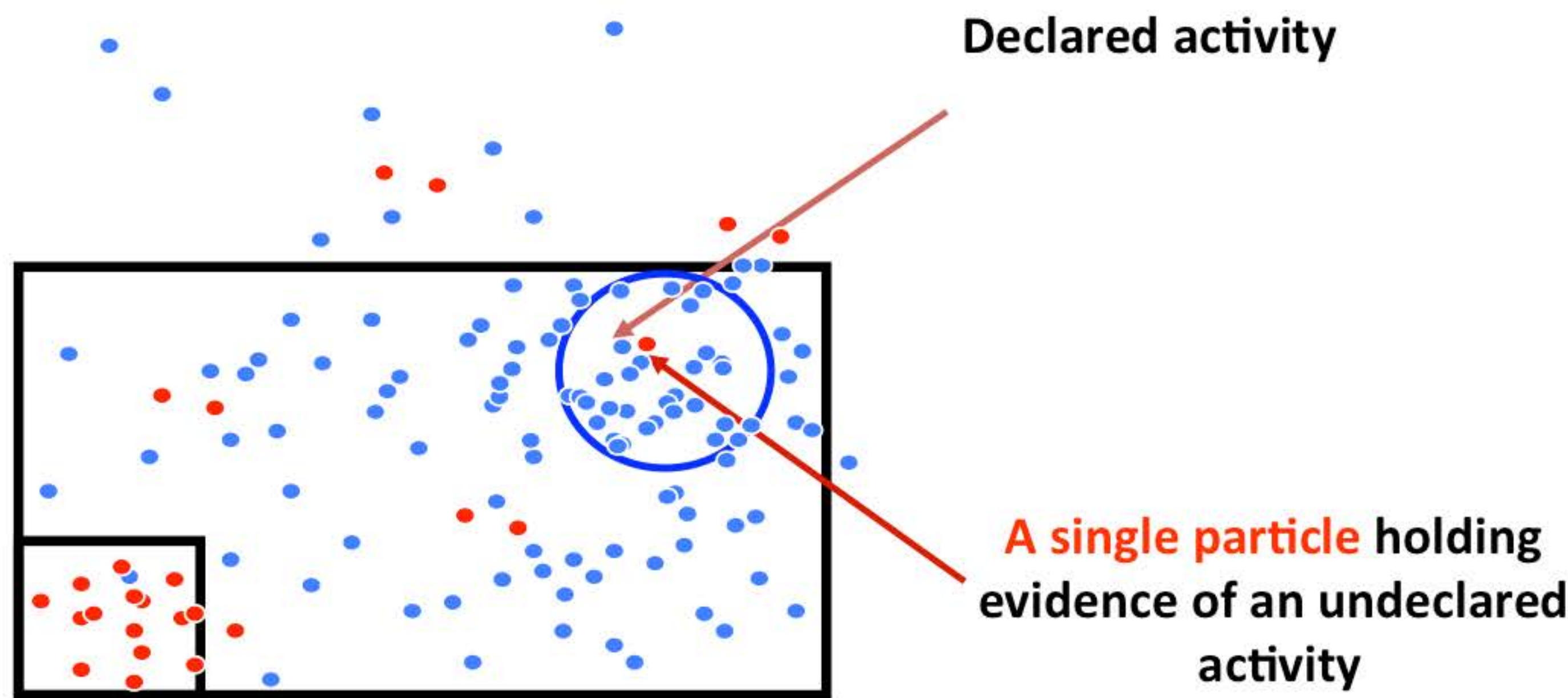
► Isotope ratios to discriminate between civilian and military use of the nuclear material :

- $^{235}\text{U}/^{238}\text{U}$, $^{234}\text{U}/^{238}\text{U}$, $^{236}\text{U}/^{238}\text{U}$
- $^{240}\text{Pu}/^{239}\text{Pu}$ ($^{241}\text{Pu}/^{239}\text{Pu}$, $^{242}\text{Pu}/^{239}\text{Pu}$)



Uranium isotopic composition of micrometric particles

- ▶ The widespread method of “bulk analysis” (dissolution, chemical purification and isotopic analysis of the cotton cloth as a whole sample) provides an average isotopic composition of the particles and may allow detecting undeclared materials.
- ▶ However, this method is not efficient when the sample contain only one particle enriched in fissile ^{235}U isotope (or a very limited number of these particles) among a vast majority of particles coming from declared materials (for instance natural uranium or uranium depleted in ^{235}U).



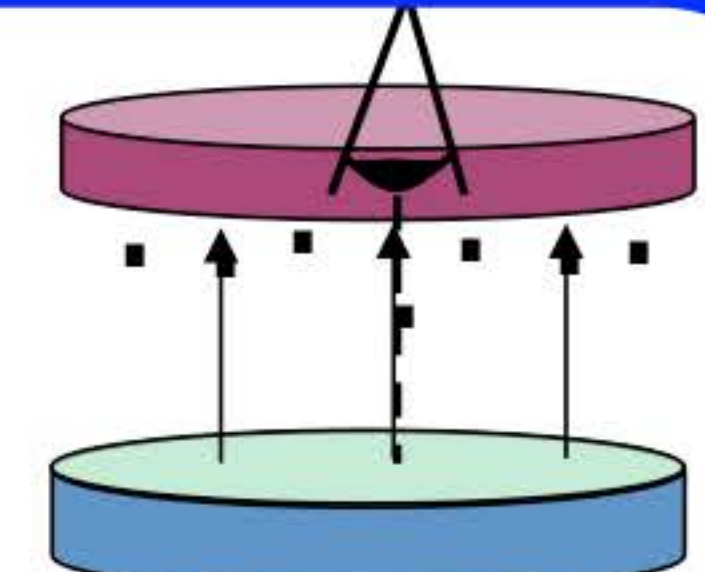
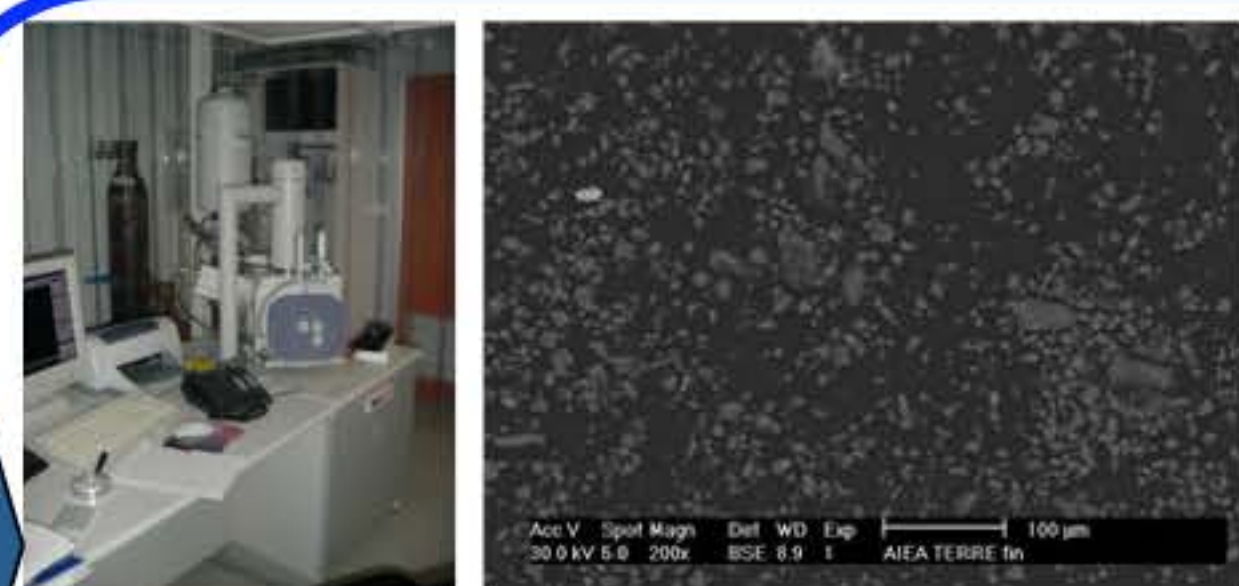
- ▶ Towards analysing isotopic signature of individual particles...

Uranium isotopic composition of particles (CEA, DAM)

1 - Particles extraction and deposition on disks



2 - Localization and selection of the most pertinent particles



Scanning Electron Microscopy
Detection and localization of the “largest” particles ($\varnothing \geq 1 \mu\text{m}$)

Fission tracks : detection and localization of the high ^{235}U content-particles

3 - Isotopic analysis of U isotopes

SIMS

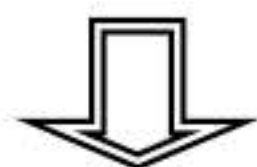


Particles are directly analyzed

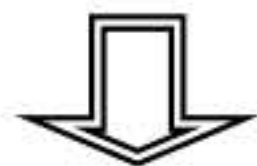


ⓘ Not selective for ^{235}U enriched-particles
☺ 4 analyses per hour

TIMS



Micro-sampling of the particles,
deposition on a Re filament and
introduction in the TIMS source



☺ Selective for ^{235}U enriched-particles
 ⓘ 1 analyses per hour

LA-ICPMS



Particles are directly analysed

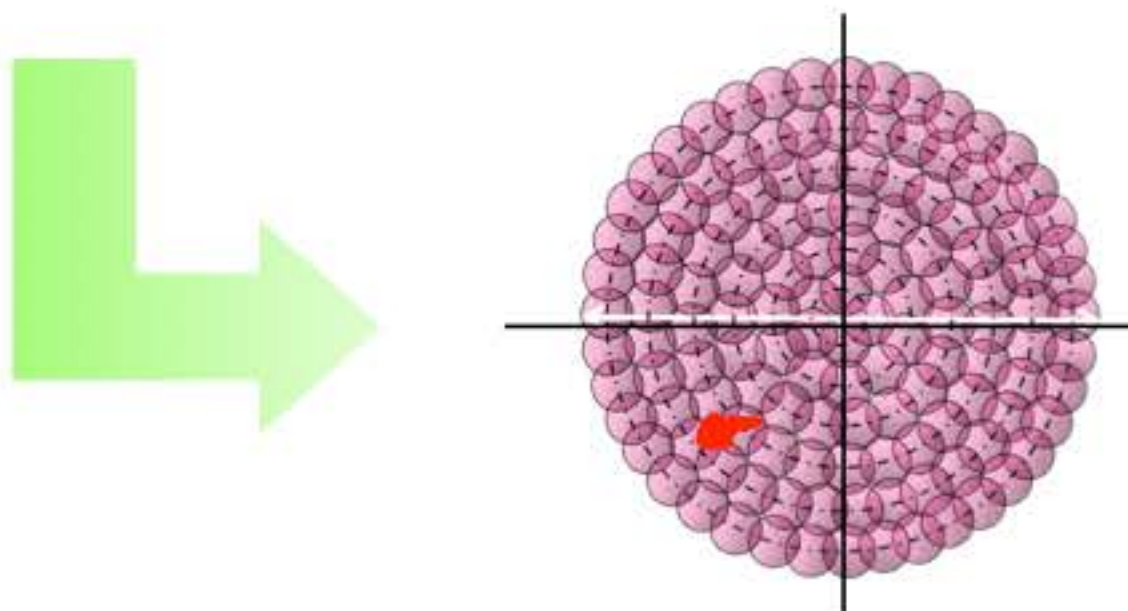


Potential??

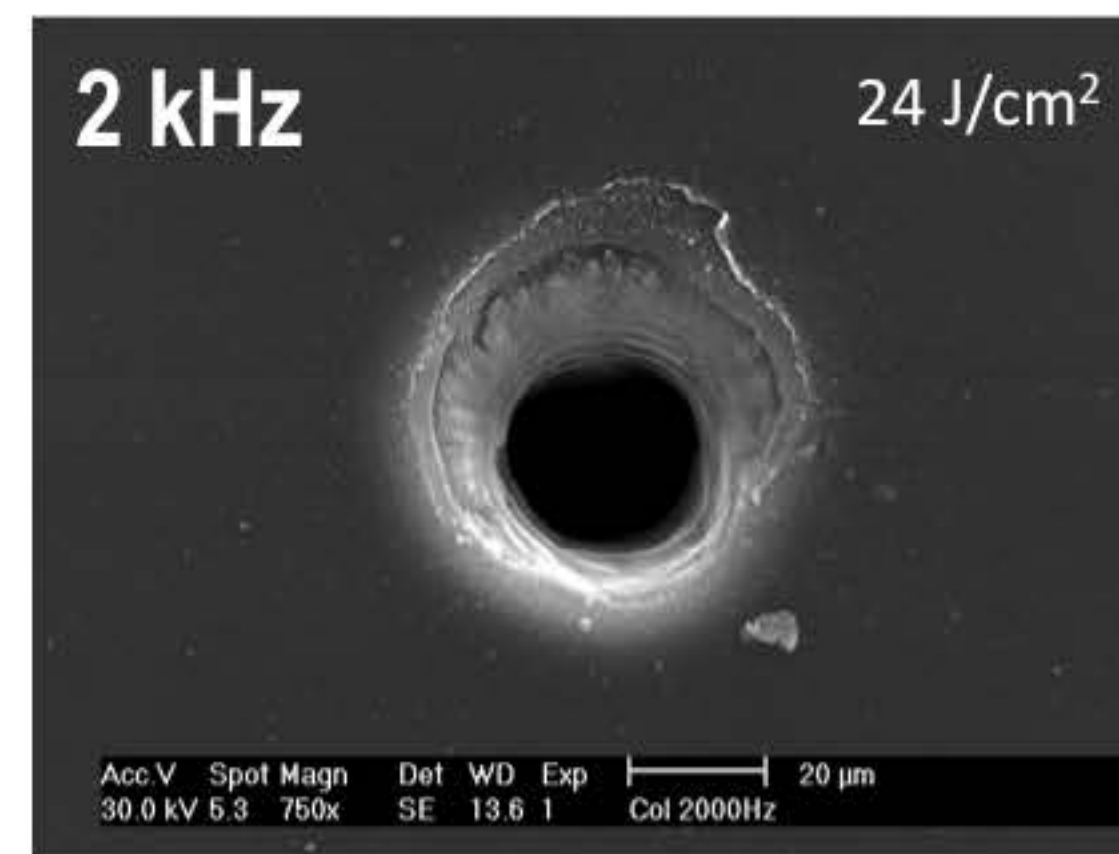
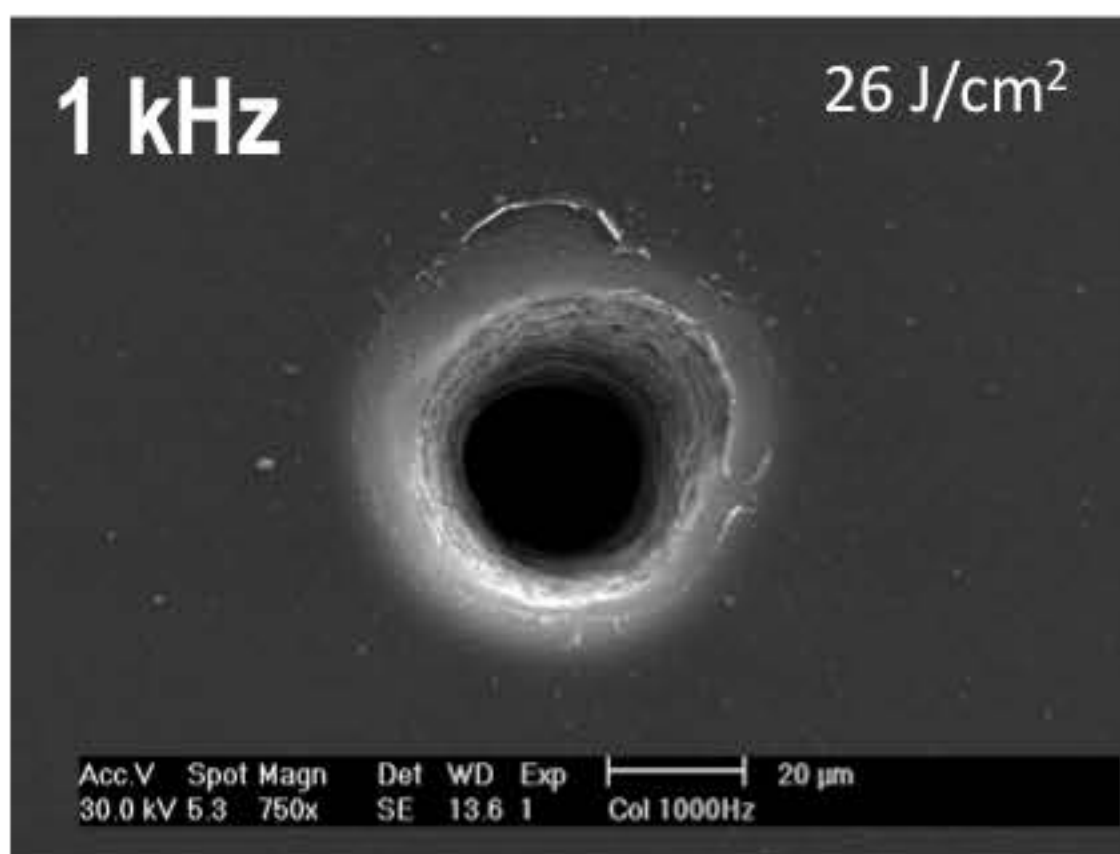
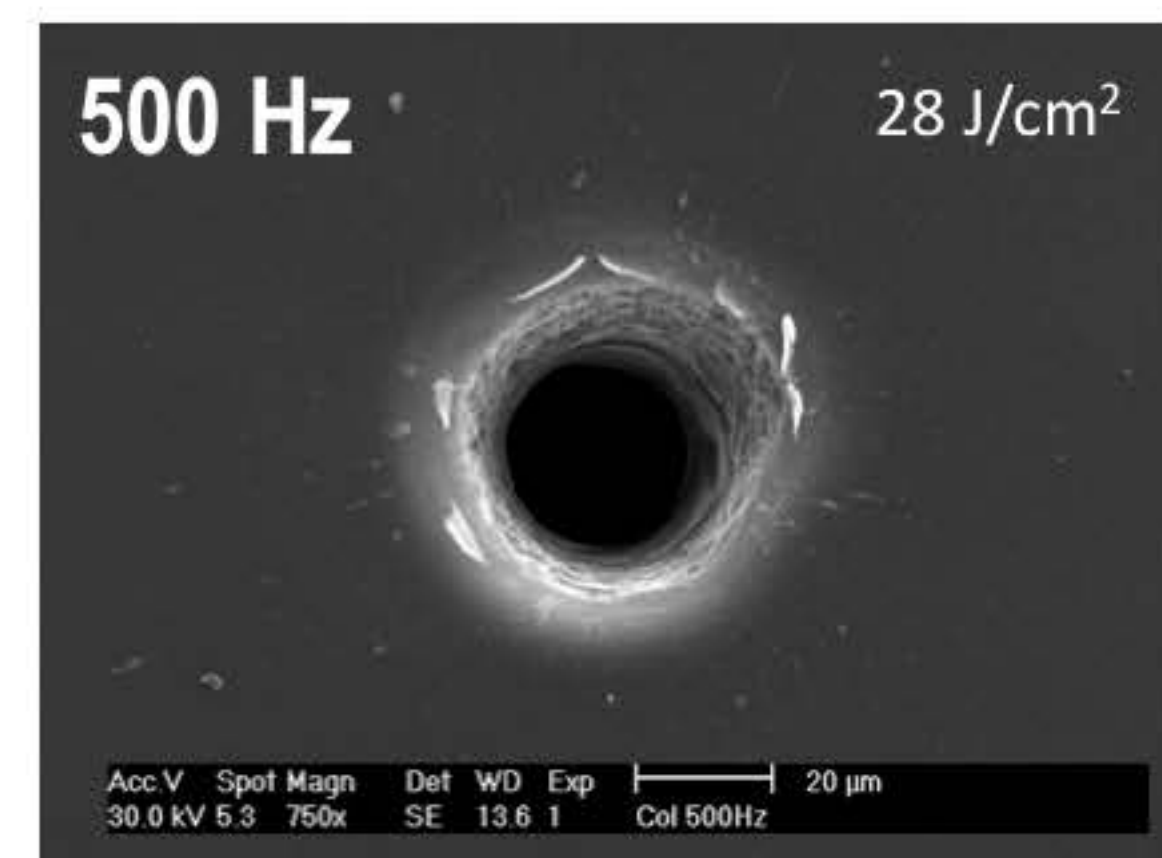
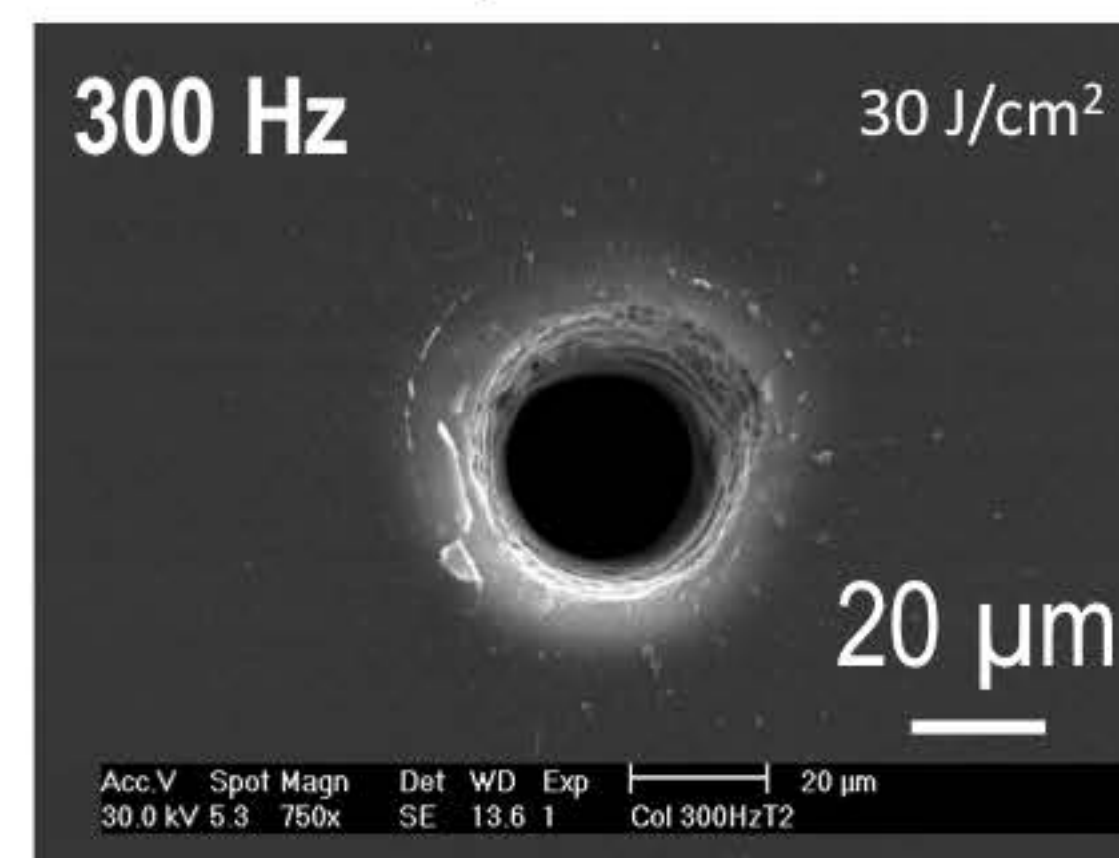
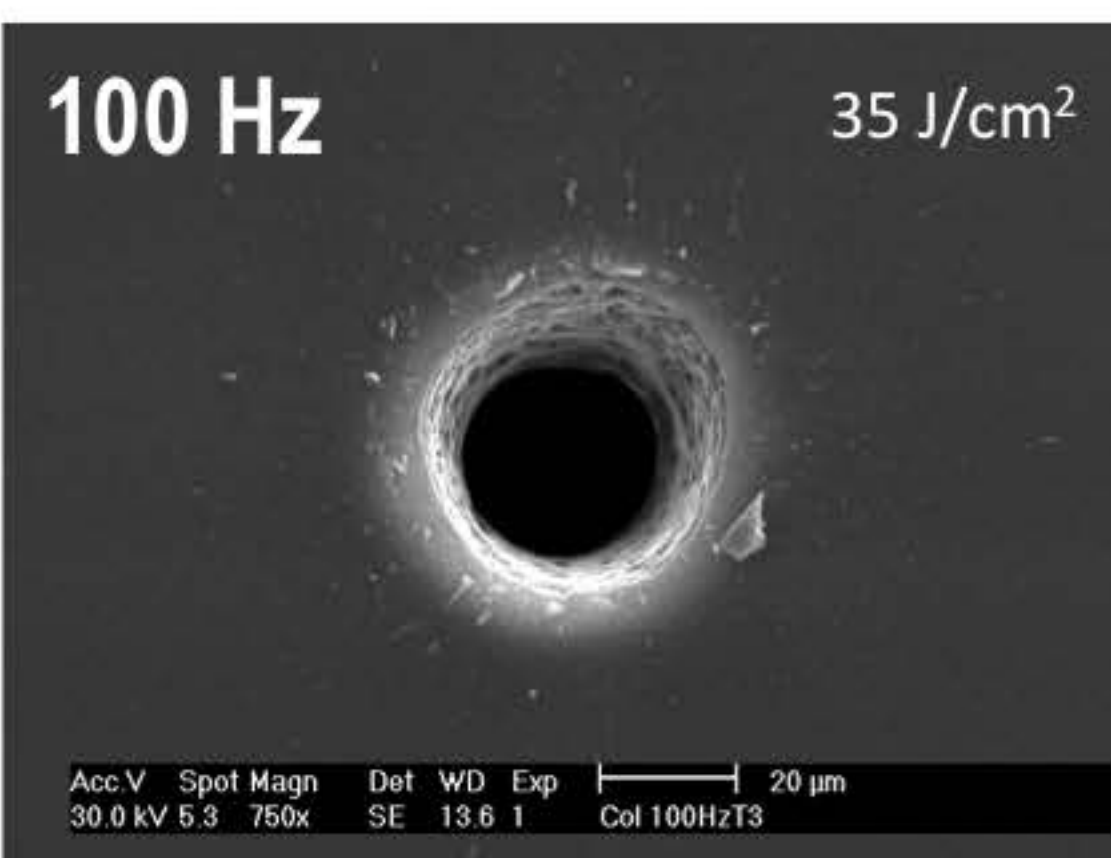
Uranium isotopic composition of micrometric particles

- ▶ Particles coordinates known at $\pm 5\text{-}10\mu\text{m}$
- ▶ Particles analysed : $< 3\ \mu\text{m}$ diameter

fsLA/ICPMS

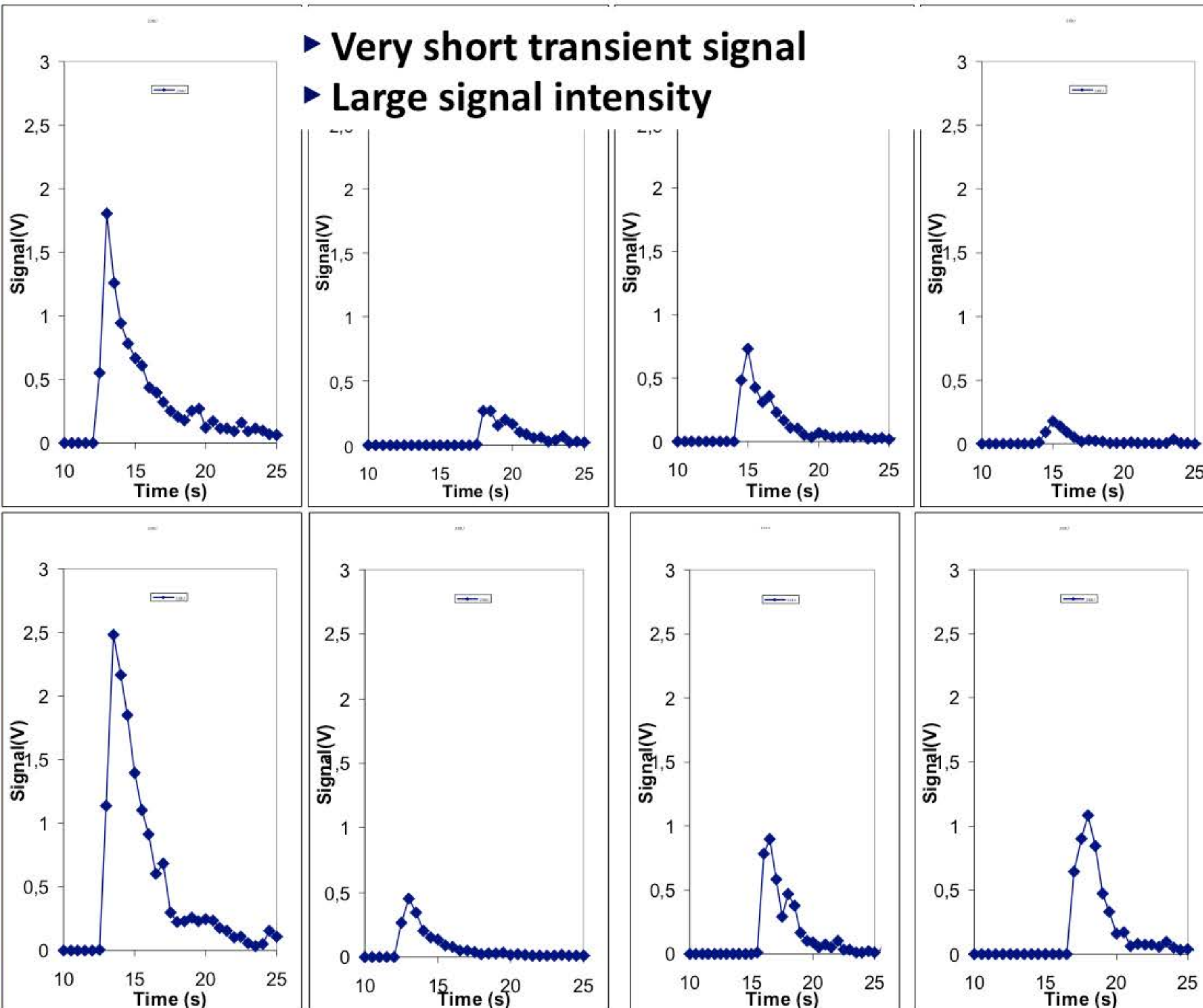


Crater of $40\ \mu\text{m}$ diameter to make sure to ablate the particles of interest



Uranium isotopic composition of micrometric particles

- Particles heterogeneity => size, shape, volume, density,...



► Particles of
Natural Isotope
 composition

$\varnothing 3 \mu\text{m} \text{ UO}_2$

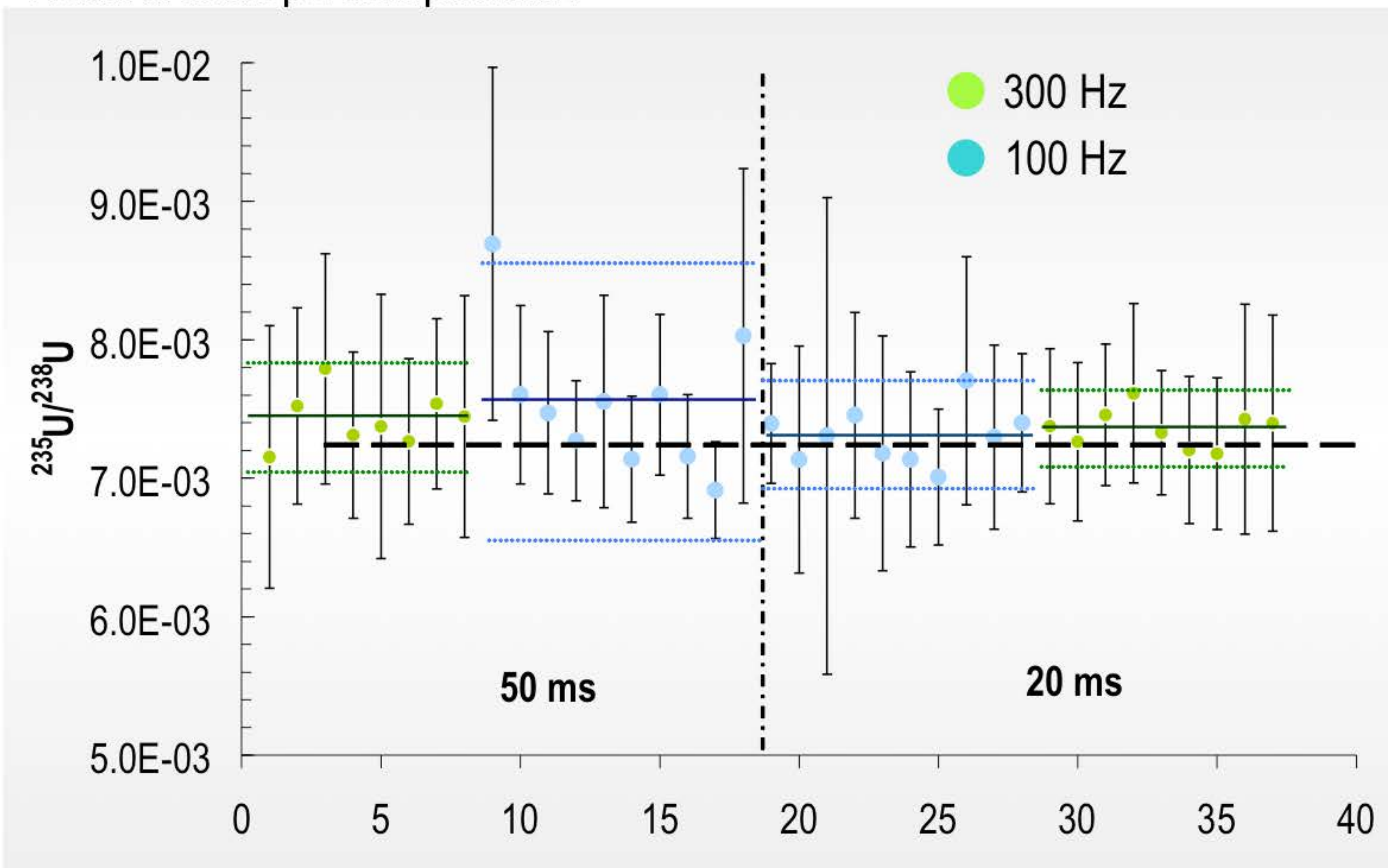
238U: 150 pg

235U: 1 pg

234U: 8 fg

FsLA/ Quad ICPMS

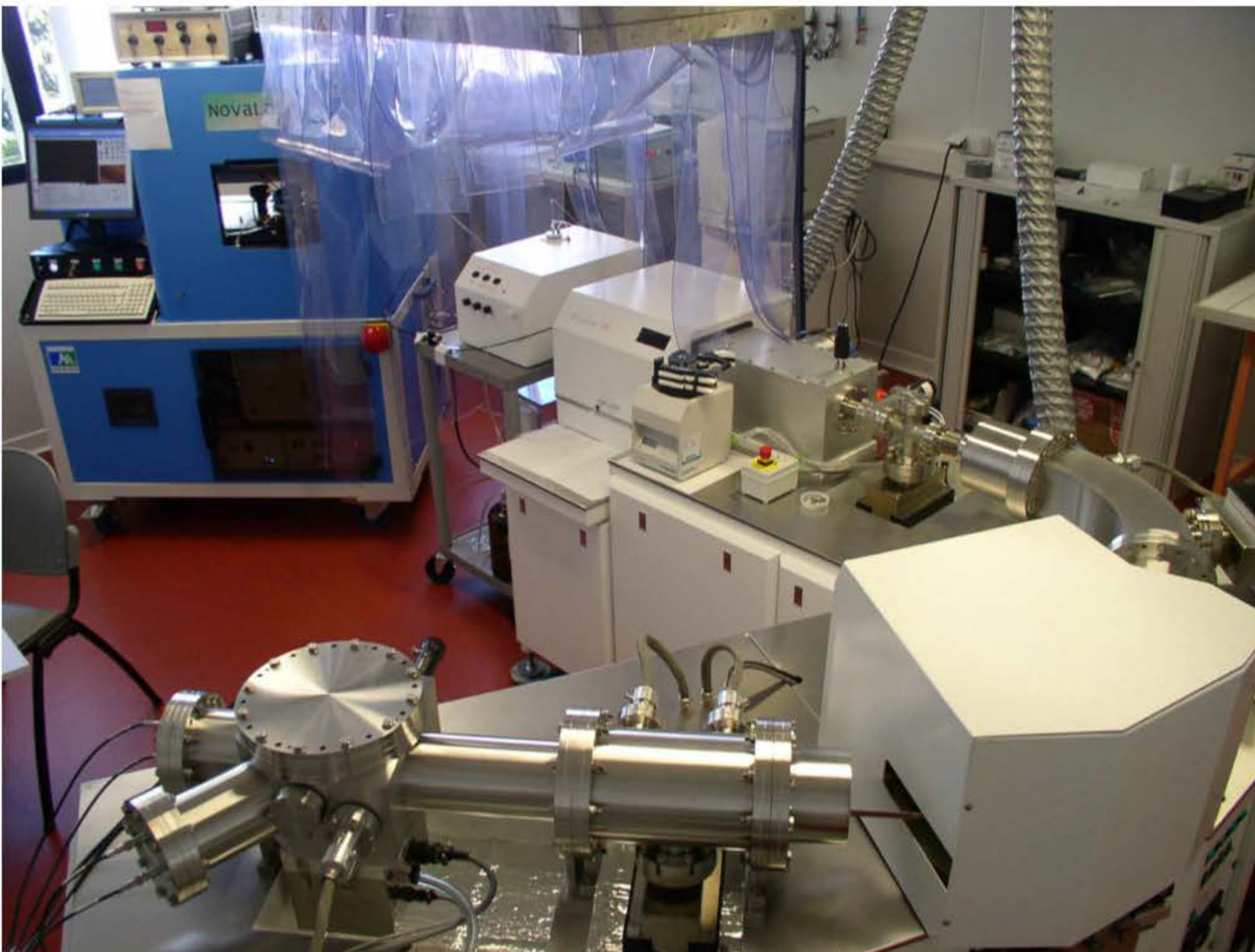
Natural Isotope composition



- ▶ Typical within run precision (1σ) = 7% to 15% for $^{235}\text{U}/^{238}\text{U}$
- ▶ No reliable information on ^{234}U nor ^{236}U

Uranium isotopic composition of micrometric particles

- ▶ **Sector Field => higher ion transmission,
=> higher sensitivity when using the IC**

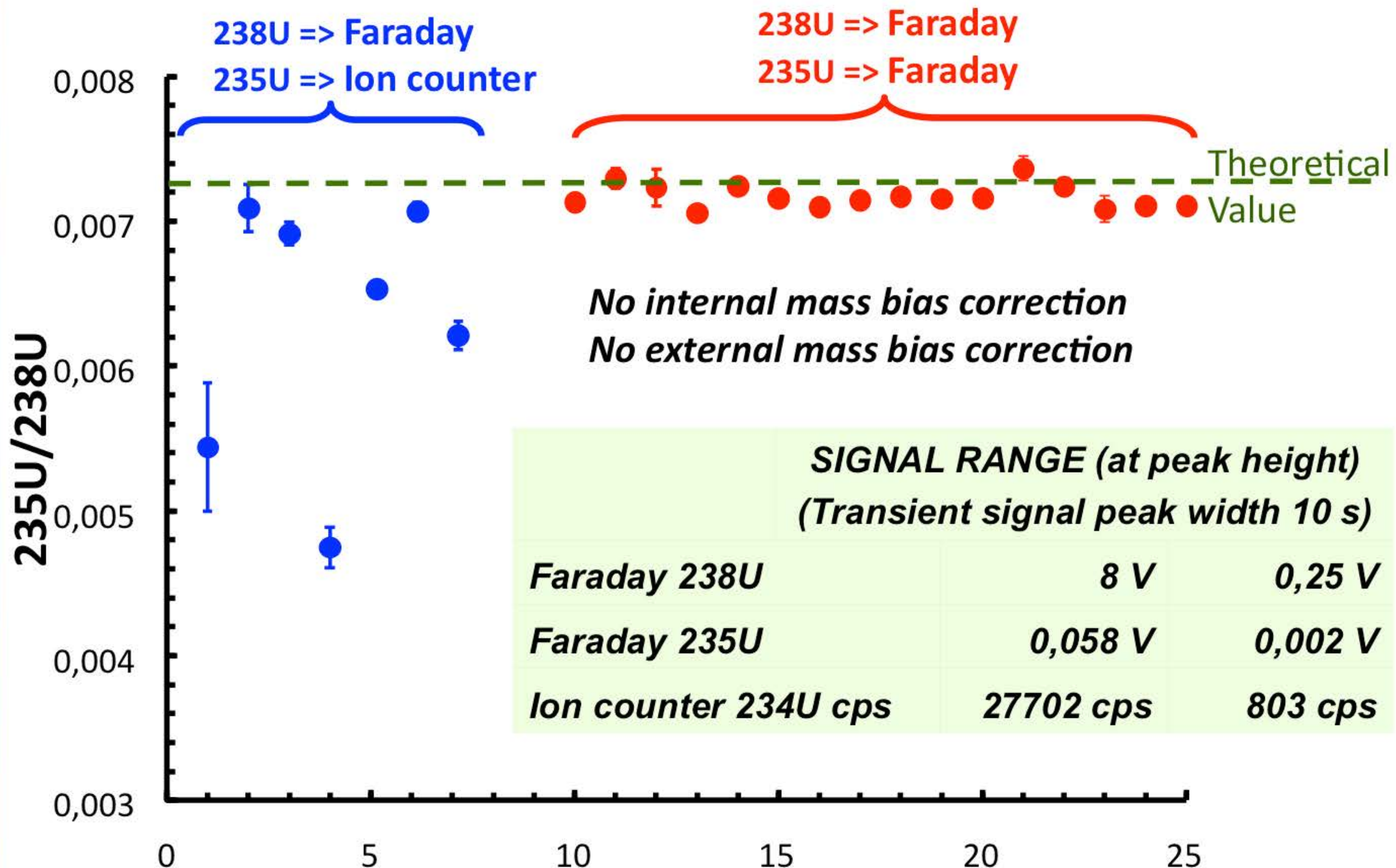


^{238}U , ^{235}U ,
 ^{234}U , ^{236}U

MC-ICPMS -Nu Plasma HR

Uranium isotopic composition of micrometric particles

► Effect of the detector...



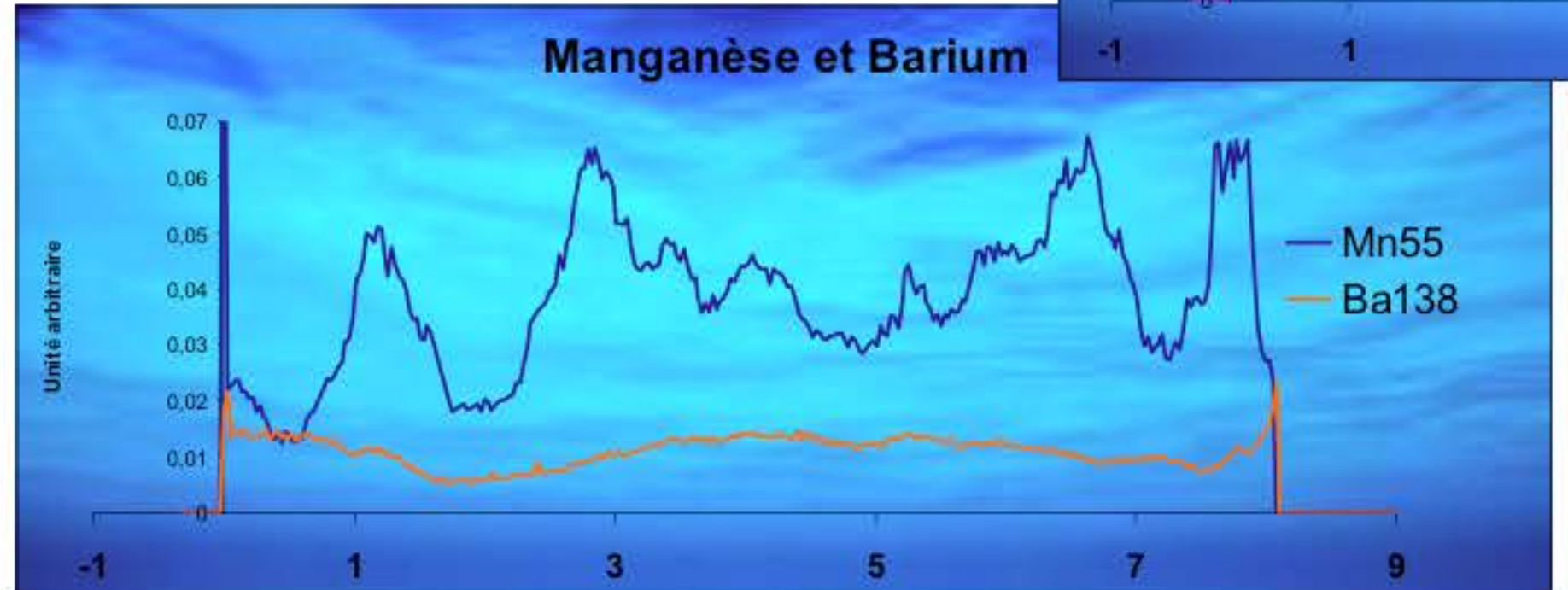
Uranium isotopic composition of micrometric particles

Comparing the analytical techniques...

	235U/238U	234U/238U	
fsLA/Q-ICPMS			
Average Internal precision	10%	-	< 100 particles /day
Mean values (n=9)	0.00736 ± 0.00027 (3,7%)	-	
Bias from theoretical value	1,5%	-	
fsLA/MC-ICPMS	<i>Faraday/Faraday</i>	<i>Ion counter/Faraday</i>	
Average Internal precision	0,68%	2.4%	< 100 particles /day
Mean values (n=16)	0.007178 ± 0.000084 (1,2%)	0.0000514 ± 0.0000014 (3.2%)	
Bias from theoretical value	-1,04%	-7.2%	
FT-TIMS			
Average Internal precision	1.5%	-	< 6 particles /day
Mean values (n=5)	0.00740 ± 0.00004 (5.2%)	-	
Bias from theoretical value	2%	-	
SIMS			
Average Internal precision	0.2%	2%	< 24 particles /day
Mean values (n=6)	0.007246 ± 0.000058 (0.8%)	0.0000540 ± 0.0000011 (2%)	
Bias from theoretical value	-0.1%	-2.5%	



**Donatien Garnier
Christophe Pécheyran**



GEANT, PROTOLITHE

An artistic installation merging science and poetry....



2 GEANT

3. Mhutule le commencement dun geant.
4. Tous les parents sont des geants des geants pour leurs enfants. Tres provisoires geants.
- 5 Chaque generation supprime la precedente croissante a la fete des deux naiss a l etape des descendances. En quoi les geants sont des gens qui vivent sur leur temps.
6. Il y a des geants a passe rapide d'autres a passe lente. Hesitants mais solides ces derniers passent leur vie entiere comme des arbres.
7. De toutes tailles les geants. Geants-géants. Geants-moyens. Geants-nains.

**5th International Otolith
Symposium 2014 (IOS2014)**



20-24 October 2014
Mallorca, Balearic Islands
Spain